Improvement of the Brillouin fermion action for heavy quark

Yong-Gwi Cho
Doctoral Program in Physics

Submitted to the Graduate School of
Pure and Applied Sciences
in Partial Fulfillment of the Requirements
for the Degree of Doctor of Philosophy in
Science

at the
University of Tsukuba

Contents

Chapter 1

Introduction

Dynamics of elementary particles can be understood by the Standard Model(SM) physics. Recently the last particle within SM, i.e. the Higgs boson, has been discovered at the Large Hadron Collider(LHC), though it could be not found for many years [1, 2]. More recently precision test of SM is significant in search for beyond SM physics, in particular after the discovery. So far the 3σ inconsistency for determinations of $|V_{ub}|$ between exclusive and inclusive semi-leptonic decay has been reported.(e.g. see [3]) In exclusive determinations from the B-meson semi-leptonic decay $B \to \pi\ell\nu$, we use the values of the B-meson decay constant computed by the lattice Quantum Chromo Dynamics(QCD) simulation(e.g. see [4, 5]). Then high precisions are required in lattice simulations, even though the heavy quark discretization error may be harmful on the lattice.

Eliminating the discretization effect is one of long-standing problem in lattice QCD, especially in the heavy quark region. Such lattice artifacts have to be improved for precise calculation for heavy quark observables. One can suppress such systematic error by brute numerical force which takes small lattice spacings so that $am_q \ll 1$, however this is very costly. For instance, the bottom quark leads to the large discretization error $am_q \sim 1$ with $1/a \sim 4GeV$ which is still not so easy from current computer resources.

Roughly speaking, there are three class of heavy-quark treatment: (A) lattice heavy quark effective theory(HQET)[6] or lattice non-relativistic QCD(NRQCD)[7], (B) relativistic heavy quark action(Fermilab[8], Tsukuba[9], RHQ[10] and Oktay-Kronfeld[11]), (C) improved light quark action. Both of (A) and (B) can treat the bottom quark without extrapolation, however for (A) matching of parameter is needed and for (B) non-trivial lattice spacing dependence has been reported at $am_q \sim 1$. In this sense, recently the light quark action approach is becoming more and more important.

In this approach, Symanzik improvement is necessary with taking lattice spacing as small as possible in order to reduce the discretization effect. Improved action should be designed to be consistent with Symanzik improvement program[12, 13]. For the staggered fermion, the improved action has been suggested which is called "HISQ" action [14] and has been widely employed in lattice QCD simulations. On the other hand, even in the case of the Wilson fermion, some improved actions have been considered. The clover improved action [15] has been widely studies in many simulations. Also the twisted mass fermion action with the maximal twist has been developed by the ETM collaboration (e.g. see [16]) which eliminate the $O(a)$ discretization effect. In recent years, the ETM collaboration introduced a novel method for B-physics with the twisted mass fermion. They have proposed that one computes some ratios of heavy quark observables when extrapolate to the B-quark mass region with the knowledge of well-known static limit of

the HQET. This is called "Ratio method" and they have achieved precise calculation with twisted mass fermion [17, 18]. Furthermore they claim that the method can be applied with any other improved actions. Also the domain-wall fermion or the overlap fermion have been recently received broad attention as a heavy quark treatment owing to the exact chiral symmetry. These actions preserve the chiral symmetry on the lattice and thus one can expect that guarantee small $O(a)$ discretization effect.

In this study, we aim to investigate $O(a^2)$-improved action or more highly improved action based on the Wilson-type fermion for precise calculation of heavy quark quantity, since highly improved actions for the Wilson-type fermion has been little studied. For construction of a highly improved action, we focus on the so-called Brillouin fermion action which has multi hopping terms within a hypercube[19]. So far some similar fermion formalisms have been suggested [20, 21, 22, 23]. These fermion actions have been investigated with focus on the aspect of the approximate Ginsparg-Wilson fermion, whereas the Brillouin fermion action is designed to reproduce both of the continuum energy dispersion relation and eigenvalue spectra of the Ginsparg-Wilson fermion. Not only at tree-level but also non-perturbatively the fermion action realizes an excellent dispersion relation and thus one can expect that it is promising for heavy quark physics.

We have investigated discretization errors for the Brillouin fermion action and have found that the action can be improved furthermore. Traditional $O(a)$ clover improvement, of course, is applicable, but we adopt the similar strategy with the D34 action for the Wilson fermion action[24, 25]. On other hand since the action has Ginsparg-Wilson like eigenvalue spectra, one can expect a suitability as a kernel of the overlap procedure. Thus we attempt to apply the overlap procedure with the Brillouin kernel as $O(a)$ improvement. Furthermore $O(a^2)$ improvement has been developed in Ref.[26] and we advance to further improvement with the approach by employing the Brillouin kernel.

Also we carry out scaling studies for our improved action on quenched configurations with $1/a = 2.0 - 3.8$ GeV compared with existing formulations: non-improved Wilson fermion and the domain-wall fermion. Here we employ the tree-level Symanzik gauge action and physical length is roughly fixed to 1.6 fm. Also we measure speed-of-light, hyperfine splitting and decay constant for heavy-heavy observables. Our scaling studies show good scaling of the improved action up to the charm quark region. Furthermore we mention to an applicable limit of the improved action and discuss unphysical poles.

This thesis is organized as follows. First of all, we briefly introduce formulations of lattice gauge theory in chapter 2. In chapter 3, we follow a basic idea of Symanzik improvement and discuss how to construct improved actions. Next we introduce chiral symmetric fermion actions and these properties in chapter 4. Also we simply review how to obtain hadron spectroscopy in chapter 5. Formulation of the Brillouin fermion will be introduced in chapter 6 and here suggest some improved actions based on the tree-level analysis. In chapter 7 we show our results of scaling studies for the improved action and additional properties of the Brillouin-type fermion will discussed in chapter 8.

Chapter 2

Quantum chromo dynamics on the lattice

We briefly review the lattice gauge theory. More detailed formulations will be discussed at later chapters.

2.1 Continuum theory

First of all, we review the continuum QCD theory. The QCD action can be described as a gauge part and a fermion part.

$$S_{QCD} = \int d^4x \left[\mathcal{L}_{gauge} + \mathcal{L}_{fermion}\right] \tag{2.1}$$

The pure-gauge part and fermion part can be defined respectively as

$$\mathcal{L}_{gauge} = -\frac{1}{2} tr\left[F^a_{\mu\nu}(x) F^{\mu\nu a}(x)\right], \tag{2.2}$$

$$F^a_{\mu\nu}(x) = \partial_\mu A^a_\nu(x) - \partial_\nu A^a_\mu(x) + igf^{abc} A^b_\mu(x) A^c_\nu(x), \tag{2.3}$$

$$\mathcal{L}_{fermion} = \bar{\psi}(x)\left[D_\mu \gamma^\mu + m\right]\psi(x), \tag{2.4}$$

$$D_\mu = \partial_\mu - igA^a_\mu(x) T^a, \tag{2.5}$$

where T^a denotes a $SU(3)$ generator and γ^μ is the gamma matrices. Also m is a bare quark mass and g is a bare coupling constant. The above lagrangian is invariant under the gauge symmetry

$$\psi(x) \to V(x)\psi(x), \tag{2.6}$$

$$A_\mu(x) \to \frac{1}{ig} V(x)\partial_\mu(x) V^\dagger(x) + V(x) A_\mu(x) V^\dagger(x), \tag{2.7}$$

where $V(x)$ is an element of $SU(3)$ group and it can be written as $V(x) = exp(i\varepsilon^a T^a)$ in terms of the generator T^a . Then an expectation value of an observable O can be measured by

$$< O > = \frac{1}{Z} \int \mathcal{D}A\mathcal{D}\bar{\psi}\mathcal{D}\psi e^{iS_{QCD}} O, \tag{2.8}$$

$$Z = \int \mathcal{D}A\mathcal{D}\bar{\psi}\mathcal{D}\psi e^{iS_{QCD}}. \tag{2.9}$$

The QCD lagrangian is quite simple, but calculations are not straightforward for low energy physics, e.g. the hadron mass or the decay constant. Since the QCD coupling is strong at low energy which is known as the asymptotic freedom, complicated non-perturbative calculations are necessary. Then lattice QCD calculation would be the unique powerful tool.

2.2 Gauge action

Simplest gauge action on the lattice is realized by the standard plaquette action.

$$\begin{aligned} S_G &= \sum_n \sum_{\mu,\nu} \beta tr U_{\mu\nu}(n) \\ U_{\mu\nu}(n) &= U_{n,\mu} U_{n+\mu,\mu} U^{\dagger}_{n+\nu,\mu} U_{n,\nu}{}^{\dagger} \end{aligned} \tag{2.10}$$

$$U_{n,\mu} \in SU(3) \tag{2.11}$$

This gauge action is invariant under the gauge transformation

$$U_{n,\mu} \to V_n^{\dagger} U_{n,\mu} V_{n+1}, \tag{2.12}$$

where V_n is an element of $SU(3)$ algebra. Also we could consider a rectangle gauge invariant objects which are introduced by Iwasaki.

$$\begin{aligned} S_G &= \beta \sum_n \sum_{\mu,\nu} tr \{ R_{\mu\mu\nu}(n) + R_{\nu\nu\mu}(n) \} \\ R_{\mu\mu\nu}(n) &= U_{n,\mu} U_{n+\mu,\mu} U_{n+2\mu,\nu} U^{\dagger}_{n+\mu+\nu,\mu} U^{\dagger}_{n+\nu,\mu} U^{\dagger}_{n,\nu} \end{aligned} \tag{2.13}$$

$$S_G = \beta \sum_n \sum_{\mu,\nu} \left[c_0 tr U_{\mu\nu} + c_1 tr \{ R_{\mu\mu\nu}(n) + R_{\nu\nu\mu}(n) \} \right] \tag{2.14}$$

In the continuum limit, the gauge action should agree with the continuum gauge action. Thus the coefficients are determined as

$$c_0 + 8c_1 = 1. \tag{2.15}$$

The rectangle action is called "Iwasaki action" and is widely used for lattice QCD simulations.

2.3 Naive discretization and fermion doubling

Here we review the well-known fermion doubling problem when the naive discretization is introduced in the fermion part. We consider a following discretized fermion action

$$S_F = a^4 \sum_n \bar{\psi}_n \left[\sum_\mu \gamma_\mu \frac{U_{n,\mu}\psi_{n+\mu} - U^\dagger_{n-\mu,\mu}\psi_{n-\mu}}{2a} + m\psi_n \right]. \tag{2.16}$$

Then if we introduce dimensionless quantities

$$\begin{aligned} \psi' &= a^{3/2}\psi, \\ M &= ma, \end{aligned} \tag{2.17}$$

Eq. (2.16) can be written as

$$S_F = \frac{1}{2}\sum_n \left[\bar{\psi}_n \gamma_\mu U_{n,\mu}\psi_{n+\mu} - \bar{\psi}_{n+\mu}\gamma_\mu U^\dagger_{n,\mu}\psi_n \right] + M\sum_n \bar{\psi}_n\psi_n \tag{2.18}$$

On the momentum space, one can read as

$$S_F = \int \frac{d^4p}{(2\pi)^4} \tilde{\bar{\psi}}(p) \left[i\gamma_\mu sin(p_\mu a) + M \right] \tilde{\psi}(p). \tag{2.19}$$

Then the fermion propagator becomes as follows

$$P_F(p) = \frac{1}{i\not{s}(p) + M} = \frac{-i\not{s}(p) + M}{s(p)^2 + M^2}, \tag{2.20}$$

where $\not{s}(p) = \sum_\mu \gamma_\mu s_\mu(p) = \sum_\mu \gamma_\mu sin(p_\mu a)$. In the limit $a \to 0$, it can be expanded as

$$sin(p_\mu a) = \begin{cases} \hat{p}_\mu a & p_\mu = \hat{p}_\mu \\ -\hat{p}_\mu a & p_\mu = \frac{\pi}{a} + \hat{p}_\mu \end{cases}, \tag{2.21}$$

then the propagator can be written as

$$\lim_{a\to 0} P_F(p) = \lim_{a\to 0} \frac{1}{a} \sum_{\hat{p}_\mu = 0, \frac{\pi}{a}} \frac{-i\sum_\mu (-1)^{\delta_\mu} \gamma_\mu \hat{p}_\mu + m}{\hat{p}^2 + m^2}, \tag{2.22}$$

where δ_μ is defined as

$$\delta_\mu = \begin{cases} 0 & \hat{p}_\mu = 0 \\ 1 & \hat{p}_\mu = \frac{\pi}{a} \end{cases}. \tag{2.23}$$

Here $\hat{p}_\mu$ has following variants

$$\hat{p}_\mu = \begin{cases} (0,0,0,0) \\ \left(0,0,0,\frac{\pi}{a}\right) \\ \left(\frac{\pi}{a},0,0,0\right) \\ \left(\frac{\pi}{a},\frac{\pi}{a},0,0\right) \\ \quad \vdots \end{cases} \tag{2.24}$$

In the quantum field theory, poles of the propagator correspond to particles. Therefore we see that 2^d doublers appear for a lattice fermion, where d is a dimension. It is called "doubling problem" and one has to avoid this problem by using some methods which will be introduced in later sections.

2.4 Nielsen-Ninomiya no-go theorem

The doubling problem is also known as Nielsen-Ninomiya no-go theorem. Here we briefly describe the derivation of the Nielsen-Ninomiya no-go theorem by following the discussion in Ref. [27]. Nielsen-Ninomiya no-go theorem says that doublers appear when following conditions are assumed.

- Translation invariance
- Hermiticity
- Locality
- Chiral symmetry
- Fermion bilinear form

Then we can prove that the doubling problem is not be avoidable. First we consider the fermion action on the momentum space

$$\begin{aligned} S_F &= \int d^4x d^4y \overline{\psi}(x) D(x,y) \psi(y) \\ &= \int d^4x d^4y \left(\int \frac{d^4p}{(2\pi)^4} e^{-ipx} \widetilde{\overline{\psi}}(-p) \right) D(x,y) \left(\int \frac{d^4q}{(2\pi)^4} e^{-iqy} \widetilde{\psi}(q) \right) \\ &= \int d^4x d^4y \int \frac{d^4p}{(2\pi)^4} \int \frac{d^4q}{(2\pi)^4} e^{-i(p+q)\left(\frac{x+y}{2}\right)} e^{-i(p-q)\left(\frac{x-y}{2}\right)} \widetilde{\overline{\psi}}(-p) D(x,y) \widetilde{\psi}(q) . \end{aligned} \tag{2.25}$$

Here we introduce absolute coordinate R and relative coordinate $r$and then the action can be written

$$
\begin{aligned}
S_F &= \int d^4Rd^4r \int \frac{d^4p}{(2\pi)^4} \int \frac{d^4q}{(2\pi)^4} e^{-i(p+q)R} e^{-i(p-q)r} \widetilde{\overline{\psi}}(-p)\, D'(R,r)\, \widetilde{\psi}(q) \\
&= (2\pi)^4 \int d^4r \int \frac{d^4p}{(2\pi)^4} \int \frac{d^4q}{(2\pi)^4} e^{-i(p-q)r} \delta^{(4)}(p+q)\, \widetilde{\overline{\psi}}(-p)\, D'(r)\, \widetilde{\psi}(q) \\
&= \int d^4r \int \frac{d^4q}{(2\pi)^4} e^{-2iqr} \widetilde{\overline{\psi}}(q)\, D'(r)\, \widetilde{\psi}(q) \\
&= \int \frac{d^4q}{(2\pi)^4} \widetilde{\overline{\psi}}(q)\, \widetilde{F}\left(-\frac{q}{2}\right) \widetilde{\psi}(q), \qquad (2.26)
\end{aligned}
$$

where we used translation invariance $D(R,r) = D(r)$ in the second line. In other words, the fermion action can be written as a function of a momentum. Furthermore the assumption of chiral symmetry restricts to the form of

$$
\widetilde{F}(p) = \sum_\mu \gamma_\mu \widetilde{F_\mu}(p). \qquad (2.27)
$$

Also $\tilde{F}_\mu(p)$ is real from hermiticity and locality guarantees continuity of $\tilde{F}_\mu(p)$. In other words, if we assume the form of

$$
\widetilde{F_\mu}(0) = \int d^4x e^{-\alpha|x|} F_\mu(x), \qquad (2.28)
$$

then continuity of $\tilde{F}_\mu(p)$ at $p=0$ is ensured as

$$
\lim_{p\to 0} \left(\frac{d}{dp}\right)^n \widetilde{F_\mu}(p) = \lim_{p\to 0} \int d^4x\, (ix)^n e^{ipx} F_\mu(x) < \infty. \qquad (2.29)
$$

Therefore we see that $\tilde{F}_\mu(p)$ is real vector field on d dimension torus

$$
\widetilde{F_\mu}(p) \in T^d. \qquad (2.30)
$$

In this context, we utilize the Poincare-Hopf theorem (e.g. see Ref. [28]) which states that the sum of the indices of zeros for the continuous vector field defined on a compact manifold is equal to the Euler numbers. For a torus, the Euler number is zero. Therefore it is found that sum of zero modes of $\tilde{F}_\mu(p)$ is zero. Expanding $\tilde{F}_\mu(p)$ at around p_0, we obtain

$$
\widetilde{F_\mu}(p) = A_{\mu,\nu}(p-p_0)_\nu + \mathcal{O}\left((p-p_0)^2\right), \qquad (2.31)
$$

where

$$
A_{\mu,\nu} = \left.\frac{\partial \widetilde{F_\mu}(p)}{\partial p_\nu}\right|_{p=p_0}. \qquad (2.32)
$$

Then the index of zeros is defined by $detA_{\mu,\nu}$ and we notice that the index of zeros corresponds to chirality. To see this, we set $p_0 = 0$ for simplicity. If we diagonalize $A_{\mu,\nu}$ by redefinition of ψ, $\tilde{F}_\mu(p)$ can be written as

$$\widetilde{F_\mu}(p) = A_\mu p_\mu. \tag{2.33}$$

When $A_\mu = (1,1,1,1)$, the index and the fermion action are

$$\begin{cases} \text{index} & 1 \\ \text{fermion action} & \tilde{\overline{\psi}}(p) \sum_\mu \gamma_\mu p_\mu \tilde{\psi}(p) \end{cases}. \tag{2.34}$$

On the other hand, for $A_\mu = (-1,1,1,1)$ these are

$$\begin{cases} \text{index} & -1 \\ \text{fermion action} & \tilde{\overline{\psi}}(p) \sum_\mu (1-2\delta_{\mu 1}) \gamma_\mu p_\mu \tilde{\psi}(p) \\ & = \left(\tilde{\overline{\psi}}(p) \gamma_5 \gamma_1\right) \sum_\mu \gamma_\mu p_\mu \left(\gamma_1 \gamma_5 \tilde{\psi}(p)\right) \end{cases}. \tag{2.35}$$

Chiral transformation ofψ is defined by

$$\psi \to e^{iQ\gamma_5}\psi, \tag{2.36}$$

where Q is the chiral charge. Then the indices ± 1 respectively correspond to

$$\psi(p) \to e^{iQ\gamma_5}\psi(p), \tag{2.37}$$

$$\gamma_5\gamma_1\psi(p) \to e^{-iQ\gamma_5}\gamma_5\gamma_1\psi(p). \tag{2.38}$$

If we combine this thing with the Poincare-Hopf theorem, Nielsen-Ninomiya no-go theorem can be proved. Namely, number of fermions with $+Q$ chiral charge must be equivalent to number of fermions with $-Q$ chiral charge.

2.5 Wilson fermion

In order to remove unphysical doublers, one adds a $O(a)$ term to the lattice fermion action

$$\begin{aligned} S_W &= -ar \int d^4x \overline{\psi} D^2 \psi \\ &\to -\frac{1}{2} r \sum_{n,\mu} \left[\overline{\psi}_n U_{n,\mu} \psi_{n+\mu} + \overline{\psi}_{n+\mu} U^\dagger_{n,\mu} \psi_n - 2\overline{\psi}_n \psi_n\right], \end{aligned} \tag{2.39}$$

which are introduced by Wilson and thus this term is called "Wilson term". Also $r$is a free parameter which usually taken to the unity. Then whole fermion action becomes

$$\begin{aligned} S_F &= \int \frac{d^4p}{(2\pi)^4} \overline{\psi}(-p) \left[i\not{s}(p) + M + r\sum_\mu (1 - cos(p_\mu a))\right] \psi(p) \\ &= \int \frac{d^4p}{(2\pi)^4} \overline{\psi}(-p) \left[i\not{s}(p) + M(p)\right] \psi(p), \end{aligned} \tag{2.40}$$

where $M(p) \equiv M + r\sum_{\mu}(1 - cos(p_\mu a))$ and we obtain the fermion propagator

$$G_F(p) = \frac{-i\not{s}(p) + M(p)}{s(p)^2 + M(p)^2}. \tag{2.41}$$

In the limit $a \to 0$, $M(p)$ can be written

$$M(p) = \begin{cases} ma & \text{physycal} \\ ma + 2r|\delta| & \text{unphysycal} \end{cases}, \tag{2.42}$$

where $|\delta|$ is number of doubles which have momentum π/a. Then dimension-full masses are

$$m_{\text{phys}} = m, \tag{2.43}$$

$$m_{\text{doubler}} = m + \frac{2r}{a}|\delta|. \tag{2.44}$$

Thus unphysical doublers decouple in the continuum limit and thus we could remove doublers by adding the Wilson term. However the Wilson term explicitly violate the chiral symmetry due to the Wilson term. It is one of disadvantage of the Wilson fermion.

2.6 Staggered fermion

The staggered fermion is also employed widely in lattice QCD simulations. Here I briefly introduce this formalism. The staggered fermion is 1 component lattice fermion and appearing 16 species are interpreted as 4flavor $\otimes$ 4Dirac fermions. The staggered fermions is given by

$$S_F = \frac{1}{2}\sum_{n,\mu}\left[\eta_\mu(n)\left(\bar{\chi}(n)U_{n,\mu}\chi(n+\hat{\mu}) - \bar{\chi}(n+\hat{\mu})U^\dagger_{n,\mu}\chi(n)\right) + m\bar{\chi}(n)\chi(n)\right], \tag{2.45}$$

where $\chi(n)$ is one component staggered fermion field and the sign function $\eta_\mu(n)$ is defined as

$$\eta_\mu(n) = (-1)^{n_1+n_2+\cdots+n_\mu-1}. \tag{2.46}$$

Then $\chi(n)$ is related to 4 component Dirac fermion as

$$\psi(N)_{\alpha,f} = N_0\sum_A\left(\frac{\gamma_A}{2}\right)_{\alpha,f}\chi(2N+A) \equiv N_0\sum_A\left(\frac{\gamma_A}{2}\right)_{\alpha,f}\chi_A(N), \tag{2.47}$$

$$\bar{\psi}(N)_{\alpha,f} = N_0\sum_A\bar{\chi}(2N+A)\left(\frac{\bar{\gamma}_A}{2}\right)_{\alpha,f} \equiv N_0\sum_A\bar{\chi}_A(N)\left(\frac{\bar{\gamma}_A}{2}\right)_{\alpha,f}, \tag{2.48}$$

where α is an index of spinor and f is an index of flavor. Also N_0 is a normalization constant and γ_A is defined by

$$\gamma_A = \gamma_1^{A_1}\gamma_2^{A_2}\gamma_3^{A_3}\gamma_4^{A_4}, \tag{2.49}$$

where $A_\mu = 0, 1$ and thus $2N + A$ represents a coordinate within a hypercube placed on $2N$. If one uses transformations Eqs. (2.47) and(2.48), Eq. (2.45) can be written as

$$S_F = \frac{1}{N_0^2}\sum_{N,\mu}\bar{\psi}(N)\left[(\gamma_\mu \otimes 1)\frac{\nabla\mu}{2} + (\gamma_5 \otimes t_\mu t_5)\frac{\nabla_\mu^2}{2} + M(1\otimes 1)\right]\psi(N), \tag{2.50}$$

where $t_\mu = \bar{\gamma}_\mu = \gamma_\mu^T$. Here N is taken only for even lattice points and thus maximum momentum becomes $\pi/2a$. Then the staggered fermion can avoid $p = \pi/a$ on which doublers are assigned. However as we have seen, the second term in Eq. (2.50) violates the flavor symmetry. Thus one may conclude that the staggered fermion is equivalent to 4 flavor Dirac fermions, but the flavor symmetry is broken. For one flavor simulations, the rooting trick is employed and it is often discussed whether 4th rooted staggered fermion can be identified with one flavor Dirac fermion. For more details, please see e.g. Ref [29].

Chapter 3

Symanzik improvement

Lattice QCD is defined on the discretized space-time and thus the discretization systematics effect is not avoidable at finite lattice spacing a. However Symanzik has proposed that one can systematically reduce discretization effects by adding higher dimensional operators up to desired order vanish [12, 13]. In this chapter, we review the Symanzik improvement program and some applications. In general, when considering improvement for lattice QCD, one needs to improve euclidean correlation function

$$\langle O \rangle = \frac{1}{Z} \int \mathcal{D}U \mathcal{D}\psi \mathcal{D}\bar{\psi} e^{-S[U,\psi,\bar{\psi}]} O\left[U, \psi, \bar{\psi}\right]. \tag{3.1}$$

In this context, we have to improved both of the action and the interpolator O. Here let us discuss improvement of action. For improvement of interpolators, please see e.g. Ref. [30].

3.1 Symanzik improvement program

As mentioned before, Symanzik have introduced a local effective lagrangian for analyzing the discretization effect. Furthermore this analysis provides a strategy for improving the lattice artifact. The idea is that lattice gauge theory which is defined on non-zero a can be described by a local effective lagrangian. Short distance behaviors are parametrized to short distance coefficients, whilst long distance effects are described by local effective lagrangian. Symanzik says that any lattice lagrangian can be written as

$$\mathcal{L}_{lat} \doteq \mathcal{L}_{Sym}, \tag{3.2}$$

where $\doteq$ means that "has the same on-shell matrix elements". The right-hand side of Eq. (3.2) is a local effective lagrangian which is used for analyzing output data. For lattice QCD, the local effective lagrangian can be written

$$\mathcal{L}_{Sym} = \mathcal{L}_{QCD} + \mathcal{L}_I, \tag{3.3}$$

where $\mathcal{L}_{QCD}$ is the continuum QCD lagrangian and $\mathcal{L}_I$ denotes the parts of lattice artifact which is describe as

$$\mathcal{L}_I = \sum_O a^{dimO-4} K_O\left(g^2, ma; \mu a\right) O_R\left(\mu\right) \tag{3.4}$$

with $dimO > 4$. Here μ denotes the renormalization scale and m is the renormalized quark mass, also g^2 represents the renormalized coupling. $a^{dimO-4} K_O\left(g^2, ma; \mu a\right)$ is a short-distance coefficient.

Furthermore the renormalized operator $O_R(\mu)$ depends on long-distance only. In the interaction picture, one can omit redundant interactions from$\mathcal{L}_I$ by the field redefinitions

$$\psi \to \psi + a^{dimX}\varepsilon X\psi, \tag{3.5}$$
$$\bar{\psi} \to \bar{\psi} + a^{dimX}\bar{\varepsilon}\bar{\psi}X, \tag{3.6}$$

where X is an arbitary gauge-covariant operator and $\varepsilon, \bar{\varepsilon}$ are free parameters. These transformations do no change on-shell quantities, e.g. hadron masses, though the measure of the path integral is changed non-significantly. Then $\mathcal{L}_I$ is changed as

$$\mathcal{L}_I \to \mathcal{L}_I + \sum_X a^{dimX}\left[\bar{\varepsilon}\bar{\psi}X\left(\not{D}+m\right)\psi\bar{\varepsilon} + \bar{\psi}\left(-\overleftarrow{\not{D}}+m\right)X\psi\right]. \tag{3.7}$$

Coefficients of higher order terms should be tuned based on the analysis of the Symanzik effective theory up to a required level .

3.2 O(a)-improvement for the Wilson fermion

For $O(a)$ -improvement of the Wilson fermion, the clover term is widely employed in lattice simulations. Historically the clover term has been introduced in the context of the field rotation [15] which corresponds to Eqs. (3.5), (3.6). Here we review the approach in Ref. [30]. First we think of the local effective lagrangian of the Wilson fermion

$$S_{\text{eff}} = \int d^4x \left(\mathcal{L}_0 + a\mathcal{L}_1 + a^2\mathcal{L}_2 + \cdots\right), \tag{3.8}$$

where $\mathcal{L}_0$ is the continuum QCD lagrangian and the lagrangians $\mathcal{L}_k$ are dimension $4+k$ operators. Requiring desirable symmetries, following 5 dimensional operator for $\mathcal{L}_1$ remain

$$O_1 = \bar{\psi}\sigma_{\mu\nu}F_{\mu\nu}\psi, \tag{3.9}$$

$$O_2 = \bar{\psi}\overrightarrow{D}_\mu\overrightarrow{D}_\nu\psi + \bar{\psi}\overleftarrow{D}_\mu\overleftarrow{D}_\nu\psi, \tag{3.10}$$

$$O_3 = m\text{tr}\left[F_{\mu\nu}F_{\mu\nu}\right], \tag{3.11}$$

$$O_4 = m\left(\bar{\psi}\gamma_\mu\overrightarrow{D}_\mu\psi - \bar{\psi}\gamma_\mu\overleftarrow{D}_\mu\psi\right), \tag{3.12}$$

$$O_5 = m^2\bar{\psi}\psi, \tag{3.13}$$

where D_μ is the continuum covariant derivative operator. However if we use the filed equation $(\gamma_\mu D_\mu + m)\psi = 0$, one obtains following relations

$$O_1 - O_2 + 2O_5 = 0, \tag{3.14}$$

$$O_4 + 2O_5 = 0. \tag{3.15}$$

Thus O_2 and O_4 are redundant in terms of the on-shell improvement. Moreover O_3 and O_5 can be absorbed into the definition of mass and coupling. Then we can write down an improved action for the Wilson fermion

$$S_{imp} = S_{Wilson} + \frac{c_{SW}}{2} a^5 \sum_{\mu<\nu} \bar{\psi} \sigma_{\mu\nu} \hat{F}_{\mu\nu} \psi, \tag{3.16}$$

which is so-called the clover-improved Wilson fermion and c_{SW} is a free parameter to be tuned. Here $\hat{F}_{\mu\nu}$ is a discretized version of the field strength tensor

$$\hat{F}_{\mu\nu} = \frac{-i}{8a} \left(Q_{\mu\nu}(x) - Q_{\nu\mu}(x) \right), \tag{3.17}$$

where $Q_{\mu\nu}(x)$ is given by

$$Q_{\mu\nu}(x) = U_{\mu,\nu}(x) + U_{\nu,-\mu}(x) + U_{-\mu,-\nu}(x) + U_{-\nu,\mu}(x)$$

and is graphically shown in Fig. 3.1. This shape is often expressed as the clover leaf.

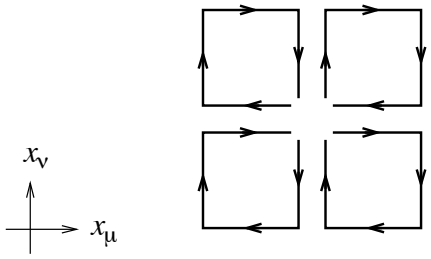

Figure 3.1: Graphical representation of the $Q_{\mu\nu}(x)$ in the $x_\mu - x_\nu$ plan used for the definition of the lattice field strength. This shape is often expressed as the clover leaf.

3.3 D234 action

Here we first review the clover improvement in terms of the field rotation or the filed redefinition which do not affect on-shell quantities. Let us start from the continuum action

$$\int \bar{\psi}_c M_c \psi_c \equiv \int d^4x \bar{\psi}_c(x) \left(\not{D} + m_c \right) \psi_c. \tag{3.18}$$

Then if we perform a following field rotation

$$\psi_c = \Omega_c \psi, \tag{3.19}$$

$$\bar{\psi}_c = \bar{\psi} \bar{\Omega}_c, \tag{3.20}$$

the action is transformed as

$$\bar{\psi}_c M_c \psi_c = \bar{\psi} M_\Omega \psi, \tag{3.21}$$

$$M_\Omega \equiv \bar{\Omega}_c M_c \Omega_c. \tag{3.22}$$

If we choose

$$\bar{\Omega}_c = \Omega_c, \tag{3.23}$$

$$\bar{\Omega}_c \Omega_c = 1 - \frac{ra}{2} \left(\not{D} - m_c \right), \tag{3.24}$$

where a is just a parameter. Note that Ω and $\bar{\Omega}$ are optionally chosen and one may think of an another choice. Then

$$\begin{aligned} M_\Omega &= \bar{\Omega}_c \left(\not{D} - m_c \right) \Omega_c \\ &= \bar{\Omega}_c \not{D} \Omega_c - m_c \left(1 - \frac{ra}{2} \left(\not{D} - m_c \right) \right) \\ &\approx \left(1 - \frac{ra}{4} \left(\not{D} - m_c \right) \right) \not{D} \left(1 - \frac{ra}{4} \left(\not{D} - m_c \right) \right) - m_c \left(1 - \frac{ra}{2} \left(\not{D} - m_c \right) \right) \\ &= m_c + \not{D} - \frac{1}{2} ra \left(\not{D}^2 - m_c^2 \right) \\ &= m_c \left(1 + \frac{1}{2} ram_c \right) + \not{D} - \frac{1}{2} ra \left(\sum_\mu D_\mu^2 + \frac{1}{2} \sigma \cdot F \right), \end{aligned} \tag{3.25}$$

where we used $\left(1 - \frac{ra}{2} \left(\not{D} - m_c \right) \right)^{1/2} \approx 1 - \frac{ra}{4} \left(\not{D} - m_c \right)$ in the third line and $\{ \gamma_\mu D_\mu, \gamma_\nu D_\nu \} = 2\delta_{\mu\nu} D_\mu^2 + \sigma_{\mu\nu} F_{\mu\nu}$ in the last line. The Shiekholeslami-Wohlert action or clover-improved Wilson action can be obtained by replacing the derivatives with leading discretized operators in Eq. (3.25)

$$M_{SW} = m_c \left(1 + \frac{1}{2} ram_c \right) + \not{\nabla} - \frac{1}{2} ra \sum_\mu \triangle_\mu - \frac{1}{4} ra \sigma \cdot \hat{F}, \tag{3.26}$$

where ∇_μ and $\triangle_\mu$ are defined as

$$\nabla_\mu \psi(x) = \frac{1}{2a} \left[U_\mu(x) \psi(x + \hat{\mu}) - U_\mu^\dagger(x - \hat{\mu}) \psi(x - \hat{\mu}) \right] \tag{3.27}$$

$$\triangle_\mu \psi(x) = \frac{1}{2a} \left[U_\mu(x) \psi(x + \hat{\mu}) + U_\mu^\dagger(x - \hat{\mu}) \psi(x - \hat{\mu}) - 2\psi(x) \right] \tag{3.28}$$

If one is interested in only on-shell quantities, we could use the propagator $G = M^{-1}$, but off-shell quantities may have $O(a)$ errors, since $\Omega_c = 1 + O(a)$ and therefore $\psi = \psi_c + O(a)$. In order to remove this error in off-shell quantities, we perform a lattice version of the inverse field rotation Ω and $\bar{\Omega}$. Then the action is changed as $\bar{\Omega}^{-1} M \Omega^{-1}$ and the propagator of the action is $G = \bar{\Omega} M^{-1} \Omega = M_c^{-1} + O(a^n)$. If one takes into account up to the next leading order in the expansion of the continuum derivatives, we obtain

$$M_{D234} = m_c \left(1 + \frac{1}{2} r a m_c\right) + \sum_\mu \gamma_\mu \nabla_\mu \left(1 - b a^2 \triangle_\mu\right), \tag{3.29}$$

$$- \frac{1}{2} r a \sum_\mu \triangle_\mu - \frac{1}{4} r a \sigma \cdot \hat{F} + c a^3 \sum_\mu \triangle_\mu^2, \tag{3.30}$$

where $b = 1/6$ and $c = r/24$. The D234 action does not have $O(a)$ and $O(a^2)$ errors. The dispersion relation of the D234 action has been discussed3 in Ref. [31]. Furthermore this action contains the unphysical additional poles which are called "Ghost" or "lattice Ghost". The ghosts may be harmful in some cases.This problem will be discussed in later chapter.

3.4 Tree-level improved Symanzik gauge action

Improved gauge actions also have been proposed based on the Symanzik improvement program [32, 33]. The improved gauge action includes higher dimensional expressions of the gauge invariant pure gage action on the lattice. The tree-level Symanzik improved action is defined as follows

$$S_{gauge} = \frac{1}{g_{lat}^2} \left[c_0 \sum_{plaquette} Tr U_{pl} + c_1 \sum_{rectangle} Tr U_{rtg} + c_2 \sum_{chair} Tr U_{chr} + c_3 \sum_{parallelogram} Tr U_{plg} \right], \tag{3.31}$$

which have higher gauge invariant objects. Then the coefficient are normalized so that

$$c_0 + 8c_1 + 16c_2 + 8c_3 = 1. \tag{3.32}$$

For the tree-level improvement, the following conditions should be imposed for the coefficients

$$c_1 - c_2 - c_3 = -\frac{1}{12}, \tag{3.33}$$

This condition was derived from a computation of the energies of excited states with the twisted periodic boundary condition. Further this improved action has been employed extensively in lattice QCD simulations.

Chapter 4

Chiral symmetry on the lattice

Chiral symmetry is the approximate symmetry in QCD. On the lattice, chiral symmetry is apparently broken by the Wilson term even in massless case. On the other hand, the Wilson term should be added to decouple doublers. The situation related to the chiral symmetry on the lattice is not straightforward. However this problem has been solved in the context of the Ginsparg-Wilson relation[34] and Neuberger presented a particular solution which is called *overlap fermion* [35]. Chiral symmetric lattice fermions are also promising for heavy quark physics, since the chiral symmetry forbid some parts of discretization errors. We will also discuss this aspect of chiral symmetric fermions.

4.1 Chiral symmetry on the continuum theory

First of all, I review violation of chiral symmetry at the classical level. Fermion actions can be written down as

$$S_F = \int d^4x \overline{\psi} \left[\not{D} + m \right] \psi. \tag{4.1}$$

Then the chiral transformation is defined as follows

$$\begin{aligned} \psi &\to e^{i\theta\gamma_5}\psi, \\ \overline{\psi} &\to \overline{\psi} e^{i\theta\gamma_5}. \end{aligned} \tag{4.2}$$

At $m = 0$, this action maintains the chiral symmetry. A non-zero mass term breaks the symmetry which is expressed by

$$\{D, \gamma_5\} \neq 0 \tag{4.3}$$

If there is the chiral symmetry,

$$\{D, \gamma_5\} = 0. \tag{4.4}$$

However this symmetry breaks down in a perturbative theory which is well-known the Adler-Bell-Jackiw anomaly. Then the conservation law of the chiral symmetry become

$$\partial^\mu A_\mu = \frac{g^2}{32\pi^2}\varepsilon^{\mu\nu\alpha\beta}F_{\mu\nu}F_{\alpha\beta}. \tag{4.5}$$

The right hand side of Eq. (4.5) is called the chiral anomaly and is strongly related to zero modes of the Dirac-operator which is well-known Atiyah-Singer index theorem [36].

4.2 Ginsparg-Wilson relation

Keeping the chiral symmetry on the lattice is difficult from the Nielsen-Ninomiya No-Go theorem. For instance, the Wilson term have to be added to naive lattice fermion in order to decouple doublers and the Wilson term explicitly breaks the chiral symmetry as $\{D, \gamma_5\} = \mathcal{O}(a)$. The Ginsparg-Wilson relation has derived through spin block transformations from chiral symmetric continuum theory.

$$\{D, \gamma_5\} = 2aDR\gamma_5 D \tag{4.6}$$

Here let us review derivation of the Ginsparg-Wilson relation [34]. We consider a chiral symmetric action $S_I\left(\phi, \bar{\phi}\right)$, that is

$$S_I\left(e^{i\varepsilon\gamma_5}\phi, \bar{\phi}e^{i\varepsilon\gamma_5}\right) = S_I\left(\phi, \bar{\phi}\right), \tag{4.7}$$

where $\phi, \bar{\phi}$ are fermion fields. Then we define a new fermion action $S\left(\psi, \bar{\psi}\right)$ by the block-spin transformation

$$e^{-S\left(\psi,\bar{\psi}\right)} = \int \mathcal{D}\phi\mathcal{D}\bar{\phi} exp\left[-\left(\bar{\psi}_n - \bar{\phi}_n\right)\alpha_{nm}\left(\psi_m - \phi_m\right) - S_I\left(\phi, \bar{\phi}\right)\right]. \tag{4.8}$$

The ϕ and $\bar{\phi}$ in the right hand side of the Eq. 22 are block variables. The matrix α may take some gamma matrices, but we focus on the form $\alpha \propto 1$ which corresponds to the chiral variant term $m\bar{\psi}\psi$. Here we perform the chiral transformation in Eq. 4.8

$$\begin{aligned} e^{-S\left(e^{i\varepsilon\gamma_5}\psi, \bar{\psi}e^{i\varepsilon\gamma_5}\right)} &= \int \mathcal{D}\phi\mathcal{D}\bar{\phi} exp\left[-\left(\bar{\psi}_n e^{i\varepsilon\gamma_5} - \bar{\phi}_n\right)\alpha_{nm}\left(e^{i\varepsilon\gamma_5}\psi_m - \phi_m\right) - S_I\left(\phi, \bar{\phi}\right)\right]. \\ &= \int \mathcal{D}\phi\mathcal{D}\bar{\phi} exp\left[-\left(\bar{\psi}_n e^{i\varepsilon\gamma_5} - \bar{\phi}_n e^{i\varepsilon\gamma_5}\right)\alpha_{nm}\left(e^{i\varepsilon\gamma_5}\psi_m - e^{i\varepsilon\gamma_5}\phi_m\right) - S_I\left(e^{i\varepsilon\gamma_5}\phi, e^{i\varepsilon\gamma_5}\bar{\phi}\right)\right] \\ &= \int \mathcal{D}\phi\mathcal{D}\bar{\phi} exp\left[-\left(\bar{\psi}_n - \bar{\phi}_n\right)e^{i\varepsilon\gamma_5}\alpha_{nm}e^{i\varepsilon\gamma_5}\left(\psi_m - \phi_m\right) - S_I\left(\phi, \bar{\phi}\right)\right], \end{aligned} \tag{4.9}$$

where if one assume that $S\left(\psi, \bar{\psi}\right) = \bar{\psi}D\psi$, we expand the left hand side

$$\begin{aligned} exp\left[-\bar{\psi}e^{i\varepsilon\gamma_5}De^{i\varepsilon\gamma_5}\psi\right] &\simeq exp\left[-\bar{\psi}\left(D + i\varepsilon\{D, \gamma_5\}\right)\psi\right] \\ &\simeq exp\left[-\bar{\psi}D\psi\right]\left(1 - i\varepsilon\bar{\psi}\{D, \gamma_5\}\psi\right) \end{aligned} \tag{4.10}$$

and for the right hand side

$$
\begin{aligned}
&\simeq \int \mathcal{D}\phi\mathcal{D}\bar{\phi} exp\left[-\left(\bar{\psi}_n-\bar{\phi}_n\right)\left(\alpha_{nm}+i\varepsilon\{\alpha_{nm},\gamma_5\}\right)\left(\psi_m-\phi_m\right)-S_I\left(\phi,\bar{\phi}\right)\right] \\
&= \int \mathcal{D}\phi\mathcal{D}\bar{\phi} exp\left[-\left(\bar{\psi}_n-\bar{\phi}_n\right)\alpha_{nm}\left(\psi_m-\phi_m\right)-S_I\left(\phi,\bar{\phi}\right)-i\varepsilon\left(\bar{\psi}_n-\bar{\phi}_n\right)\{\alpha_{nm},\gamma_5\}\left(\psi_m-\phi_m\right)\right] \\
&\simeq \int \mathcal{D}\phi\mathcal{D}\bar{\phi}\left(1-i\varepsilon\left(\bar{\psi}_n-\bar{\phi}_n\right)\{\alpha_{nm},\gamma_5\}\left(\psi_m-\phi_m\right)\right) exp\left[-\left(\bar{\psi}_n-\bar{\phi}_n\right)\alpha_{nm}\left(\psi_m-\phi_m\right)-S_I\left(\phi,\bar{\phi}\right)\right] \\
&= \left[1-i\varepsilon\frac{\delta}{\delta\psi}\alpha^{-1}\{\alpha,\gamma_5\}\alpha^{-1}\frac{\delta}{\delta\bar{\psi}}\right]\int \mathcal{D}\phi\mathcal{D}\bar{\phi} exp\left[-\left(\bar{\psi}-\bar{\phi}\right)\alpha\left(\psi-\phi\right)-S_I\left(\phi,\bar{\phi}\right)\right]. \qquad (4.11)
\end{aligned}
$$

Then the transformation in the last line is not trivial. To check this, we perform

$$
\begin{aligned}
&\frac{\delta}{\delta\psi}\alpha^{-1}\{\alpha,\gamma_5\}\alpha^{-1}\frac{\delta}{\delta\bar{\psi}}\int \mathcal{D}\phi\mathcal{D}\bar{\phi} exp\left[-\left(\bar{\psi}-\bar{\phi}\right)\alpha\left(\psi-\phi\right)-S_I\left(\phi,\bar{\phi}\right)\right] \\
&= \frac{\delta}{\delta\psi}\alpha^{-1}\{\alpha,\gamma_5\}\alpha^{-1}\int \mathcal{D}\phi\mathcal{D}\bar{\phi}\left[-\alpha+\alpha\left(\psi-\phi\right)\right] exp\left[-\left(\bar{\psi}-\bar{\phi}\right)\alpha\left(\psi-\phi\right)-S_I\left(\phi,\bar{\phi}\right)\right] \\
&= \int \mathcal{D}\phi\mathcal{D}\bar{\phi}\left[-Tr\left[\alpha^{-1}\{\alpha,\gamma_5\}\right]+\left(\bar{\psi}-\bar{\phi}\right)\{\alpha,\gamma_5\}\left(\psi-\phi\right)\right] exp\left[-\left(\bar{\psi}-\bar{\phi}\right)\alpha\left(\psi-\phi\right)-S_I\left(\phi,\bar{\phi}\right)\right], \qquad (4.12)
\end{aligned}
$$

where the first term vanishes due to

$$
Tr\left[\alpha^{-1}\{\alpha,\gamma_5\}\right]=2Tr\left[\gamma_5\right]=0. \qquad (4.13)
$$

Furthermore one can immediately notice that

$$
\alpha^{-1}\{\alpha,\gamma_5\}\alpha^{-1}=\{\gamma_5,\alpha^{-1}\} \qquad (4.14)
$$

Therefore we could prove that

$$
\begin{aligned}
&\int \mathcal{D}\phi\mathcal{D}\bar{\phi}\left[\left(\bar{\psi}-\bar{\phi}\right)\{\alpha,\gamma_5\}\left(\psi-\phi\right)\right] exp\left[-\left(\bar{\psi}-\bar{\phi}\right)\alpha\left(\psi-\phi\right)-S_I\left(\phi,\bar{\phi}\right)\right] \\
&\qquad = \frac{\delta}{\delta\psi}\alpha^{-1}\{\alpha,\gamma_5\}\alpha^{-1}\frac{\delta}{\delta\bar{\psi}}e^{-S\left(\psi,\bar{\psi}\right)}. \qquad (4.15)
\end{aligned}
$$

Then if we compare the $O\left(\varepsilon\right)$ term in Eq. (4.9), we obtain a following relation

$$
e^{-S\left(\psi,\bar{\psi}\right)}\bar{\psi}\{D,\gamma_5\}\psi=\frac{\delta}{\delta\psi}\{\gamma_5,\alpha^{-1}\}\frac{\delta}{\delta\bar{\psi}}e^{-S\left(\psi,\bar{\psi}\right)}. \qquad (4.16)
$$

By using a following formula

$$
D\psi e^{-\bar{\psi}D\psi}=-\frac{\delta}{\delta\bar{\psi}}e^{-\bar{\psi}D\psi}, \qquad (4.17)
$$

$$
\bar{\psi}De^{-\bar{\psi}D\psi}=\frac{\delta}{\delta\psi}e^{-\bar{\psi}D\psi}, \qquad (4.18)
$$

we found that

$$\begin{aligned} e^{-S(\psi,\bar{\psi})}\bar{\psi}\{D,\gamma_5\}\psi &= -\frac{\delta}{\delta\psi}\{\gamma_5,\alpha^{-1}\}D\psi e^{-S(\psi,\bar{\psi})} \\ &= \left(-Tr\left[\{\gamma_5,\alpha^{-1}\}D\right] + \bar{\psi}D\{\gamma_5,\alpha^{-1}\}D\psi\right) e^{-S(\psi,\bar{\psi})} \end{aligned} \tag{4.19}$$

In general the term $Tr\left[\{\gamma_5,\alpha^{-1}\}D\right]$ remains, for instance in the case of $D \propto \gamma_5$. However now we assume that $D \propto \gamma_\mu$ and recall $\alpha^{-1} \propto 1$. Then $Tr\left[\{\gamma_5,\alpha^{-1}\}D\right] = 0$ and thus we obtain finally a relation

$$\{D,\gamma_5\} = 2D\gamma_5\alpha^{-1}D, \tag{4.20}$$

which is called Ginsparg-Wilson relation. Here α^{-1} is often represented as $R = \alpha^{-1}$ and thus one sees the usual expression of the Ginsparg-Wilson relations. Note that generally one can not ignore the term $Tr\left[\{\gamma_5,\alpha^{-1}\}D\right]$, but if we restrict to a non-singlet transformation in $\psi \to e^{i\varepsilon^a\tau^a}\psi$, the term vanishes due to $tr\left[\tau^a\right] = 0$ with $a \neq 0$.

4.3 Neuberger's overlap fermion

The overlap fermions is introduced by Neuberger as

$$D = \frac{1}{a}\left[1 + \frac{A}{\sqrt{A^\dagger A}}\right], \tag{4.21}$$

where $A = -M_0 + aD_W$ and D_W is the massless Wilson Dirac-operator. Here A is often called a kernel o the overlap Dirac-operator. This is one of solution for the Ginsparg-Wilson relation $\{D,\gamma_5\} = aD\gamma_5 D$. To check this, we define a quantity

$$V \equiv \frac{A}{\sqrt{A^\dagger A}}, \tag{4.22}$$

where V satisfies following relations

$$\gamma_5 V \gamma_5 = V^\dagger, \tag{4.23}$$

which is often called the gamma5 hermiticity. Then we can transform

$$\begin{aligned} \gamma_5\frac{1}{aD}\gamma_5 &= \gamma_5\left(1+V\right)^{-1}\gamma_5 \\ &= \gamma_5\left(\sum_n a_n V^n\right)\gamma_5 \\ &= \sum_n a_n\left(\gamma_5 V\gamma_5\right)^n \\ &= \sum_n a_n\left(V^\dagger\right)^n \\ &= \left(1+V^\dagger\right)^{-1} \\ &= \frac{V}{V+1} \\ &= 1 - \frac{1}{aD}. \end{aligned} \tag{4.24}$$

If we use this relation, one can obtains

$$\begin{aligned} \gamma_5 D^{-1}\gamma_5 &= a - D^{-1} \\ \gamma_5 D^{-1} + D^{-1}\gamma_5 &= a\gamma_5 \end{aligned} \tag{4.25}$$

also it can be read as the Ginsparg-Wilson

$$\{D, \gamma_5\} = aD\gamma_5 D. \tag{4.26}$$

Also it may be convenient to write the overlap fermion by using the hermitian Wilson Dirac-operator $H_W = \gamma_5 D_W$ as follows

$$\begin{aligned} D &= \frac{1}{a}\left[1 + \gamma_5 \frac{H_W}{\sqrt{H_W^2}}\right] \\ &= \frac{1}{a}\left[1 + \gamma_5 \mathrm{sgn}\left(H_W\right)\right], \end{aligned} \tag{4.27}$$

where $\mathrm{sgn}\left(x\right)$ is the sign function of a variable x. As we see, the overlap Dirac-operator includes the propagator of the Wilson Dirac-operator. Thus a implementation of the overlap Dirac-operator is generally intensive from the viewpoint of numerical costs. Moreover if near zeros of the H_W is harmful for the locality of the overlap Dirac-operator, but it has been discussed in Refs. [37, 38, 39, 40, 41].

4.4 Chiral symmetry and discretization errors

I would like to review a relation between the chiral symmetry and discretization errors. An open question is that why we need to impose the chiral symmetry for heavy quarks. Here I follow the discussion of Ref [9] in order to reveal a relation between the chiral symmetry and discretization error. For convenience, we define the following mass matrix

$$M = \begin{pmatrix} m_1 & 0 & \cdots & 0 \\ 0 & m_2 & \ddots & \vdots \\ \vdots & \ddots & \ddots & 0 \\ 0 & \cdots & 0 & m_N \end{pmatrix} \tag{4.28}$$

on the N_f flavor space with spurious filed transformations

$$\mathcal{M} \to V_R \mathcal{M} V_L^\dagger \tag{4.29}$$

$$\mathcal{M}^\dagger \to V_L \mathcal{M}^\dagger V_R^\dagger \tag{4.30}$$

under $SU(N_f)_L \times SU(N_f)_R$ symmetry. Here $.V_L$ and V_R denotes respectively elements of the fundamental representation. Quark fields are expressed as

$$q_L = P_- q, \tag{4.31}$$

$$\bar{q}_L = \bar{q} P_+, \tag{4.32}$$

$$q_R = P_+ q, \tag{4.33}$$

$$\bar{q}_R = \bar{q}_R P_-, \tag{4.34}$$

where $P_\pm = (1 \pm \gamma_5)/2$ and are transformed by

$$q_L \to V_L q_L, \tag{4.35}$$

$$\bar{q}_L \to \bar{q}_L V_L^\dagger, \tag{4.36}$$

$$q_R \to V_R q_R, \tag{4.37}$$

$$\bar{q}_R \to \bar{q}_R V_R^\dagger, \tag{4.38}$$

under the symmetry. Here we choose $\mathcal{M} = \mathcal{M}^\dagger = M$ for the spurious field transformations. We observe that allowing operator are

$$M^{2n} \cdot \left(SU\left(N_f\right)_L \times SU\left(N_f\right)_R \text{invariant operator} \right). \tag{4.39}$$

In this context, for instance following operators are allowed

$$\bar{q} M^{2n+1} q, \tag{4.40}$$

$$\bar{q} M^{2n} \gamma_\mu D_\mu q, \tag{4.41}$$

$$\bar{q} M^{2n+1} \sigma_{\mu\nu} F_{\mu\nu} q, \tag{4.42}$$

however operators

$$\bar{q} M^{2n} q, \tag{4.43}$$

$$\bar{q} M^{2n+1} \gamma_\mu D_\mu q, \tag{4.44}$$

$$\bar{q} M^{2n} \sigma_{\mu\nu} F_{\mu\nu} q, \tag{4.45}$$

are forbidden with $n \geq 0$. Here we show this mechanism with focus on the case of $\bar{q}M^{2n+1}q$ and $\bar{q}M^{2n}q$.

$$\begin{aligned}\bar{q}M^{2n+1}q &= \left(\bar{q}_L + \bar{q}_R\right) M^{2n+1} \left(q_L + q_R\right) \\ &\to \left(\bar{q}_L V_L^\dagger + \bar{q}_R V_R^\dagger\right) M^{2n+1} \left(V_L q_L + V_R q_R\right) \\ &= \bar{q}_L V_L^\dagger M^{2n+1} V_L q_L + \bar{q}_R V_R^\dagger M^{2n+1} V_L q_L \\ &\quad + \bar{q}_L V_L^\dagger M^{2n+1} V_R q_R + \bar{q}_R V_R^\dagger M^{2n+1} V_R q_R V_R q_R,\end{aligned}$$

where we still do not perform the spurious field transformations of M. If we consider this transformation, above terms are invariant as

$$\begin{aligned}\bar{q}_L V_L^\dagger M^{2n+1} V_L q_L &\to \bar{q}_L V_L^\dagger V_L M V_R^\dagger V_R M V_L^\dagger \cdots V_R M V_L^\dagger V_L q_L \\ &= \bar{q}_L M^{2n+1} q_L\end{aligned} \tag{4.46}$$

$$\begin{aligned}\bar{q}_R V_R^\dagger M^{2n+1} V_L q_L &\to \bar{q}_R V_R^\dagger V_R M V_L^\dagger \cdots V_R M V_L^\dagger V_L q_L \\ &= \bar{q}_R M^{2n+1} q_L\end{aligned} \tag{4.47}$$

In a similar way, other two terms also can be proved as above transformations. Thus we observe that the operator $\bar{q}M^{2n+1}q$ is invariant under the transformations. At this point the essential properties is that odd powers of M. By contrast, we think of the transformation of the $\bar{q}M^{2n}q$. Firstly a following term is invariant the under current transformations

$$\begin{aligned}\bar{q}_L V_L^\dagger M^{2n} V_L q_L &\to \bar{q}_L V_L^\dagger V_L M V_R^\dagger V_R M V_L^\dagger \cdots V_L q_L \\ &= \bar{q}_L M^{2n} q_L,\end{aligned} \tag{4.48}$$

however following kind of terms can not be invariant.

$$\begin{aligned}\bar{q}_R V_R^\dagger M^{2n} V_L q_L &\to \bar{q}_R V_R^\dagger V_R M V_L^\dagger V_L M V_R^\dagger \cdots V_L M V_R^\dagger V_L q_L \\ &= \bar{q}_R M^{2n} V_R^\dagger V_L q_L\end{aligned} \tag{4.49}$$

Thus we see that $\bar{q}M^{2n}q$ is not invariant and such terms is forbidden in the chiral symmetric action. In this way, the chiral symmetry can suppress some parts of discretization errors and it would be an advantage of the chiral symmetric fermion in heavy quark physics.

4.5 Standard domain-wall fermion

Conventional domain-wall fermions are defined on the 5 dimensional space time with the Wilson Dirac operator $D_W\left(-M\right)$. Then the Wilson Dirac operator has a large negative mass which is called a domain-wall height. In this section and next section, I will follow discussions of Ref. [42]. The domain-wall fermion action is defined by

$$S_{DW} = \sum_x \bar{\psi} D^5_{DW} \psi, \tag{4.50}$$

where the 5-dimensional Dirac operator is given as follows

$$D^5_{DW} = \begin{pmatrix} D_{||} & -P_- & 0 & \cdots & 0 & mP_+ \\ -P_+ & D_{||} & \ddots & \ddots & \cdots & 0 \\ 0 & \ddots & D_{||} & \ddots & \ddots & \vdots \\ \vdots & \ddots & \ddots & \ddots & \ddots & 0 \\ 0 & \cdots & 0 & -P_+ & D_{||} & -P_- \\ mP_- & 0 & \cdots & \cdots & -P_+ & D_{||} \end{pmatrix}. \tag{4.51}$$

Here $D_{||} = 1 + D_W(-M)$ and $D_\perp = P_- \delta_{s+1,s'} + P_+ \delta_{s-1,s'}$. The chiral projection is defined as $P_\pm = (1 \pm \gamma_5)/2$. Then physical fields in 4D can be defined as

$$q = \left(\mathcal{P}^{-1}\psi\right)_1, \tag{4.52}$$

$$\bar{q} = \left(\bar{\psi} R_5 \mathcal{P}\right)_1, \tag{4.53}$$

where $(\cdots)_1$ represents taking the first component in 5-dimension and $\mathcal{P}, \mathcal{P}^{-1}, R$ are respectively defined as follows

$$\mathcal{P} = \begin{pmatrix} P_- & P_+ & 0 & \cdots & \cdots & 0 \\ 0 & P_- & P_+ & \ddots & \ddots & \vdots \\ \vdots & \ddots & P_- & P_+ & \ddots & \vdots \\ \vdots & \ddots & \ddots & P_- & P_+ & 0 \\ 0 & \ddots & \ddots & \ddots & \ddots & P_+ \\ P_+ & 0 & \cdots & \cdots & 0 & P_- \end{pmatrix}, \tag{4.54}$$

$$\mathcal{P}^{-1} = \begin{pmatrix} P_- & 0 & \cdots & \cdots & 0 & P_+ \\ P_+ & P_- & \ddots & \ddots & \ddots & 0 \\ 0 & \ddots & P_- & \ddots & \ddots & \vdots \\ \vdots & \ddots & \ddots & P_- & \ddots & \vdots \\ \vdots & \ddots & \ddots & \ddots & \ddots & 0 \\ 0 & \cdots & \cdots & 0 & P_+ & P_- \end{pmatrix}, \tag{4.55}$$

$$R_5 = \begin{pmatrix} 0 & 0 & \cdots & \cdots & 0 & 1 \\ 0 & 0 & \cdots & \cdots & 1 & 0 \\ \vdots & \vdots & \ddots & \ddots & \vdots & \vdots \\ \vdots & \vdots & \ddots & \ddots & \vdots & \vdots \\ 0 & 1 & \cdots & \cdots & 0 & 0 \\ 1 & 0 & \cdots & \cdots & 0 & 0 \end{pmatrix}. \tag{4.56}$$

Then if we perform a basis transformation

$$\chi = \mathcal{P}^{-1}\psi, \tag{4.57}$$

$$\bar{\chi} = \bar{\psi}\gamma_5 Q_-, \tag{4.58}$$

the standard domain-wall action can be written

$$S_{DW} = \sum \bar{\psi} D_{DW} \psi = \sum \left(\bar{\psi}\gamma_5 Q_-\right)\left(Q_-^{-1}\gamma_5 D_{DW}^5 \mathcal{P}\right)\left(\mathcal{P}^{-1}\psi\right) = \bar{\chi} D_\chi^5 \chi, \tag{4.59}$$

where

$$Q_- = H_{||}P_- - P_+ = \frac{1}{2}\gamma_5\left[D_W - (2 + D_W)\,\gamma_5\right] \tag{4.60}$$

and we may define

$$Q_+ = H_{||}P_+ + P_- = \frac{1}{2}\gamma_5\left[D_W + (2 + D_W)\,\gamma_5\right] \tag{4.61}$$

$$T^{-1} = -Q_-^{-1}Q_+ = \frac{1 + H_T}{1 - H_T} \tag{4.62}$$

Here the Shamir kernel H_T is written as

$$H_T = \gamma_5 \frac{D_W}{2 + D_W} \tag{4.63}$$

Then the transformed Dirac-operator D_χ^5 can be expressed

$$
\begin{aligned}
D_\chi^5 &= Q_-^{-1}\gamma_5 D_{DW}^5 \mathcal{P} \\
&= \begin{pmatrix}
P_- - mP_+ & -T^{-1} & 0 & \cdots & \cdots & 0 \\
0 & 1 & -T^{-1} & \ddots & \ddots & \vdots \\
\vdots & 0 & 1 & -T^{-1} & \ddots & \vdots \\
\vdots & \vdots & \ddots & \ddots & \ddots & 0 \\
\vdots & \vdots & \ddots & \ddots & 1 & -T^{-1} \\
-T^{-1}\left(P_+ - mP_-\right) & 0 & \cdots & \cdots & 0 & 1
\end{pmatrix} \qquad (4.64) \\
&\equiv \begin{pmatrix} D & C \\ B & A \end{pmatrix}. \qquad (4.65)
\end{aligned}
$$

To be specific, D, C, B and A are respectively

$$D_{1\times 1} = P_- - mP_+, \qquad (4.66)$$

$$C_{1\times(N_s-1)} = \begin{pmatrix} -T^{-1} & 0 & \cdots & \cdots & 0 \end{pmatrix}, \qquad (4.67)$$

$$B_{(N_s-1)\times 1} = \begin{pmatrix} 0 \\ \vdots \\ \vdots \\ 0 \\ -T^{-1}\left(P_+ - mP_-\right) \end{pmatrix}, \qquad (4.68)$$

$$A_{(N_s-1)\times(N_s-1)} = \begin{pmatrix}
1 & -T^{-1} & 0 & \cdots & 0 \\
0 & 1 & -T^{-1} & \ddots & \vdots \\
\vdots & \ddots & \ddots & \ddots & 0 \\
\vdots & \ddots & \ddots & \ddots & -T^{-1} \\
0 & \cdots & \cdots & 0 & 1
\end{pmatrix}, \qquad (4.69)$$

Then we perform the block diagonalization of the D_χ^5 by using the UDL decomposition

$$\begin{pmatrix} D & C \\ B & A \end{pmatrix} = \begin{pmatrix} 1 & CA^{-1} \\ 0 & 1 \end{pmatrix} \begin{pmatrix} S_\chi & 0 \\ 0 & A \end{pmatrix} \begin{pmatrix} 1 & 0 \\ A^{-1}B & 1 \end{pmatrix}. \qquad (4.70)$$

with $S_\chi = D - CA^{-1}B$. We note that $det\,(A) = 1$. The inverse matrix of A can be calculated easily as

$$A^{-1} = \begin{pmatrix} 1 & -T^{-1} & 0 & \cdots & 0 \\ 0 & 1 & -T^{-1} & \ddots & \vdots \\ \vdots & \ddots & \ddots & \ddots & 0 \\ \vdots & \ddots & \ddots & 1 & -T^{-1} \\ 0 & \cdots & \cdots & 0 & 1 \end{pmatrix}^{-1}$$
$$= \begin{pmatrix} 1 & T^{-1} & T^{-2} & \cdots & T^{-L_s+2} \\ 0 & 1 & T^{-1} & \ddots & T^{-Ls+3} \\ \vdots & \ddots & \ddots & \ddots & \vdots \\ \vdots & \ddots & \ddots & 1 & T^{-1} \\ 0 & \cdots & \cdots & 0 & 1 \end{pmatrix}$$

Then one can write down $S_\chi\,(m)$ as follows

$$\begin{aligned} S_\chi\,(m) &= (P_- - mP_+) - T^{-L_s}\,(P_+ - mP_-) \\ &= -\left(T^{-L_s}+1\right)\gamma_5\left[\frac{1+m}{2} + \frac{1-m}{2}\gamma_5\frac{T^{-L_s}-1}{T^{-L_s}+1}\right], \end{aligned} \tag{4.71}$$

also 4-dimensional effective operator can be written as

$$\begin{aligned} D^4 &= S_\chi^{-1}\,(m=1)\,S_\chi\,(m) \\ &= \frac{1+m}{2} + \frac{1-m}{2}\gamma_5\frac{T^{-L_s}-1}{T^{-L_s}+1} \end{aligned}$$

with $S_\chi^{-1}\,(m=1) = -\left(T^{-L_s}+1\right)\gamma_5$ which corresponds to the Pauli-Villars field in the domain-wall fermion formalism. Now let me describe the 4D effective operator in 5D space. The 4D effective operator can be expressed by

$$D^4 = S_\chi^{-1}\,(m=1)\,S_\chi\,(m) = \left[\mathcal{P}^{-1}\left(D_{DW}^5\,(m=1)\right)^{-1} D_{DW}\,(m)\,\mathcal{P}\right]_{11}.$$

In order to confirm this relation, we start from $\left(D_{DW}^5\,(m=1)\right)^{-1} D_{DW}\,(m)$

$$\begin{aligned}\left(D^5_{DW}(m=1)\right)^{-1} D_{DW}(m) &= \left(\gamma_5 Q_- D^5_\chi(m=1)\,\mathcal{P}^{-1}\right)^{-1}\gamma_5 Q_- D^5_\chi(m)\,\mathcal{P}^{-1}\\ &= \mathcal{P}\left(D^5_\chi(m=1)\right)^{-1} D^5_\chi(m)\,\mathcal{P}^{-1}\\ &= \mathcal{P}\left[\begin{pmatrix}1 & CA^{-1}\\ 0 & 1\end{pmatrix}\begin{pmatrix}S_\chi(m=1) & 0\\ 0 & A\end{pmatrix}\begin{pmatrix}1 & 0\\ A^{-1}B & 1\end{pmatrix}\right]^{-1}\\ &\quad\left[\begin{pmatrix}1 & CA^{-1}\\ 0 & 1\end{pmatrix}\begin{pmatrix}S_\chi(m) & 0\\ 0 & A\end{pmatrix}\begin{pmatrix}1 & 0\\ A^{-1}B & 1\end{pmatrix}\right]\mathcal{P}^{-1}\end{aligned}$$

$$\begin{aligned}&= \mathcal{P}\begin{pmatrix}1 & 0\\ A^{-1}B & 1\end{pmatrix}^{-1}\begin{pmatrix}S_\chi^{-1}(m=1) & 0\\ 0 & A^{-1}\end{pmatrix}\\ &\quad\begin{pmatrix}S_\chi(m) & 0\\ 0 & A\end{pmatrix}\begin{pmatrix}1 & 0\\ A^{-1}B & 1\end{pmatrix}\mathcal{P}^{-1}\\ &= \mathcal{P}\begin{pmatrix}1 & 0\\ A^{-1}B & 1\end{pmatrix}^{-1}\begin{pmatrix}S_\chi^{-1}(m=1)\,S_\chi(m) & 0\\ 0 & 1\end{pmatrix}\begin{pmatrix}1 & 0\\ A^{-1}B & 1\end{pmatrix}\mathcal{P}^{-1}\\ &= \mathcal{P}\begin{pmatrix}1 & 0\\ A^{-1}B & 1\end{pmatrix}^{-1}\begin{pmatrix}S_\chi^{-1}(m=1)\,S_\chi(m) & 0\\ A^{-1}B & 1\end{pmatrix}\mathcal{P}^{-1}\end{aligned}\tag{4.72}$$

Therefore we obtain a following relation

$$\mathcal{P}^{-1}\left(D^5_{DW}(m=1)\right)^{-1} D^5_{DW}(m)\,\mathcal{P} = \begin{pmatrix}S_\chi^{-1}(m=1)\,S_\chi(m) & 0\\ A^{-1}B\left(1-S_\chi^{-1}(m=1)\,S_\chi(m)\right) & 1\end{pmatrix},\tag{4.73}$$

and define a 4D effective operator by taking the $(1,1)$ component of the this relation

$$\left[\mathcal{P}^{-1}\left(D^5_{DW}(m=1)\right)^{-1} D^5_{DW}(m)\,\mathcal{P}\right]_{11} = S_\chi^{-1}(m=1)\,S_\chi(m) = D^4.\tag{4.74}$$

Then the propagator of the 4D effective operator can be found as

$$\begin{aligned}(1-m)^{-1}\left[\left(D^4\right)^{-1}-1\right] &= (1-m)^{-1}\left[\mathcal{P}^{-1}\left(D^5_{DW}(m)\right)^{-1} D^5_{DW}(m=1)\,\mathcal{P}\right]_{11} - 1\\ &= (1-m)^{-1}\left[\mathcal{P}^{-1}\left(D^5_{DW}(m)\right)^{-1}\left(D^5_{DW}(m=1)-D^5_{DW}(m)\right)\mathcal{P}\right]_{11}.\end{aligned}\tag{4.75}$$

By the subtraction in the right-hand side, almost parts vanish and remained parts are

$$\left(D^5_{DW}(m=1) - D^5_{DW}(m)\right)\mathcal{P} = \begin{pmatrix} 0 & \cdots & \cdots & \cdots & 0 & (1-m)\,P_+ \\ \vdots & \ddots & \ddots & \ddots & \ddots & 0 \\ \vdots & \ddots & \ddots & \ddots & \ddots & \vdots \\ \vdots & \ddots & \ddots & \ddots & \ddots & \vdots \\ 0 & \ddots & \ddots & \ddots & \ddots & \vdots \\ (1-m)\,P_- & 0 & \cdots & \cdots & \cdots & 0 \end{pmatrix} \times \begin{pmatrix} P_- & P_+ & 0 & \cdots & \cdots & 0 \\ 0 & P_- & P_+ & 0 & \ddots & \vdots \\ \vdots & \ddots & \ddots & \ddots & \ddots & \vdots \\ \vdots & \ddots & \ddots & \ddots & \ddots & 0 \\ 0 & \ddots & \ddots & \ddots & \ddots & P_+ \\ P_+ & 0 & \cdots & \cdots & 0 & P_- \end{pmatrix}$$

$$= (1-m) \begin{pmatrix} P+ & \cdots & \cdots & \cdots & 0 & 0 \\ \vdots & \ddots & \ddots & \ddots & \ddots & 0 \\ \vdots & \ddots & \ddots & \ddots & \ddots & \vdots \\ \vdots & \ddots & \ddots & \ddots & \ddots & \vdots \\ 0 & \ddots & \ddots & \ddots & \ddots & \vdots \\ P_- & 0 & \cdots & \cdots & \cdots & 0 \end{pmatrix}. \tag{4.76}$$

On the other hand, $R_5\mathcal{P}$ is written as follows

$$R_5\mathcal{P} = \begin{pmatrix} P+ & 0 & \cdots & \cdots & 0 & P_- \\ 0 & \cdots & \cdots & 0 & P_- & 0 \\ \vdots & \iddots & \iddots & P_- & 0 & \vdots \\ \vdots & \iddots & \iddots & \iddots & \iddots & \vdots \\ 0 & \iddots & \iddots & \iddots & \iddots & \vdots \\ P_- & 0 & \cdots & \cdots & \cdots & 0 \end{pmatrix}. \tag{4.77}$$

Here we found that the first row is same among two expressions. If one takes into account the operation $[\cdots]_{11}$, we obtain a following relation

$$(1-m)^{-1}\left[\left(D^4\right)^{-1}-1\right]=\left[\mathcal{P}^{-1}\left(D^5_{DW}(m)\right)^{-1}R_5\mathcal{P}\right]_{11} \tag{4.78}$$

Thus the standard domain-wall fermions corresponds to Neuberger's overlap Dirac operator

$$D_N(m)=\frac{1+m}{2}+\frac{1-m}{2}\gamma_5 sgn(H_K), \tag{4.79}$$

with the kernel H_K being H_T and the sign function can be written as

$$sgn_{tanh}(H_T)=\frac{T^{-L_s}-1}{T^{-L_s}+1}=\frac{(1+H_T)^{L_s}-(1-H_T)^{Ls}}{(1+H_T)^{L_s}+(1-H_T)^{Ls}}. \tag{4.80}$$

Then if we consider a following quantity $x=tanh^{-1}(H_T)$, one can derive these relations

$$\begin{aligned} H_T=tanh(x)&=\frac{e^x-e^{-x}}{e^x+e^{-x}}\\ &=\frac{1-e^{-2x}}{1+e^{2x}}, \end{aligned} \tag{4.81}$$

$$\begin{aligned} \left(1+e^{2x}\right)H_T&=1-e^{-2x}\\ e^{-2x}&=\frac{1-H_T}{1+H_T}. \end{aligned} \tag{4.82}$$

By using above relations,

$$\begin{aligned} \frac{(1+H_T)^{L_s}-(1-H_T)^{Ls}}{(1+H_T)^{L_s}+(1-H_T)^{Ls}}&=\frac{1-e^{-2L_sx}}{1+e^{-2L_sx}}\\ &=\frac{e^{L_sx}-e^{-L_sx}}{e^{L_sx}+e^{-L_sx}}\\ &=tanh(L_sx)\\ &=tanh\left(L_s tanh^{-1}(H_T)\right) \end{aligned} \tag{4.83}$$

Thus we can write down an approximate sign function

$$sgn_{tanh}(H_T)=tanh\left(L_s tanh^{-1}(H_T)\right). \tag{4.84}$$

4.6 Generalized domain-wall fermions

At $L_s\to\infty$, the domain-wall fermion has the exact chiral symmetry in terms of the Ginsparg-Wilson relation. In other words, the domain-wall fermion can be identified with the overlap fermion in this limit. Here we generalize the conventional domain-wall fermion formulation for tuning of

violation the chiral symmetry. Let us define a generalized domain-wall fermion formulation as follows

$$S_{GDW} = \sum \bar{\psi} D^5_{GDW} \psi, \tag{4.85}$$

$$D^5_{GDW} = \begin{pmatrix} \tilde{D^1} & -P_- & 0 & \cdots & 0 & mP_+ \\ -P_+ & \tilde{D^2} & -P_- & 0 & \cdots & 0 \\ 0 & -P_+ & \tilde{D^3} & \ddots & \ddots & \vdots \\ \vdots & \ddots & \ddots & \ddots & \ddots & 0 \\ 0 & \ddots & \ddots & \ddots & \ddots & -P_- \\ mP_- & 0 & \cdots & 0 & -P_+ & \tilde{D^{L_s}} \end{pmatrix}, \tag{4.86}$$

where

$$\tilde{D^s} = \left(D^s_-\right)^{-1} D^s_+ \tag{4.87}$$

$$\tilde{D^s}_+ = a_s \left(1 + b_s D_W\left(-M\right)\right), \tag{4.88}$$

$$\tilde{D^s}_- = a_s \left(1 - c_s D_W\left(-M\right)\right). \tag{4.89}$$

with some constant a_s, b_s and c_s. By a change of the basis as the case of the standard domain-wall fermion, we obtain

$$S_{GDW} = \sum \bar{\psi} D_{GDW} \psi = \sum \left(\bar{\psi}\gamma_5 Q_-\right)\left(Q_-^{-1}\gamma_5 D^5_{GDW}\mathcal{P}\right)\left(\mathcal{P}^{-1}\psi\right) = \sum \bar{\chi} D^5_\chi \chi, \tag{4.90}$$

where D^5_χ and $Q\_$ are respectively

$$\begin{aligned} D^5_\chi &= Q_-^{-1}\gamma_5 D^5_{DW}\mathcal{P} \\ &= \begin{pmatrix} P_- - mP_+ & -T_1^{-1} & 0 & \cdots & \cdots & 0 \\ 0 & 1 & -T_2^{-1} & \ddots & \ddots & \vdots \\ \vdots & 0 & 1 & -T_3^{-1} & \ddots & \vdots \\ \vdots & \vdots & \ddots & \ddots & \ddots & 0 \\ \vdots & \vdots & \ddots & \ddots & 1 & -T_{L_s-1}^{-1} \\ -T^{-1}\left(P_+ - mP_-\right) & 0 & \cdots & \cdots & 0 & 1 \end{pmatrix}, \end{aligned}$$

$$Q_- = \begin{pmatrix} Q_-^1 & 0 & \cdots & \cdots & 0 \\ 0 & Q_-^2 & \ddots & \ddots & \vdots \\ \vdots & \ddots & Q_-^3 & \ddots & \vdots \\ \vdots & \ddots & \ddots & \ddots & 0 \\ 0 & \cdots & \cdots & 0 & Q_-^{L_s} \end{pmatrix} \tag{4.91}$$

with $Q_\pm^s = \tilde{D}^s P_\mp - P_\pm$. Then by doing Schur decomposition as Eq. (4.72), we obtain

$$\begin{aligned} S_\chi(m) &= (P_- - mP_+) - T_1^{-1}T_2^{-1}\cdots T_{L_s}^{-1}(P_+ - mP_-) \\ &= -\left(1 + T_1^{-1}T_2^{-1}T_3^{-1}\cdots T_{L_s}^{-1}\right)\gamma_5 \\ &\times \left[\frac{1+m}{2} + \frac{1-m}{2}\gamma_5 \frac{T_1^{-1}T_2^{-1}T_3^{-1}\cdots T_{L_s}^{-1} - 1}{T_1^{-1}T_2^{-1}T_3^{-1}\cdots T_{L_s}^{-1} + 1}\right], \end{aligned} \tag{4.92}$$

and

$$\begin{aligned} T_s^{-1} &= -\left(Q_-^s\right)^{-1} Q_+^s \\ &= -\left[1 - \gamma_5 \frac{(b_s + c_s) D_W}{2 + (b_s - c_s) D_W}\right]^{-1} \left[1 + \gamma_5 \frac{(b_s + c_s) D_W}{2 + (b_s - c_s) D_W}\right]. \end{aligned} \tag{4.93}$$

If we introduce new parameters

$$b_s + c_s = b\omega_s, \tag{4.94}$$

$$b_s - c_s = c, \tag{4.95}$$

one may define the Moebius kernel

$$H_M = \gamma_5 \frac{bD_W}{2 + cD_W}, \tag{4.96}$$

where the case of $b = c = 1$ corresponds to the Shamir kernel. Then the transfer matrix for the Moebius kernel can be written as

$$T_s^{-1} = \frac{1 + \omega_s H_M}{1 - \omega_s H_M}. \tag{4.97}$$

Then we may optimize b and c so that the violation of the Ginsparg-Wilson relation is smaller than the standard domain-wall fermion.

4.7 A relation between the domain-wall fermion and the overlap fermion

In this section, we review a relation between the domain-wall fermion and the overlap fermion in context of Ref. [43]. Here we start from the domain-wall fermion formalism on the 5-dimensional space time with finite N_s.

$$S_{DW} = \sum_{s,t}\sum_{n} \bar{\psi}_{n,s}\{\gamma_\mu \frac{1}{2}\left(\nabla_\mu + \nabla_\mu^\dagger\right)\delta_{s,t} + P_L M_{st} + P_R M_{st}^\dagger\}\psi_{n,t}, \tag{4.98}$$

where

$$a_5 M_{st} = [\delta_{s,t}B - \delta_{s,t+1}] \tag{4.99}$$

$$= \begin{pmatrix} B & -1 & 0 & \cdots & \cdots & 0 \\ 0 & B & -1 & \ddots & \ddots & \vdots \\ \vdots & 0 & \ddots & \ddots & \ddots & \vdots \\ \vdots & \ddots & \ddots & \ddots & \ddots & 0 \\ \vdots & \ddots & \ddots & \ddots & \ddots & -1 \\ 0 & \cdots & \cdots & \cdots & 0 & B \end{pmatrix} \tag{4.100}$$

and $B = 1 - a_5\left(\frac{a}{2}\nabla_\mu\nabla_\mu^\dagger + M_0/a\right)$. Here $a$and a_5 are respectively the lattice spacing of the 4 dimensions and the 5 dimension and the lattice derivatives are defined by

$$a\nabla_\mu\psi(x) = U_{n,\mu}\psi(n+\hat{\mu}) - \psi(x), \tag{4.101}$$

$$a\nabla_\mu^\dagger\psi(x) = \psi(n) - U_{n-\hat{\mu},\mu}^\dagger\psi(x-\hat{\mu}). \tag{4.102}$$

Here we aim to derive the 4D effective action by integrating the 5-dimension fields.

$$S^{\text{eff}} = a^4\sum_{n,m}\bar{q}_n D_{nm}^{\text{eff}} q_n \tag{4.103}$$

To do that, we introduce external fields J and $\bar{J}$ coupled to q and $\bar{q}$. For simplicity, we work in the specific case $L_s = 4$ and speculate a general form at L_s. In this case the fermion fields are written as

$$\bar{\Psi} = \left(\bar{\psi}_1^L, \bar{\psi}_1^R, \bar{\psi}_2^L, \bar{\psi}_2^R, \bar{\psi}_3^L, \bar{\psi}_3^R, \bar{\psi}_4^L, \bar{\psi}_4^R\right) \tag{4.104}$$

$$\Psi = \begin{pmatrix} \psi_1^L \\ \psi_1^R \\ \psi_2^L \\ \psi_2^R \\ \psi_3^L \\ \psi_3^R \\ \psi_4^L \\ \psi_4^R \end{pmatrix} \tag{4.105}$$

and the Dirac-operator is

$$a_5 D_{DW} = \begin{pmatrix} B & C & 0 & 0 & 0 & 0 & 0 & 0 \\ -C^\dagger & B & 0 & -1 & 0 & 0 & 0 & 0 \\ -1 & 0 & B & C & 0 & 0 & 0 & 0 \\ 0 & 0 & -C^\dagger & B & 0 & -1 & 0 & 0 \\ 0 & 0 & -1 & 0 & B & C & 0 & 0 \\ 0 & 0 & 0 & 0 & -C^\dagger & B & 0 & -1 \\ 0 & 0 & 0 & 0 & -1 & 0 & B & C \\ 0 & 0 & 0 & 0 & 0 & 0 & -C^\dagger & B \end{pmatrix}, \tag{4.106}$$

where the chiral representation of the gamma matrix are employed

$$\gamma_\mu = \begin{pmatrix} 0 & \sigma_\mu \\ \sigma_\mu^\dagger & 0 \end{pmatrix}, \tag{4.107}$$

$$\gamma_5 = \begin{pmatrix} 1 & 0 \\ 0 & -1 \end{pmatrix}, \tag{4.108}$$

and C and $C^\dagger$ and defined as $C = a_5\sigma_\mu \left(\nabla_\mu + \nabla_\mu^*\right)/2$ and $C^\dagger = -a_5\sigma_\mu \left(\nabla_\mu + \nabla_\mu^*\right)/2$. Here we may exchange the left-handed and the right-handed component for every ψ in Ψ

$$\begin{pmatrix} \psi_s^L \\ \psi_s^R \end{pmatrix} \Rightarrow \begin{pmatrix} \psi_s^R \\ \psi_s^L \end{pmatrix} = \begin{pmatrix} 0 & 1 \\ 1 & 0 \end{pmatrix} \begin{pmatrix} \psi_s^L \\ \psi_s^R \end{pmatrix}. \tag{4.109}$$

Then the Dirac-operator of the domain-wall fermion is changed as follows. Furthermore we move the first low down to the last row

$$a_5 D'_{DW} \Rightarrow a_5 D''_{DW} = \begin{pmatrix} B & -C^\dagger & -1 & 0 & 0 & 0 & 0 & 0 \\ 0 & -1 & C & B & 0 & 0 & 0 & 0 \\ 0 & 0 & B & -C^\dagger & -1 & 0 & 0 & 0 \\ 0 & 0 & 0 & -1 & C & B & 0 & 0 \\ 0 & 0 & 0 & 0 & B & -C^\dagger & -1 & 0 \\ 0 & 0 & 0 & 0 & 0 & -1 & C & B \\ 0 & 0 & 0 & 0 & 0 & 0 & B & -C^\dagger \\ C & B & 0 & 0 & 0 & 0 & 0 & 0 \end{pmatrix} \tag{4.110}$$

Consequently the components of the domain-wall fermion filed are transformed as

$$\begin{aligned} \bar{\Psi} \Rightarrow \bar{\Psi}'' &\equiv \begin{pmatrix} \bar{\psi}''^R_1 & \bar{\psi}''^L_1 & \bar{\psi}''^R_2 & \bar{\psi}''^L_2 & \bar{\psi}''^R_3 & \bar{\psi}''^L_3 & \bar{\psi}''^R_4 & \bar{\psi}''^L_4 \end{pmatrix} \\ &= \begin{pmatrix} \bar{\psi}^R_1 & \bar{\psi}^L_2 & \bar{\psi}^R_2 & \bar{\psi}^L_3 & \bar{\psi}^R_3 & \bar{\psi}^L_3 & \bar{\psi}^R_4 & \bar{\psi}^L_1 \end{pmatrix} \end{aligned} \tag{4.111}$$

$$\Psi \Rightarrow \Psi'' \equiv \begin{pmatrix} \psi''^L_1 \\ \psi''^R_1 \\ \psi''^L_2 \\ \psi''^R_2 \\ \psi''^L_3 \\ \psi''^R_3 \\ \psi''^L_4 \\ \psi''^R_1 \end{pmatrix} = \begin{pmatrix} \psi^L_1 \\ \psi^R_1 \\ \psi^L_2 \\ \psi^R_2 \\ \psi^L_3 \\ \psi^R_3 \\ \psi^L_4 \\ \psi^R_4 \end{pmatrix} \tag{4.112}$$

If we use new fields, 5D quark field can be written as

$$q_n = P_L \psi_{n,1} + P_R \psi_{n,N_s} = P_L \begin{pmatrix} 0 & 1 \\ 1 & 0 \end{pmatrix} \psi''_{n,1} + P_R \begin{pmatrix} 0 & 1 \\ 1 & 0 \end{pmatrix} \psi''_{n,N_s}, \tag{4.113}$$

$$\begin{aligned} \bar{q}_n &= \bar{\psi}_{n,1} P_R + \bar{\psi}_{n,N_s} P_L \\ &= \left(\bar{\psi}^L_{n,1}, \bar{\psi}^R_{n,1}\right) P_R + \left(\bar{\psi}^L_{n,1}, \bar{\psi}^R_{n,1}\right) P_L \\ &= \left(\bar{\psi}''^R_{n,N_s}, \bar{\psi}''^L_{n,1}\right) P_R + \left(\bar{\psi}''^R_{n,N_s-1}, \bar{\psi}''^L_{n,N_s}\right) P_L \\ &= \left(\bar{\psi}''^R_{n,N_s}, 0\right) + \left(0, \bar{\psi}''^L_{n,N_s}\right) \\ &= \left(\bar{\psi}''^R_{n,N_s}, \bar{\psi}''^L_{n,N_s}\right) \\ &= \bar{\psi}''_{n,N_s} \begin{pmatrix} 0 & 1 \\ 1 & 0 \end{pmatrix}, \end{aligned} \tag{4.114}$$

therefore the external field part becomes

$$a^4\sum_n\{\bar{J}_n\left[P_L\begin{pmatrix}0&1\\1&0\end{pmatrix}\psi''_{n,1}+P_R\begin{pmatrix}0&1\\1&0\end{pmatrix}\psi''_{n,N_s}\right]+\bar{\psi}_{n,N_s}\begin{pmatrix}0&1\\1&0\end{pmatrix}J_n\}. \tag{4.115}$$

In order to express the two by two blocks of D''_{DW}, we define following quantities

$$\alpha=\frac{1}{a_5}\begin{pmatrix}B&-C^\dagger\\0&-1\end{pmatrix}, \tag{4.116}$$

$$\beta=\frac{1}{a_5}\begin{pmatrix}-1&0\\C&B\end{pmatrix}, \tag{4.117}$$

$$\alpha_0=\frac{1}{a_5}\begin{pmatrix}B&-C^\dagger\\0&0\end{pmatrix}, \tag{4.118}$$

$$\beta_0=\frac{1}{a_5}\begin{pmatrix}0&0\\C&B\end{pmatrix}. \tag{4.119}$$

If one uses above definitions, we obtain

$$a_5D''_{DW}=\begin{pmatrix}\alpha&\beta&0&0\\0&\alpha&\beta&0\\0&0&\alpha&\beta\\\beta_0&0&0&\alpha_0\end{pmatrix}. \tag{4.120}$$

Now we have a following partition function

$$\begin{aligned}Z=\int\mathcal{D}\Psi''\mathcal{D}\bar{\Psi}''\mathcal{D}U exp[\bar{\Psi}D''_{DW}\Psi''\\+a^4\sum_n\{\bar{J}_n\left[P_L\begin{pmatrix}0&1\\1&0\end{pmatrix}\psi''_{n,1}+P_R\begin{pmatrix}0&1\\1&0\end{pmatrix}\psi''_{n,N_s}\right]+\bar{\psi}_{n,N_s}\begin{pmatrix}0&1\\1&0\end{pmatrix}J_n\}].\end{aligned} \tag{4.121}$$

Next we integrate out the coupled terms with the external fields. Firstly we perform integration for the $s=1$ part

$$\left[\bar{J}_nP_L\begin{pmatrix}0&1\\1&0\end{pmatrix}+\bar{\psi}''_{n,N_s}\beta_0\right]\psi''_{n,1}+\bar{\psi}''_{n,1}\alpha\psi''_{n,1}+\bar{\psi}''_{n,1}\beta\psi''_{n,2}. \tag{4.122}$$

Here we introduce abbreviations $X = \bar{J}P_L \begin{pmatrix} 0 & 1 \\ 1 & 0 \end{pmatrix} + \bar{\psi}_{N_s}\beta_0$ and $Y = \beta\psi''_2$ and then integration are implemented as

$$\begin{aligned}
&\int \mathcal{D}\psi''_1\mathcal{D}\bar{\psi}''_1 e^{X\psi''_1+\bar{\psi}''_1\alpha\psi''_1+\bar{\psi}''_1 Y} \\
&= det\,[\alpha]\int \mathcal{D}\eta\mathcal{D}\bar{\psi}''_1 e^{\left(X\alpha^{-1}+\bar{\psi}''_1\right)\eta+\bar{\psi}''_1 Y} \\
&= det\,[\alpha]\, e^{-X\alpha^{-1}Y}\int \mathcal{D}\eta\mathcal{D}\bar{\psi}''_1 e^{\left(\bar{\psi}''_1+X\alpha^{-1}\right)(Y+\eta)} \\
&= det\,[\alpha]\, e^{-X\alpha^{-1}Y}\int \mathcal{D}\eta\mathcal{D}\bar{\xi} e^{\bar{\xi}\eta'} \\
&= det\,[\alpha]\, e^{-X\alpha^{-1}Y}
\end{aligned}$$

In the second line, we perform the field transform $\eta = \alpha\psi''_1$ with Jacobian $det\,[\alpha]$ and in the forth line we used $\eta' = \eta + Y$ and $\bar{\xi} = \bar{\psi}''_1 + X\alpha^{-1}$. Also $det\,[\alpha]$ will be divided by the contribution the Pauli-Villars fields and thus the we obtain the $s = 2$ part

$$\left[\bar{J}_n P_L \begin{pmatrix} 0 & 1 \\ 1 & 0 \end{pmatrix} + \bar{\psi}''_{n,N_s}\beta_0\right]\left(-\alpha^{-1}\beta\right)\psi''_{n,2} + \bar{\psi}''_{n,2}\alpha\psi''_{n,2} + \bar{\psi}''_{n,2}\beta\psi''_{n,3}. \tag{4.123}$$

In the same way, we can calculate up to the $N_s - 1$ part

$$\begin{aligned}
&\left[\bar{J}_n P_L \begin{pmatrix} 0 & 1 \\ 1 & 0 \end{pmatrix}\left(-\alpha^{-1}\beta\right)^{N_s-1} + P_R \begin{pmatrix} 0 & 1 \\ 1 & 0 \end{pmatrix}\right]\psi''_{n,N_s} \\
&\qquad + \bar{\psi}''_{n,N_s}\left[\alpha_0 + \beta_0\left(-\alpha^{-1}\beta\right)^{N_s-1}\right]\psi''_{n,N_s} + \bar{\psi}''_{n,N_s}\begin{pmatrix} 0 & 1 \\ 1 & 0 \end{pmatrix} J_n.
\end{aligned} \tag{4.124}$$

In order to calculate this term, we prepare some quantities

$$\alpha^{-1} = a_5 \begin{pmatrix} B^{-1} & -B^{-1}C^\dagger \\ 0 & -1 \end{pmatrix}, \tag{4.125}$$

$$\beta^{-1} = a_5 \begin{pmatrix} -1 & 0 \\ B^{-1}C & B^{-1} \end{pmatrix}, \tag{4.126}$$

$$\alpha_0\alpha^{-1} = \begin{pmatrix} 1 & 0 \\ 0 & 0 \end{pmatrix} = \begin{pmatrix} 0 & 1 \\ 1 & 0 \end{pmatrix} P_L \begin{pmatrix} 0 & 1 \\ 1 & 0 \end{pmatrix}, \tag{4.127}$$

$$\beta_0\beta^{-1} = \begin{pmatrix} 0 & 0 \\ 0 & 1 \end{pmatrix} = \begin{pmatrix} 0 & 1 \\ 1 & 0 \end{pmatrix} P_R \begin{pmatrix} 0 & 1 \\ 1 & 0 \end{pmatrix}, \tag{4.128}$$

also the transfer matrix can be defined as

$$T = e^{-a_5 H} = \begin{pmatrix} B^{-1} & -B^{-1}C^\dagger \\ -CB^{-1} & B + C^\dagger B^{-1} C \end{pmatrix}. \tag{4.129}$$

Then we can derive

$$\begin{aligned} -\beta\alpha^{-1} &= \begin{pmatrix} B^{-1} & -B^{-1}C^\dagger \\ -CB^{-1} & B + C^\dagger B^{-1} C \end{pmatrix} \\ &= \begin{pmatrix} 0 & 1 \\ 1 & 0 \end{pmatrix} \gamma_5 e^{a_5 H} \gamma_5 \begin{pmatrix} 0 & 1 \\ 1 & 0 \end{pmatrix} \end{aligned} \tag{4.130}$$

and then Eq. (4.124) becomes

$$\begin{aligned} \bar{J}_n \left[-a_5 \left(P_L e^{N_5 a_5 H} + P_R \right) \gamma_5 \begin{pmatrix} 0 & 1 \\ 1 & 0 \end{pmatrix} \right] \alpha\psi''_{n,N_s} \\ - \bar{\psi}''_{n,N_s} \begin{pmatrix} 0 & 1 \\ 1 & 0 \end{pmatrix} \left[P_L + P_R e^{N_5 a_5 H} \right] \gamma_5 \begin{pmatrix} 0 & 1 \\ 1 & 0 \end{pmatrix} \alpha\psi''_{n,N_s} + \bar{\psi}''_{n,N_s} \begin{pmatrix} 0 & 1 \\ 1 & 0 \end{pmatrix} J_n. \end{aligned} \tag{4.131}$$

Furthermore if one uses $\eta = \alpha\psi''_{N_s}$, $\bar{\eta} = \bar{\psi}''_{Ns} \begin{pmatrix} 0 & 1 \\ 1 & 0 \end{pmatrix}$ and $J' = \begin{pmatrix} 0 & 1 \\ 1 & 0 \end{pmatrix} J$,

$$\begin{aligned} \bar{J}_n \left[-a_5 \left(P_R + P_L e^{N_5 a_5 H} \right) \gamma_5 \begin{pmatrix} 0 & 1 \\ 1 & 0 \end{pmatrix} \right] \eta_n \\ - \bar{\eta}_n \left[P_L + P_R e^{N_5 a_5 H} \right] \gamma_5 \begin{pmatrix} 0 & 1 \\ 1 & 0 \end{pmatrix} \eta_n + \bar{\psi}''_{n,N_s} J'_n. \end{aligned} \tag{4.132}$$

After integrating this, we obtain a following partition function

$$Z = a_5 a \sum \bar{J}_n \left[\frac{P_R + P_L e^{a_5 N_s H}}{P_L + P_R e^{a_5 N_s H}} \right] J_n, \tag{4.133}$$

and the propagator

$$\langle q\bar{q} \rangle = \frac{\delta}{\delta J} \frac{\delta}{\delta \bar{J}} \log Z|_{J=\bar{J}=0} = \frac{a_5}{a} \frac{1 - \gamma_5 tanh\left(a_5 \frac{N_s}{2} H \right)}{1 + \gamma_5 tanh\left(a_5 \frac{N_s}{2} H \right)}. \tag{4.134}$$

Thus the effective operator can be found as

$$D_{\text{eff}} = \frac{1}{a}\langle q\bar{q}\rangle^{-1} = \frac{1}{a_5}\frac{1+\gamma_5 tanh\left(a_5\frac{N_s}{2}H\right)}{1-\gamma_5 tanh\left(a_5\frac{N_s}{2}H\right)}. \tag{4.135}$$

Moreover we obtain a similar effective operator for the Pauli-Villars fields

$$a^4\sum\bar{Q}\left[D_{eff}+\frac{1}{a_5}\right]Q \tag{4.136}$$

and thus we finally write down

$$aD_{DW} = \frac{D_{\text{eff}}}{D_{\text{eff}}+\frac{1}{a_5}} = \frac{1}{2}\left(1+\gamma_5 \text{tanh}a_5\frac{N_s}{2}H\right). \tag{4.137}$$

Then D_{DW} asymptotically can be identified with the overlap Dirac-operator aD_{ov} at $N_s\to\infty$

$$D_{DW}\to D_{ov} = \frac{1}{2a}\left(1+\gamma_5\frac{H}{\sqrt{H^2}}\right), \tag{4.138}$$

however here H is defined from the transfer matrix $H=-\ln T/a_5$. If we think of a limit $a_5\to 0$

$$\begin{aligned} T &= \begin{pmatrix} 1 & 0 \\ 0 & 1 \end{pmatrix} + a_5 \begin{pmatrix} \left(\frac{a}{2}\nabla_\mu\nabla_\mu^\dagger+\frac{M_0}{a}\right) & -\sigma_\mu\frac{1}{2}\left(\nabla_\mu\nabla_\mu^\dagger\right) \\ \sigma_\mu^\dagger\frac{1}{2}\left(\nabla_\mu\nabla_\mu^\dagger\right) & -\left(\frac{a}{2}\nabla_\mu\nabla_\mu^\dagger+\frac{M_0}{a}\right) \end{pmatrix} + O\left(a_5^2\right) \\ &= 1-a_5\gamma_5 D_W\left(-M_0\right)+O\left(a_5^2\right), \end{aligned} \tag{4.139}$$

thus asymptotic form of the domain-wall fermion is

$$\lim_{a_5\to 0}\lim_{N_s\cdot a_5\to 0} D_{overlap} = \frac{1}{2a}\left(1+\gamma_5\frac{H_W\left(-M_0\right)}{\sqrt{H_W^2\left(-M_0\right)}}\right). \tag{4.140}$$

Then we finally obtained the overlap Dirac-operator as the asymptotic form at $N_s\to\infty$. In other words, the domain-wall fermion approximately satisfies .

4.8 Ward-Takahashi identity for the domain-wall axial vector current

In the case of the continuum N_f flavor QCD, Ward-Takahashi identity can be written

$$\langle 0|\{\partial_\mu A_\mu(x)+2mP^a(x)\}O(y)|0\rangle + \langle 0|\delta_x^a O(y)|0\rangle = 0, \tag{4.141}$$

where $|0\rangle$ is a vacuum state , m is a quark mass and

$$A_\mu^a(x) = \bar{\psi}(x)\gamma_5\gamma_\mu\tau^a\psi(x), \tag{4.142}$$

$$P^a(x) = \bar{\psi}(x)\gamma_5\tau^a\psi(x). \tag{4.143}$$

Here τ^a is an element of $SU(N_f)$ and δ_x^a is the infinitesimal local chiral transformation

$$\delta_x^a \psi(y) = i\delta(x-y)\tau^a\gamma_5\psi(x), \tag{4.144}$$

$$\delta_x^a \bar{\psi}(y) = i\delta(x-y)\bar{\psi}(x)\tau^a\gamma_5, \tag{4.145}$$

also $O(y)$ is an arbitary local operator. We can derive the PCAC (Partially Conserved Axial-vector Current) relation from the Ward-Takahashi identity

$$m_\pi^2 = 2m\langle 0|P^a(0)|\overrightarrow{0},\pi\rangle \tag{4.146}$$

which describes how the pion mass behaves if the quark mass is turned out to be non-zero. Now we are interested in the Ward-Takahashi identity when the domain-wall fermion is employed. To begin with, we consider following transformations for the domain-wall fermion

$$\psi_s(x) \to \psi_s'(x) = e^{i\theta_s^a\tau^a}\psi_s(x), \tag{4.147}$$

$$\bar{\psi}_s(x) \to \bar{\psi}_s'(x) = \bar{\psi}_s(x)e^{-i\theta_s^a\tau^a}, \tag{4.148}$$

where θ_s^a is defined as

$$\theta_s^a = \begin{cases} -\theta^a & \text{for } s = 1,2,\cdots,N_s/2 \\ \theta^a & \text{for } s = N_s/2+1,\cdots,N_s \end{cases}. \tag{4.149}$$

Here s denotes a fifth dimension's index. Furthermore we can check that this transformation corresponds to the conventional chiral transformation for the physical quark fields q and $\bar{q}$ which are defined as

$$q(x) = P_L\psi_1(x) + P_R\psi_{N_s}(x), \tag{4.150}$$

$$\bar{q}(x) = \bar{\psi}_1(x)P_R + \bar{\psi}_{N_s}(x)P_L. \tag{4.151}$$

By using this transformation, we obtain the Ward-Takahashi identity for the domain-wall fermion

$$\langle\left(\nabla_\mu^- A_\mu^a(x) + 2m_f P^a(x)\right)O(y) + \delta_x^a O(y)\rangle = 2 < J_{5q}^a(x)O(y) >, \tag{4.152}$$

where $\nabla_\mu^- f(x) = (f(x) - f(x-\hat{\mu}))/a$, $P^a(x) = \bar{q}(x)\gamma_5\tau^a q(x)$ is the pseudo-scalar density and the axial-vector current is given by

$$A_\mu^a(x) = \frac{1}{2}\sum_s \mathrm{sgn}(s-(N_s+1)/2)\left[\bar{\psi}_s(x+\hat{\mu})(1+\gamma_\mu)U_\mu^\dagger(x)\tau^a\psi_s(x) - \bar{\psi}_s(x)(1-\gamma_\mu)U_\mu(x)\tau^a\psi_s(x+\hat{\mu})\right]. \tag{4.153}$$

The right-hand side of Eq. (4.152) resembles the conventional lattice Ward-Takahashi identity except for the complexity of $A_\mu^a(x)$, thus the left-hand side represents violation of the Ward-Takahashi identity. $J_5^a(x)$ is defined by

$$J_5^a(x) = \frac{1}{2}\left[\bar{\psi}_{N_s/2+1}(x)(1+\gamma_5)\tau^a\psi_{N_s/2}(x) - \bar{\psi}_{N_s/2+1}(x)(1-\gamma_5)\tau^a\psi_{N_s/2+1}(x)\right] \tag{4.154}$$

At $N_s \to \infty$, $\langle 2J_5^a O\rangle$ vanishes for the non-singlet case, but for the singlet case it yields the chiral anomaly. Therefore we may conclude that the domain-wall fermion reproduce the continuum QCD.

4.9 Numerical test for the residual mass

As we have seen in the previous section, the domain-wall fermion has the chiral symmetry at $N_s \to \infty$, but at finite N_s violation of the chiral symmetry may remains. Residual mass is often used as an indicatory of violation of the Ginsparg-Wilson relation [44, 45]. Residual mass is defined via the axial Ward-Takahashi identity Eq. (4.152). Close to the continuum limit, the sum of the second term of left-hand side and the term of the right-hand side must be equivalent to $m_{\text{eff}} = m_f + m_{\text{res}}$

$$m_f < P^a(x)\, O(y) > + < J_5^a(x)\, O(y) > \approx m_{\text{eff}} < P^a(x)\, O(y) >, \tag{4.155}$$

with understanding $J_5^a \approx m_{res} P^a$. Then we may define a following ratio ratio

$$R(t) = \frac{\sum\limits_{x,y} < J_5^a(x,t)\, P^a(y,0) >}{\sum\limits_{x,y} < P^a(x,t)\, P^a(y,0) >}. \tag{4.156}$$

For t greater than $t_{\min}$, the ratio should be equivalent to a residual mass m_{res}

$$m_{\text{res}} = \left. \frac{\sum\limits_{x,y} < J_5^a(x,t)\, P^a(y,0) >}{\sum\limits_{x,y} < P^a(x,t)\, P^a(y,0) >} \right|_{t \geq t_{\min}} . \tag{4.157}$$

The residual mass plays a role in an indicator for the explicit chiral symmetry breaking. In order to maintain small violation of the Ginsparg-Wilson relation, some tests of the residual mass have been done by the JLQCD collaborations by adjusting the tunable parameters b, c [46]. Firstly they implemented a test on the 8^4 lattice with quenched Iwasaki gauge action at $\beta = 2.43$. By varying the parameter b, then search for an optimal choice. Fig. 4.1 shows residual masses measured for $L_s = 6, 8, 12$, and 16. We observe that $b = 2 - 2.3$ is good choice such that the smallest residual mass is given and the dependence on L_s is not significant for the parameter b. On $16^3 \times 32$ lattice with the tree-level Symanzik gauge action and $1/a = 2.5$ GeV, following possible variants were tested

- $(b = 1,\ c = 1)$ with $N_{smr} = 0$ and $M_0 = -1.0$,
- $(b = 1,\ c = 1)$ with $N_{smr} = 0$ and $M_0 = -1.6$,
- $(b = 1,\ c = 1)$ with $N_{smr} = 3$ and $M_0 = -1.0$,
- $(b = 2,\ c = 1)$ with $N_{smr} = 0$ and $M_0 = -1.0$,
- $(b = 2,\ c = 1)$ with $N_{smr} = 0$ and $M_0 = -1.6$,
- $(b = 2,\ c = 1)$ with $N_{smr} = 3$ and $M_0 = -1.0$.

Fig. 4.2 shows the residual masses with various parameters plotted as a function of L_s . Here the Tanh approximation is employed. We see that the choice of $b = 2,\ c = 1$ with $N_{smr} = 3$ and $M_0 = -1.0$ gives the smallest residual mass. In this context, we did not tune c value, the choice of $c = 1$ has been determined from a viewpoint of numerical costs of CG inversions. From JLQCD's studies, it was found that choosing $c = 1$ is few times faster than when $c = 0$ are chosen.

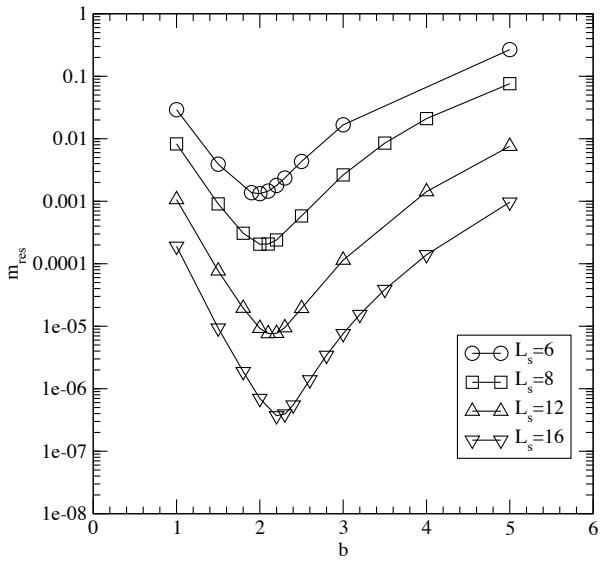

Figure 4.1: Residual masses are plotted as a function of b for the some choices of L_s . We observe that $b = 2 - 2.3$ gives the smallest residual mass.

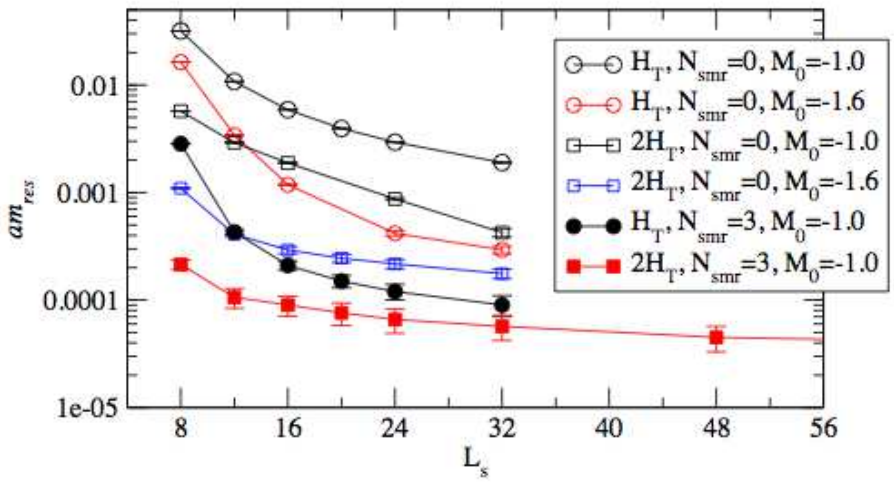

Figure 4.2: Residual mass for the various choices of generalized domain-wall fermions as a function of L_s. This figure is reprinted from Ref. [46].

4.10 $O\left(a^2\right)$-improvement for overlap Dirac operator

An $O(a^2)$-improved Dirac operator has been suggested by Ikeda-Hashimoto [26] and then the usual Ginsparg-Wilson relation is generalized. Here I review the formulation briefly. According to their analysis, whole improvement process should be done by two steps: improvement of a kernel and improvement of the overlap-Dirac operator. They employ the D34 action for the kernel of the overlap-Dirac operator and also suggest a following improved operator

$$D_c^{imp} = D_c + \frac{a^2}{4\rho} D_{ov}^\dagger D_{ov} D_c, \tag{4.158}$$

where D_{ov} is the standard overlap-Dirac operator and D_c is defined as $D_c = D_{ov}\left(1 - \frac{a}{2\rho}D_{ov}\right)^{-1}$ which is a non-local operator. Then D_{ov} satisfies the Ginsparg-Wilson relation $\{D_{ov}, \gamma_5\} = \frac{a}{\rho} D_{ov}\gamma_5 D_{ov}$, where ρ is a kernel mass. D_c^{imp} has the continuum chiral symmetry $\{D_c^{imp}, \gamma_5\} = 0$ and we can construct a local operator by a field rotation $\left(1 - \frac{a}{2\rho}D_{ov}\right)$

$$\begin{aligned} D_{ov}^{imp} &= D_c^{imp}\left(1 - \frac{a}{2\rho}D_{ov}\right) \\ &= D_{ov} + \frac{a^2}{4\rho^2} D_{ov}^\dagger D_{ov}^2. \end{aligned} \tag{4.159}$$

Then D_{ov}^{imp} is more costly than D_{ov}, but the $O(a^2)$ discretization errors is removed. Furthermore one observes that the improved overlap operator satisfies a generalized Ginsparg-Wilson relation

$$\{D_{ov}^{imp}, \gamma_5\} = \frac{a}{\rho} D_{ov}^{imp} R D_{ov}^{imp}, \tag{4.160}$$

where $R = \left(1 + \frac{a}{4\rho^2} D_{ov}^\dagger D_{ov}\right)^{-1}$. We can understand that the above relation is a alternative expression of the Ginsparg-Wilson relation in term of Ref. [34]. In Ref. [34], R is taken as $R \propto 1$, but essentially R may be generalized an operator which satisfies $[R, \gamma_5] = 0$. Then we can show that R satisfies this relation. In order to check this, first we expand the operator R as $R = \sum_n c_n \left(D_{ov}^\dagger D_{ov}\right)^n$ for $n = 0, 1, 2, \cdots$. If $\left[\left(D_{ov}^\dagger D_{ov}\right)^n, \gamma_5\right] = 0$ is satisfied for any integer n, we can conclude that $[R, \gamma_5] = 0$. By using mathematical induction, we are able to prove this relation. The case of $n = 0$ is trivial. To prove the case of $n = 1$ i.e. $[D_{ov}^\dagger D_{ov}, \gamma_5] = 0$, we use following formulas

$$\{AB, C\} = A[B, C] + \{A, C\}B \tag{4.161}$$

$$= [C, A]B + A\{B, C\}, \tag{4.162}$$

$$[AB, C] = A\{B, C\} - \{A, C\}B. \tag{4.163}$$

Then we obtain

$$\begin{aligned} \left[D_{ov}^\dagger D_{ov}, \gamma_5\right] &= D_{ov}^\dagger \{D_{ov}, \gamma_5\} - \{D_{ov}^\dagger, \gamma_5\} D_{ov} \\ &= \gamma_5 D_{ov}\gamma_5 \left(2\frac{a}{\rho} D_{ov}\gamma_5 D_{ov}\right) - \{D_{ov}^\dagger, \gamma_5\} D_{ov} \\ &= 2\frac{a}{\rho}\left(\gamma_5 D_{ov}\right)^3 - \{D_{ov}^\dagger, \gamma_5\} D_{ov}, \end{aligned} \tag{4.164}$$

where the Ginsparg-Wilson relation is used in the second line. Here the second term of Eq. (4.164) can be written as

$$\begin{aligned}\{D_{ov}^{\dagger},\gamma_5\} &= \{\gamma_5 D_{ov}\gamma_5,\gamma_5\}\\ &= \gamma_5 D_{ov}\left[\gamma_5,\gamma_5\right]+\{\gamma_5 D_{ov},\gamma_5\}\gamma_5\\ &= \left([\gamma_5,\gamma_5]D_{ov}+\gamma_5\{D_{ov},\gamma_5\}\right)\gamma_5\\ &= 2\frac{a}{\rho}\gamma_5 D_{ov}\gamma_5 D_{ov}\gamma_5,\end{aligned}$$

where we used the γ_5 hermiticity in the first line. Then we found

$$\begin{aligned}\left[D_{ov}^{\dagger}D_{ov},\gamma_5\right] &= 2\frac{a}{\rho}\left(\gamma_5 D_{ov}\right)^3-2\frac{a}{\rho}\left(\gamma_5 D_{ov}\right)^3\\ &= 0.\end{aligned}$$

If one assumes that $\left[\left(D_{ov}^{\dagger}D_{ov}\right)^k,\gamma_5\right]=0$, we obtain

$$\begin{aligned}\left[\left(D_{ov}^{\dagger}D_{ov}\right)^{k+1},\gamma_5\right] &= \left[\left(D_{ov}^{\dagger}D_{ov}\right)^k D_{ov}^{\dagger}D_{ov},\gamma_5\right]\\ &= \left(D_{ov}^{\dagger}D_{ov}\right)^k\left[D_{ov}^{\dagger}D_{ov},\gamma_5\right]+\left[\left(D_{ov}^{\dagger}D_{ov}\right)^k,\gamma_5\right]D_{ov}^{\dagger}D_{ov}\\ &= 0,\end{aligned}$$

where $\left[\left(D_{ov}^{\dagger}D_{ov}\right)^k,\gamma_5\right]=0$ and $\left[D_{ov}^{\dagger}D_{ov},\gamma_5\right]=0$ are used. From mathematical induction, we finally obtain $[R,\gamma_5]=0$. For comparison of the dispersion relation with the standard overlap operator, please see later chapter.

Chapter 5

Hadron spectroscopy

In this chapter, we discuss how to extract hadron spectroscopy, e.g. hadron mass. Furthermore various methods have been proposed to obtain better signals so far. We also review such technical improvements in this chapter.

5.1 Hadron interpolators and correlators

We concentrate on the meson interpolators. First of all, we consider the pions as an example. The u quark has $I = 1/2$, $I_z = +1/2$ and charge $Q = 2/3e$. The d quark has $I = 1/2$, $I_z = -1/2$ and charge $Q = -1/3e$. The pions are composed of the u, d quarks. Then we can write down the pion operators as follows

$$M_{\pi^+}(n) = \bar{d}(n)\gamma_5 u(n), \tag{5.1}$$

$$M_{\pi^-}(n) = \bar{u}(n)\gamma_5 d(n). \tag{5.2}$$

These operators corresponds each required quantum numbers. For instance, charge conjugation for M_{π^+} gives M_{π^-} . Here charge conjugation of mesons are defined through charge conjugation for quarks

$$\psi(n) \to C^{-1}\bar{\psi}(n)^T, \tag{5.3}$$

$$\bar{\psi}(n) \to -\psi(n)^T C, \tag{5.4}$$

where C obeys the relation

$$C\gamma_\mu C^{-1} = -\gamma_\mu^T. \tag{5.5}$$

In a similar way, other meson operators can be constructed from the quark fields. Generally a meson operator is given by

$$M(n) = \bar{\psi}^{(f_1)}(n)\,\Gamma\psi^{(f_2)}(n). \tag{5.6}$$

Next we consider two point meson correlators. Then one needs to find a interpolator which generate the meson state from the vacuum. If we ignore an overall sign factor such operators can be written as follows

$$\bar{M}(m) = \bar{\psi}^{(f_2)}(m)\,\Gamma\psi^{(f_1)}(m) \tag{5.7}$$

also two-point meson correlators is written by using Wick's theorem

$$\begin{aligned}\langle M(n)\bar{M}(m)\rangle &= \langle \bar{\psi}^{(f_1)}(n)\,\Gamma\psi^{(f_2)}(n)\,\bar{\psi}^{(f_2)}(m)\,\Gamma\psi^{(f_1)}(m)\rangle \\ &= -\mathrm{tr}\left[D_{f_1}^{-1}(n,m)\,\Gamma D_{f_2}^{-1}(m,n)\,\Gamma\right], \end{aligned} \tag{5.8}$$

where if $\Gamma = \gamma_5$ and $f_1 = f_2$, we may use $\gamma_5 D \gamma_5 = D^\dagger$. However in the case of $f_1 = f_2$, there is a disconnected part and it may be significant for precise calculation. Some methods have been suggested for computing the disconnected part of correlators, e.g. see Ref. [47].

5.2 Extracting hadron mass

Hadron mass is one of interesting observables which have to be calculated from lattice QCD. We review the calculation of hadron mass in lattice QCD and discuss how to get better signals.

5.2.1 How to extract the hadron mass

We demonstrate how to extract the hadron mass. I start from a two point correlation function of the form

$$\left\langle 0|M(\overrightarrow{x},t)\,M\left(\overrightarrow{0},0\right)|0\right\rangle, \tag{5.9}$$

where M is a field operator that create or annihilate states. Here we consider a complete set

$$1 = |0\rangle\langle 0| + \sum_k \int \frac{d^3p}{(2\pi)^3}\,|E_k(\overrightarrow{p})\rangle\langle E_k(\overrightarrow{p})|\,\frac{1}{2E_k(\overrightarrow{p})} + \textit{multi particle states}, \tag{5.10}$$

where $|0\rangle$ is a vacuum state and $|E_k(\overrightarrow{p})\rangle$ is a one-particle state with a momentum $\overrightarrow{p}$ and a energy $E_k(\overrightarrow{p})$. Furthermore $|E_k(\overrightarrow{p})\rangle$ is normalized as

$$\langle E_k(\overrightarrow{p})\,|E_l(\overrightarrow{q})\rangle = 2E_k(\overrightarrow{p})\,\delta_{k,l}\delta^{(3)}(p-q)\,(2\pi)^3. \tag{5.11}$$

If one substitutes Eq. (5.10) to Eq. (5.9),

$$\begin{aligned}\langle 0|\,M(\overrightarrow{x},t)\,M\left(\overrightarrow{0},0\right)|0\rangle &= \langle 0|\,M(\overrightarrow{x},t)\,|0\rangle\langle 0|\,M\left(\overrightarrow{0},0\right)|0\rangle \\ &+ \sum_k \int \frac{d^3p}{(2\pi)^3}\frac{1}{2E_k(\overrightarrow{p})}\langle 0|\,M(\overrightarrow{x},t)\,|E_k(\overrightarrow{p})\rangle\langle E_k(\overrightarrow{p})|\,M\left(\overrightarrow{0},0\right)|0\rangle + \cdots \\ &= \langle 0|\,e^{-i\hat{p}x}M\left(\overrightarrow{0},0\right)e^{i\hat{p}x}\,|0\rangle\langle 0|\,M\left(\overrightarrow{0},0\right)|0\rangle \\ &+ \sum_k \int \frac{d^3p}{(2\pi)^3}\frac{1}{2E_k(\overrightarrow{p})}\langle 0|\,e^{-i\hat{p}x}M\left(\overrightarrow{0},0\right)e^{i\hat{p}x}\,|E_k(\overrightarrow{p})\rangle\langle E_k(\overrightarrow{p})|\,M\left(\overrightarrow{0},0\right)|0\rangle + \cdots \\ &= \left|\langle 0|\,M\left(\overrightarrow{0},0\right)|0\rangle\right|^2 \\ &+ \sum_k \int \frac{d^3p}{(2\pi)^3}\frac{1}{2E_k(\overrightarrow{p})}e^{-E_k(\overrightarrow{p})t}e^{i\overrightarrow{p}\cdot\overrightarrow{x}}\left|\langle 0|\,M\left(\overrightarrow{0},0\right)|E_k(\overrightarrow{p})\rangle\right|^2 + \cdots \end{aligned}$$

Then we define a connected correlation function as

$$\langle 0|\, M\left(\overrightarrow{x},t\right) M\left(\overrightarrow{0},0\right)|0\rangle_{connected} = \langle 0|\, M\left(\overrightarrow{x},t\right) M\left(\overrightarrow{0},0\right)|0\rangle - \langle 0|\, M\left(\overrightarrow{x},t\right)|0\rangle \langle 0|\, M\left(\overrightarrow{0},0\right)|0\rangle$$

and also if one takes summation over $\overrightarrow{x}$, we obtain a following formula

$$\begin{aligned}
&\sum_{\overrightarrow{x}} \langle 0|\, M\left(\overrightarrow{x},t\right) M\left(\overrightarrow{0},0\right)|0\rangle_{conneted} \\
&= \sum_k \int \frac{d^3p}{(2\pi)^3} \frac{1}{2E_k\left(\overrightarrow{p}\right)} e^{-E_k\left(\overrightarrow{p}\right)t} (2\pi)^3 \delta^{(3)}\left(\overrightarrow{p}\right) \left|\langle 0|\, M\left(\overrightarrow{0},0\right)|E_k\left(\overrightarrow{p}\right)\rangle\right|^2 + \cdots \\
&= \sum_k \frac{1}{2m_k} e^{-m_k t} |Z_k|^2 + \cdots \\
&= \frac{|Z_0|^2}{2m_0} e^{-m_0 t}\left[1 + e^{-\triangle m_k t}\right]
\end{aligned}$$

where $Z_k = \langle 0|\, M\left(\overrightarrow{0},0\right)|m_k\rangle$ and $\triangle m_k = m_k - m_0$. For extracting the ground state of corresponding hadrons, one has to take a large t in order to suppress the excited states contribution in the factor $e^{-\triangle m_k t}$. If one imposes a periodic boundary condition against the t direction with $0 < t < T$, we obtain

$$\langle 0|\, M\left(\overrightarrow{x},t\right) M\left(\overrightarrow{0},0\right)|0\rangle^{PBC}_{connected} = \frac{|Z_0|^2}{2m_0} e^{-m_0 T/2} \cosh\left[m_0\left(t - \frac{T}{2}\right)\right] + \cdots . \tag{5.12}$$

5.2.2 Source smearing

The effective mass is often used for a check of validity

$$m_{eff}\left(t\right) a = -\log \frac{Corr(t+a)}{Corr(t)}. \tag{5.13}$$

Then if the excited states is well-removed, the effective mass takes a constant value which do not depend t. However taking a large t would be difficult due to a limit of numerical computational costs. In order to get a clear signal, some optimizations for source are employed. Now we consider a general form of a meson interpolator as

$$M\left(x_0\right) = \sum_{x_1, x_2} F\left(x_0; x_1, x_2\right) \bar{\psi}\left(x_1\right) \Gamma \psi\left(x_2\right),$$

where $F\left(x_0; x_1, x_2\right)$ is a distribution function and Γ is an element of the Clifford algebra. In the simplest case, we take $F\left(x_0; x_1, x_2\right) = \delta\left(x_1 - x_0\right)\delta\left(x_2 - x_0\right)$ which is called *local source* or *point source*. However a realistic wave function can be obtained from a less trivial function as

$$F\left(x_0; x_1, x_2\right) = S_i\left(x_0; x_1\right) S_k\left(x_0; x_2\right)$$

For instance, $S_i\left(x_0; x_1\right)$ may be taken a exponential form

$$S_i\left(x_0; x_1\right) = e^{-\alpha |x_1 - x_0|},$$

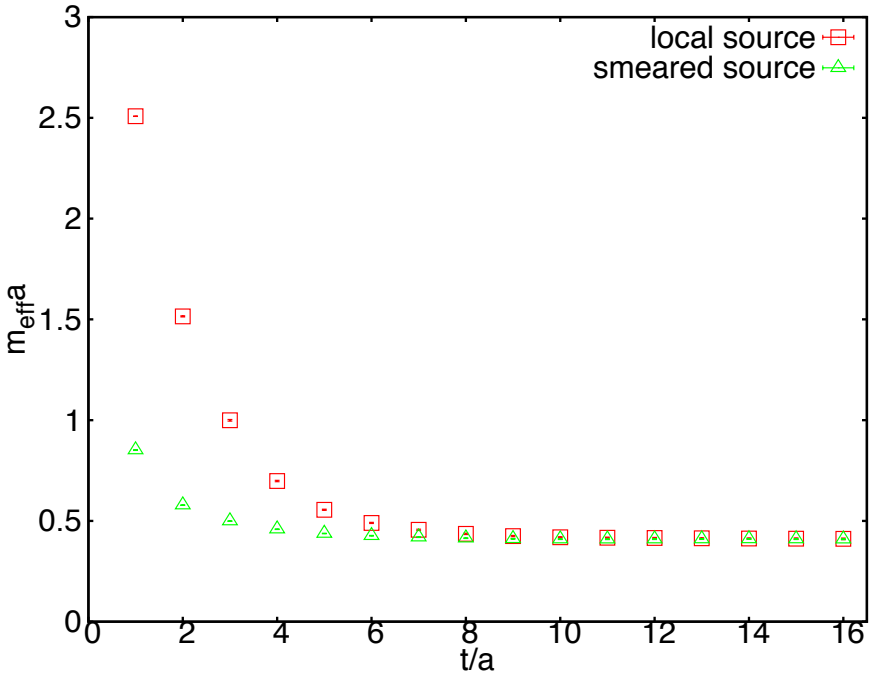

Figure 5.1: Effective masses with the point source and the exponentially smeared source. We observe that the effective mass become a constant at smaller t than the case of the local source when the smeared source is employed.

where a parameter α can be tuned for a better signal. In a similar way, $S_k(x_0; x_2)$ can be taken some functions. This kind of source is called a *smeard source*. Here we show effective masses with the local source and the exponentially smeared source at Fig. 5.1. We observe that the effective mass become a constant at smaller t than the case of the local source when the smeared source is employed.

5.3 Link smearing

When we calculate correlation functions one is manly interested in the long distance behavior. Then one can improved the correlation signal by smearing the gauge field. Here we introduce the APE smearing [48] and the stout smearing [49] which are employed in our scaling studies on quenched lattices at Chapter 5. In the smearing process, one typically replaces the original link variables $U_\mu(n)$ by local averaged link variables $V_\mu(n)$

$$V_\mu(n) = (1-\alpha)\, U_\mu(n) + \frac{\alpha}{6}\sum_{\nu\neq\mu} C_{\mu\nu}(n)\,, \tag{5.14}$$

$$C_{\mu\nu}(n) = U_\nu(n)\, U_\mu(n+\hat{\nu})\, U_\nu(n+\hat{\mu})^\dagger + U_\nu(n-\hat{\nu})^\dagger\, U_\mu(n-\hat{\nu})\, U_\nu(n-\hat{\nu}+\hat{\mu})\,, \tag{5.15}$$

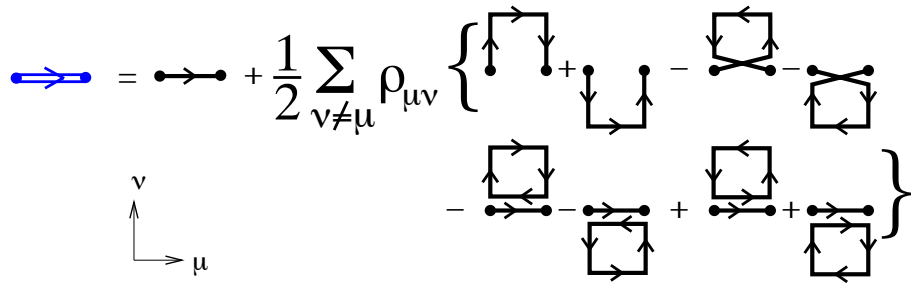

Figure 5.2: Sketch of smeared gauge links. The expansion up to first order in the $\rho_{\mu\nu}$ of the new link gauge link. ˜This figure is quoted from [49].

where α is a real parameter which can be tuned. Then $V_\mu(n)$ is not an element of $SU(3)$ and one needs to project it to $SU(3)$. The projection is usually done by maximizing Retr $\left[XV_\mu(n)^\dagger\right]$ and using X as new link variable $U'_\mu(n)$. This is called the APE smearing. Next we introduce stout smearing which is similar way with the APE smearing. In this process, the new link variable $U'_\mu(n)$ is defined as

$$U'_\mu(n) = e^{iQ_\mu(n)}U_\mu(n)\,, \tag{5.16}$$

where $Q_\mu(n)$ is a traceless and hermitian matrix and thus $e^{iQ_\mu(n)}$ is an element of $SU(3)$ or generally $SU(N)$. Here $Q_\mu(n)$ is defined as

$$Q_\mu(n) = \frac{i}{2}\left(\Omega_\mu(n)^\dagger - \Omega_\mu(n) - \frac{1}{3}tr\left[\Omega_\mu(n)^\dagger - \Omega_\mu(n)\right]\right), \tag{5.17}$$

$$\Omega_\mu(n) = \left(\sum_{\nu\neq\mu}\rho_{\mu\nu}C_{\mu\nu}\right)U_\mu(n)^\dagger\,, \tag{5.18}$$

where $C_{\mu\nu}$ is common with the APE smearing and we schematically describe . In order to obtain the new gauge link variables, we can employ this smearing process (5.16) iteratively with keeping that the new link variable is an element of $SU(3)$. Usual choices of $\rho_{\mu\nu}$ are $\rho_{\mu4} = \rho_{4\mu} = 0$, $\rho_{\mu\nu} = \rho$.

Such smearing method leads to smooth gauge fluctuations and reducing the radiative correction for observables [50]. In Ref. [50], radiative corrections for renormalization factors of the fermion bilinear operator and the four fermi operator can be suppressed by the APE smearing and the HYP smearing [51]. Note that these processes are gauge covariant procedures and thus we do not need to fix the gauge.

5.4 Scale setting

In the lattice formalism all observables are calculated as dimensionless quantities. In order to introduce the dimension, we have to set the scale. Here we discuss how to set the scale. Then we can relate the lattice spacing a to the inverse coupling β.

5.4.1 Static quark potential

Firstly we introduce the well-known traditional method to set the scale on the lattice. We can extract the static quark potential from the Wilson loop and determine the lattice spacing a from the so-called Sommer scale r_0 on the lattice. In physical unit, the Sommer scale is $r_0 \simeq 0.49$fm [52]. The Wilson loop is defined as

$$L[U] = tr\left[\prod_{(n,\mu)\in C} U_\mu(n)\right], \tag{5.19}$$

where C is a closed loop of links on the lattice and it has the asymptotic behavior at large $t = an_t$

$$L[U] \propto \exp\left(-an_t V(r)\right). \tag{5.20}$$

Then the static QCD potential can be parametrized by

$$V(r) = A + \frac{B}{r} + \sigma r, \tag{5.21}$$

where σ is called the sting tension. r_0 is determined from

$$F(r_0)\, r_0^2 = 1.65, \tag{5.22}$$

where the force between the two static quarks is $F(r) = dV(r)/dr$. If one uses the parametrized potential Eq. (5.21), we obtain

$$F(r) = -\frac{B}{r^2} + \sigma, \tag{5.23}$$

and then Eq. (5.22) implies

$$\frac{r_0}{a} = \sqrt{\frac{1.65 + B}{\sigma a^2}}. \tag{5.24}$$

Here the dimensionless r_0/a can be calculated from lattice calculation. Then the lattice spacing a is determined through the Sommer scale.

5.4.2 Yang-Mils gradient flow

Wilson flow or Yang-Mils gradient flow has been recently proposed in Ref. [53]. In order to determine scale on the lattice, we may employ the w_0 or the $t_0^{1/2}$ in terms of the Wilson flow instead of the the static quark potential method. w_0 is introduced in Ref. [54] in order for high-precision scale setting. Here we briefly introduce this approach.

In this method, we calculate the Wilson flow by following steps

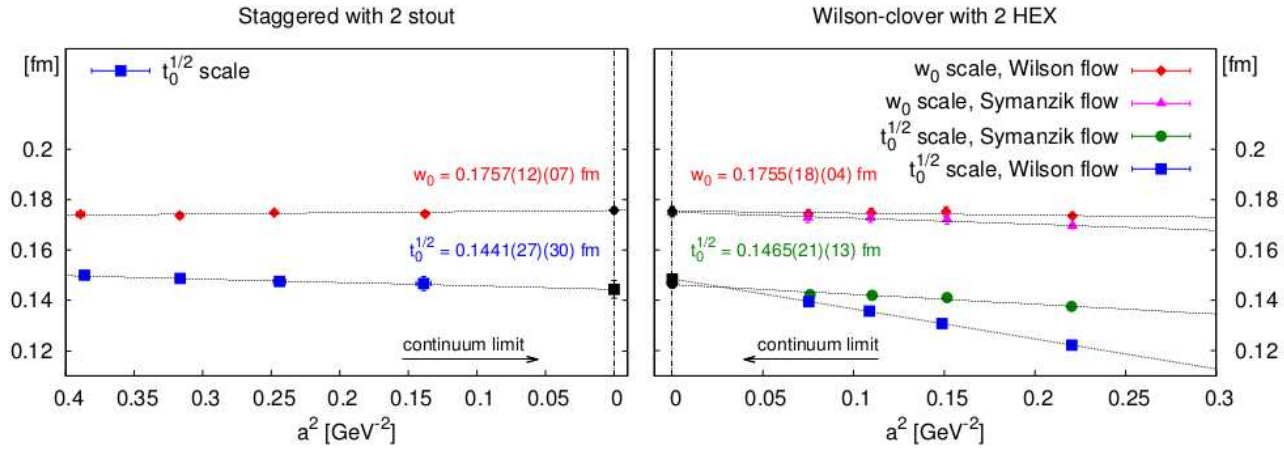

Figure 5.3: w_0 and $t_0^{1/2}$ are plotted as a function of a^2 in both case of staggered fermion computation and Wilson fermion computation. This figure is reprinted from [54].

$$\dot{V}_t = Z\left(V_t\right) V_t, \quad V_0 = U \tag{5.25}$$

where V_t are the gauge links at flow time t and U is the original link variables. In Ref. [53], the Wilson gauge action is used and $Z\left(V_t\right)$ is the derivative of the plaquette action. This steps are performed up to a scale t and this scale is expressed as t_0 which is defined as $t^2\left\langle E\left(t\right)\right\rangle|_{t=t_0} = 0.3$. Here $\left\langle E\left(t\right)\right\rangle$ is the expectation value of $G^a_{\mu\nu}\left(t\right) G^a_{\mu\nu}\left(t\right)$ with flow time t , where $G^a_{\mu\nu}\left(t\right)$ is the lattice chromoelectric field-strength which is defined by the clover term. The BMW collaboration introduced the w_0 scale as an alternative way. They proposed a related following observable

$$W\left(t\right) \equiv t\frac{d}{dt}\{t^2\langle E\left(t\right)\rangle\} \tag{5.26}$$

and defined the w_0 scale as

$$W\left(t\right)|_{t=w_0^2} = 0.3. \tag{5.27}$$

Then $W\left(t\right)$ take a less cutoff effect. We show the lattice spacing dependence of the w_0 and $t_0^{1/2}$ in both case of 2HEX smeared Wilson fermion computation and 2-stout smeared staggered fermion simulations. Here the HEX smearing means the stout smearing based on the HYP smearing [55]. Also in Fig. 5.3, the Wilson flow represent using the derivative of the plaquette gauge action for $Z\left(V_t\right)$ and the Symanzik flow indicate employing the tree-level Symanzik gauge action instead. We observe that good scaling of w_0 and $t_0^{1/2}$ against a^2.

Chapter 6

The Brillouin fermion

The Brillouin fermion was introduced in [19]. As mentioned in introduction, this fermion formalism was designed to respect the rotational symmetry and produces an excellent energy dispersion relation on the non-trivial gauge fields as well as on the free gauge fields. On the other hand, it has Ginsparg-Wilson like eigenvalue spectra and thus the suitability as a kernel of overlap fermions could be expected as indicated in [19]. There are some similar approaches[20, 21, 22, 56], while the Brillouin fermion is optimized for both of the continuum dispersion relation and the Ginsparg-Wilson eigenvalues spectra. From these continuum like characteristic, one could expect that the Brillouin fermion is promising for heavy quark physics. The action is defined as follows

$$D^{Bri}(n,m) = \sum_{\mu}\gamma_{\mu}\nabla_{\mu}^{iso}(n,m) - \frac{a}{2}\triangle^{bri}(n,m) + m_0\delta_{n,m} - \frac{c_{SW}}{2}\sum_{\mu<\nu}\sigma_{\mu\nu}F_{\mu\nu}\delta_{n,m}, \tag{6.1}$$

$$S_F = \sum_{n,m}\overline{\psi}_n D^{Bri}(n,m)\,\psi_m$$

where ∇_{μ}^{iso} and $\triangle^{bri}$ have 2 hopping terms, 3 hopping term, and 4 hopping terms as well as usual 1 hopping terms. However many hopping in same direction is forbidden, thus all of hopping is within a hypercube.

6.1 Overall Smearing Strategy

One can summarize the Brillouin operator on free gauge fields as following formula[19],

$$D^{Bri}(n,m) = \sum_{\mu}\gamma_{\mu}\rho_{\mu}(n,m) + \lambda(n,m) \tag{6.2}$$

$$\rho_{\mu}(n,m) = \rho_1\left[\delta_{n+\hat{\mu},m} - \delta_{n-\hat{\mu},m}\right] + \rho_2\sum_{\nu}\left[\delta_{n+\hat{\mu}+\hat{\nu},m} - \delta_{n-\hat{\mu}+\hat{\nu},m}\right] + \rho_3\sum_{\nu,\rho}\left[\delta_{n+\hat{\mu}+\hat{\nu}+\hat{\rho},m} - \delta_{n-\hat{\mu}+\hat{\nu}+\hat{\rho},m}\right]$$
$$+ \rho_4\sum_{\nu,\rho,\sigma}\left[\delta_{n+\hat{\mu}+\hat{\nu}+\hat{\rho}+\hat{\sigma},m} - \delta_{n-\hat{\mu}+\hat{\nu}+\hat{\rho}+\hat{\sigma},m}\right] \tag{6.3}$$

$$\lambda(n,m) = \lambda_0\delta_{n,m} + \lambda_1\sum_{\mu}\left[\delta_{n+\hat{\mu},m} + \delta_{n-\hat{\mu},m}\right] + \lambda_2\sum_{\mu,\nu}\left[\delta_{n+\hat{\mu}+\hat{\nu},m} + \delta_{n-\hat{\mu}+\hat{\nu},m}\right] + \lambda_3\sum_{\mu,\nu,\rho}\left[\delta_{n+\hat{\mu}+\hat{\nu}+\hat{\rho},m} + \delta_{n-\hat{\mu}+\hat{\nu}+\hat{\rho},m}\right]$$
$$+ \lambda_4\sum_{\mu,\nu,\rho,\sigma}\left[\delta_{n+\hat{\mu}+\hat{\nu}+\hat{\rho}+\hat{\sigma},m} + \delta_{n-\hat{\mu}+\hat{\nu}+\hat{\rho}+\hat{\sigma},m}\right] \tag{6.4}$$

with $(\rho_1,\rho_2,\rho_3,\rho_4) = \frac{1}{432}(64,16,4,1)$, $(\lambda_0,\lambda_1,\lambda_2,\lambda_3,\lambda_4) = \frac{1}{128}(240,-8,-4,-2,-1)$. Then summation is taken over $\mu = \pm1,\pm2,\pm3,\pm4$. The simplest way of constructing gauge covariant operator is summing over all shortest paths. It means that one consider off-axis link variables. There are following 2-hopping contributions

$$V_{\hat{\mu}+\hat{\nu}}(n) = \frac{1}{2}\left[U_\mu(n)\,U_\nu(n+\hat{\mu}) + U_\nu(n)\,U_\mu(n+\hat{\nu})\right] \tag{6.5}$$

$$V_{-\hat{\mu}-\hat{\nu}}(n) = \frac{1}{2}\left[U_\mu^\dagger(n-\hat{\mu})\,U_\nu^\dagger(n-\hat{\mu}-\hat{\nu}) + U_\nu^\dagger(n-\hat{\nu})\,U_\mu^\dagger(n-\hat{\mu}-\hat{\nu})\right] \tag{6.6}$$

$$V_{\hat{\mu}-\hat{\nu}}(n) = \frac{1}{2}\left[U_\mu(n)\,U_\nu^\dagger(n+\hat{\mu}-\hat{\nu}) + U_\nu^\dagger(n-\hat{\nu})\,U_\mu(n-\hat{\nu})\right] \tag{6.7}$$

$$V_{-\hat{\mu}+\hat{\nu}}(n) = \frac{1}{2}\left[U_\nu(n)\,U_\mu^\dagger(n+\hat{\nu}-\hat{\mu}) + U_\mu^\dagger(n-\hat{\mu})\,U_\nu(n-\hat{\mu})\right] \tag{6.8}$$

with(or without) back projection to SU(3). We schematically show a diagonal link variable at figure 6.1. Then we have to take a average of all possible paths for corresponding hopping terms. For 3-hopping terms and 4 hopping terms, there are respectively a following diagonal link variable

$$V_{\hat{\mu}+\hat{\nu}+\hat{\rho}}(n) = \frac{1}{3}\left[V_{\hat{\mu}+\hat{\nu}}(n)\,U_\rho(n+\hat{\mu}+\hat{\nu}) + V_{\hat{\mu}+\hat{\rho}}(n)\,U_\nu(n+\hat{\mu}+\hat{\rho}) + V_{\hat{\nu}+\hat{\rho}}(n)\,U_\mu(n+\hat{\nu}+\hat{\rho})\right], \tag{6.9}$$

$$V_{\hat{\mu}+\hat{\nu}+\hat{\rho}+\hat{\sigma}}(n) = \frac{1}{4}\left[\,V_{\hat{\mu}+\hat{\nu}+\hat{\rho}}(n)\,U_\sigma(n+\hat{\mu}+\hat{\nu}+\hat{\rho}) + V_{\hat{\mu}+\hat{\nu}+\hat{\sigma}}(n)\,U_\rho(n+\hat{\mu}+\hat{\nu}+\hat{\sigma})\right.$$
$$\left. V_{\hat{\mu}+\hat{\rho}+\hat{\sigma}}(n)\,U_\nu(n+\hat{\mu}+\hat{\rho}+\hat{\sigma}) + V_{\hat{\nu}+\hat{\rho}+\hat{\sigma}}(n)\,U_\mu(n+\hat{\nu}+\hat{\rho}+\hat{\sigma})\,\right], \tag{6.10}$$

, where we did not show all of diagonal link variables. Note that the Brillouin fermion has 80 nearest-neighbors, thus 80 diagonal link variables are necessary. Generating diagonal link variables should be implemented before the CG iteration as a kind of preconditioning with or without link smearing. This can be done independently with measurements and it might be good to store these off-axis link variables before real calculation. Thus one may exclude this cost from implementation numerical cost of the Brillouin fermion. This method/strategy is called "Overall Smearing Strategy" which is suggested by original authors.

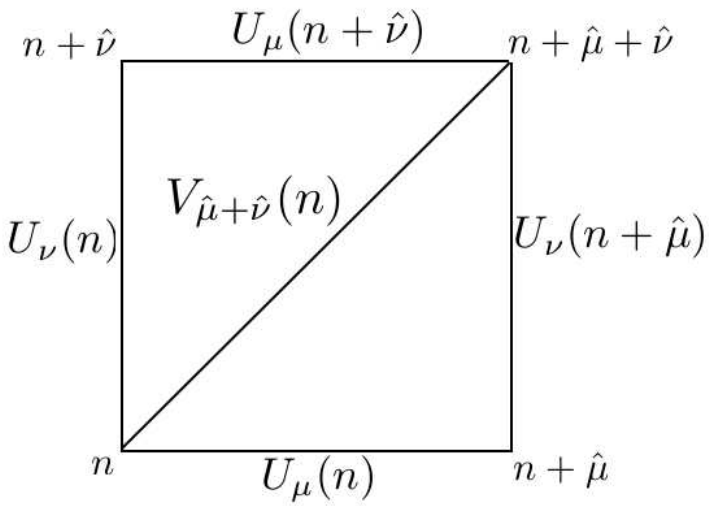

Figure 6.1: sketch of a diagonal link variable

6.2 Recursive formula

We also can consider a alternative building method for a covariant form of the Brillouin laplacian and the isotropic derivative with gauge fields. For the Brillouin laplacian, we can take a following recursive formulation

$$a\triangle^{bri}(n,m)\,\psi_m = \frac{1}{64}\sum_\mu D_\mu^+\psi_n''' - \frac{15}{4}\psi_n, \tag{6.11}$$

$$\psi_n''' \equiv 8\psi_n + \frac{1}{2}\sum_{\nu\neq\mu} D_\nu^+\psi_n'', \tag{6.12}$$

$$\psi_n'' \equiv 4\psi_n + \frac{1}{3}\sum_{\rho\neq\mu,\nu} D_\rho^+\psi_n', \tag{6.13}$$

$$\psi_n' \equiv 2\psi_n + \frac{1}{4}\sum_{\sigma\neq\mu,\nu,\rho} D_\sigma^+\psi_n, \tag{6.14}$$

where $D_\mu^\pm$ is defined by

$$D_\mu^\pm\psi_n = U_\mu(n)\,\psi_{n+\hat{\mu}} \pm U_\mu^\dagger(n-\hat{\mu})\,\psi_{n-\hat{\mu}}. \tag{6.15}$$

Final expressions should be calculated using step by step process. We also write a formula of the isotropic derivative for the x-direction. To maintain the γ_5-hermiticity, we have to take all paths. In the case of derivative term, the formula becomes slightly complicated form as follows

$$\nabla_x^{iso}(n,m)\,\psi_m = \frac{1}{432}\left(D_x^-\xi_n''' + \frac{1}{2}\sum_{\nu\neq x} D_\nu^+\eta_n'''\right) \tag{6.16}$$

$$\xi_n''' \equiv 64\psi_n + \frac{1}{2}\sum_{\nu\neq x} D_\nu^+\xi_n'' \tag{6.17}$$

$$\xi_n'' \equiv 16\psi_n + \frac{1}{3}\sum_{\rho\neq x,\nu} D_\rho^+\xi_n' \tag{6.18}$$

$$\xi_n' \equiv 4\psi_n + \frac{1}{4}\sum_{\sigma\neq x,\nu,\rho} D_\sigma^+\psi_n \tag{6.19}$$

$$\eta_n''' \equiv D_x^-\xi_n'' + \frac{1}{3}\sum_{\rho\neq x,\nu} D_\rho^+\eta_n'' \tag{6.20}$$

$$\eta_n'' \equiv D_x^-\xi_n' + \frac{1}{4}\sum_{\sigma\neq x,\nu,\rho} D_\sigma^+\eta_n' \tag{6.21}$$

$$\eta_n' \equiv D_x^-\psi_n \tag{6.22}$$

This formula is exactly consistent with previous one which is shown at the last section. Numerical implementation of this recursive formula is difficult to achieve high-performance, however sometimes it may be useful for a convenience e.g. for automatic perturbative calculation.

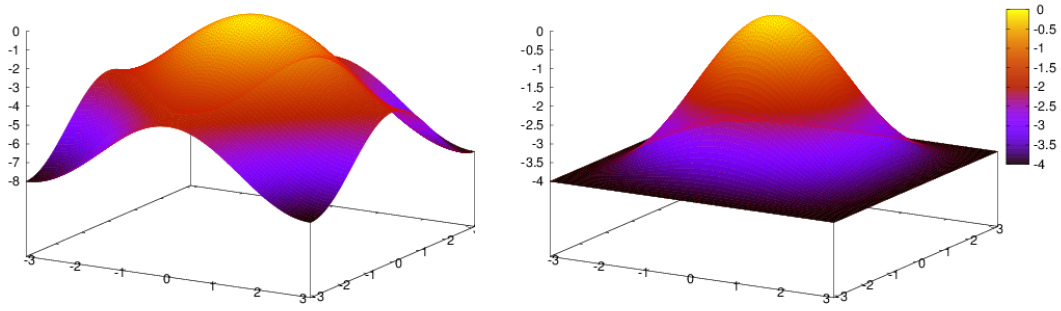

Figure 6.2: standard(left) and Brillouin(right) laplacian in 2d momentum space

6.3 Tree-level analysis for Wilson type fermions

We would like to investigate discretization effects for the Brillouin fermion. First let us review the free-field dispersion relation for three Dirac operators: the Wilson fermion, the Brillouin fermion and the D34 action. Here we systematically mention to dispersion relation for later convenience.

6.3.1 Wilson fermions

First of all , we review the free-field dispersion relation for the Wilson fermion. Dispersion relation easily can be compared with continuum theory $E = \sqrt{\overrightarrow{p}^2 + m^2}$, thus one can see discretization effect via deviation from that. Dispersion relation can be extracted from a fermion propagator. In this section, we only work at tree-level, however one can easily extend this study to one-loop level and non-perturbative. A general form of a Dirac operator D could be defined as follows

$$D(x,y) = \sum_{\mu} \gamma_\mu \rho_\mu (x,y) + \lambda (x,y), \tag{6.23}$$

also we can obtain a propagator of the form

$$D^{-1} = \frac{-\sum_{\mu} \gamma_\mu \rho_\mu + \lambda}{\lambda^2 - \sum_{\mu} \rho_\mu^2}. \tag{6.24}$$

In the case of Wilson fermions, these are respectively $\rho_\mu (x,y) = \nabla_\mu^{std}(x,y)$ and $\lambda(x,y) = -\frac{a}{2} r \Delta^{std}(x,y) + m$ where ∇_μ^{std} and Δ^{std} are defined by

$$\nabla_\mu^{std}(x,y) = \frac{1}{2a} \left(\delta_{y,x+a\hat{\mu}} - \delta_{y,x-a\hat{\mu}}\right), \tag{6.25}$$

$$\Delta^{std}(x,y) = \sum_{\mu} \frac{1}{a^2} \left(\delta_{y,x+a\hat{\mu}} + \delta_{y,x-a\hat{\mu}} - 2\delta_{y,x}\right). \tag{6.26}$$

Also the Fourier form of these operator are given by

$$\tilde{\nabla}_\mu^{std}(p) = \frac{i}{a} \sin(p_\mu a) \equiv i S_\mu^{std}(p) \tag{6.27}$$

$$\tilde{\Delta}^{std}(p) = \sum_{\mu} \frac{2}{a^2} \left(\cos(p_\mu a) - 1\right) \tag{6.28}$$

These operator can be expanded by a as

$$S_\mu^{std}(p) = p_\mu - \frac{1}{6} p_\mu^3 a^2 + O\left(a^4\right) \tag{6.29}$$

$$\tilde{\triangle}^{std}(p) = -p_\mu^2 + \frac{1}{12} p_\mu^4 a^2 + O\left(a^4\right) \tag{6.30}$$

At $\overrightarrow{p} = 0$, we can obtain a following exact solution by using $p_4 = iE$ for the Wilson Dirac-operator $Ea = ln(1 + ma)$ which is a well-known factor m_1 as shown at [8]. If one expand the energy up to $(ma)^5$, we obtain

$$(Ea)^2(\overrightarrow{0}, ma) = (ma)^2 - (ma)^3 + \frac{11}{12}(ma)^4 - \frac{5}{6}(ma)^5 + \mathcal{O}\left((ma)^6\right). \tag{6.31}$$

If spacing momenta are turned out to be non-zero, the above expression will be changed as follows,

$$
\begin{aligned}
Ea(\overrightarrow{p}, ma)^2 &= (ma)^2 - (ma)^3 + \frac{11}{12}(ma)^4 - \frac{5}{6}(ma)^5 \\
&\quad + A(ma)\sum_i (p_i a)^2 + B(ma)\left(\sum_{i\le j} p_i^2 p_j^2 a^4 + \sum_i (p_i a)^4\right) \qquad (6.32)\\
A(ma) &= 1 - \frac{2}{3}(ma)^2 + \frac{7}{6}(ma)^3 \\
B(ma) &= -\frac{2}{3} + \frac{ma}{2}
\end{aligned}
$$

From the above analysis, we see that discretization errors of the Wilson fermion starts from $O(a)$ which is mostly improved by the clover term[15] up to a required level. Also we can estimate the dispersion relation numerically by a solving zero point by the Newton method as shown at figure 6.3. Here red line denotes the continuum dispersion relation $E = \sqrt{\overrightarrow{p}^2 + m^2}$ and different pattern of dots show solutions for each directions of spacing momentum $\overrightarrow{p}$, where three directions are chosen: $\overrightarrow{p} = (1,1,1), (1,1,0), (1,0,0)$. From the massless dispersion relation, we see that the dispersion relation deviate from the continuum theory around at $\overrightarrow{p}a \sim 0.5$. In the case of the massive dispersion relation, the energy of the Wilson fermion differ from the continuum one even at $\overrightarrow{p}a = 0.0$ because of $Ea = \ln(1 + ma)$. One may shift the energy to the continuum one at $\overrightarrow{p}a = 0.0$, because constant shift of the energy is not essential for physics. However we do not tune this problem in our plots to show discretization effects explicitly. In terms of Ref. [8], the rest mass M_1 can be expressed as

$$
(M_1 a)^2 = (ma)^2 - (ma)^3 + \frac{11}{12}(ma)^4 - \frac{5}{6}(ma)^5, \qquad (6.33)
$$

also in fact $A(ma)$ corresponds to the speed-of-light M_1/M_2 . Then M_2 can be obtained

$$
M_2 a = ma - \frac{1}{2}(ma)^2 + (ma)^3 . \qquad (6.34)
$$

6.3.2 Brillouin operator

Now we are ready to discuss discretization effect for the Brillouin fermion. In the case of the Brillouin operator, the momentum representation of the Dirac operator on the free field is given by

$$
\tilde{D}^{Bri}(p) = \sum_\mu \gamma_\mu \tilde{\nabla}_\mu^{iso}(p) - \frac{a}{2}\tilde{\triangle}^{bri}(p) + m \qquad (6.35)
$$

$$
a^2\tilde{\triangle}^{bri}(p) = 4\left(\prod_\mu \cos^2(p_\mu a/2) - 1\right) \qquad (6.36)
$$

$$
a\tilde{\nabla}_\mu^{iso}(p) = \frac{i}{27}\sin(p_\mu a)\prod_{\nu\neq\mu}(\cos(p_\nu a) + 2) \qquad (6.37)
$$

For later convenience, we define

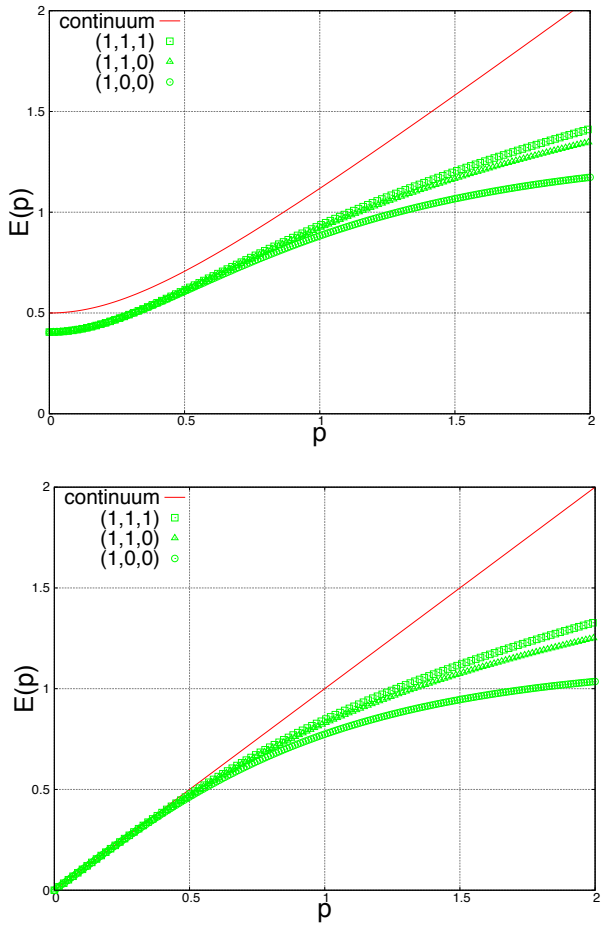

Figure 6.3: The dispersion relation for the Wilson fermion

$$S_{\mu}^{iso}(p) = \frac{1}{27}\sin(p_{\mu}a)\prod_{\nu\neq\mu}(\cos(p_{\nu}a)+2). \tag{6.38}$$

Thus the dispersion relation can be written by

$$\left(\frac{1}{2}\tilde{\triangle}^{bri}(p) - ma\right)^2 - \sum_{\mu}\left(\tilde{\nabla}_{\mu}^{\ iso}(p)\right)^2 = 0. \tag{6.39}$$

Using the Taylor expansion, the energy can be estimated as

$$Ea\left(\overrightarrow{0}, ma\right)^2 = (ma)^2 - (ma)^3 + \frac{11}{12}(ma)^4 - \frac{5}{6}(ma)^5 + \mathcal{O}\left((ma)^6\right), \tag{6.40}$$

where we found that the Brillouin fermions has a similar discretization effect as Wilson fermions at $\overrightarrow{p} = 0$ which gives $Ea = \ln(1+ma)$, because the Brillouin fermion can be identified with the Wilson fermion at $\overrightarrow{p} = 0$. At non-zero spacing momenta, the energy differ form the Wilson fermion

$$
\begin{aligned}
Ea(\overrightarrow{p}, ma)^2 &= (ma)^2 - (ma)^3 + \frac{11}{12}(ma)^4 - \frac{5}{6}(ma)^5 \\
&\quad + A(ma)\sum_i (p_i a)^2 + B(ma)\left(\sum_{i\le j} p_i^2 p_j^2 a^4 + \sum_i (p_i a)^4\right) \qquad (6.41)\\
A(ma) &= 1 + \frac{1}{12}(ma)^3 \\
B(ma) &= \frac{ma}{12}
\end{aligned}
$$

The dispersion relation for Wilson fermions and Brillouin fermions is shown at Figure6.4, where momentum $\overrightarrow{p}$ is taken to $(1, 1, 1)$. In the massless case, very continuum-like dispersion relation can be observed up to $pa \simeq 1.5$ when the Brillouin fermion is employed. For the massive dispersion relation, however, a deviation can be observed even at $pa = 0$ by the $Ea = \ln(1 + ma)$. Also we compare tree-level eigenvalue spectra between the Wilson fermion and the Brillouin fermion at figure6.5. From this figure, we see that the Brillouin fermion has very Ginsparg-Wilson like property and can expect a suitability of a kernel as the overlap procedure. Furthermore we estimate M_1 and M_2 as the last section. Now we are able to identify M_1 with the Wilson fermion's one, but M_2 can be written by

$$M_2 a = ma - \frac{1}{2}(ma)^2 + \frac{1}{3}(ma)^3 \qquad (6.42)$$

Then we found that the leading effect is suppressed in the speed-of-light $M_1/M_2 = A(ma)$ for the Brillouin fermion. This would be an advantage of the Brillouin fermion.

6.3.3 D34 action

Here it might be good to review the D34 action for comparison. The D34 action is suggested by Eguchi-Kawamoto [25] and Hamber-Wu [24]. This action has third and fourth order derivative terms, but no second-order Wilson term. The Dirac operator is given as

$$D_{D34} = \sum_\mu \gamma_\mu \nabla_\mu^{std}\left(1 - \frac{1}{6}a_\mu^2 \triangle_\mu^{std}\right) + \sum_\mu c_\mu a^3 \left(\triangle_\mu^{std}\right)^2, \qquad (6.43)$$

where $\triangle_\mu^{std}$ are defined as follows,

$$\Delta_\mu^{std}(x, y) = \frac{1}{a^2}\left(\delta_{y,x+a\hat{\mu}} + \delta_{y,x-a\hat{\mu}} - 2\delta_{y,x}\right). \qquad (6.44)$$

Also here we assume isotropic lattices $a_\mu = a$ for every μ. Note that the D34 action is introduced without the conventional field rotation which does not affect spectral quantities in terms of on-shell improvement. On the other hand, an advantage of unisotropic lattices has been discussed at [31]. On the momentum space, these operators are described by following expression,

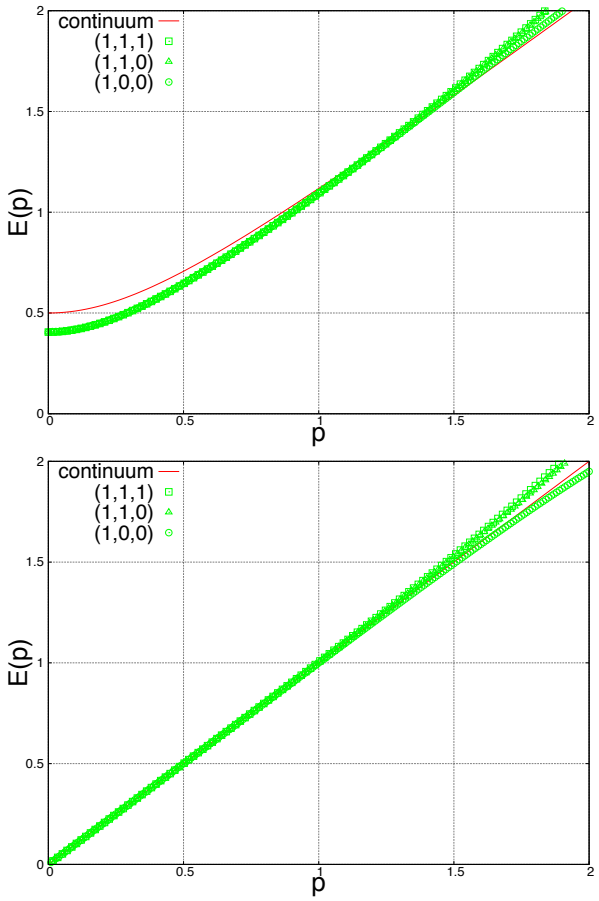

Figure 6.4: The dispersion relation of the Brillouin fermion

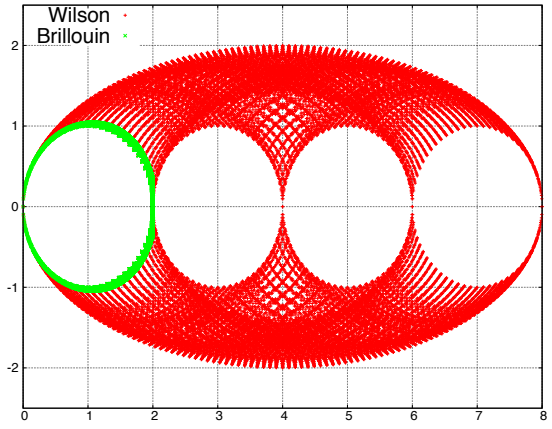

Figure 6.5: Eigenvalue spectra for the Wilson fermion and the Brillouin fermion

$$\tilde{\nabla}_{\mu}^{std}(p) = \frac{i}{a}\sin(ap_{\mu}) \tag{6.45}$$

$$\tilde{\triangle}_{\mu}^{std}(p) = \frac{2}{a^2}(\cos(p_{\mu}a) - 1) = -\frac{4}{a^2}\sin^2\left(\frac{ap_{\mu}}{2}\right). \tag{6.46}$$

, also the improved term can be written as

$$\left(1-\frac{1}{6}a^2\tilde{\triangle}_\mu^{std}(p)\right)\tilde{\nabla}_\mu^{std}(p)=\frac{i}{3}\left(4-\cos\left(ap_\mu\right)\right)\sin\left(ap_\mu\right) \tag{6.47}$$

If one take isotropically $c_\mu = c_{D34}$, again we obtain the dispersion relation for the D34 action

$$\left(c_{D34}\sum_\mu a^3\left(\tilde{\triangle}_\mu^{std}(p)\right)^2+ma\right)^2-\sum_\mu\left((1-\frac{1}{6}a^2\tilde{\triangle}_\mu^{std}(p))\tilde{\nabla}_\mu^{std}(p)\right)^2 \;=\; 0, \tag{6.48}$$

and the energy is given by

$$Ea\left(\overrightarrow{0},ma\right)^2=(ma)^2+2c_{D34}(ma)^5+\mathcal{O}\left((ma)^6\right), \tag{6.49}$$

and for finite $\overrightarrow{p}$

$$Ea(\overrightarrow{p},ma)^2=(ma)^2+2c_{D34}(ma)^5+A\left(ma\right)\sum_i\left(p_ia\right)^2+B(ma)\left(\sum_{i\leq j}p_i^2p_j^2a^4+\sum_i\left(p_ia\right)^4\right) \tag{6.50}$$

$$A(ma)=1+4c_{D34}(ma)^3$$
$$B(ma)=4mc_{D34}$$

Dispersion relations and eigenvalue spectra of the D34 action at tree-level respectively are shown in figure6.6 and figure6.7, where we chose $c_{D34} = 1/6$. Massive dispersion relation starts from around $E\left(\overrightarrow{p}=0\right)=0.5$ which means that some parts of the discretization effect $Ea=\ln(1+ma)$ is restoring. From figure 6.7, we observe that eigenvalue spectra of the D34 action get close to the imaginary axis which is eigenvalue distributions of the continuum theory. Also the laplacian of the D34 action is shown at figure 6.8, behavior around the Brillouin zone is similar with the Wilson fermion, however at low momentum region this figure show $O\left(a^2\right)$ scaling.

6.4 Improvement for the Brillouin operator

Up to here we have reviewed various schemes via dispersion relation, eigenvalue spectra and investigated discretization effects for each fermions. Here, we explore the Symanzik improvement for the Brillouin fermion and discuss discretization effects of improved actions. In general, an improvement needs higher-order derivative and these terms may generate unphysical poles which interfere with a physical solution. Let us mention about this problem in a later section.

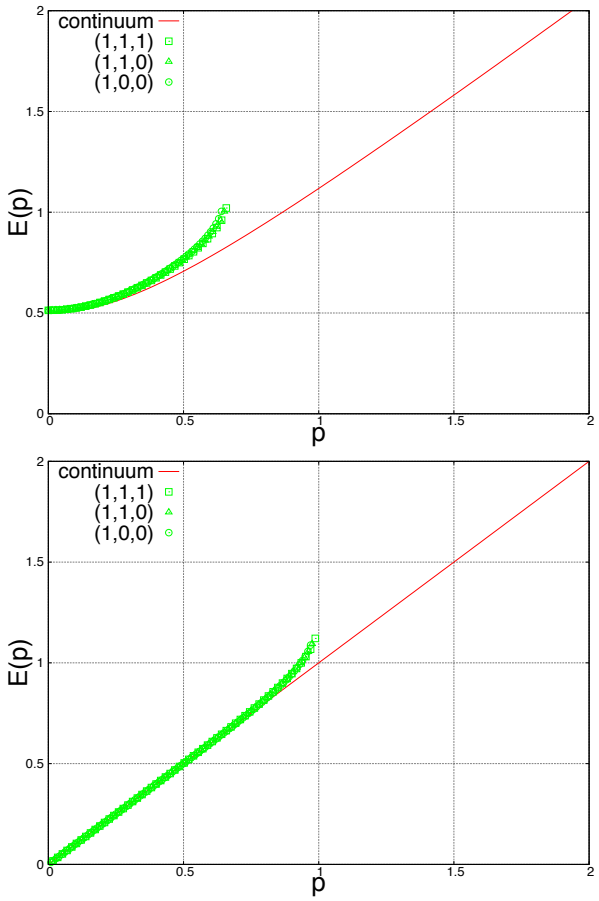

Figure 6.6: The dispersion relation of the D34 action

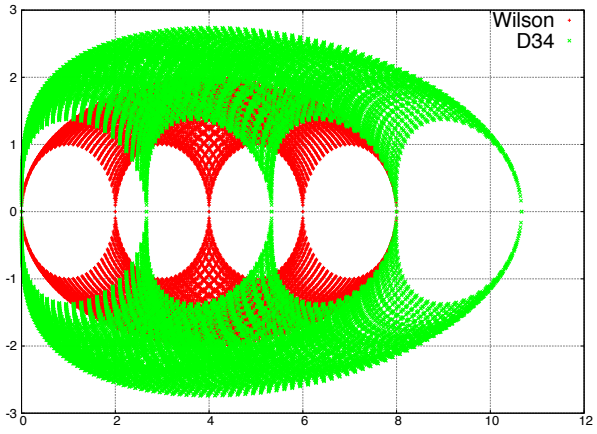

Figure 6.7: Eigenvalue spectra for the D34 action against the Wilson fermion

6.4.1 Tree-level $O\left(a^2\right)$ improvement

We have shown that the Brillouin fermion still has $O\left(a\right)$ discretization error. For the $O\left(a\right)$ improvement based on the Symanzik improvement, the clover term is widely employed with tuning

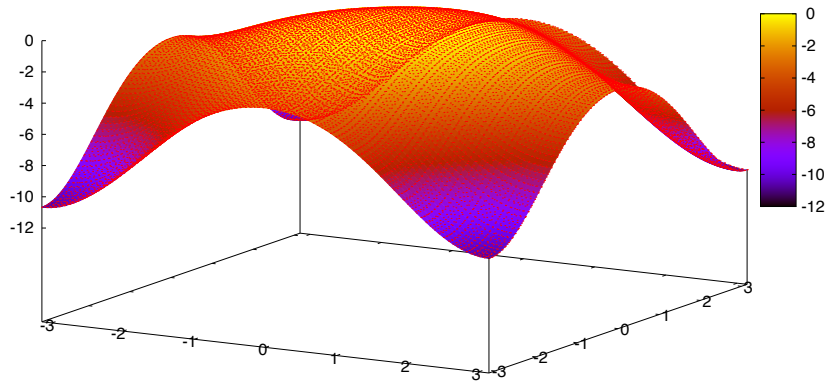

Figure 6.8: The laplacian of the D34 action in 2d momentum space

the coefficient c_{SW} at perturbative level or non-perturbative level. Usually perturbative tuning c_{SW} would be carried out analytically, however the Brillouin fermion is composed of many terms which include 2 link, 3link and 4link terms. Therefore analytic calculation seem to be intensive, thus it might be good to utilize an numerical automatic perturbative system. Our studies for perturbative calculation is on-going. This will be published another paper soon. Here we improve the Brillouin fermions by eliminating up to its $O\left(a^2\right)$ discretization effects without the field rotation which is often used for the improvement. To do that, we think of classical actions on the momentum space and expand by the lattice spacing a up to needed order.

$$aS_{\mu}^{iso}\left(p\right) = p_{\mu}a - \frac{1}{6}\left(p_{\mu}a\right)\sum_{\mu}\left(p_{\mu}a\right)^2 + O\left(\left(pa\right)^5\right)$$

$$a^2\tilde{\triangle}^{bri}\left(p\right) = -\sum_{\mu}\left(p_{\mu}a\right)^2 + O\left(\left(pa\right)^4\right)$$

Then if one add higher derivative terms to the action, leading errors can be eliminated from the action

$$a\tilde{\nabla}_{\mu}^{iso}\left(p\right) \rightarrow \left(1 - \frac{1}{12}a^2\tilde{\triangle}^{bri}\left(p\right)\right) a\tilde{\nabla}_{\mu}^{iso}\left(p\right)\left(1 - \frac{1}{12}a^2\tilde{\triangle}^{bri}\left(p\right)\right)$$

From above analysis we suggest a following improved action

$$D^{imp} = \sum_{\mu}\gamma_{\mu}(1 - \frac{a^2}{12}\triangle^{bri})\nabla_{\mu}^{iso}(1 - \frac{a^2}{12}\triangle^{bri}) + c_{imp}a^3(\triangle^{bri})^2, \tag{6.51}$$

,where we remain a tunable parameter c_{imp} which is similar with the Wilson parameter r in the Wilson fermion. Note that sandwiching symmetric factor $(1 - \frac{a^2}{12}\triangle^{bri})$ is introduced to eliminate the $O\left(a^2\right)$ errors while keeping the γ_5 hermiticity property and a Wilson term which is considered to suppress the contribution of doublers is a $O\left(a^3\right)$ term. This improved action resembles the D34

action, however this action is still keeping an excellent energy dispersion relation and Ginsparg-Wilson like eigenvalue spectra which are respectively shown at figure6.9 and figure 6.12. By expanding the energy of D^{imp} p to $O\left(a^5\right)$ and taking the space momentum to zero,

$$(Ea)^2 = (ma)^2 + 2c_{imp}(ma)^5 \tag{6.52}$$

We compare discretization effect for every Dirac operators in table6.1. This table show dispersion relation at finite momenta expanded up to $O\left(a^5\right)$. The D34 action and the Brillouin fermion are better than Wilson fermion. Also D34 action is restored $O\left(a\right)$ and $O\left(a^2\right)$ error. The improved Brillouin operator does not have $O\left(a\right)$ and $O\left(a^2\right)$ error like the the D34 action, however moreover this action is close to continuum theory up to this order. Note that $(pa)^0$ coefficient is same between the Wilson fermion and the Brillouin fermion, however there seem to be an advantage in $\sum_i (p_i a)^2$ and $\sum_i (p_i a)^4 + \sum_{i<j} p_i p_j a^4$ coefficients. Also we show improved laplacian in Figure6.11. At near the Brillouin zone, the laplacian is similar with the unimproved version, however near $ap \simeq 0$ behavior differ. From eigenvalues spectra, we see that eigenvalue spectra of the improved Brillouin fermion get close to the imaginary axis.

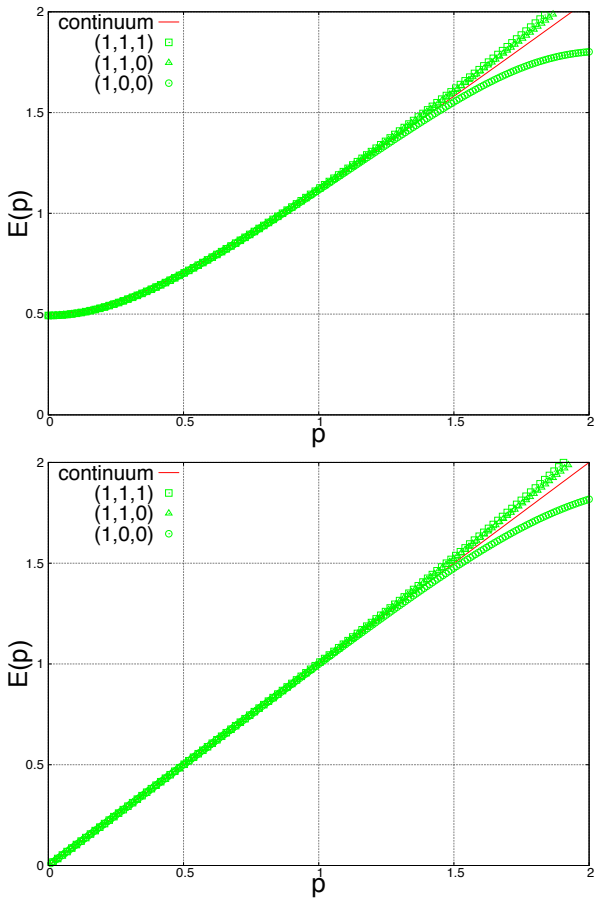

Figure 6.9: Dispersion relation of improved Brillouin operator

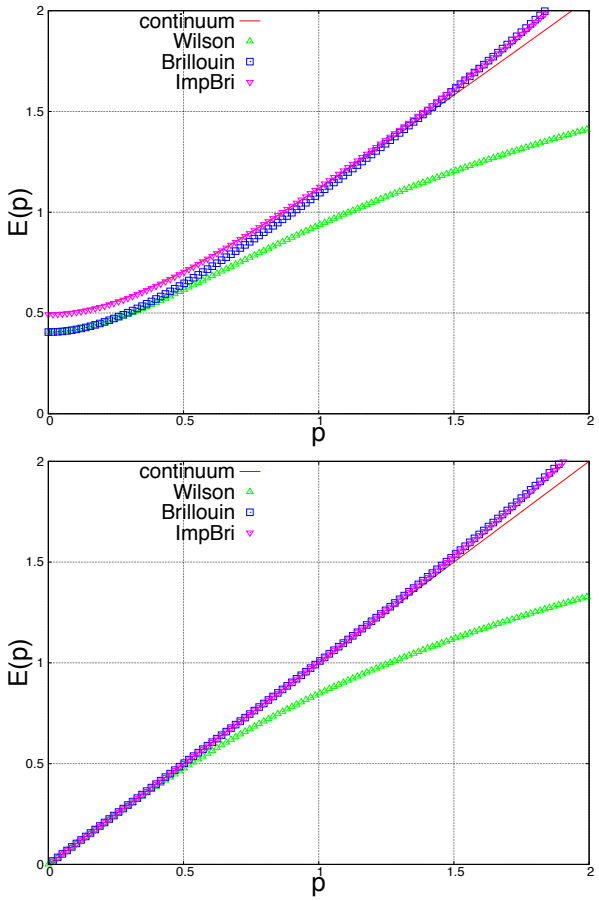

Figure 6.10: Comparison via dispersion relations

6.4.2 Reducing the numerical cost

Numerical implementation of the improved action D^{imp} which is suggested in previous section is expensive. For feasible simulations, we might think of any cheeper formulation with a similar scaling, i.e. the dispersion relation. First we consider a following cheeper version of the improved action

$$D^{imp1} = \sum_{\mu} \gamma_\mu (1 - \frac{1}{12} a^2 \triangle^{std}) \nabla_\mu^{iso} (1 - \frac{1}{12} a^2 \triangle^{std}) + c_{imp} a^3 (\triangle^{std})^2, \tag{6.53}$$

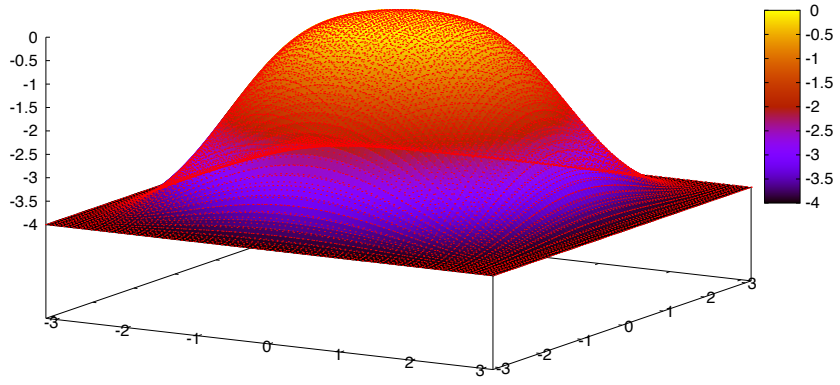

Figure 6.11: improved laplacian in 2d momentum space

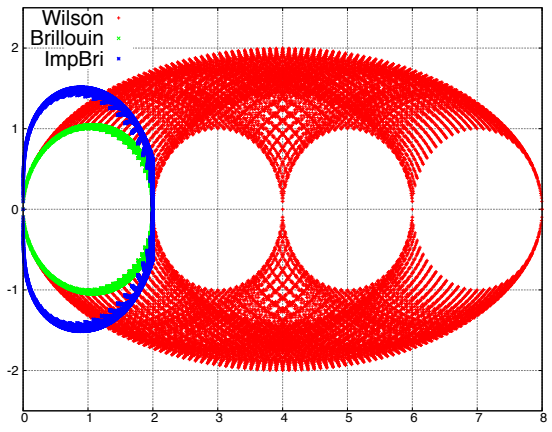

Figure 6.12: Comparison eigenvalues

	$(pa)^0$	$\sum_i (p_i a)^2$	$\sum_i (p_i a)^4 + \sum_{i<j} p_i p_j a^4$
Wilson	$(ma)^2 - (ma)^3 + \frac{11}{12}(ma)^4 - \frac{5}{6}(ma)^5$	$1 - \frac{2}{3}(ma)^2 + \frac{7}{6}(ma)^3$	$-\frac{2}{3} + \frac{ma}{2}$
Brillouin	$(ma)^2 - (ma)^3 + \frac{11}{12}(ma)^4 - \frac{5}{6}(ma)^5$	$1 + \frac{1}{12}(ma)^3$	$\frac{ma}{12}$
D34	$(ma)^2 + 2c_{D34}\,(ma)^5$	$1 + 4c_{D34}(ma)^3$	$4c_{D34}ma$
Improved Brillouin	$(ma)^2 + 2c_{imp}(ma)^5$	1	0

Table 6.1: Comparison of the energy expansions among Dirac-operators

where $\left(\triangle^{std}\right)^2$ is employed instead of $\triangle^{bri}$ in eq(6.51). Then we get rid of a suitability as a kernel of overlap fermions and focus the dispersion relation for heavy quark actions. In figure6.14, we show eigenvalue spectra which is rather close to the Wilson fermion than the Brillouin fermion, where $c_{imp} = 1/8$ is chosen. On the other hand, the dispersion relation is good up to $pa \sim 1.0$ as shown at fig 6.13, however this is rather worse than improved Brillouin operator. It seems convenient to keep scaling property and reduce numerical const at once. Thus any another approach should be considered. Then we introduce parameter δ as suggested in[57]

$$\nabla_x^{iso}(\delta) = \left(1 + \delta a^2 \partial_y^2\right) \nabla_x^{std}.$$

and optimize this parameter for scaling properties at tree-level, in particular the dispersion relation. From Kumar's trick, it is defined as $\delta = 1/6$ which is employed at[19]. In 4-dimension, the δ-dependent isotropic derivative can be defined as

$$\nabla_\mu^{iso}(\delta) = \nabla_\mu^{std} \prod_{i \neq \mu} \left(1 + \delta a^2 \partial_i^2\right) \tag{6.54}$$

The Fourier form of the δ-dependent isotropic derivative can be written

$$\tilde{\nabla}_\mu^{iso}(\delta) = \tilde{\nabla}_\mu^{std} \prod_i \left[1 + 2\delta\left(cos\left(p_i a\right) - 1\right)\right] = i S_\mu^{iso}(\delta). \tag{6.55}$$

By expanding pa up to $(pa)^3$,

$$\begin{aligned} S_\mu^{iso}(\delta) &= \left(p_\mu a - \frac{1}{6}(p_\mu a)^3 + O\left((pa)^5\right)\right) \prod_{i \neq \mu} \left[2\delta\left(1 - \frac{1}{2}(p_i a)^2 + O\left((pa)^4\right)\right) + 1 - 2\delta\right] \\ &= p_\mu a + \left(\delta - \frac{1}{6}\right)(p_\mu a)^3 - \delta\,(p_\mu a)\,\hat{p}^2 + O\left((pa)^5\right), \end{aligned}$$

where $\hat{p}^2 \equiv \sum_\mu (p_\mu a)^2$. Thus an improved action can be written as

$$\begin{aligned} a S_\mu^{iso}(\delta) &\to \left(1 - c(\delta)\, a^2 \tilde{\triangle}^{std}\right) a S_\mu^{iso}(\delta) \left(1 - c(\delta)\, a^2 \tilde{\triangle}^{std}\right) \\ &= p_\mu a + \left(\delta - \frac{1}{6}\right)(p_\mu a)^3 + (2c(\delta) - \delta)\,\hat{p}^2\,(p_\mu a) + O\left((pa)^5\right). \end{aligned}$$

An improvement condition should be imposed as follows so that $O\left(a^2\right)$ discretization effects are eliminated

$$\delta = \frac{1}{6},\ c(\delta) = \frac{\delta}{2}. \tag{6.56}$$

To tune the parameter δ for optimizing, a new term is needed and we introduce a following term to improved actions

$$\begin{aligned} aS_\mu^{iso}(\delta) \to & \left(1 - c(\delta) a^2 \tilde{\triangle}^{std} - d(\delta) a^2 \tilde{\triangle}_\mu^{std}\right) aS_\mu^{iso}(\delta) \left(1 - c(\delta) a^2 \tilde{\triangle}^{std} - d(\delta) a^2 \tilde{\triangle}_\mu^{std}\right) \\ & = p_\mu a + \left(\delta - \frac{1}{6} + 2d(\delta)\right) (p_\mu a)^3 + (2c(\delta) - \delta) \hat{p}^2 (p_\mu a) + O\left((pa)^5\right) \end{aligned}$$

Thus a new improvement condition becomes

$$c(\delta) = \frac{1}{2}\left(\frac{1}{6} - \delta\right),\ d(\delta) = \frac{\delta}{2}, \tag{6.57}$$

which includes the previous case when $\delta = 1/6$. In other words, we define a following improved action with above improvement conditions

$$D^{imp2} = \sum_\mu \gamma_\mu \left(1 - a^2 \triangle_\mu^{imp}\right) a\nabla_\mu^{iso}(\delta) \left(1 - a^2 \triangle_\mu^{imp}\right) + c_{imp} a^3 (\triangle^{std})^2, \tag{6.58}$$

where $\triangle_\mu^{imp}$ is defined as

$$\triangle_\mu^{imp} = \frac{1}{12}\triangle_\mu^{std} + \frac{\delta}{2}\sum_{\nu \neq \mu} \triangle_\nu^{std}. \tag{6.59}$$

From viewpoint of numerical costs, $\triangle_\mu^{imp}$ is compatible with $\triangle^{std}$. We may employ this "hybrid" improved action without the overlap projection. However we found that tuning of δ is not significant for dispersion relations. Also we may tune the parameter δ and c_{imp} at one-loop or non-perturbative level.

6.4.3 The overlap procedure with the Brillouin kernel

For further improved lattice fermion actions, we would like to employ the overlap formulation with some kernels, because the chiral symmetry suppress $O\left(a^{2n+1}\right)$ discretization errors for the integer n. Also the Brillouin operator might reduce a cost of the projection of overlap procedure as indicated in [19]. Here we also employ an improved overlap operator which is suggested by Ikeda-Hashimoto[26] for further improvements which suppress $O\left(a^2\right)$ discretization errors. We

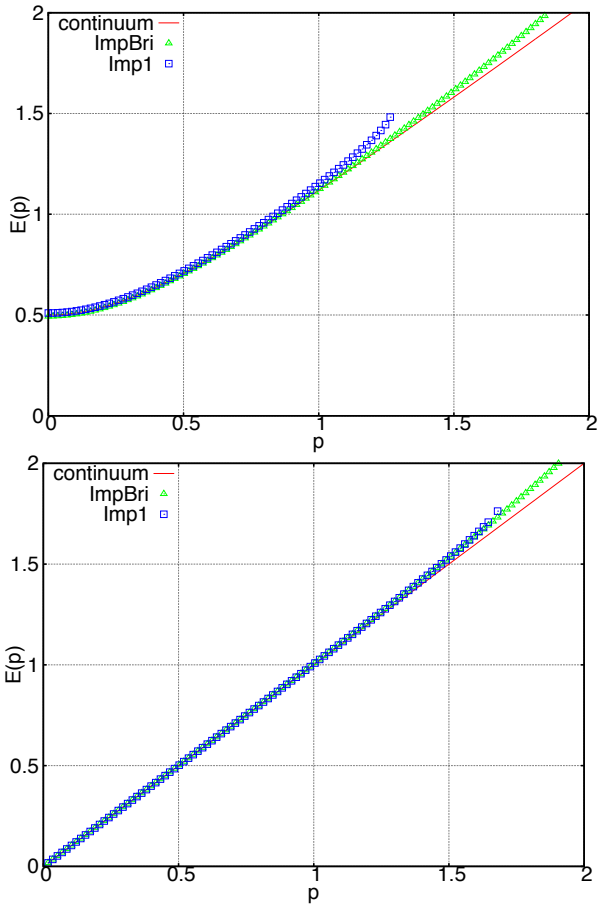

Figure 6.13: Dispersion relation of D^{imp1}

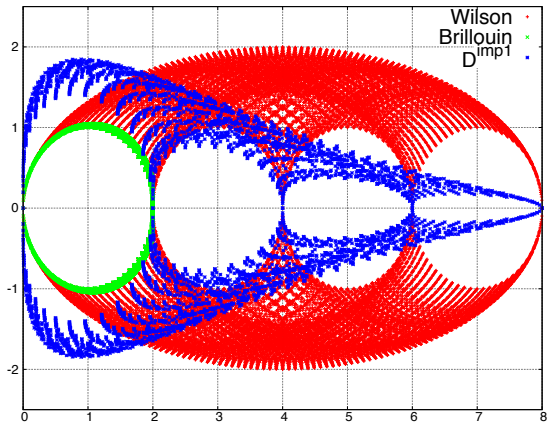

Figure 6.14: Eigenvalue spectra of D^{imp1}

consider the dispersion relation of overlap type fermions. The standard massless overlap Dirac

operator can be defined as follows.

$$D_{ov} = \frac{1}{Ra}\left[1 + X\frac{1}{\sqrt{X^\dagger X}}\right], \tag{6.60}$$

where X denotes the massless Wilson Dirac operator with a large negative mass. On the momentum space, the Wilson kernel $X(p)$ can be written as

$$\begin{aligned} X(p) &= aD_w(p) - \rho \\ &= i\sum_\mu \gamma_\mu \alpha_\mu(p) + \beta(p) \end{aligned} \tag{6.61}$$

$$\alpha_\mu(p) = -i\tilde{\nabla}^{std}_\mu(p), \tag{6.62}$$

$$\beta(p) = -\frac{r}{2}\tilde{\triangle}^{std}(p) - \rho, \tag{6.63}$$

where ρ means a kernel mass which should be positive. Thus $X^\dagger X$ is written as follows,

$$X^\dagger X = \sum_\mu \alpha_\mu(p)^2 + \beta(p)^2 \equiv \omega(p)^2. \tag{6.64}$$

One can write massless Dirac operator on the momentum space as

$$D_{ov}(p) = \frac{\rho}{\omega(p)}\left(i\not{\alpha}(p) + \omega(p) + \beta(p)\right) \tag{6.65}$$

Here we introduce the effective operator D_c which is anti-commute with γ_5.

$$D_c = D_{ov}\left(1 - \frac{a}{2\rho}D_{ov}\right)^{-1} \tag{6.66}$$

$$\{D_c, \gamma_5\} = 0 \tag{6.67}$$

$$\psi_c = \left(1 - \frac{a}{2\rho}D_{ov}\right)\psi \tag{6.68}$$

$$\bar{\psi}_c = \bar{\psi} \tag{6.69}$$

Then the fermion action is invariant.

$$S_F = \int d^4x d^4y \bar{\psi} D_{ov} \psi = \int d^4x d^4y \bar{\psi}_c D_c \psi_c \tag{6.70}$$

This operator is non-local exactly, however this Dirac operator has a continuum like property. The massive overlap operator $D_{ov}(m)$ is given by

$$\begin{aligned} D_{ov}(m) &= (D_c + m)\left(1 - \frac{a}{2\rho}D_{ov}\right) \\ &= D_{ov} + m\left(1 - \frac{a}{2\rho}D_{ov}\right) \end{aligned} \tag{6.71}$$

Thus the massive overlap Dirac operator can be written as

$$D_{ov}(m) = \frac{1}{2\omega(p)}\left[(2\rho a - ma)\, i\not{\alpha}(p) + 2\rho\left\{\omega(p) + \beta(p)\right\} + am\left\{\omega(p) - \beta(p)\right\}\right] \tag{6.72}$$

Then the dispersion relation of the massive overlap operator is expressed as (6.73).

$$4(\rho a)^2\left\{\omega(p) + \beta(p)\right\} + (ma)^2\left\{\omega(p) - \beta(p)\right\} = 0 \tag{6.73}$$

If one solve the energy at $\overrightarrow{p} = 0$ and expand up to a^5, we obtain a following relation

$$(Ea)^2 = (ma)^2 + \frac{1}{6}(ma)^4, \tag{6.74}$$

where $\rho a = 1.0$ is chosen. Then we see that $O(a^{2n+1})$ discretization effects for the integer n is suppressed in the case of overlap fermions. For finite spacing momentum, we calculate the dispersion relation numerically in the massive case and the massless case at $\rho a = 1.0$ for overlap type fermions. For the overlap fermions of Brillouin kernel , we choose

$$\alpha_\mu(p) = -i\tilde{\nabla}^{iso}_\mu(p), \tag{6.75}$$

$$\beta(p) = -\frac{r}{2}\tilde{\triangle}^{bri}(p) - \rho. \tag{6.76}$$

In this case, the energy at tree-level at $\overrightarrow{p} = 0$ is completely same with standard overlap fermions, even though the value differ from the standard overlap fermion when finite $\overrightarrow{p}$ are taken. For finite $\overrightarrow{p}$, the dispersion relation of the overlap operator of Brillouin kernel can be shown as follows. For $O(a^2)$ improvement of the overlap fermion, one may think that we can employ improved action as a kernel of the action, however actually it is not straightforward as mentioned in [26]. Let us show discretization effects for the standard overlap fermion with improved Brillouin kernel. For the improved kernel,

$$\alpha_\mu(p) = -i(1 - \frac{a^2}{12}\tilde{\triangle}^{bri}(p))\tilde{\nabla}^{iso}_\mu(p)\,(1 - \frac{a^2}{12}\tilde{\triangle}^{bri}(p)), \tag{6.77}$$

$$\beta(p) = c_{imp}\left(\tilde{\triangle}^{bri}(p)\right)^2 - \rho, \tag{6.78}$$

are chosen and the energy solution can be shown as

$$(Ea)^2 = (ma)^2 - \frac{1}{2}(ma)^4, \tag{6.79}$$

which still has an $O(a^2)$ discretization error which comes from the leading term of $\alpha_\mu(p)$ in the $\omega(p)$. Then we may advance a subsequent step on $O(a^2)$ improvement as proposed in [26] which will be discussed in next section. Here we compare the dispersion relation of the overlap operator of Wilson kernel and Brillouin kernel with the Wilson fermion and the Brillouin fermion at figure6.17, where we chose a spacing momentum proportional to $(1, 1, 1)$. From figure6.17, one observe that the overlap operator with Brillouin kernel has a continuum like property more than the Brillouin operator, particularly at the massive case. We can think that this continuum like property is

due to the chiral symmetry which can suppress $O(a)$ discretization effects. Also we find that the standard overlap fermion remove such as discretization errors which can be shown at low momentum $\overrightarrow{p}$ region. However the dispersion relation of the standard overlap fermion deviate from the continuum theory around at $pa \sim 0.5$ as the Wilson fermion. Here we see that overlap fermion can be employed to reduce discretization effects, especially the Brillouin overlap fermion has an excellent dispersion relation.

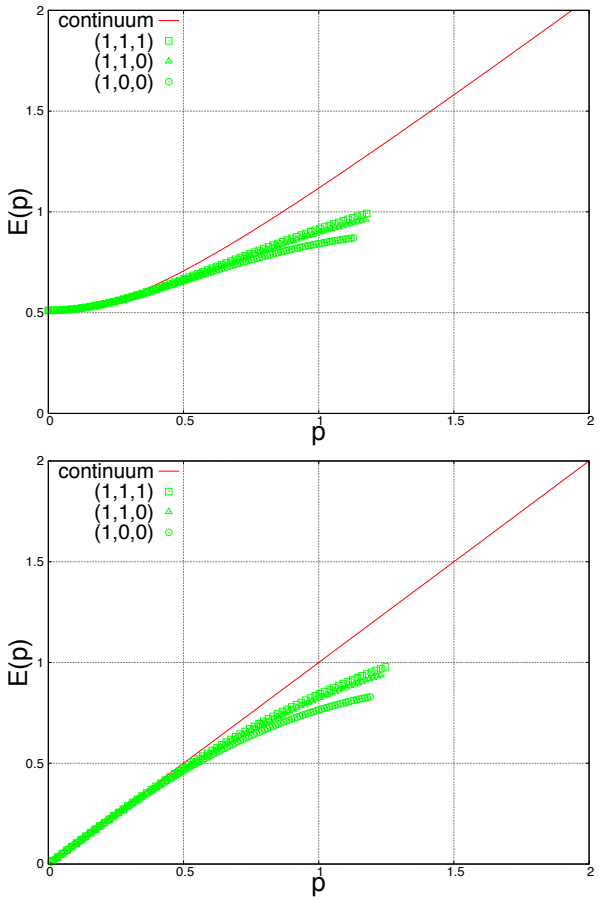

Figure 6.15: Dispersion relations of the overlap Dirac operator with Wilson kernel

6.5 $\mathcal{O}\left(a^2\right)$ improvement for the overlap-type fermion

We have shown discretization effects for the overlap fermion of the Brillouin kernel. If one improves $O(a^2)$ discretization errors within the overlap formulation, we obtain a highly improved action of

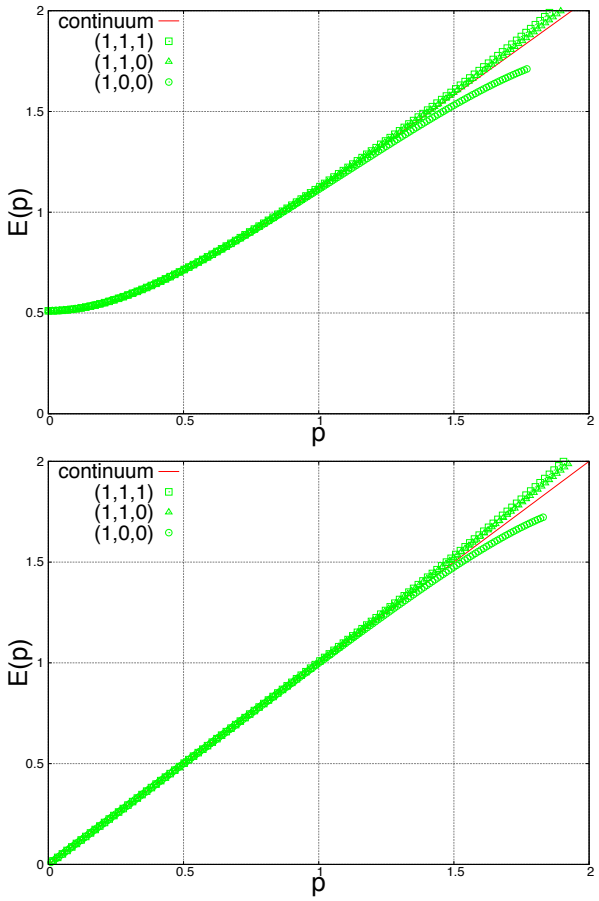

Figure 6.16: Dispersion relations of Brillouin overlap operator

which discretization effects start from $O\left(a^4\right)$. For the purpose, following $O(a^2)$-improved overlap-Dirac operator have been suggested by using the effective operator D_c in [26]

$$D_c^{imp} = D_c + \frac{a^2}{4\rho} D_{ov}^{\dagger} D_{ov} D_c, \tag{6.80}$$

which has been discussed in chapter 5. This operator has a continuum like chiral symmetry as (6.68)$\{D_c^{imp}, \gamma_5\} = 0$ and the massive improved overlap is defined as

$$\begin{aligned} D_{ov}^{imp}(m) &= \left(D_c^{imp} + m\right)\left(1 - \frac{a}{2\rho} D_{ov}\right) \\ &= m + \left(1 - \frac{am}{2\rho}\right) D_{ov} + \frac{a^2}{2\rho} D_{ov}^{\dagger} D_{ov}^2. \end{aligned} \tag{6.81}$$

Again, in terms of $\alpha_\mu(p), \beta(p), \omega(p)$, the operator can be written as

$$\begin{aligned} a D_{ov}^{imp}(m) = \frac{1}{2\omega(p)^2} &[\{\rho(3\omega(p) + \beta(p)) - am\omega(p)\} i\not{\alpha}(p) \\ &+ \{\rho(3\omega(p) + \beta(p))(\omega(p) + \beta(p)) + am\omega(p)(\omega(p) - \beta(p))\}], \end{aligned} \tag{6.82}$$

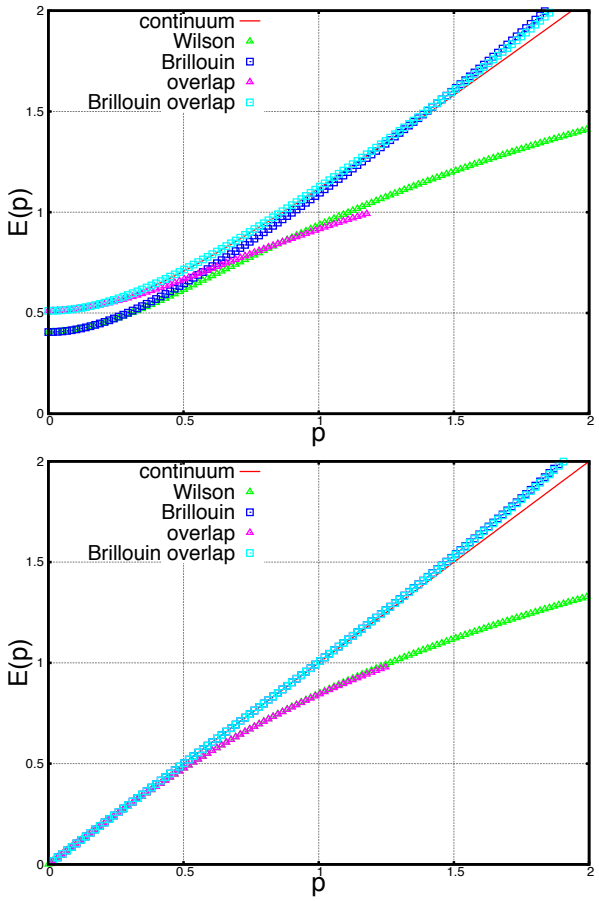

Figure 6.17: Comparison of dispersion relations for various type Dirac operators. (Wilson, Brillouin, standard overlap, Brillouin overlap)

and also the dispersion relation of improved overlap operator can be shown

$$\rho^2 \left\{3\omega\left(p\right)+\beta\left(p\right)\right\}^2 \left\{\omega\left(p\right)+\beta\left(p\right)\right\}+a^2m^2\omega\left(p\right)^2\left\{\omega\left(p\right)-\beta\left(p\right)\right\}=0. \tag{6.83}$$

We calculate the dispersion relation for improved Dirac operator which kernel is improved Brillouin operator numerically the same way with previous section as shown at figure (6.18). From this figure, we see that the dispersion relation for the action is very continuum like up $a\overrightarrow{p} \sim 1.5$ in both of case of massless and massive. We can expect that this action has $O\left(a^4\right)$ scaling at tree-level because of our improvement and the chiral symmetry: $O\left(\alpha_s\left(am\right)^2,\left(am\right)^4\right)$. In actual, if one the expand energy up to $O\left(a^5\right)$, we obtain at $a\overrightarrow{p}=0$

$$\left(Ea\right)^2=\left(ma\right)^2+O\left(a^6\right). \tag{6.84}$$

Expansions of the energy for various Dirac operators are summarized at table (6.2). Finally we compare various Dirac operators via the dispersion relation at figure(6.19): Wilson, Brillouin, improved Brillouin, standard overlap, Brillouin overlap, improved overlap operator with improved Brillouin kernel. However differences between different Dirac operator are invisible in this scale. Figure6.20 is magnified figure of figure6.19($ma=0.5$case). From these comparison, we conclude

that a most improved action is improved overlap fermions with improved Brillouin kernel which is $O(a^2)$-improved at tree-level. Note that in general the overlap procedure is expensive for feasible lattice calculation, thus we do not extend our studies of the overlap action with some kernels for one-loop and non-perturbative calculation. Also one may employ the domain-wall fermion instead of the overlap fermion as improvement. If one reduce the residual mass sufficiently, remaining $O(a)$ discretization effect can be neglected. Note that the Brillouin kernel may be able to reduce cost of the overlap procedure, because eigenvalue of the Dirac operator is very close to the overlap Dirac operator's one.

overlap type	kernel type	$E^2(\vec{0}, m)$ (ρ=1.0)
standard	wilson	$m^2 + \frac{m^4}{6} + O(a^4)$
standard	Brillouin	$m^2 + \frac{m^4}{6} + O(a^4)$
standard	improved Brillouin	$m^2 - \frac{1}{2}m^4 + O(a^4)$
improved	improved Brillouin	$m^2 + O(a^4)$

Table 6.2: The energy of various overlap type fermions

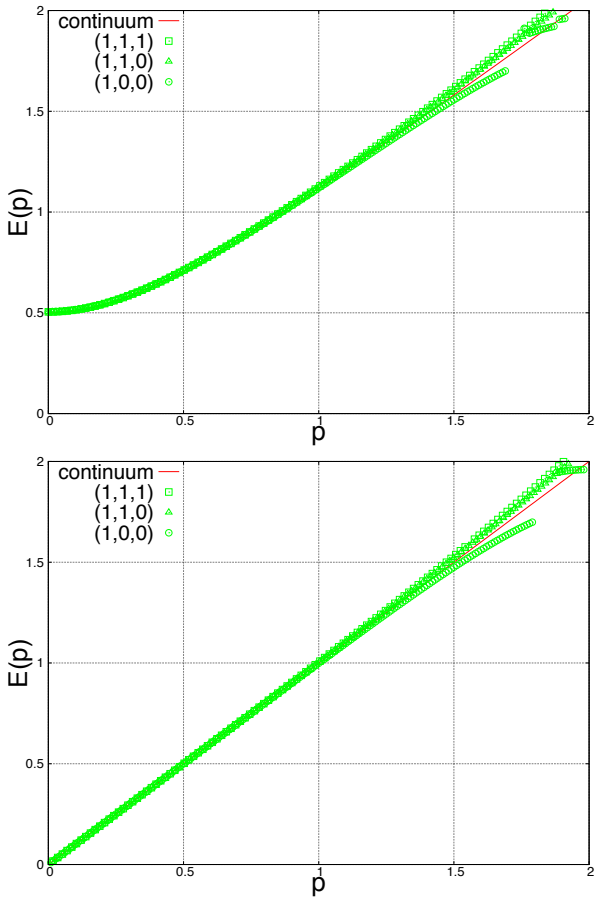

Figure 6.18: Dispersion relations for the improved overlap operator of the improved Brillouin kernel

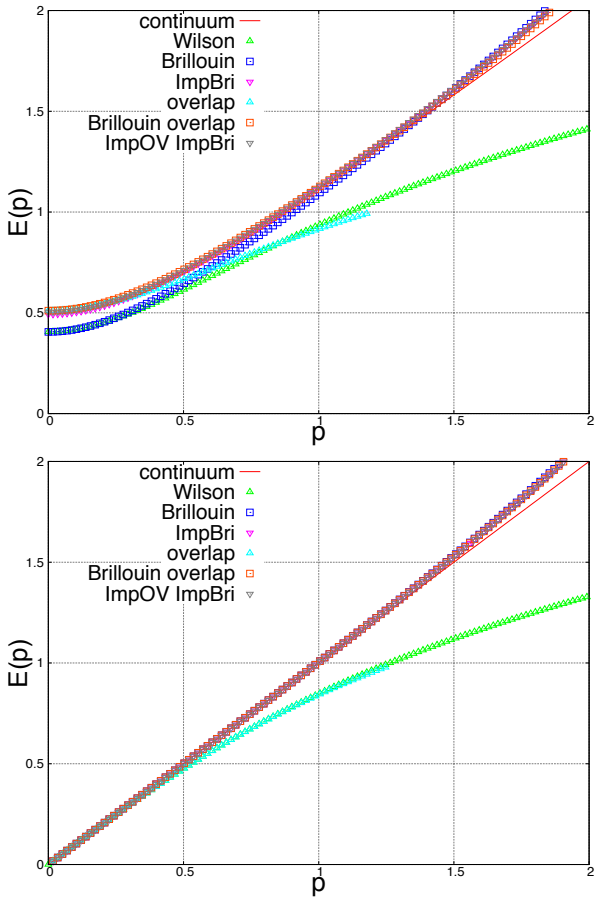

Figure 6.19: Dispersion relations for various Dirac operators

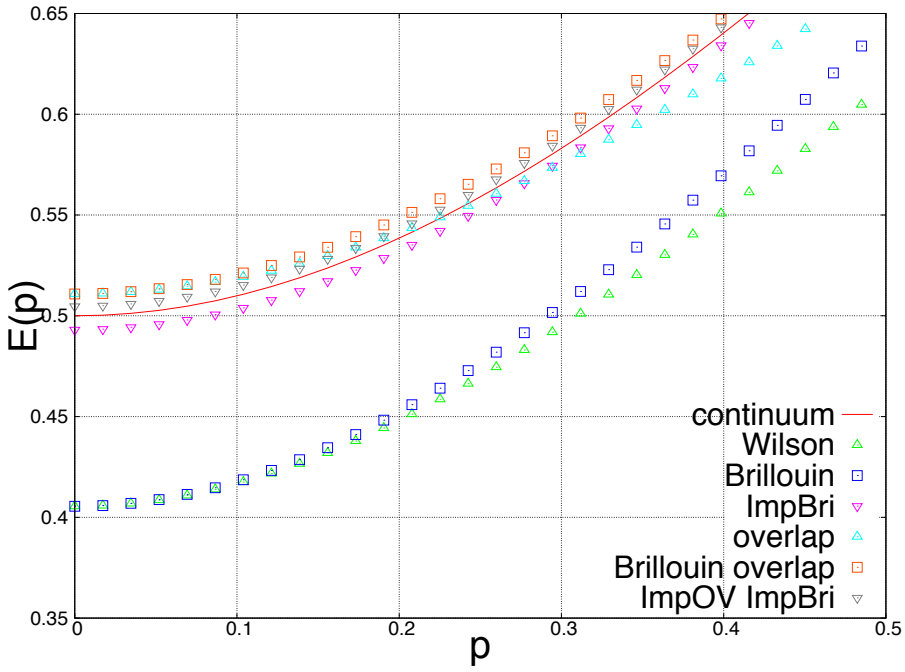

Figure 6.20: a magnified figure of the figure6.19

Chapter 7

Scaling studies on the quenched configurations

In previous section, we have explored various possibilities of Symanzik improvements for the Brillouin fermion. Here we concentrate on the improved action Eq. (6.51) and demonstrate non-perturbative scaling studies of it against existing other formulations on the quenched configurations. We are interested in scaling of heavy-heavy or heavy-light quantities as a function of lattice spacing. Here we focus on heavy-heavy quantities: speed-of-light, hyperfine splitting and decay constant.

7.1 Simulation details

We carry out scaling studies on quenched configurations. Quenched ensembles are generated by the Southampton group[58]. We employ the tree-level Symanzik gauge action [32, 33] and the improved Brillouin fermion action Eq. (6.51). Here for the tunable parameter of the improved action $c_{imp} = 1/8$ is chosen. Physical length of all lattices is kept fixed to $L \approx 1.6fm$ to avoid different finite volume effects. For comparison of fermion actions, we also employ the naive Wilson fermion and the generalized Domain-wall fermion which respectively have $O(a)$ and $O(a^2)$ discretization errors.

For the domain-wall fermion, the JLQCD collaboration has investigated a parameter set which give $m_{res} = 0.1 - 0.5[MeV]$:$b = 2$, $c = 1$ for the Moebius kernel with the stout smearing $N_{smr} = 3$ [59, 60, 46]. In this scaling study, length of the fifth dimension $Ls = 8$ and domain-wall height $M_0 = -1$ are chosen. We expect that good chiral symmetry guarantees small $O(a)$ discretization effect. Computational code is implemented on the Iroiro++ package[61].

For comparison among different Dirac operators, we tune quarks masses so that the pseudo-scalar meson mass become $m_{ps} = 1.0, 1.5, 2.0, 2.5, 3.0$ and 3.5 [GeV]. Table. 7.2 shows parameters used in this simulations. To be specific, after roughly tuning quark masses we have interpolated to aimed meson mass scale as function of the bare quark mass. In order to reduce uncertainty about interpolation, we have connected linearly between nearest two mass points. Source function is set to the smeared source $e^{-\alpha|x-y|}$ of which a parameter α can be tuned for every masses and scales. For all measurements we calculate heavy-heavy meson correlators with 4 different source points in time direction.

Here we show effective masses for every Dirac operators at Figs. 9.1-9.45. Lines show fitted

L/a	β	N_{HB}	N_{sep}	a^{-1} [GeV]
16	4.41	10000	100	2.0(07)
24	4.66	20000	200	2.81(09)
32	4.89	60000	500	3.80(12)

Table 7.1: Quenched configurations

values and fit-ranges in Figs. 9.1-9.36. On the other hand, filed dots represents fit-ranges in Figs. 9.37-9.45 and effective masses for $\langle AA \rangle$, $\langle AP \rangle$ and $\langle PP \rangle$ are plotted simultaneously in these figures. For more details, please see the later section. Also we note that effective masses of the improved Brillouin operator behave differently compared with others at small time slices. It is interpreted that this shape is an effect of additional doublers which may interfere the physical pole. As we see in later chapter, the improved action has the unphysical poles in the time direction and it may appear at small t regions. However in effective mass plots there seem to be not serious problems at large time slices which is used for extracting the energy.

7.2 Scale setting

In this section, we mention to our scale setting. Lattice spacing is determined through w_0 in terms of the Yang-Mils gradient flow [54, 53]. Here we use the Wilson flow and employ the value $w_0 = 0.1755(18)(04)$ fm [54], but this w_0 value has been estimated in $N_f = 2 + 1$ simulations. Thus here we did not take into account a systematic effect due to the quenching. Evolution of the w_0 on each lattices are plotted in Figs 7.1, 7.2 and 7.3. Furthermore we have computed $t_0^{1/2}$ in terms of the Wilson flow. Bottom of Fig. 7.7 describes scaling of ratio $t_0^{1/2}/w_0$ against a/w_0. Here we observe good scaling of the ratios, which means that the choice of $t_0^{1/2}$ or w_0 is not substantial for scale setting in current configurations. In addition, we have double-checked from the Sommer scale r_0 by calculating the static quark potential which are shown Figs. 7.4, 7.5 and 7.6. In this calculation, we have applied 10-20 times smearing which is introduced in Ref. [62] to suppress the UV fluctuations and computed the Wilson loops in various directions which is expressed as different symbols in Figs.7.4-7.6. We summarize our measurement of w_0/a, t_0/a^2 and r_0/a for all three lattices at Table. 7.3. Moreover we display scaling of ratio for r_0 and w_0 or $t_0^{1/2}$ at top of Fig. 7.7. From this scaling, very mild dependence is observed both of $r_0/t_0^{1/2}$ and r_0/w_0 . Note that we finally chose the values of lattice spacing which are determined from the w_0.

$m_{1S}[GeV]$	Dirac ops	$L/a = 16$		$L/a = 24$		$L/a = 32$	
		ma	α_{smr}	ma	α_{smr}	ma	α_{smr}
	Wilson	1.038	1.12	0.4946		0.2929	
3.5	Improved Brillouin	0.6675	1.12	0.4517	0.56	0.316	0.4
	Domain-wall	0.728	0.38	0.495		0.3446	
	Wilson	0.69		0.35		0.2	
3.0	Improved Brillouin	0.55	1.0	0.36	0.5	0.25	0.37
	Domain-wall	0.6		0.398		0.2785	
	Wilson	0.45		0.2102		0.1105	
2.5	Improved Brillouin	0.416	0.84	0.268	0.45	0.184	0.3
	Domain-wall	0.465		0.303		0.2115	
	Wilson	0.2125		0.1		0.0267	
2.0	Improved Brillouin	0.2808	0.8	0.1705	0.4	0.119	0.25
	Domain-wall	0.3305		0.2154		0.149	
	Wilson	0.0361		-0.0197		-0.061	
1.5	Improved Brillouin	0.1428	0.7	0.0789	0.35	0.059	0.15
	Domain-wall	0.191		0.1264		0.0765	
	Wilson	-0.1554		-0.1447		-0.1180	
1.0	Improved Brillouin	0.0182	0.63	-0.0157	0.3	-0.0036	0.12
	Domain-wall	0.0555		0.0408		0.012	

Table 7.2: Parameters: α_{smr} is a smearing parameter of $e^{-\alpha_{smr}r}$, ma denotes a bare quark mass which is not taken into account critical quark mass. Here ma of Wilson-type Dirac operator may take the minus value.

L/a	β	w_0/a	t_0/a^2	r_0/a
16	4.41	1.767(3)	3.099(16)	5.12(10)(5)
24	4.66	2.499(8)	6.050(26)	7.16(36)(5)
32	4.89	3.374(11)	10.948(37)	9.46(23)(5)

Table 7.3: w_0/a, t_0/a^2 and r_0/a for all three lattices.

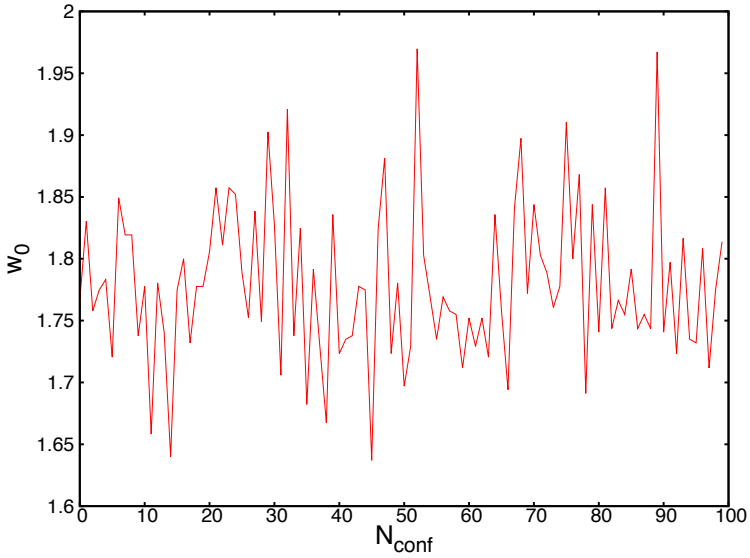

Figure 7.1: The evolution of the Wilson flow parameter w_0 for each configurations at $L/a = 16$ lattice.

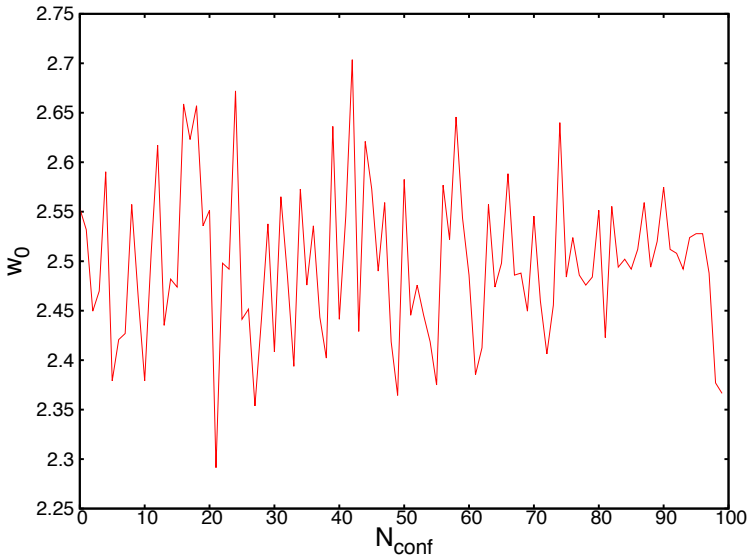

Figure 7.2: The evolution of the Wilson flow parameter w_0 at $L/a = 24$ lattice.

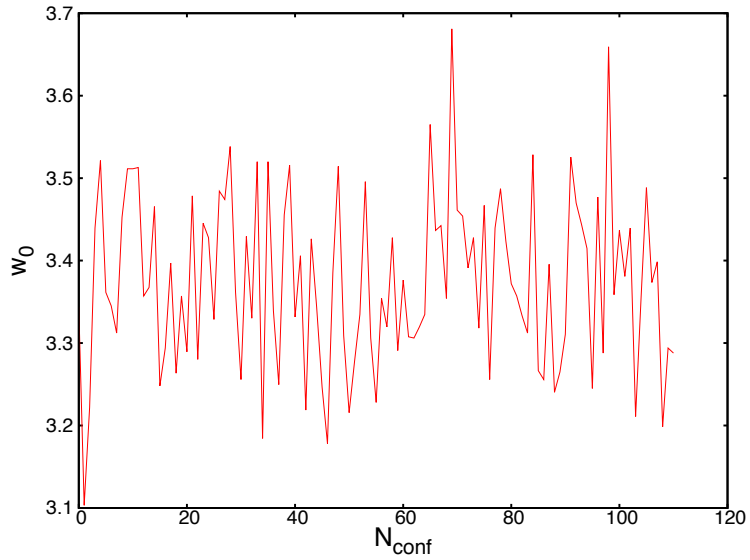

Figure 7.3: The evolution of the Wilson flow parameter w_0 at $L/a = 32$ lattice.

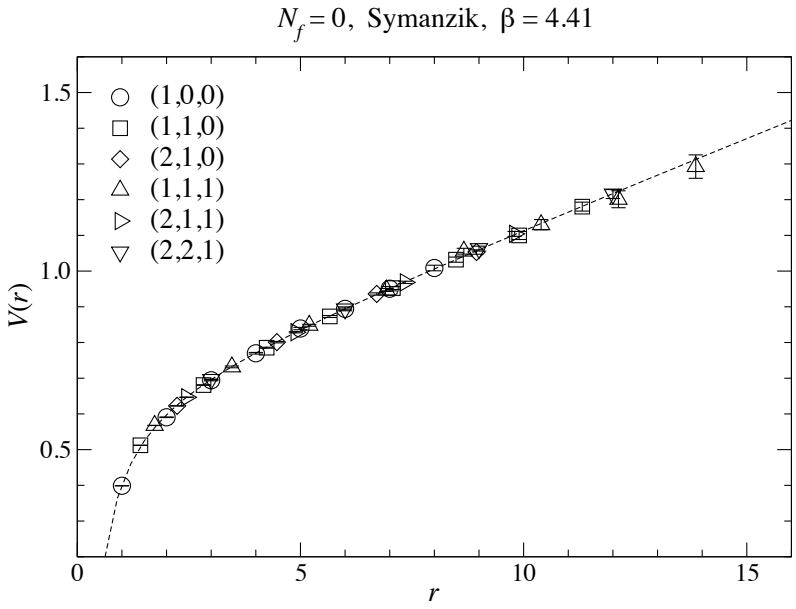

Figure 7.4: The static quark potential at $L/a = 16$ lattice.

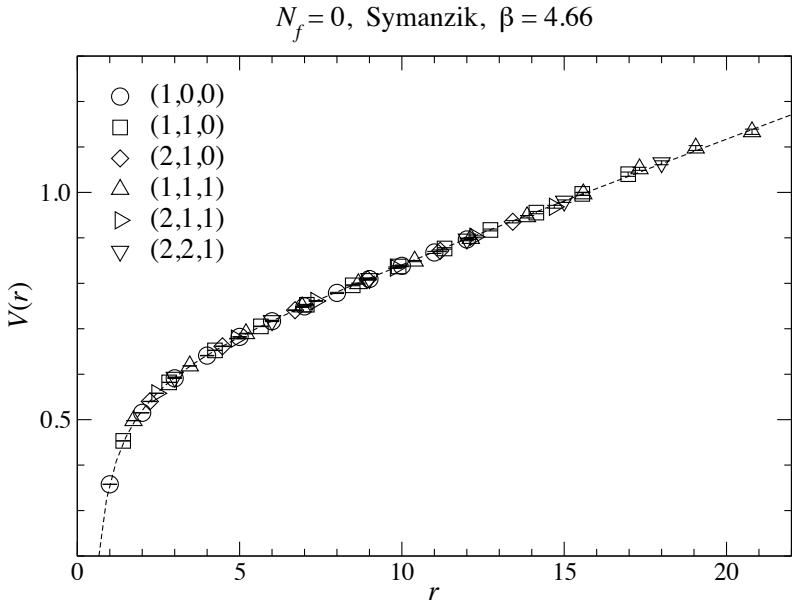

Figure 7.5: The static quark potential at $L/a = 24$ lattice.

7.3 Speed-of-light

Speed-of-light is defined as

$$c_{eff}^2(p) = \frac{E^2(\overrightarrow{p}) - E^2\left(\overrightarrow{0}\right)}{\overrightarrow{p}^2} \tag{7.1}$$

which should be unity in continuum theory. This is one of interested quantities at heavy quark region to see discretization effect. In actual, the speed-of-light is almost equivalent to the dispersion relation. In previous section, we have investigated various dispersion relations for quark. Here we measure the dispersion relation(or the speed-of-light) for mesons. For our purpose, one calculate two point correlation functions for various momenta as

$$C(t, \overrightarrow{p}) = \sum_{\overrightarrow{x}} \left\langle M(\overrightarrow{x}, t)\, \overline{M}\left(\overrightarrow{0}, 0\right)\right\rangle e^{i\overrightarrow{p}\,\overrightarrow{x}}. \tag{7.2}$$

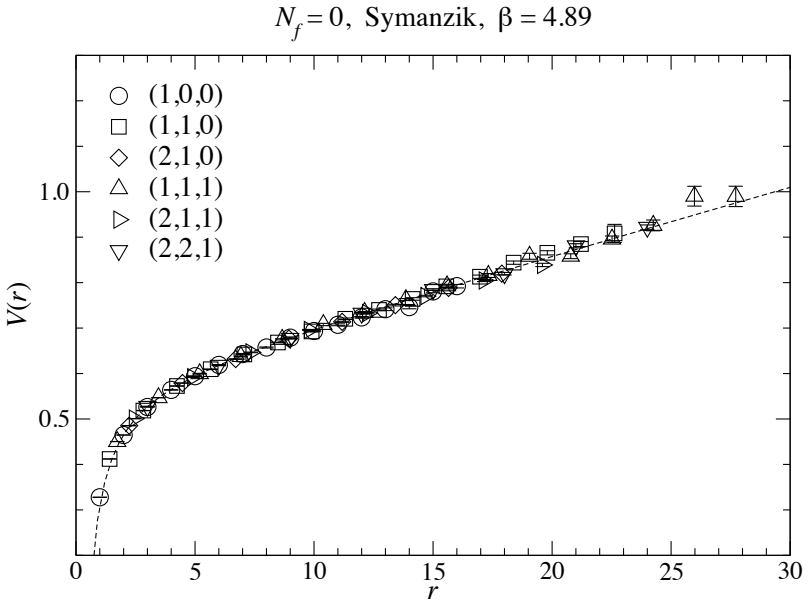

Figure 7.6: The static quark potential at $L/a = 32$ lattice.

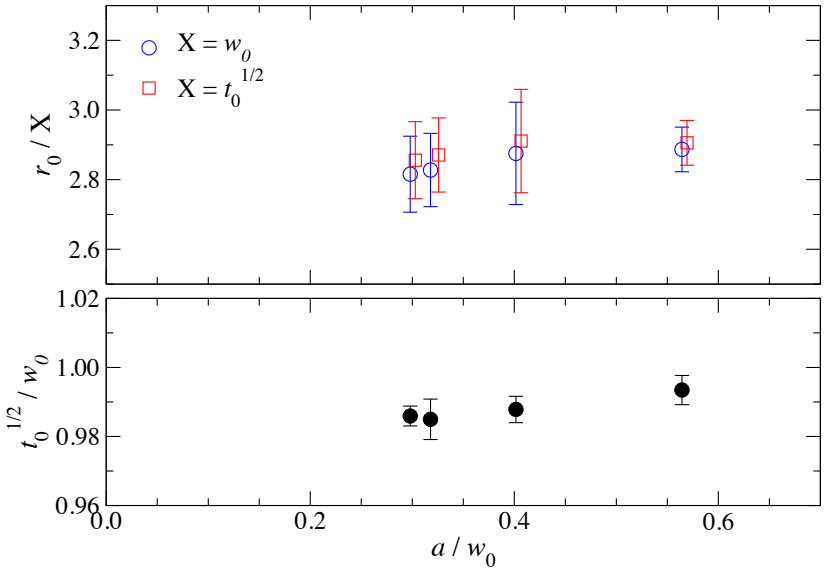

Figure 7.7: Ratio of the r_0 scale and the w_0 scale or the $t_0^{1/2}$ scale.

meson(orbit)	J^{PC}	operator	mass[GeV](experiment)
$\eta_c(1S)$	0^{-+}	$\overline{\psi}_c\gamma_5\psi_c$	2.980(1)
$J/\psi(1S)$	1^{--}	$\overline{\psi}_c\gamma_i\psi_c$	3.097(0)
$\chi_{c0}(1P)$	0^{++}	$\overline{\psi}_c\psi_c$	3.415(0)
$\chi_{c1}(1P)$	1^{++}	$\overline{\psi}_c\gamma_i\gamma_5\psi_c$	3.511(0)
$h_c(1P)$	1^{+-}	$\overline{\psi}_c\gamma_i\gamma_j\psi_c$	3.525(0)

Table 7.4: charmonium

Here the meson operator $M\left(\overrightarrow{x},t\right)$ can be taken operators as shown at table7.4. If we take into account to summation over momenta $p_i = \cdots, -2, -1, 0, 1, 2, \cdots$, we can write down as follows

$$C\left(t,\overrightarrow{p}\right) = \sum_{\overrightarrow{x}} \cos\left(p_1x_1\right)\cos\left(p_2x_2\right)\cos\left(p_3x_3\right)\left\langle M\left(\overrightarrow{x},t\right)M\left(\overrightarrow{0},0\right)\right\rangle. \tag{7.3}$$

The table shows operators and corresponding charmonium with experimental values. In this studies, we assume that quark masses are degenerated. We are able to obtain the energy from the exponential tail of Euclidean correlators and extract effective speed-of-light of the form (7.1). At the coarsest lattice, the speed-of-light is estimated as Fig. 7.8, where left panel is a results of $m_{ps} = 1.5GeV$ and right one denotes $m_{ps} = 3.0GeV$. Also at both of figure, red dots correspond to data based on the Wilson fermion, blue dots are the domain-wall fermion and magenta shows the improved Brillouin fermion. From this figure, we see that the improved Brillouin is very close to the unity, though the Wilson fermion and the domain-wall fermion are quite far from the unity, especially at $m_{ps} = 3.0[GeV]$. It is a typical advantage of the Brillouin fermion. We show scaling of speed-of-light in Fig.7.9 for $m_{ps} = 3.0$GeV and three momenta $|p|^2\left(L/2\pi\right)^2 = 1, 2, 3$ against a[fm]. Then very mild dependence against lattice spacing is observed when the improved action is employed. Here let us estimate scaling properties by fitting the data with some ansatz. The results are summarized in Tables. 7.5 ,7.6 and 7.7. For the Wilson fermion, we use the ansatz $f\left(a\right) = 1 + c_1a + c_2a^2$, whereas $f\left(a\right) = 1 + c_2a^2 + c_3a^4$ is employed for the domain-wall fermion. The improved action has $O\left(\alpha_s a\right)$ and $O\left(\alpha_s a^2\right)$ effect, thus we should adopt $f\left(a\right) = 1 + c_1a + c_2a^2$. However this choice leads unreasonably large coefficient. Therefore here we adopt an arbitary choice $f\left(a\right) = 1 + c_2a^2 + c_3a^3$. Note that our fittings are not so systematic way and thus we do not have a strong opinion about these scaling ansatz. It may be chosen by an alternative function. To end this, we may increase lattice spacing data points and try to fit as various functions. However we do not attempt to do such thing for the moment. If we assume that above fitting functions we see that the c_2 coefficient of the improved action is smaller than other formalisms. Therefore here we conservatively conclude that scaling of the improved action is good.

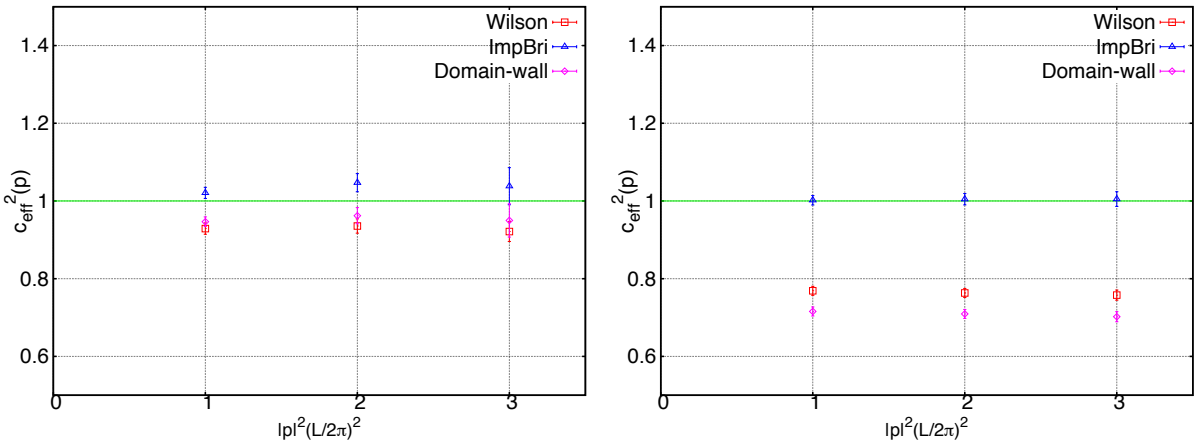

Figure 7.8: The speed-of-light with $a^{-1} = 1.973GeV$

Dirac operators	c_1	c_2	c_3	c_4
Wilson	0.005	-1.0	-	-
improved Brillouin	-	0.4	-0.8	-
domain-wall	-	-1.0	-	-0.7

Table 7.5: Fitting results for the data of speed-of-light at $|p|^2(L/2\pi)^2 = 1$, where the used ansatz is $f(a) = 1 + c_1 a + c_2 a^2$ for the Wilson fermion, $f(a) = 1 + c_2 a^2 + c_3 a^3$ for the improved action and $f(a) = 1 + c_2 a^2 + c_4 a^4$ for the domain-wall fermion. Then $\chi^2/d.o.f = 0.003$.

7.4 Hyperfine splitting

Hyperfine splitting $m_V - m_{PS}$ is also an interesting quantity for heavy quarks and has been investigated on various lattice actions. As is well-known (e.g. see[63, 64]), the charmonium hyperfine splitting strongly depends on the choice of Dirac operator. It means that the hyperfine splitting is very sensitive to the discretization error. We show our results for scaling of hyperfine splitting in Figs. 7.10-7.13.

From these figures, scaling of the improved action seems mild against lattice spacings. Here again let estimate scaling via fitting with continuum ansatz. Here we use the $f\,(a) = 1 + c_1 a + c_2 a^2$ for the Wilson fermion and $f\,(a) = 1 + c_2 a^2 + c_4 a^4$ for the domain-wall fermion. For the improved action, we adopt $f\,(a) = 1 + c_1 a + c_2 a^2$. If one assumes that these ansatz, we obtain the smaller c_1 and c_2 of the improved action than other formalisms at $m_{PS} = 3.0$ GeV which indicates good scaling of the action. The results of fitting are shown in Table.7.8. Other results of fitting almost agree with this statement, though some results disagree, e.g. the c_2 coefficient of the improved

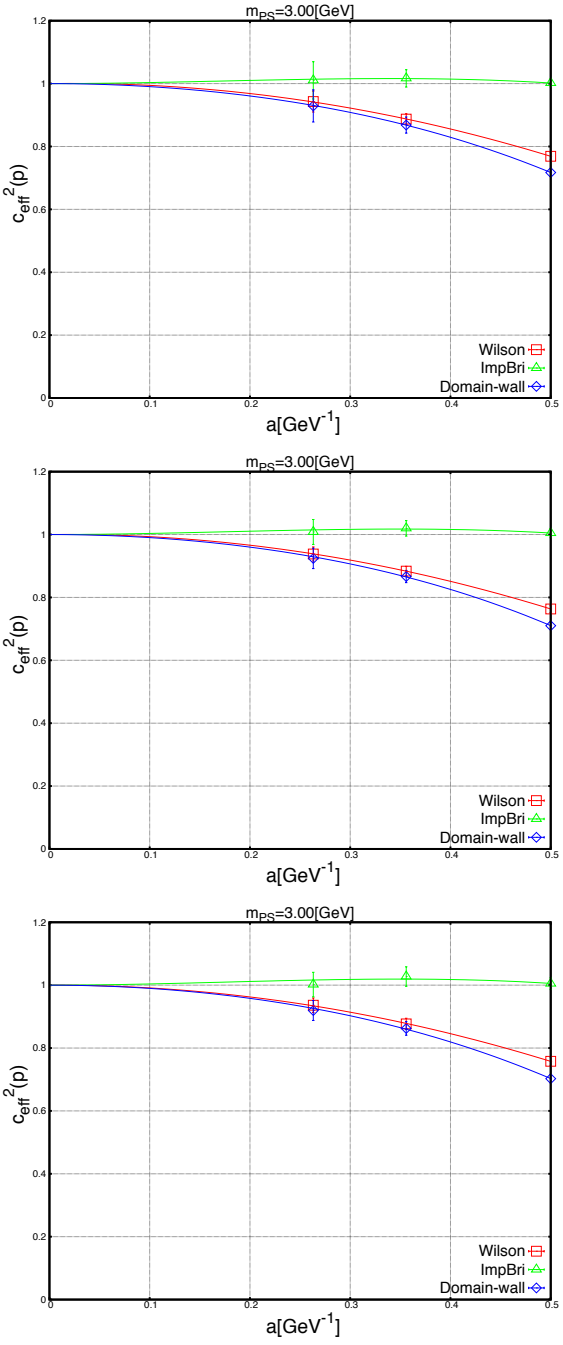

Figure 7.9: Scaling of speed-of-light against a^2

Dirac operators	c_1	c_2	c_3	c_4
Wilson	0.03	-1.0	-	-
improved Brillouin	-	0.4	-0.8	-
domain-wall	-	-1.0	-	-0.8

Table 7.6: Fitting results for the data of speed-of-light at $|p|^2(L/2\pi)^2 = 2$, where the used ansatz is $f(a) = 1 + c_1 a + c_2 a^2$ for the Wilson fermion, $f(a) = 1 + c_2 a^2 + c_3 a^3$ for the improved action and $f(a) = 1 + c_2 a^2 + c_4 a^4$ for the domain-wall fermion. Then $\chi^2/d.o.f = 0.02$.

Dirac operators	c_1	c_2	c_3	c_4
Wilson	0.01	-1.0	-	-
improved Brillouin	-	0.5	-0.9	-
domain-wall	-	-1.0	-	-0.7

Table 7.7: Fitting results for the data of speed-of-light at $|p|^2(L/2\pi)^2 = 3$, where the used ansatz is $f(a) = 1 + c_1 a + c_2 a^2$ for the Wilson fermion, $f(a) = 1 + c_2 a^2 + c_3 a^3$ for the improved action and $f(a) = 1 + c_2 a^2 + c_4 a^4$ for the domain-wall fermion. Then $\chi^2/d.o.f = 0.09$.

action at $m_{PS} = 2.0$ is not smaller than the domain-wall. However here we did not estimate statistical or systematic errors for fitting and thus we may say that this is compatible. Therefore here again we conclude that scaling of the improved action is excellent.

7.5 Decay constant

Furthermore we are interested in decay constant, since it is significant for determination of the CKM matrix elements. For decay constant studies, one has to calculate the renormalization constant Z such that $f_{PS}^{\bar{M}S} = Z f_{PS}^{lat}$. In order to avoid determining the renormalization factor, we consider a ratio of the decay constant R as

$$R = \frac{\sqrt{m_{PS}} f_{PS}}{\sqrt{m_{\rm ref}} f_{\rm ref}} \tag{7.4}$$

from the amplitude of $\langle A_4(x) A_4(0)\rangle$,$\langle P(x) P(0)\rangle$ and $\langle A_4(x) P(0)\rangle$ with a local source and a local sink, where $A_4 = \bar{\psi}\gamma_4\gamma_5\psi$. In other words, we fit these correlators simultaneously by following functions respectively

$$C_{AA}^{local-local}(t) = \frac{\left(Z_A^{local}\right)^2}{2m}\left(e^{-mt} + e^{-m(N_t - t)}\right), \tag{7.5}$$

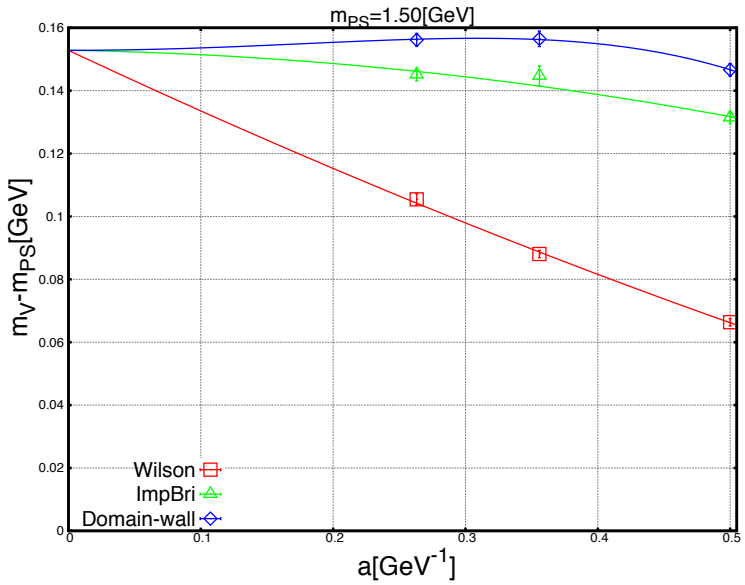

Figure 7.10: Scaling for the hyperfine splitting against a^2 at $m_{PS} = 1.5$ GeV

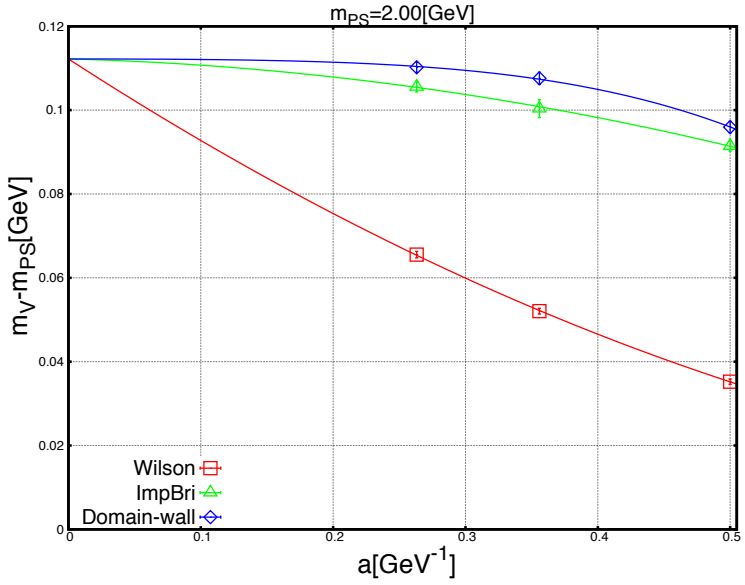

Figure 7.11: Scaling for the hyperfine splitting against a^2 at $m_{PS} = 2.0$ GeV

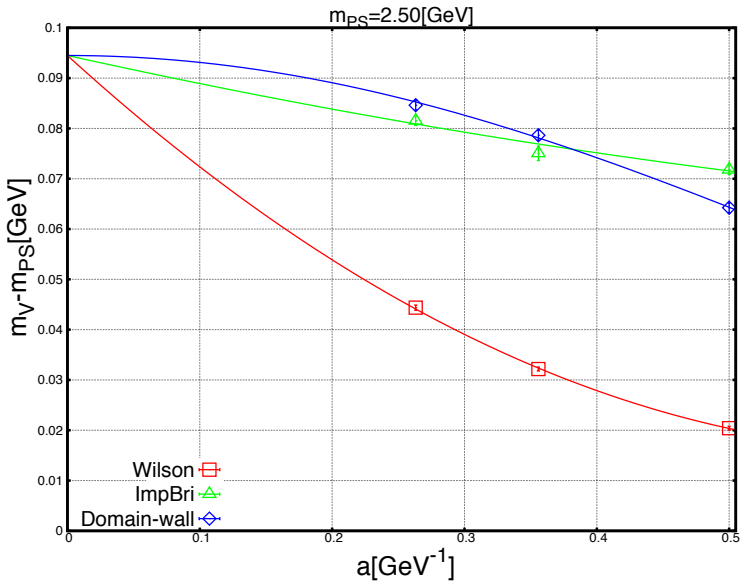

Figure 7.12: Scaling for the hyperfine splitting against a^2 at $m_{PS} = 2.5$ GeV

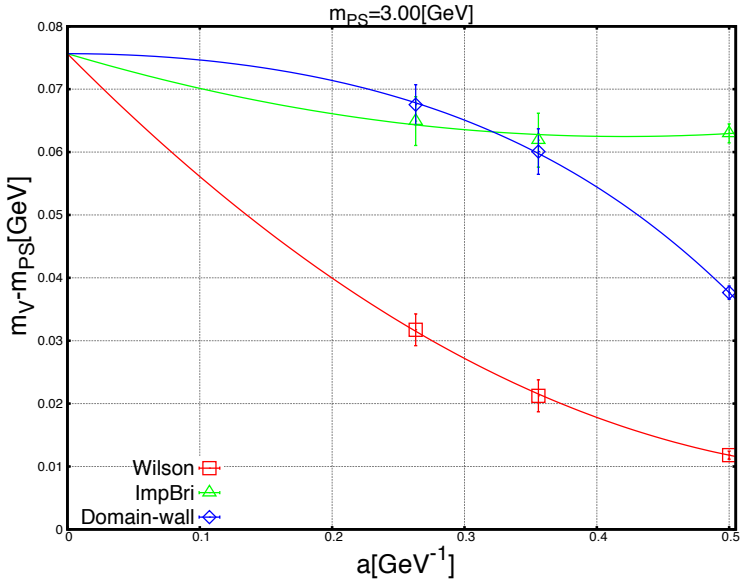

Figure 7.13: Scaling for the hyperfine splitting against a^2 at $m_{PS} = 3.0$ GeV

Dirac-operator	c_1	c_2	c_3	c_4	c_0
$m_{PS} = 1.5$ GeV					$\chi^2/d.o.f = 1.1$
Wilson	-0.2	0.05	-	-	0.153
improved Brillouin	0.007	-0.07	-	-	
domain-wall	-	-0.08	-	-0.4	
$m_{PS} = 2.0$ GeV					$\chi^2/d.o.f = 0.1$
Wilson	-0.2	0.1	-	-	0.112
improved Brillouin	-0.008	-0.07	-	-	
domain-wall	-	-0.01	-	-0.2	
$m_{PS} = 2.5$ GeV					$\chi^2/d.o.f = 1.7$
Wilson	-0.2	0.2	-	-	0.094
improved Brillouin	-0.06	0.02	-	-	
domain-wall	-	-0.1	-	-0.07	
$m_{PS} = 3.0$ GeV					$\chi^2/d.o.f = 0.05$
Wilson	-0.2	0.2	-	-	0.076
improved Brillouin	-0.06	0.07	-	-	
domain-wall	-	-0.1	-	-0.2	

Table 7.8: Fitting results for the data of the hyperfine splitting, where the used ansatz is $f(a) = 1 + c_1 a + c_2 a^2$ for the Wilson fermion and the improved action and $f(a) = 1 + c_2 a^2 + c_4 a^4$ for the domain-wall fermion.

$$C_{AP}^{local-local}(t) = \frac{Z_A^{local} Z_P^{local}}{2m} \left(e^{-mt} + e^{-m(N_t - t)}\right), \tag{7.6}$$

$$C_{PP}^{local-local}(t) = \frac{\left(Z_P^{local}\right)^2}{2m} \left(e^{-mt} + e^{-m(N_t - t)}\right). \tag{7.7}$$

We illustrate scaling of the decay constant ration at Figs. 7.14,7.15,7.16 and 7.17 and also attempt to fit all data simultaneously by $R(a) = c_0 + c_1 a + c_2 a^2$, however for the domain-wall fermion $R(a) = c_0 + c_2 a^2 + c_4 a^4$ is employed. The results are shown in Table 7.9. Here one observes that the coefficient c_1 for the improved action is slightly smaller than Wilson's c_1 in particular at heavy mass regions, but c_2 of the improved action is compatible with c_2 of the Wilson fermion. Then we may conclude that $\alpha_s a$ and $\alpha_s a^2$ are not small contributions for the improved action and thus one may advance one-loop or non-perturbative level improvement. However our fittings are not so reliable, because we did not estimate errors and did not take into account correlations between data. Also for the decay constant we did not estimate systematic errors for choosing fit-ranges,

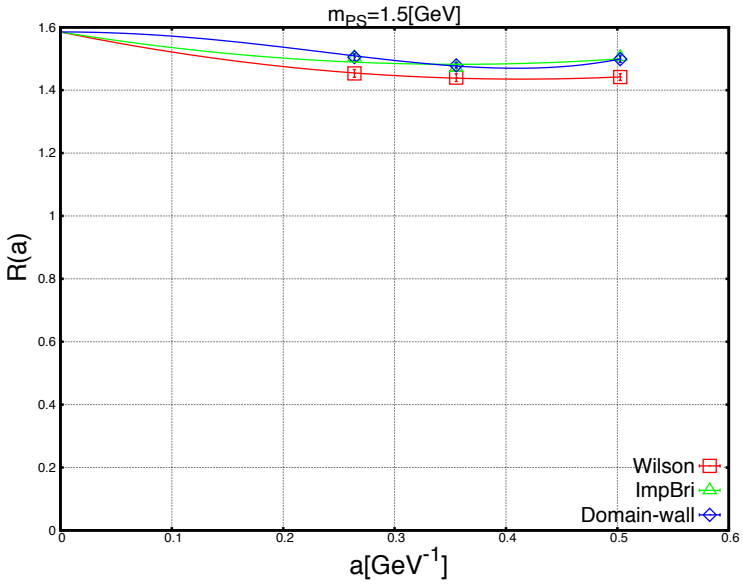

Figure 7.14: Scaling of the decay constant ratio against a at $m_{PS} = 1.5$ GeV.

though it has been done for the both of speed-of-lights and hyperfine splitting. Furthermore as we discuss in later chapter, the improved action has unphysical temporal doublers, thus it may corrupt the physical poles. Then for instance, we may discard data of the coarsest lattice. Also it may be a good idea to calculate more finer lattice and then we may are able to reveal whether its scaling is correct. For discussion of the unphysical poles of the improved action, please see the last chapter.

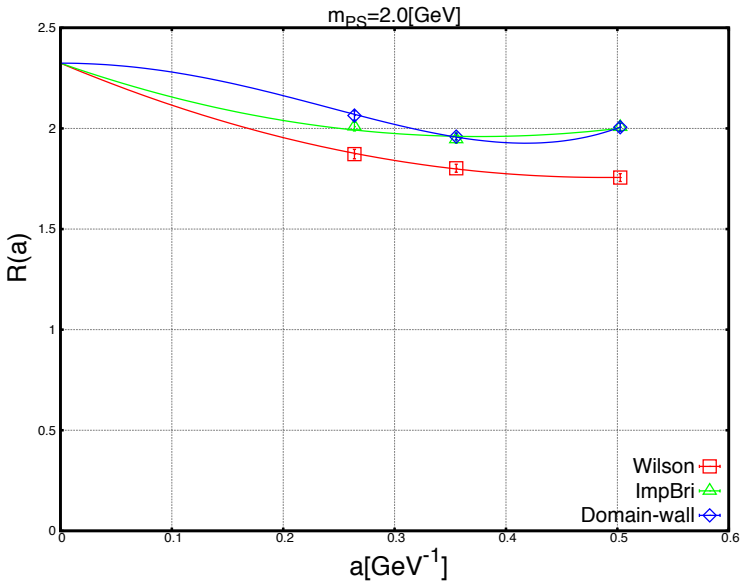

Figure 7.15: Scaling of the decay constant ratio against a at $m_{PS} = 2.0$ GeV.

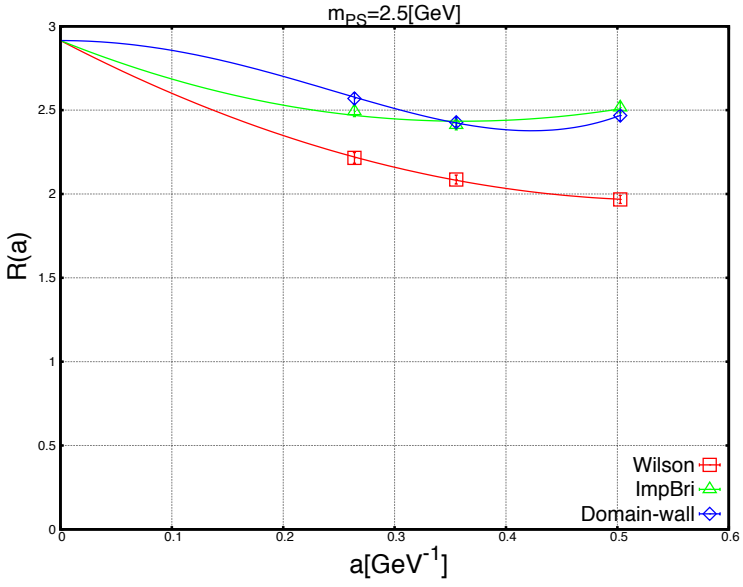

Figure 7.16: Scaling of the decay constant ratio against a at $m_{PS} = 2.5$ GeV.

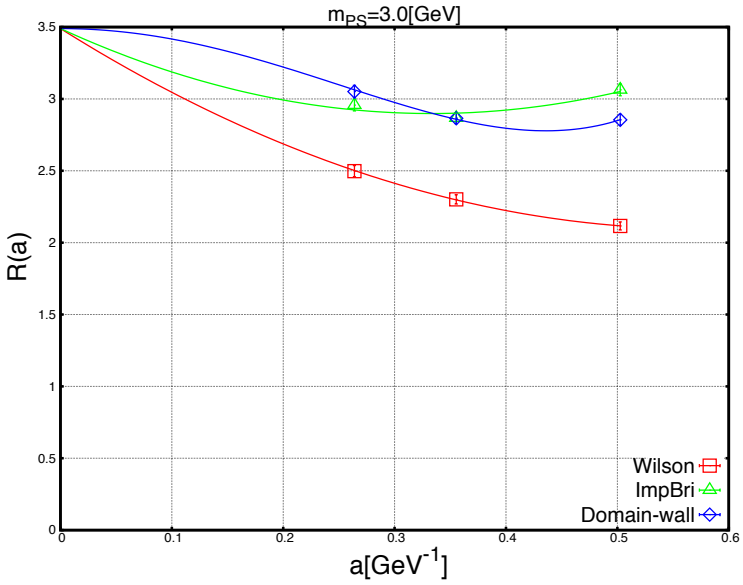

Figure 7.17: Scaling of the decay constant ratio against a at $m_{PS} = 3.0$ GeV.

Dirac operators	c_1	c_2	c_3	c_4	c_0
$m_{PS} = 1.5$ GeV					$\chi^2/d.o.f = 1.9$
Wilson	-0.7	0.9	-	-	1.6
improved Brillouin	-0.6	0.8	-	-	
domain-wall	-	-1.4	-	4.1	
$m_{PS} = 2.0$ GeV					$\chi^2/d.o.f = 0.7$
Wilson	-2.3	2.4	-	-	2.3
improved Brillouin	-1.9	2.6	-	-	
domain-wall	-	-4.6	-	13.1	
$m_{PS} = 2.5$ GeV					$\chi^2/d.o.f = 0.7$
Wilson	-3.5	3.1	-	-	2.9
improved Brillouin	-2.7	3.7	-	-	
domain-wall	-	-6.0	-	16.8	
$m_{PS} = 3.0$ GeV					$\chi^2/d.o.f = 0.9$
Wilson	-4.8	4.2	-	-	3.5
improved Brillouin	-3.5	5.3	-	-	
domain-wall	-	-7.5	-	19.7	

Table 7.9: Fitting results for the data of the decay constant, where the used ansatz is $R(a) = 1 + c_1 a + c_2 a^2$ for the Wilson fermion and the improved action and $R(a) = 1 + c_2 a^2 + c_4 a^4$ for the domain-wall fermion.

Chapter 8

Non-perturbative study for the Brillouin fermion

In this section, we discuss some non-perturbative properties for the Brillouin fermion and its improved version. For this analysis, we also use the coarsest quenched configuration in Table. 7.3.

8.1 Numerical cost of the Brillouin-type Dirac operator

We naively estimate computational costs of Brillouin Dirac-operator compared with the Wilson fermion and the domain-wall fermion. Here we employ the CG solver for solving a quark propagator. Numerical tests are implemented at a 32node in BlueGene/Q with task_per_node = 16 and stopping condition is set to $\|r\|^2 \sim 1.0E^{-22}$, where r is the residual vector. Also the meson mass is roughly tuned around $m_{PS} = 3.0$ GeV. Here the Brillouin Dirac-operator is constructed from the two different ways (Rec, OSS) which have been introduced in Chapter 6. "Rec" means using the reclusive formula for the Brillouin Dirac-operator and "OSS" represents an implementation by using the overall smearing strategy. "OSS" can exclude the cost of generating diagonal link variable, thus it is faster than constructing of the Brillouin Dirac-operator using the recursive formula. It is found that the Brillouin fermion is the 4-5 times costlier than the Wilson fermion, though Dirac application is about 100 times costly. Our improved action is only about 10 times of the Wilson fermion. In addition, we display a history of the squared residual vector at every CG iteration steps in Fig. 8.2. Then we observe that convergence of CG iteration is significantly faster than the Wilson fermion when the Brillouin-type fermion is employed. It would be an advantage of the Brillouin-type fermion and this will be explained from Dirac eigenvalue spectra in the next section.

8.2 Dirac eigenvalue spectra

We calculate eigenvalue spectra on the quenched gauge configuration. Here, we calculate eigenvalues of the $D^\dagger D$ for three kind of Dirac-operator D. Just 10 configurations are used in this

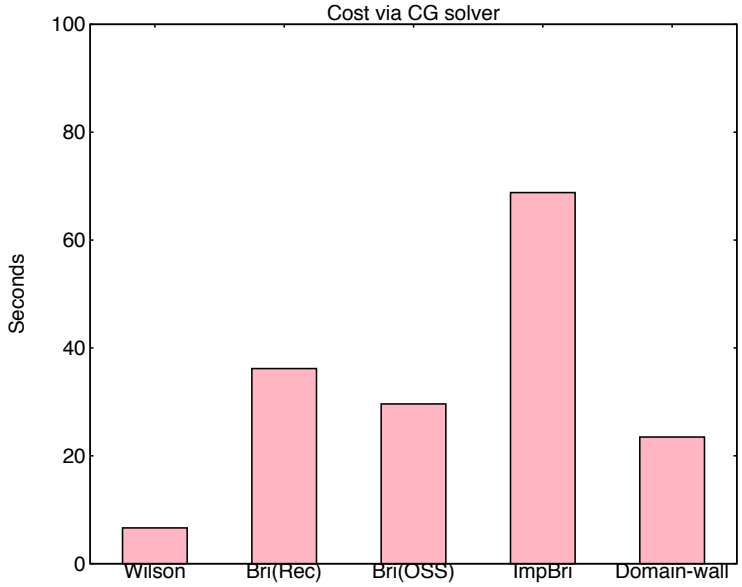

Figure 8.1: Comparison of numerical cost via CG solver

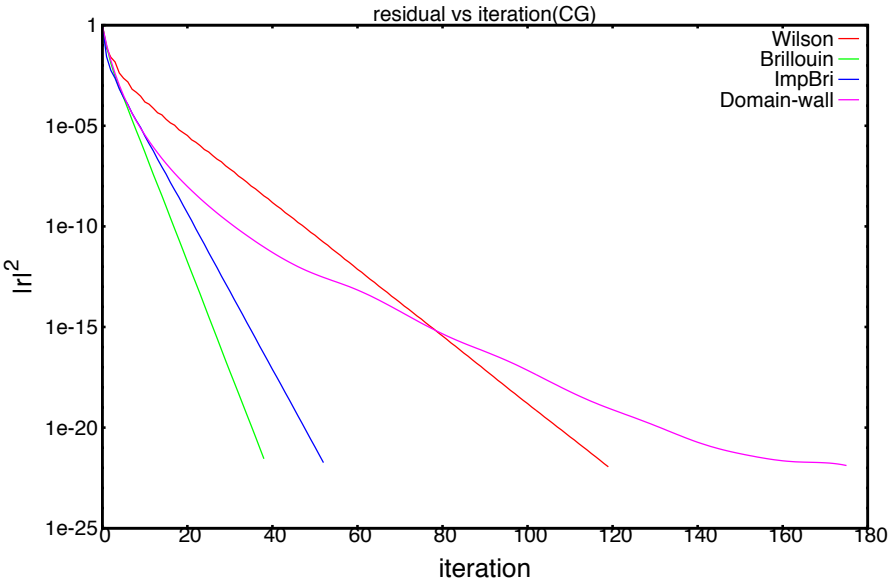

Figure 8.2: A history of squared residual vector at CG iteration steps.

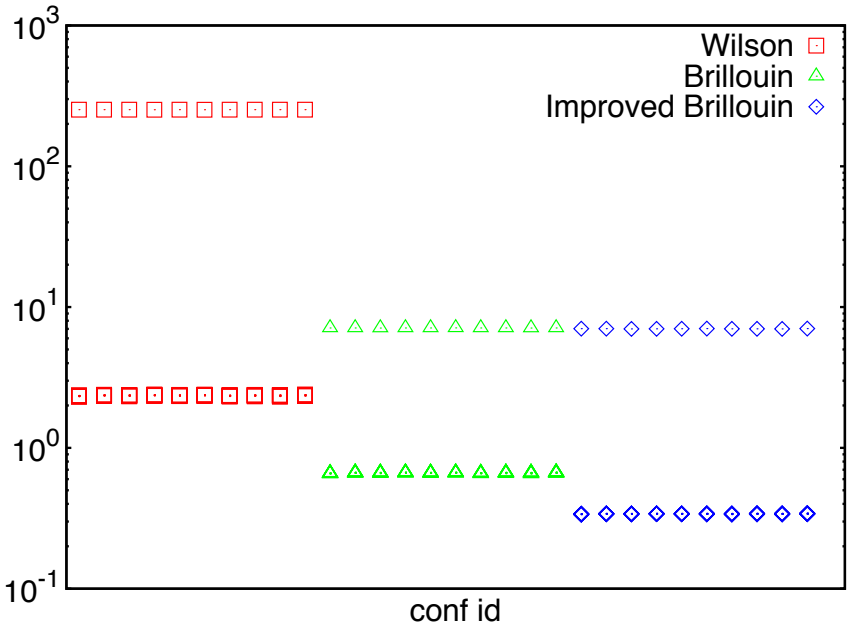

Figure 8.3: A highest eigenvalue and 10 lowest eigenvalues of $D^\dagger D$ for three Dirac operators on quenched configurations are plotted. Different colors represent different Dirac-operators. Here we used coarsest lattice. We roughly tuned for $m_{PS} = 3.0$ GeV. Note that differences of 10 lowest eigenvalues are invisible.

calculation with 3 times stout smearing. We show the highest eigenvalue and 10 lowest eigenvalues in Fig. 8.3. Different colors represent different Dirac-operators and quark masses are roughly adjusted for the $m_{PS} = 3.0$ GeV. Here we observe that ratio between the highest and the lowest modes of eigenvalues are significantly reduced when the Brillouin-type Dirac-operator is employed. Then we are able to explain the thing of the previous section. The condition number of the CG solver is typically given by the ratio between a highest mode and a lowest mode of Dirac eigenvalues. Then we see that the eigenvalue distribution significantly affects the convenience of the CG solver. We note that differences of the lowest modes among Dirac-operators comes from differences of the additive mass renormalization.

8.3 Large mass behavior of the improved action

Higher derivative terms give rise to some unphysical poles which are discussed in Ref. [31]. Also they show that such ghosts can be pushed up on the anisotropic lattices. If ghost's mass is very large, it would be harmless. However if it gets close to a physical pole, ghosts might interrupt the real pole. Also it was found that the physical energy solution become a complex value at large mass region. From our tree-level analysis, this threshold is almost $ma \sim 0.84$ for the improved Brillouin fermion. Then we found a oscillation of the Euclidian propagator on non-trivial gauge

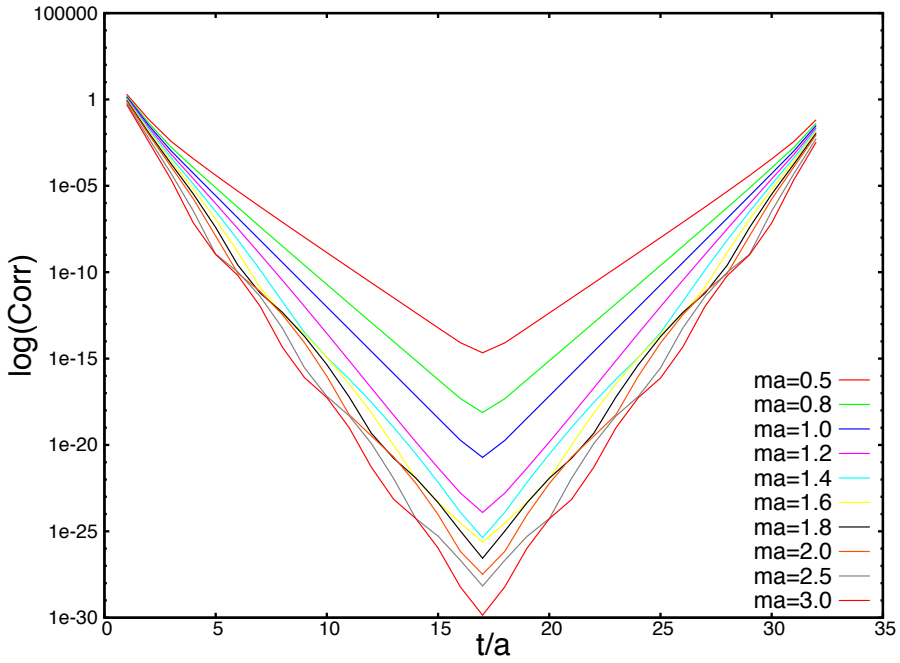

Figure 8.4: This figure shows oscillations of pseudo-scalar meson propagators on the quenched configuration. Every color lines corresponds to different quark masses.

configurations as shown at Figure8.4. Fortunately a coefficient c_{imp} can be chosen freely like the Wilson parameter in the Wilson fermion action. For instance, if we set $c_{imp} = 0.0625$, the tree-level threshold can be pushed up to $ma \sim 0.97$. Simultaneously risk of unphysical pole might be able to avoided by tuning the parameter. From analogy of the improved Brillouin action, we also found a similar phenomenon even for the D34 action by tree-level analysis at $ma \sim 0.77$, even though we have not checked at non-perturbative studies in this case. We note that the Oktay-Kronfeld action[11] might have such as problem, because it contains operators of dimensions 6 and 7. These phenomena are related to a hopping in time direction. Thus if one consider improvement which gives higher derivative terms, one would encounter this kind of problem. However in the case of the standard Brillouin fermions, there should be not such as problem, because the standard Brillouin fermion has only 1hopping term in same direction. In actual, this problem was not found from our tree-level analysis for the standard Brillouin fermion. These phenomena indicate that there might be not the reflection positivity which has been not yet proved rigorously for this kinds of improved action. However in practice, we may employ the improved actions which have higher order terms on a certain level of fine lattices. Furthermore, if we take into account to unphysical poles, we should not employ the our improved action in $ma \geq 0.5 - 0.6$. That is, we have to carefully check effect of the unphysical poles, especially for improved actions which include higher dimension terms.

Chapter 9

Summary and prospects

In this thesis, we firstly review formulation of the lattice gauge theory and Symanzik improvement. Next we have focused on the Brillouin fermion which has an excellent dispersion relation and have analyzed these discretization effects via massive dispersion relations. Furthermore we have shown various possibility of improvement for the Brillouin fermion. At tree-level, we illustrate that the Brillouin fermion can be improved to be $O(a^3)$ discretization effect. Furthermore one can employ the overlap procedure with Brillouin kernel for further improvement with the improved overlap Dirac-operator. Also we have carried out non-perturbative scaling studies on the quenched configurations. From scaling of speed-of-lights, we see that scaling of the improved action is excellent, the speed-of-light is on the unity. From scaling of hyperfine splitting, good scaling of the improved action is observed. Our results of decay constant is slightly different results with the two former results. However we think that this outcome is not so reliable and measurements of decay constant should be more improved, since we did not use smeared source and not take into account correlation between data. Also we saw that numerical cost of the improved action is currently only about 10 times higher than the non-improved Wilson fermion, though our implementation of Dirac application still can be accelerated. Finally we mentioned an application limit of the improved action. The improved action seem not have the reflection positivity, but we may employ the action practically. We note that one has to check carefully the unphysical doubler effect.

In this study, our improvement is still tree-level, thus one-loop level or non-perturbative tuning is necessary. However perturbative calculation for the Brillouin-type fermion is intensive, thus we may employ the automatic numerical perturbative system [65]. This system automatically derive Feynman rules and calculate observables e.g. the one-loop quark propagator, then lattice loop integral is implemented numerically. Our perturbative computation is still on-going, but it would be an interesting study. Furthermore JLQCD collaboration have generated $N_f = 2+1$ domain-wall dynamical configurations and thus charm quark physics with the our improved action would be expected on these configurations. However unfortunately we can not extend to B-quark region due to the restriction of am_q . Then we have to consider an other approach. From our scaling study, we also observed that the domain-wall fermion shows good scaling, thus one may adopt the domain-wall fermion for B-quark region. However we found that the domain-wall fermion also have the restriction of am_q. Residual mass of the domain-wall fermion suddenly increase over a threshold as going large mass region. Then we may take large L_s of the domain-wall fermion. In this study, we employed $L_s = 8$, however we may have to tune it so that the residual mass becomes constant up to $am_q \sim$1.0-1.5. Alternatively we may adopt the overlap fermion which has exact chiral symmetry. In terms of the domain-wall fermion, the residual mass of the overlap fermion would be tiny even

at large am_q. Then it seems to be interesting that we employ the Brillouin-kernel overlap fermion, since the Brillouin kernel may reduce numerical cost of the overlap procedure with keeping the good properties of the Brillouin fermion. Combing with the ETM ratio method, precise calculation of B-physics would become available.

Acknowledgements: First of all, I would like to gratefully thank to Professor S. Hashimoto in KEK. Also I am grateful to J.Noaki, T.Kaneko, G.Cossu and other JLQCD members for many discussions and helps. Furthermore I am thankful to A.Juttner, M.Marincovic and J.Tsang in the University of Southampton for generating configurations and useful discussions. Here I also would like thanks S.Dürr for detailed discussions and offering codes which were much helpful for our codings. Professor N.Ishizuka often gives useful suggestions. I am greatly thanks to him and also I would like to thanks to other members of the elementary particle physics group in the University of Tsukuba.

Numerical simulations are performed on the IBM System Blue Gene Solution at High Energy Accelerator Research Organization (KEK) under a support of its Large Scale Simulation Program (No. 13/14-04). This work is supported in part by the Grant-in-Aid of the Japanese Ministry of Education (No. 26247043) and the SPIRE (Strategic Program for Innovative Research) 36 Field5 project. The research leading to these results has received funding from the European Research Council under the European Union's Seventh Framework Programme (FP7/2007- 2013) / ERC Grant agreement 279757.

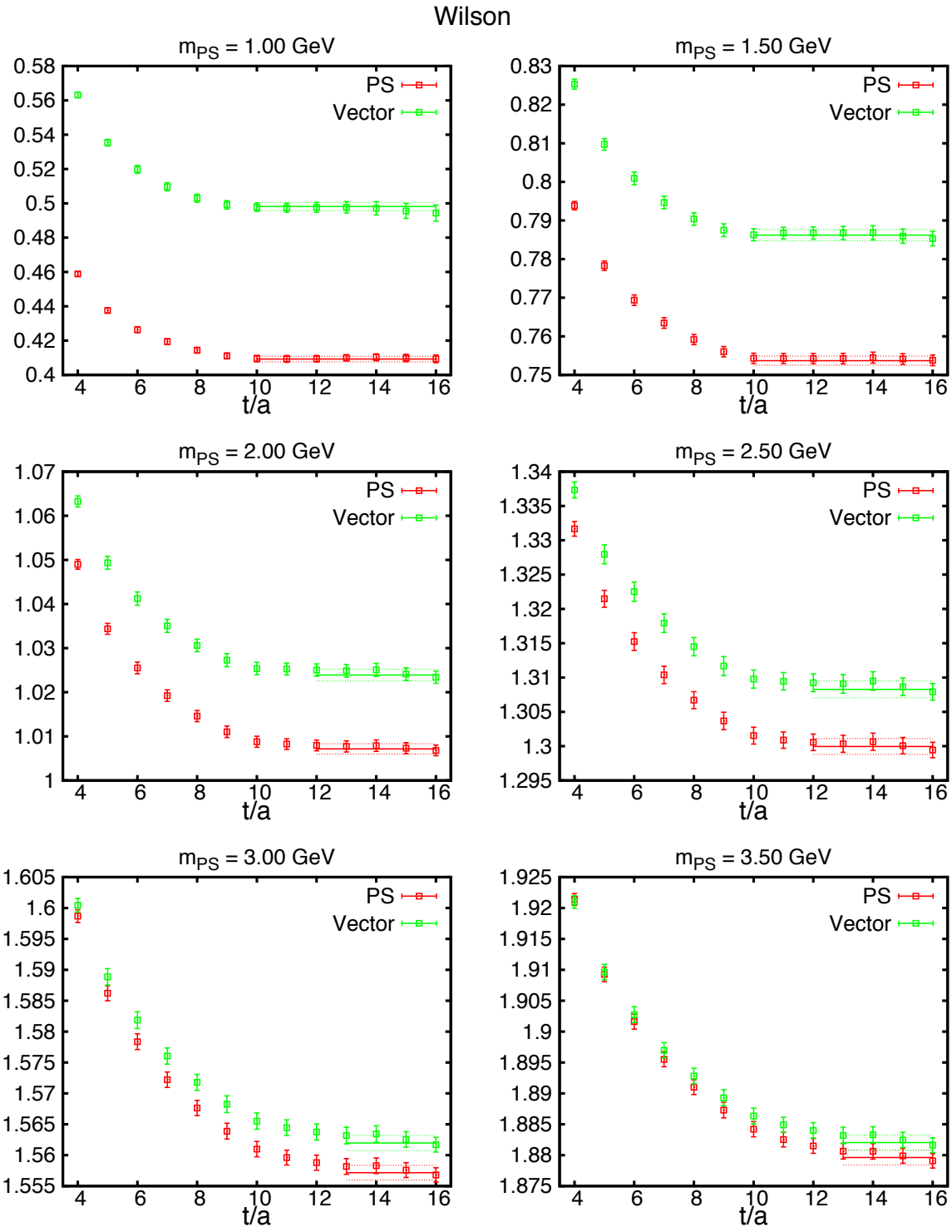

Figure 9.1: Effective masses for the Wilson fermion on the $L/a = 16$ lattice.

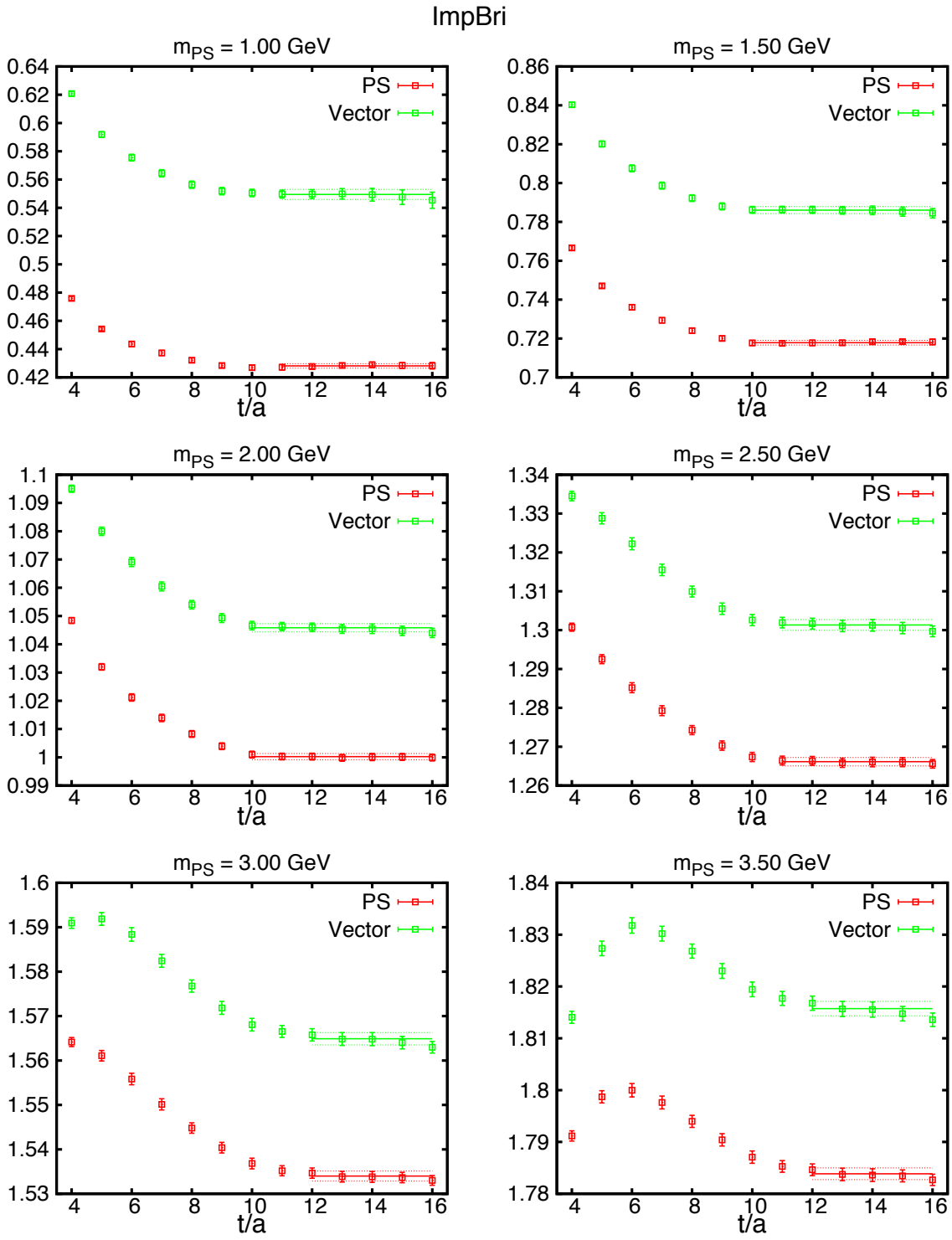

Figure 9.2: Effective masses for the improved Brillouin fermion on the $L/a = 16$ lattice.

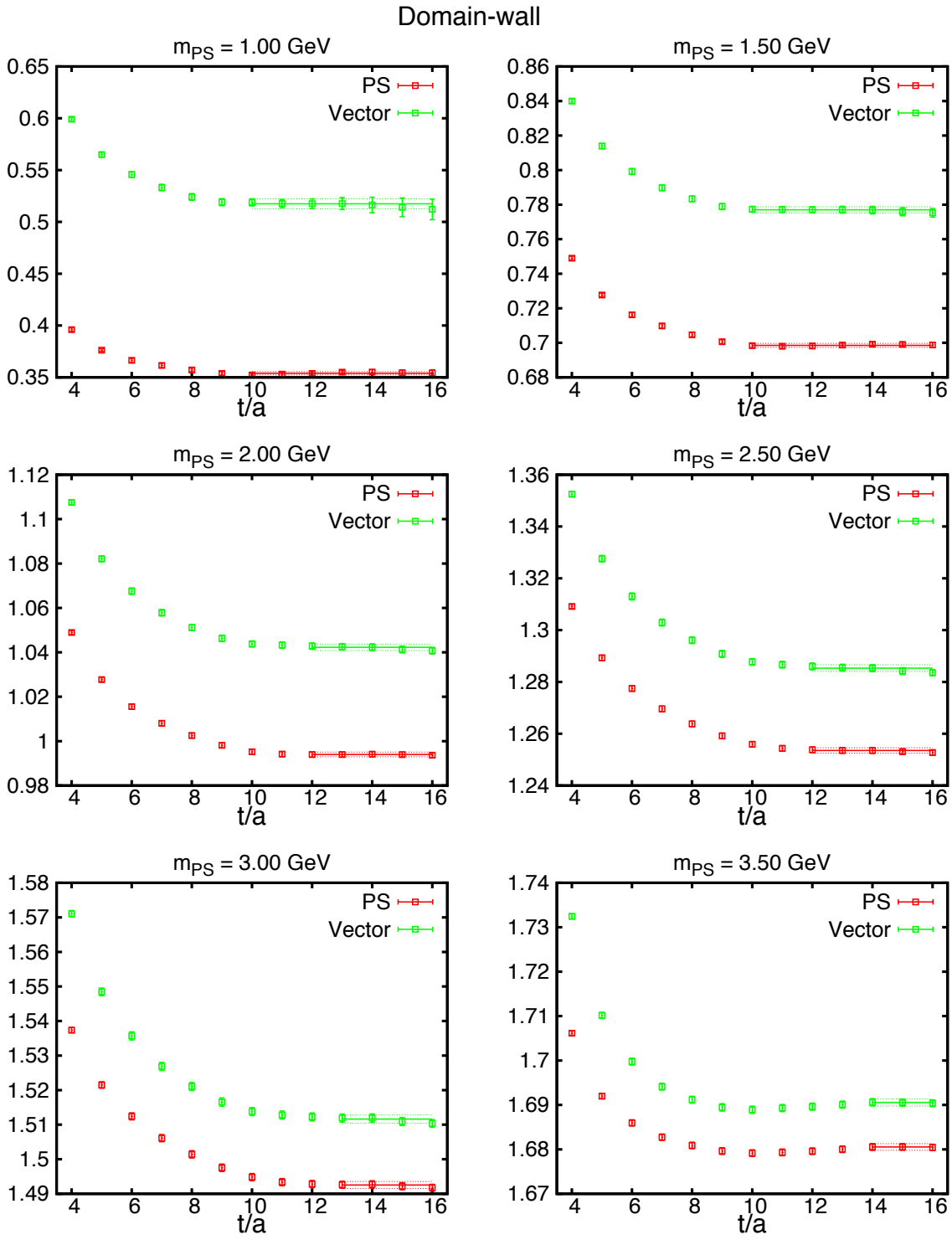

Figure 9.3: Effective masses for the domain-wall fermion on the $L/a = 16$ lattice.

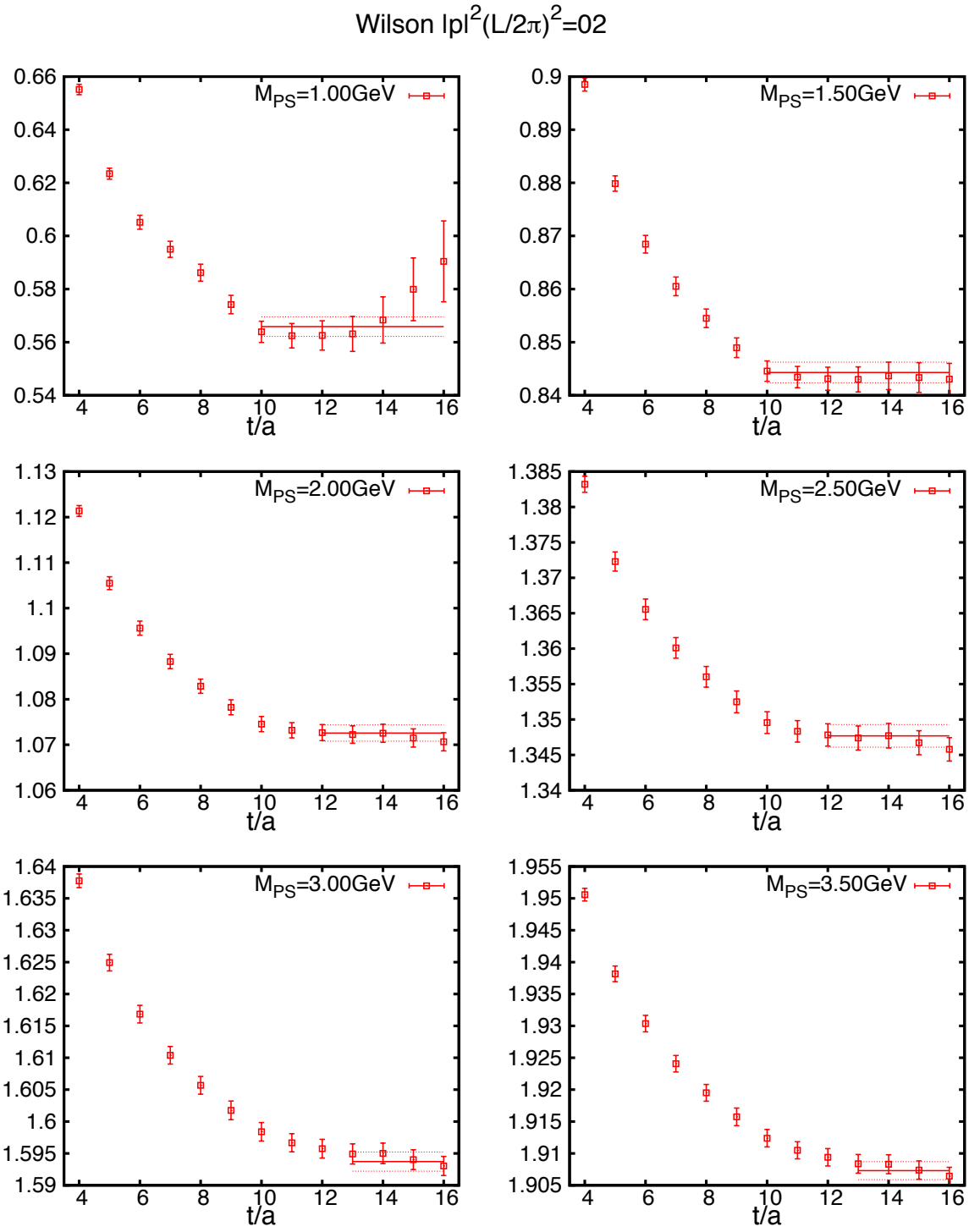

Figure 9.4: Effective masses for the Wilson fermion on the $L/a = 16$ lattice.

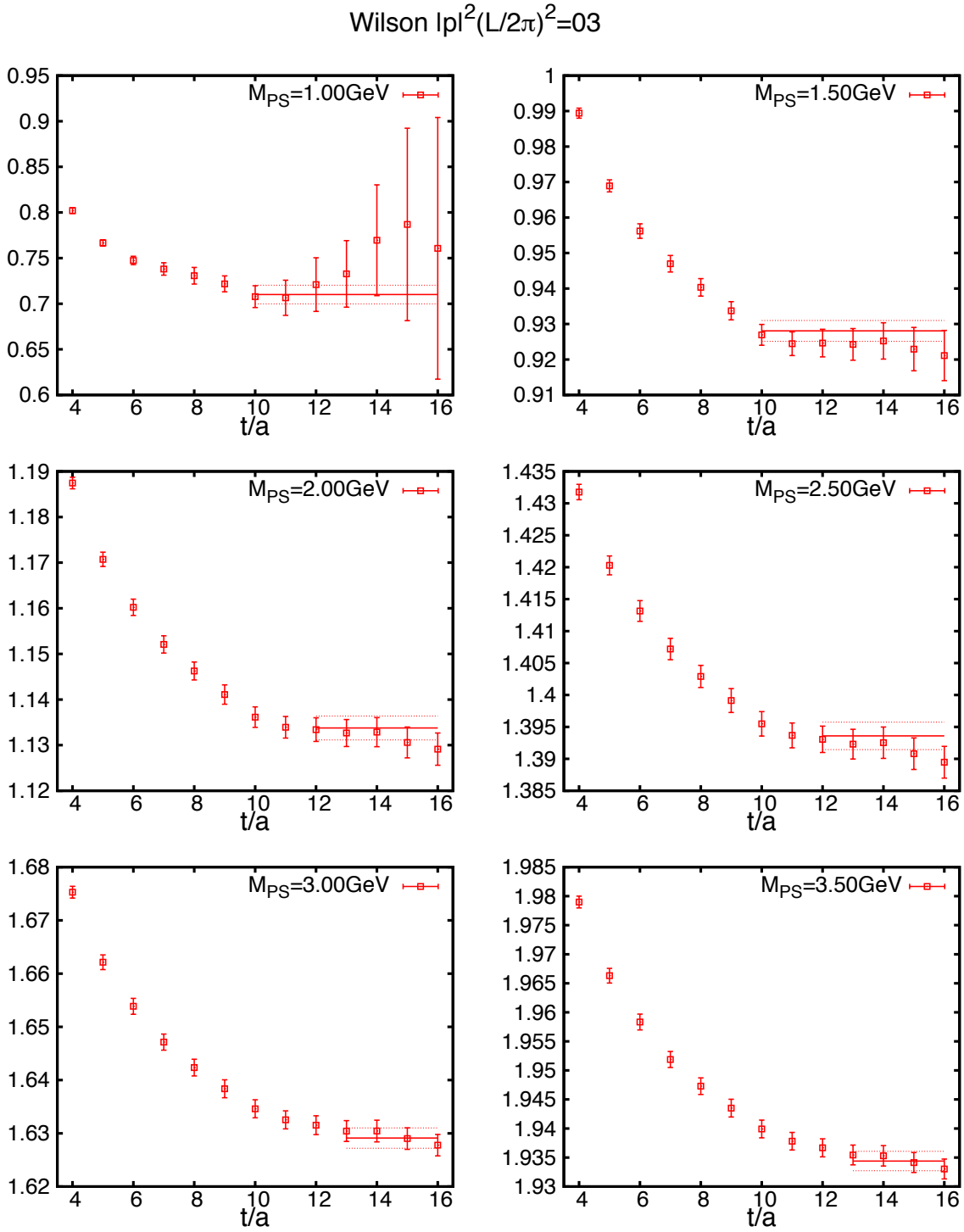

Figure 9.5: Effective masses for the Wilson fermion on the $L/a = 16$ lattice.

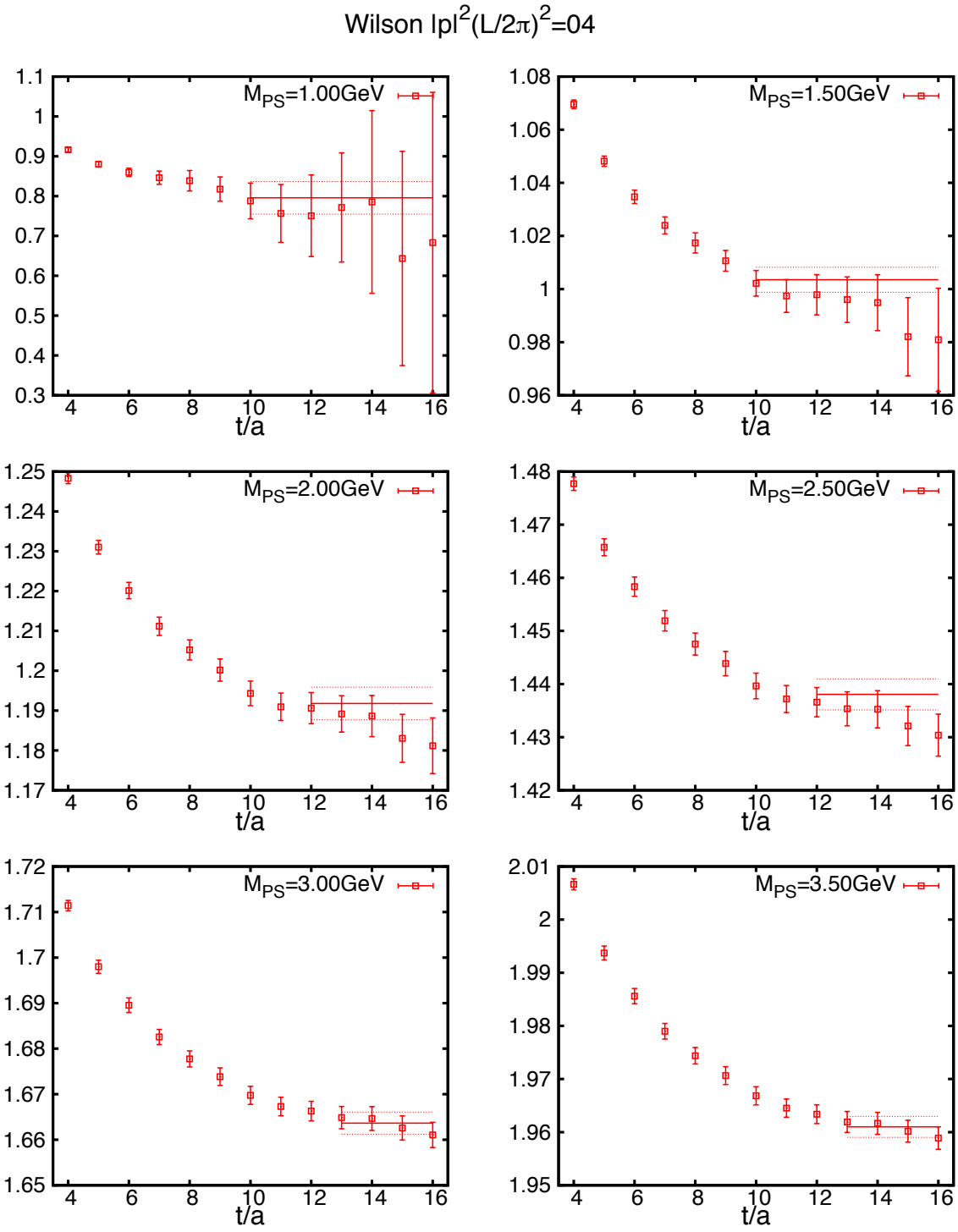

Figure 9.6: Effective masses for the Wilson fermion on the $L/a = 16$ lattice.

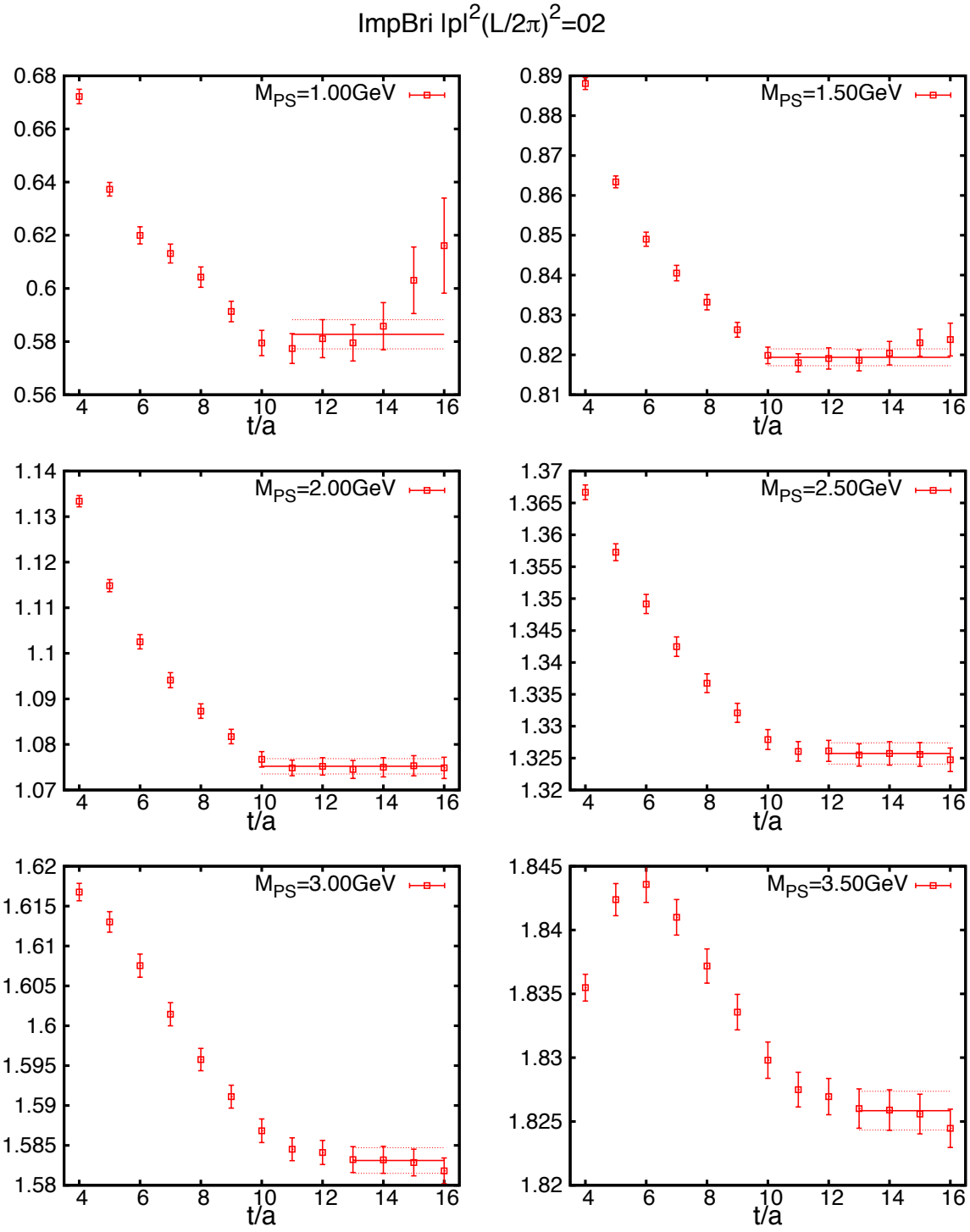

Figure 9.7: Effective masses for the improved Brillouin fermion on the $L/a = 16$ lattice.

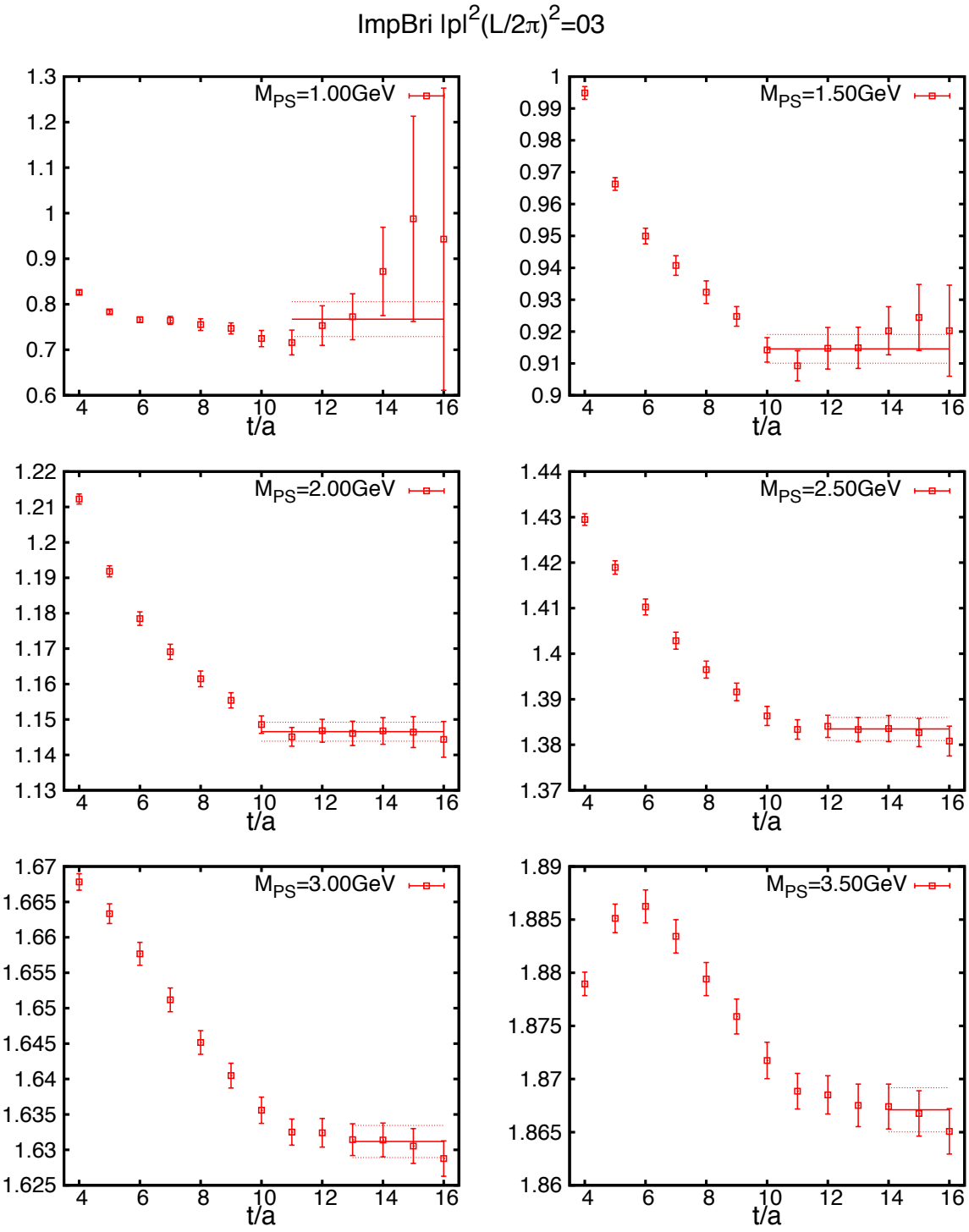

Figure 9.8: Effective masses for the improved Brillouin fermion on the $L/a = 16$ lattice.

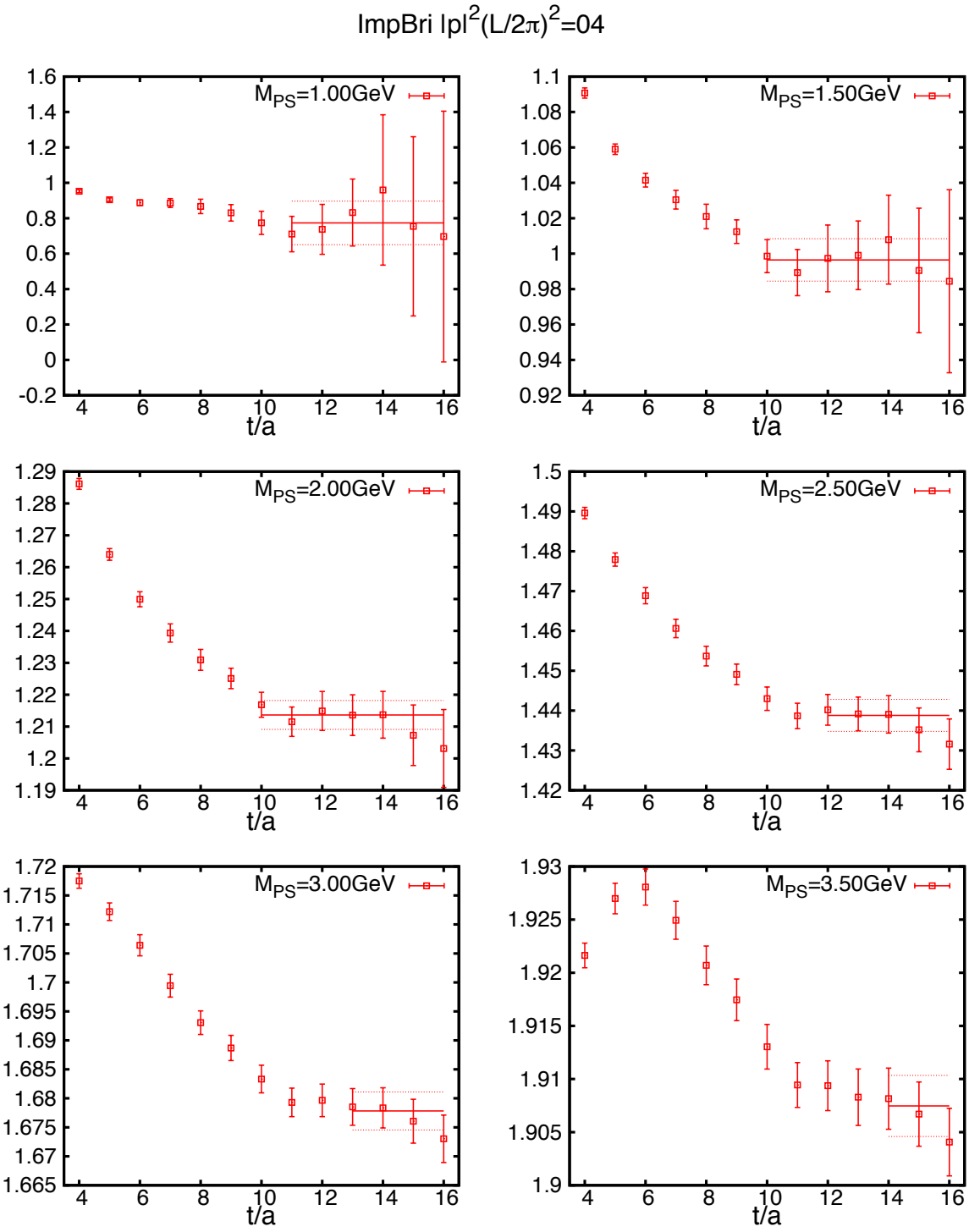

Figure 9.9: Effective masses for the improved Brillouin fermion on the $L/a = 16$ lattice.

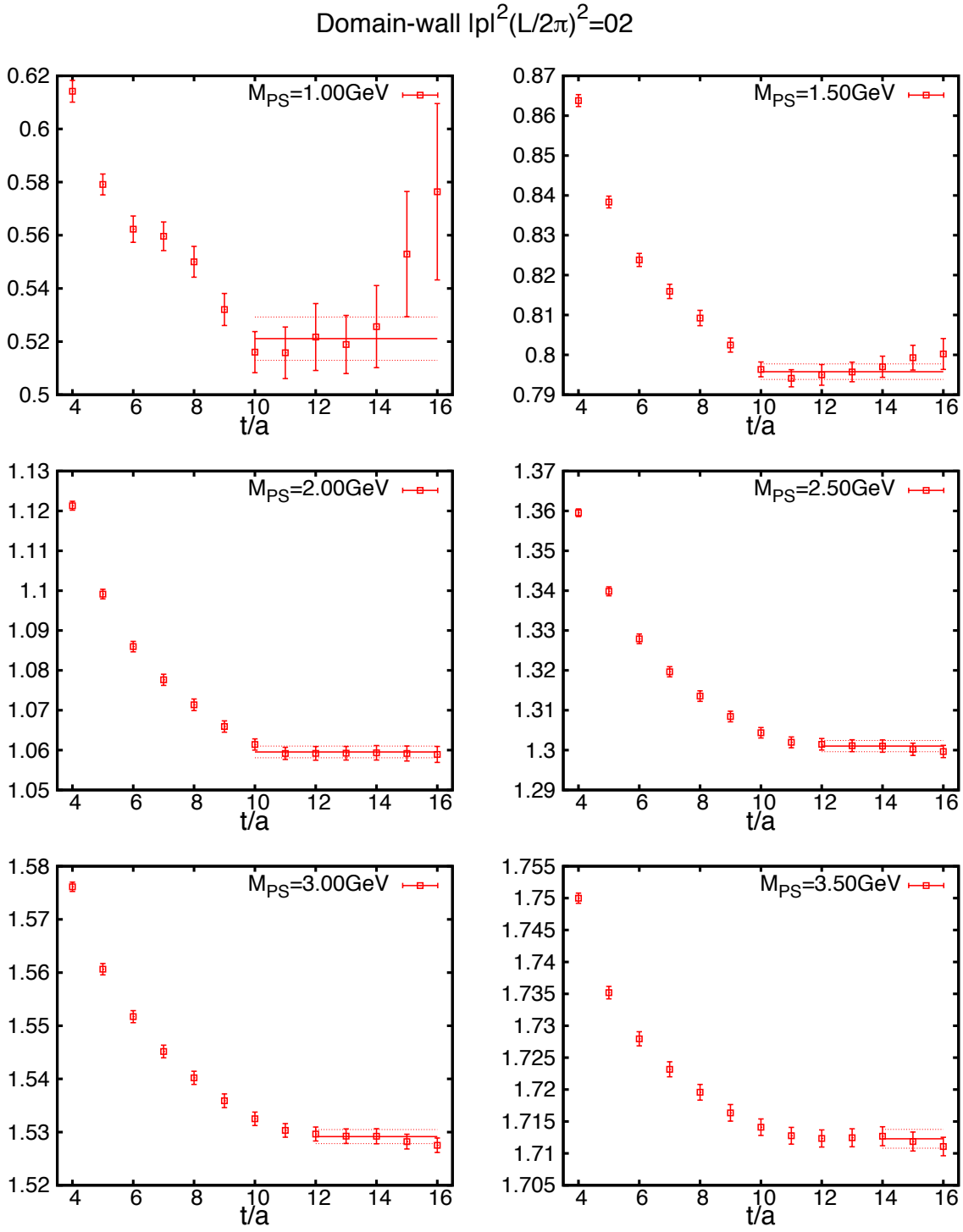

Figure 9.10: Effective masses for the domain-wall fermion on the $L/a = 16$ lattice.

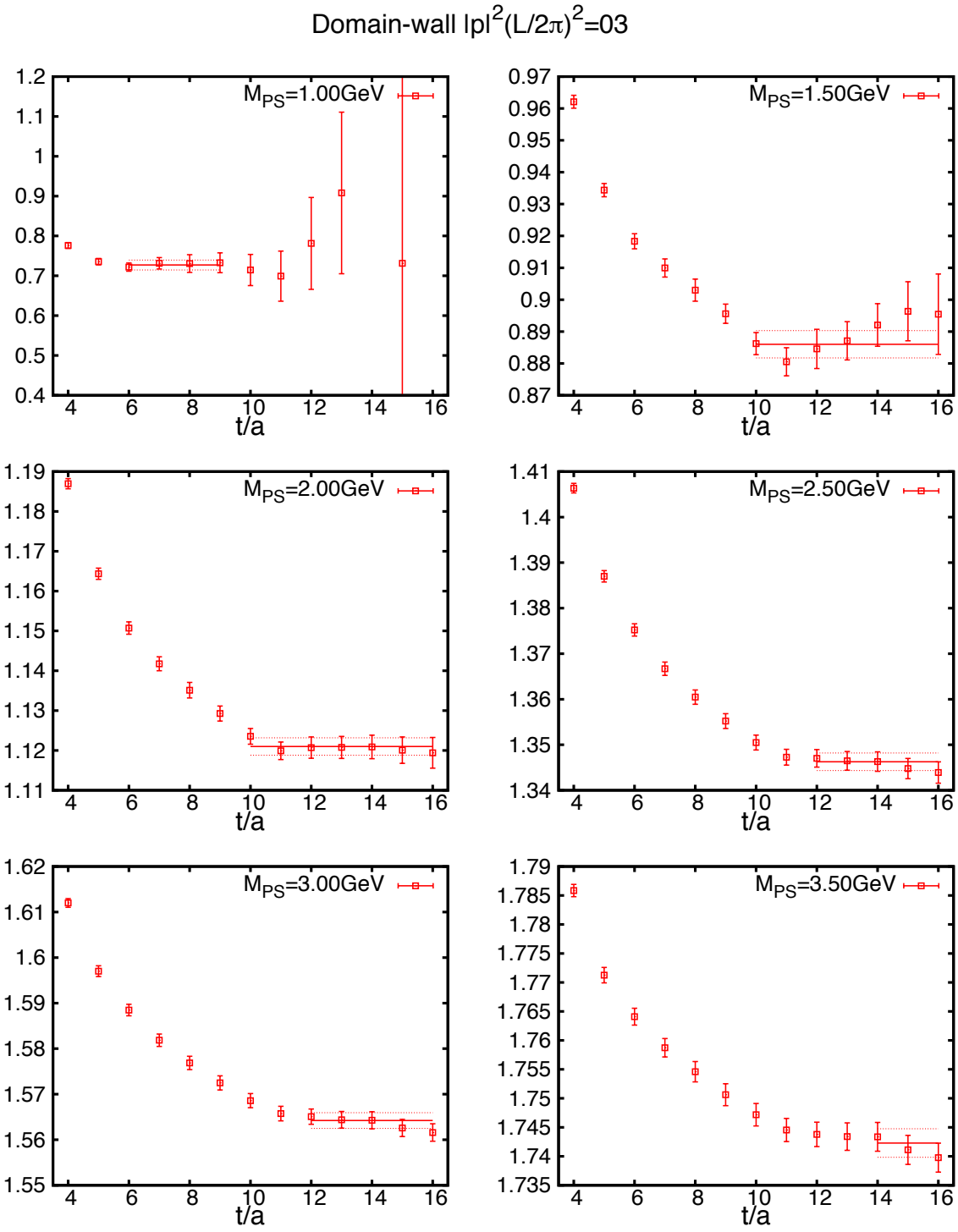

Figure 9.11: Effective masses for the domain-wall fermion on the $L/a = 16$ lattice

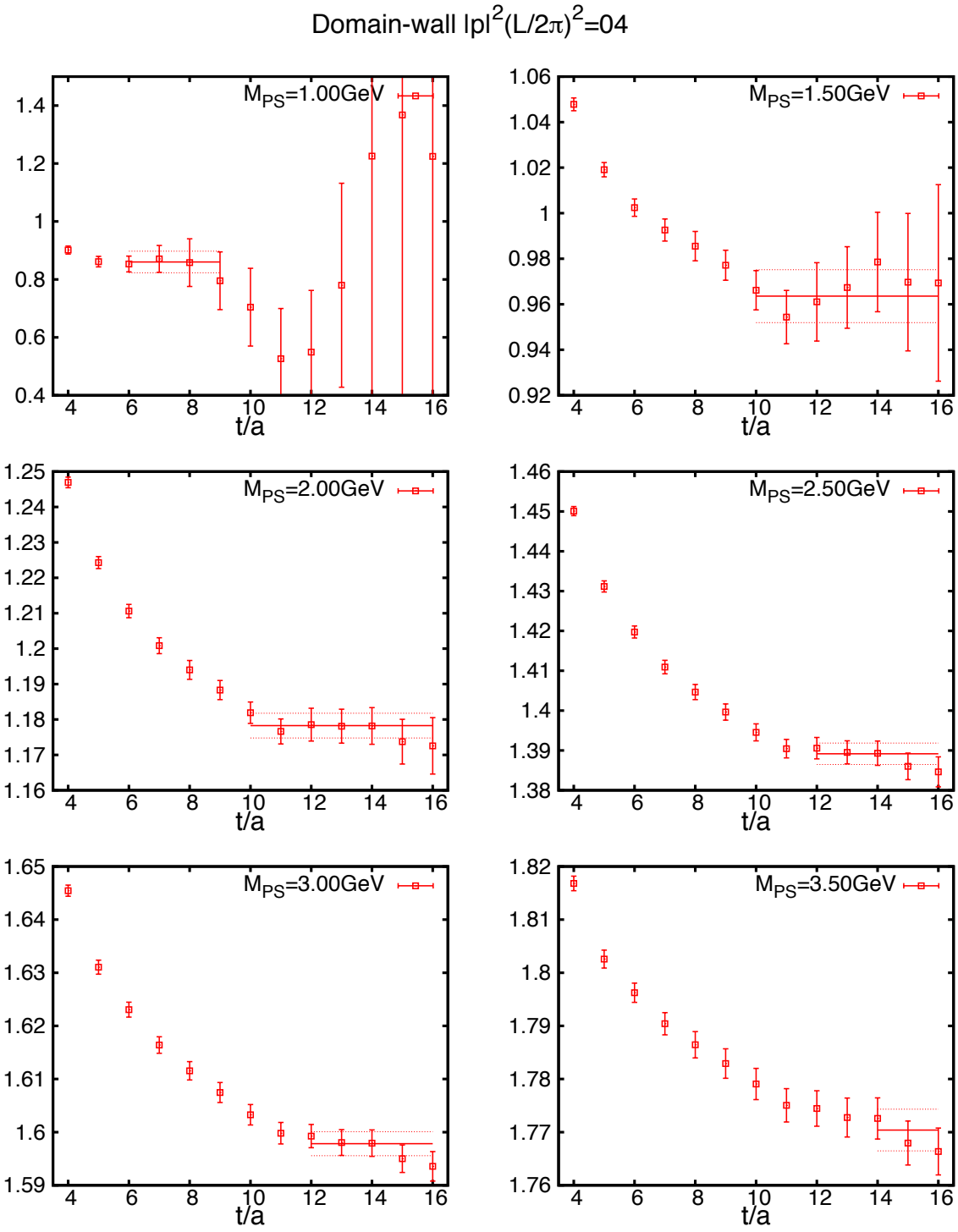

Figure 9.12: Effective masses for the domain-wall fermion on the $L/a = 16$ lattice

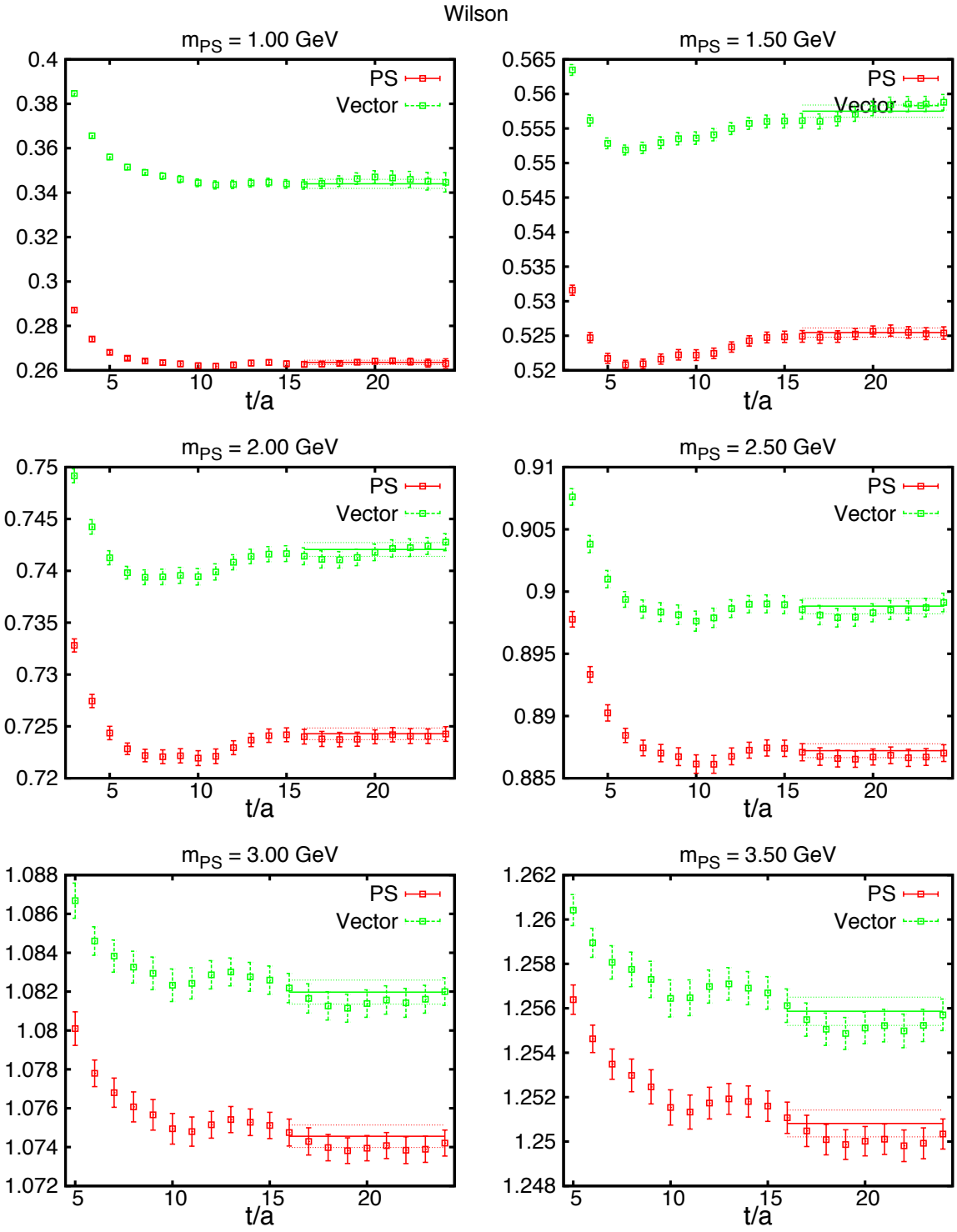

Figure 9.13: Effective masses for the Wilson fermion on the $L/a = 24$ lattice.

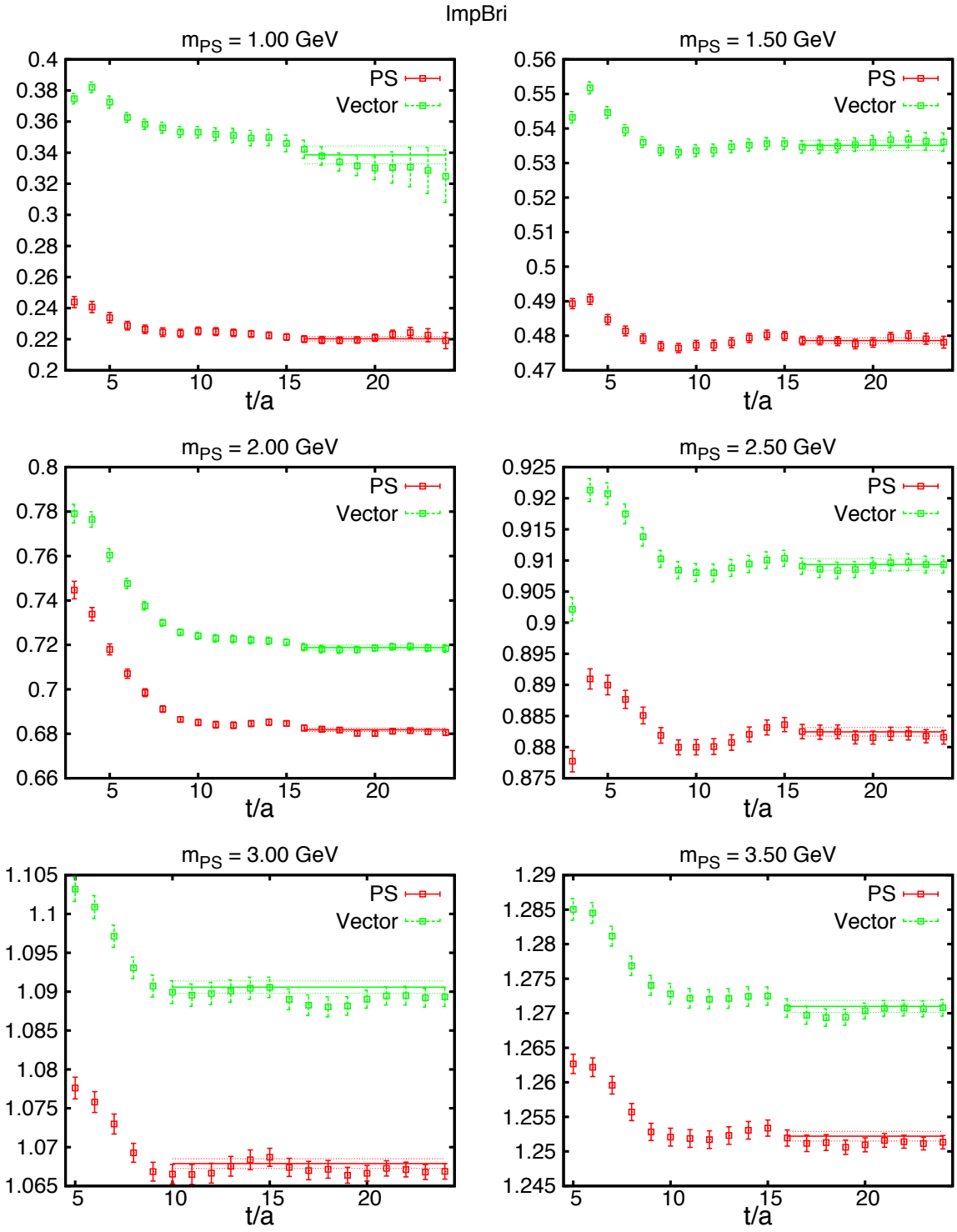

Figure 9.14: Effective masses for the improved Brillouin fermion on the $L/a = 24$ lattice.

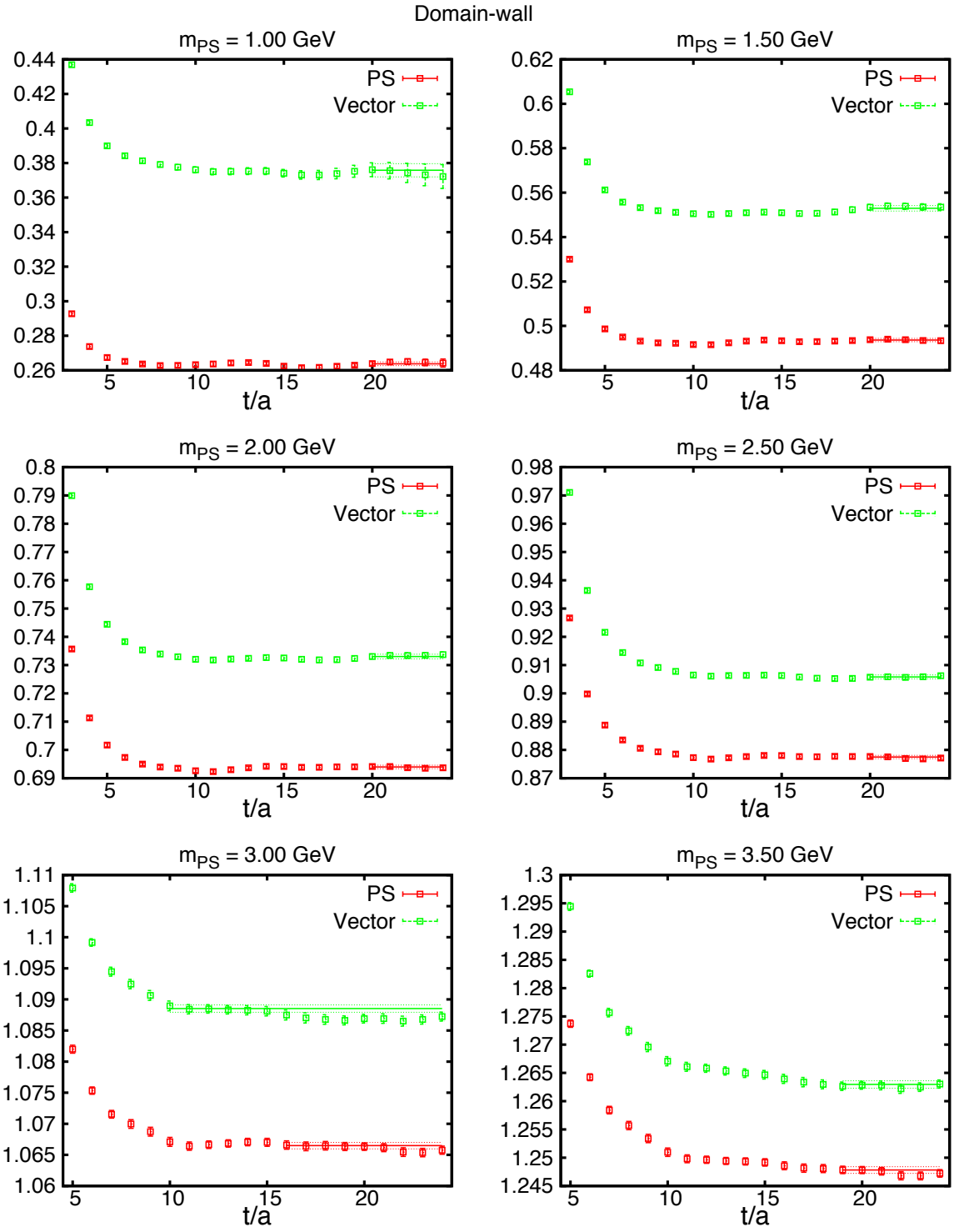

Figure 9.15: Effective masses for the domain-wall fermion on the $L/a = 24$ lattice.

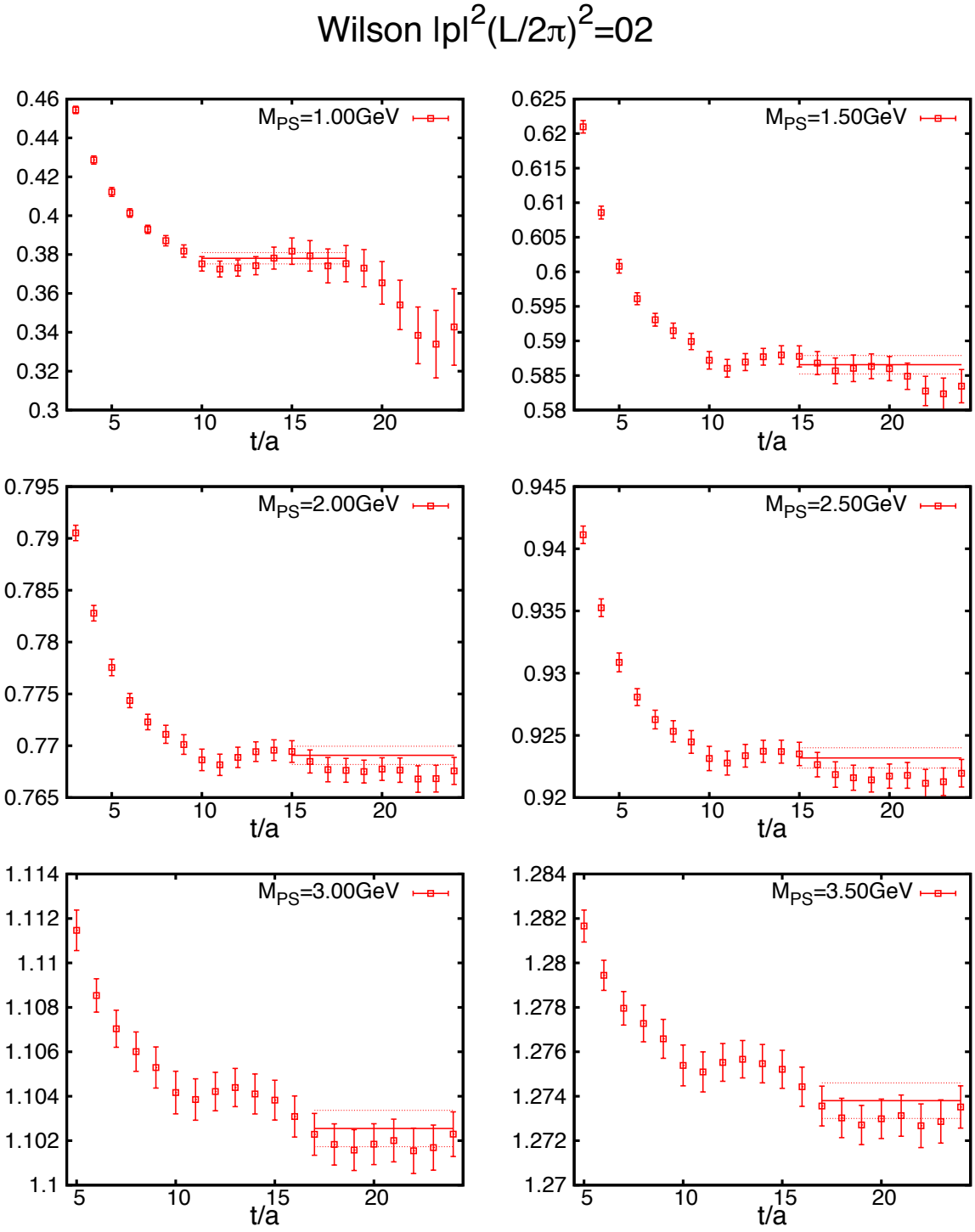

Figure 9.16: Effective masses for the Wilson fermion on the $L/a = 24$ lattice.

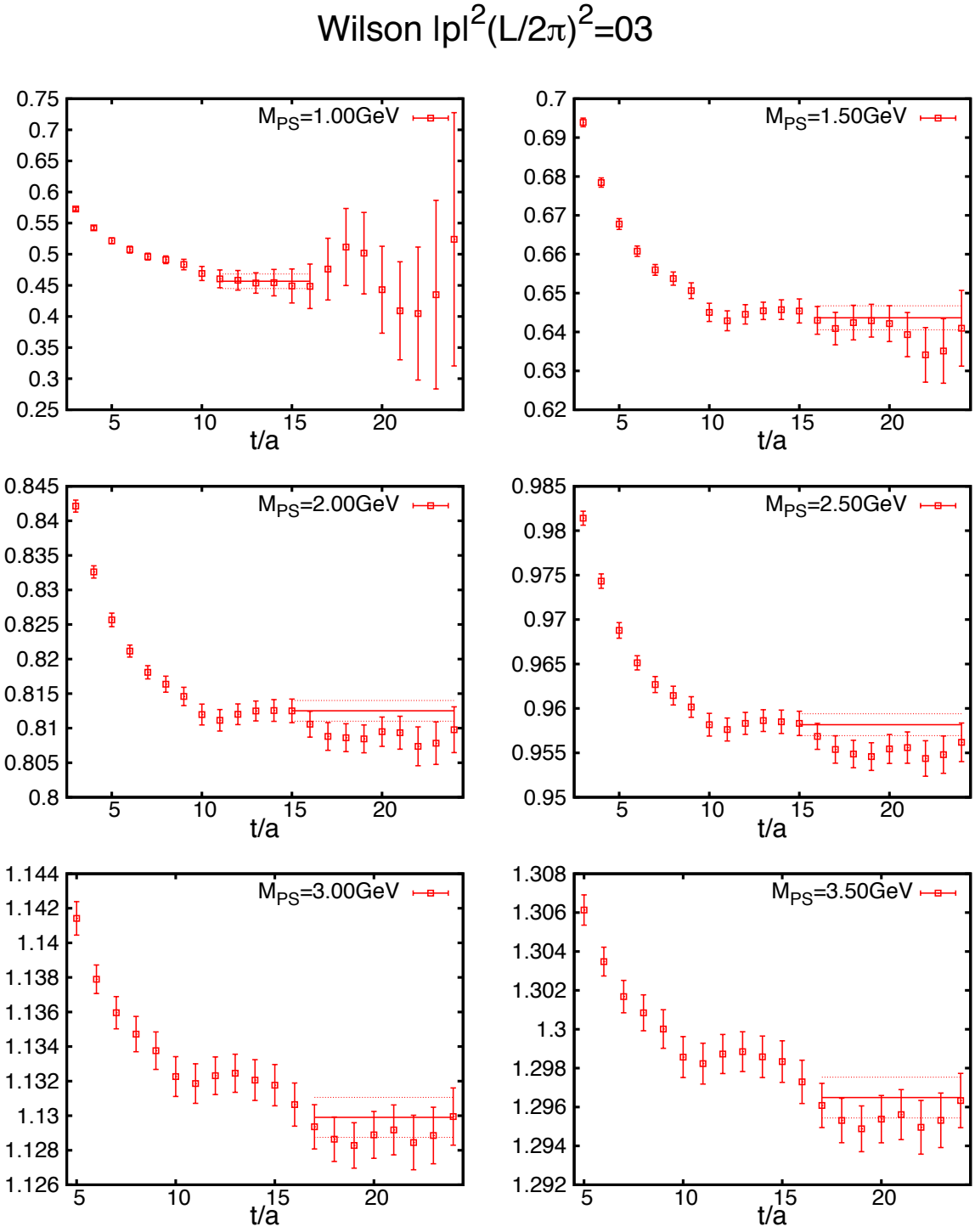

Figure 9.17: Effective masses for the Wilson fermion on the $L/a = 24$ lattice.

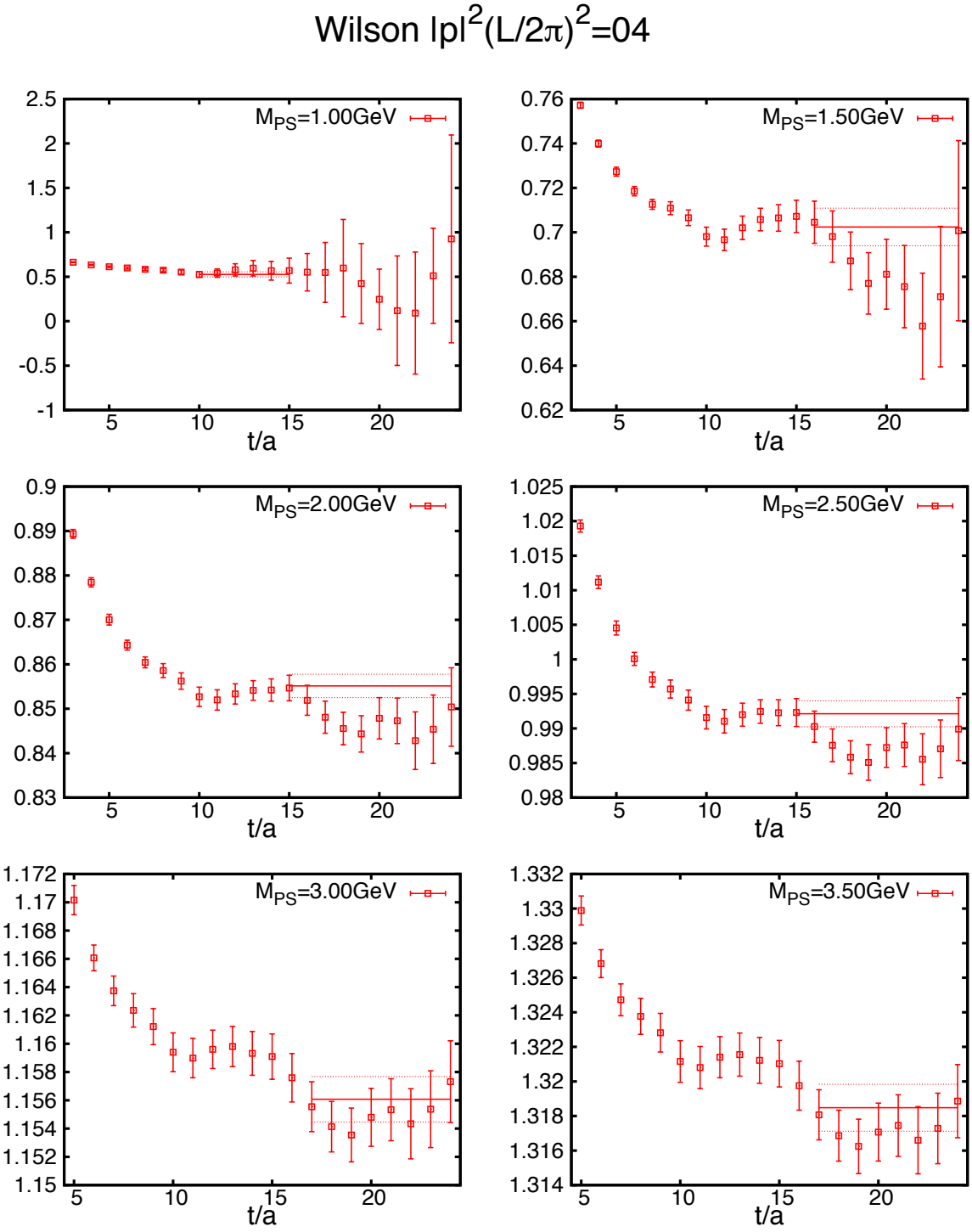

Figure 9.18: Effective masses for the Wilson fermion on the $L/a = 24$ lattice.

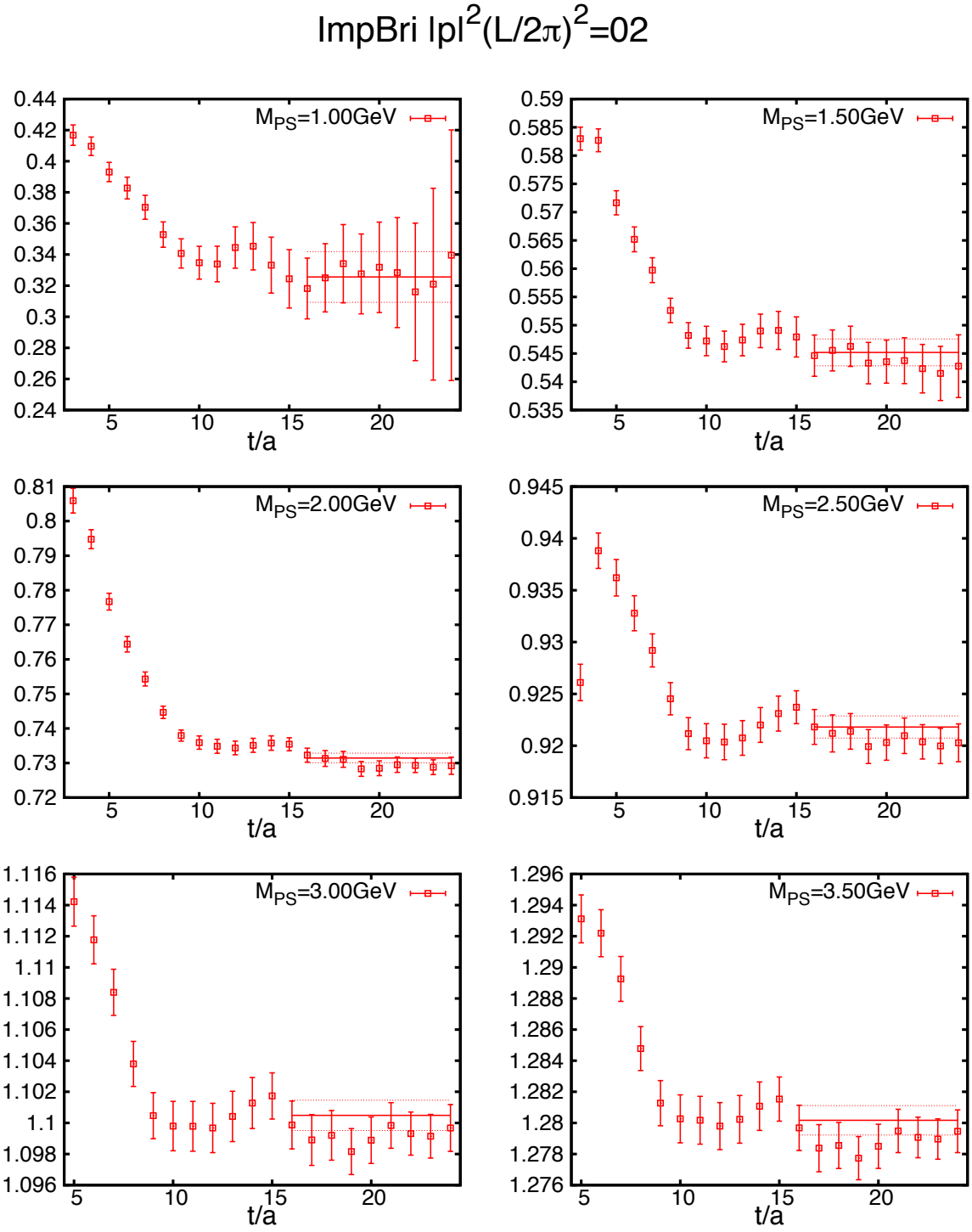

Figure 9.19: Effective masses for the improved Brillouin fermion on the $L/a = 24$ lattice.

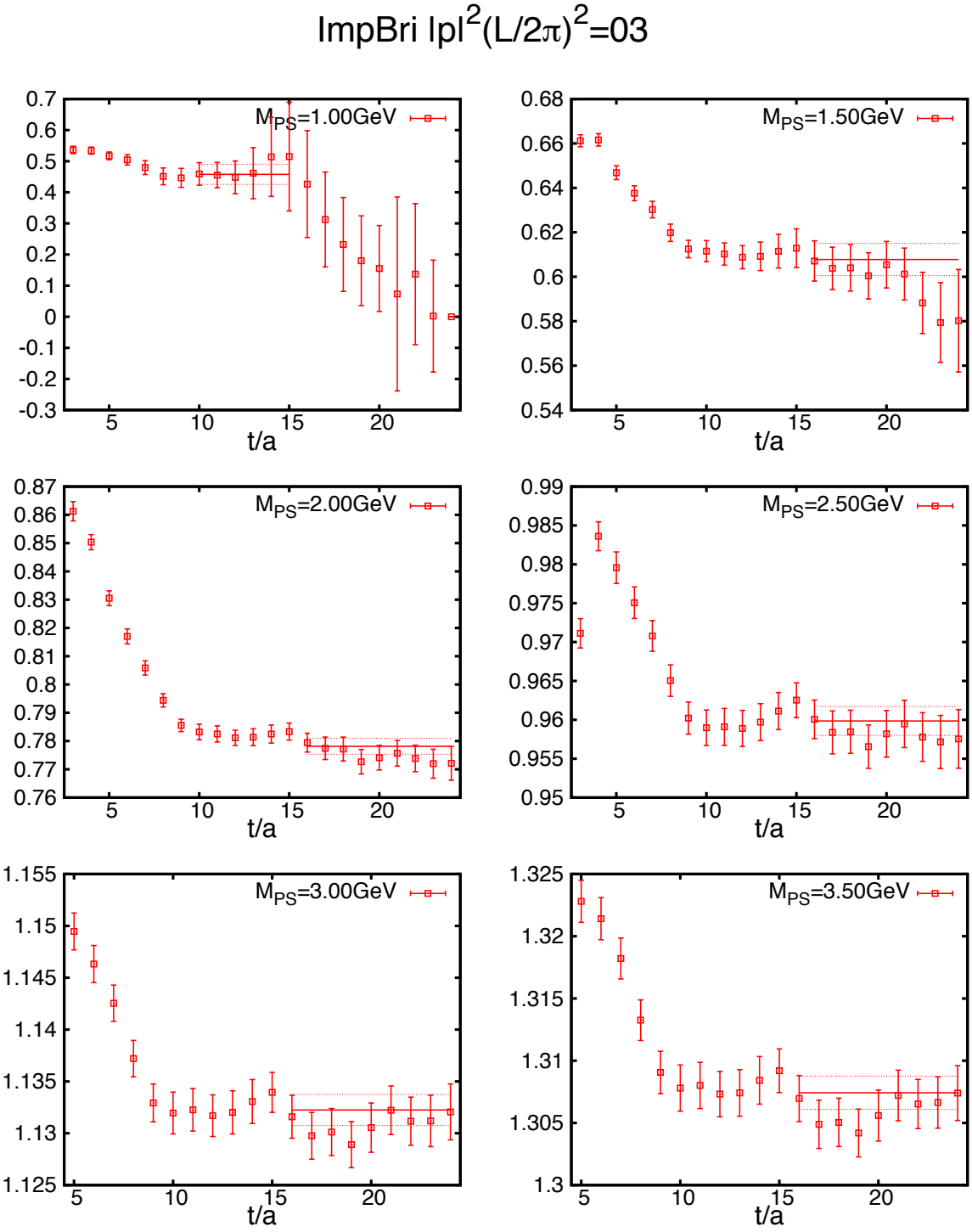

Figure 9.20: Effective masses for the improved Brillouin fermion on the $L/a = 24$ lattice.

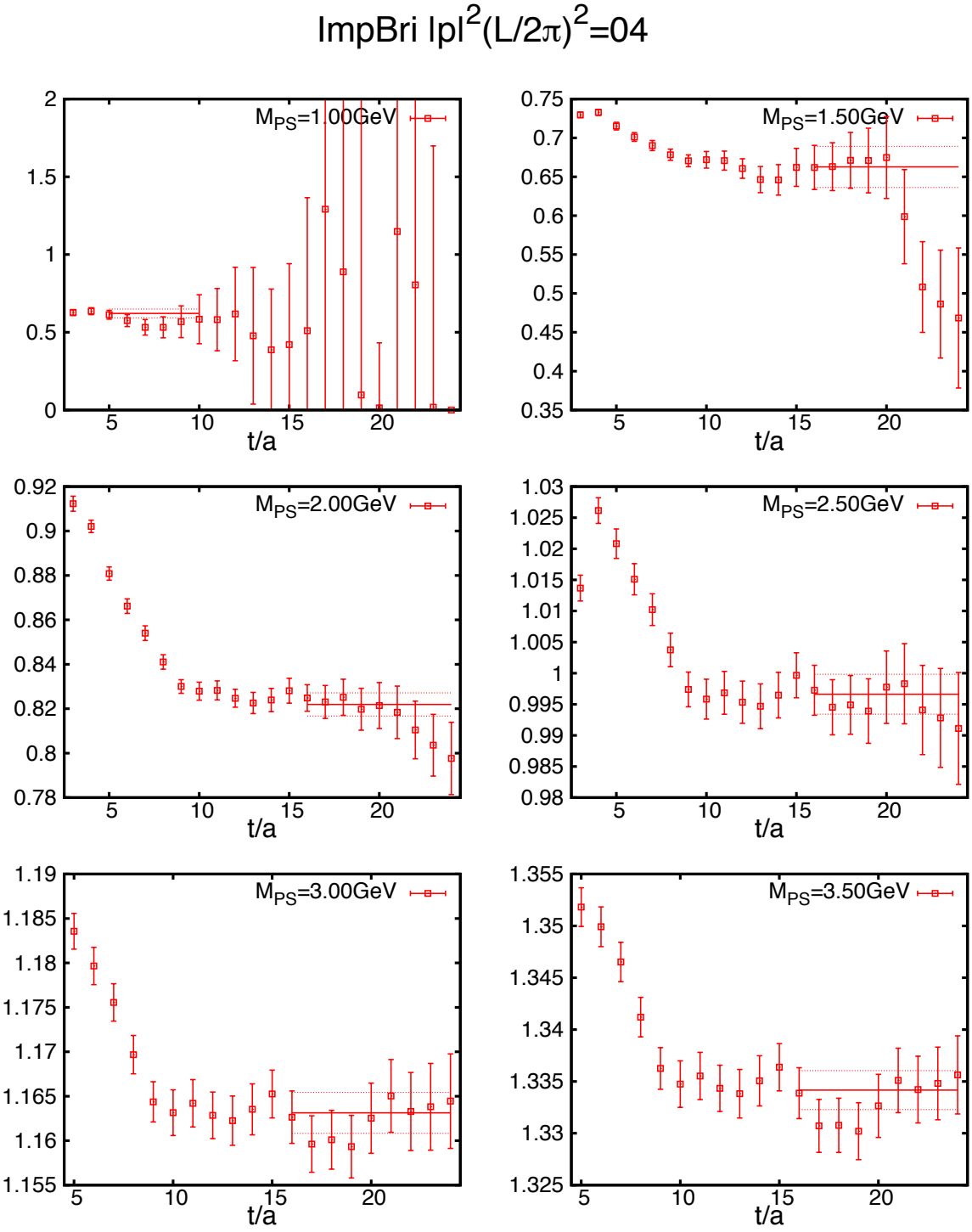

Figure 9.21: Effective masses for the improved Brillouin fermion on the $L/a = 24$ lattice.

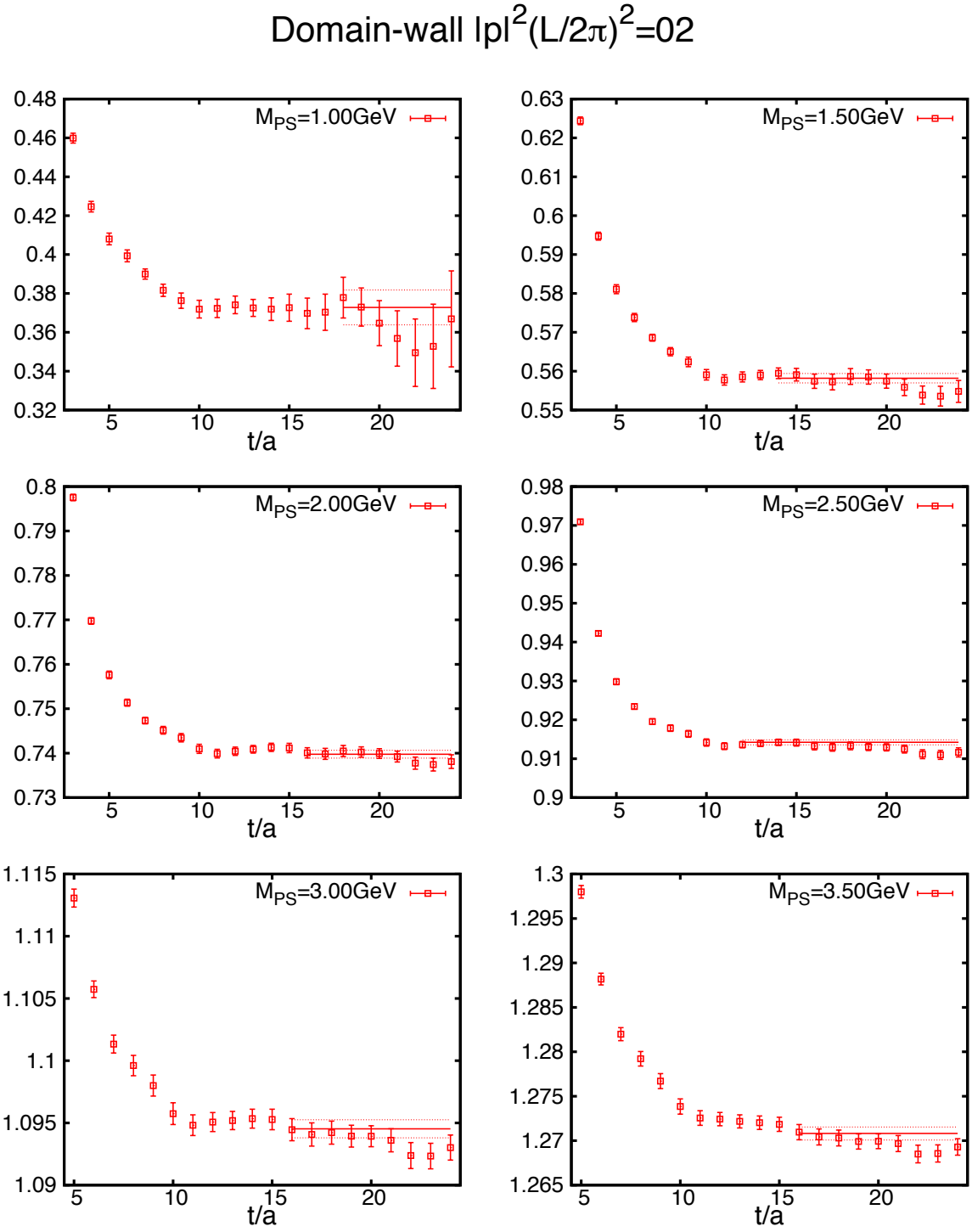

Figure 9.22: Effective masses for the domain-wall fermion on the $L/a = 24$ lattice.

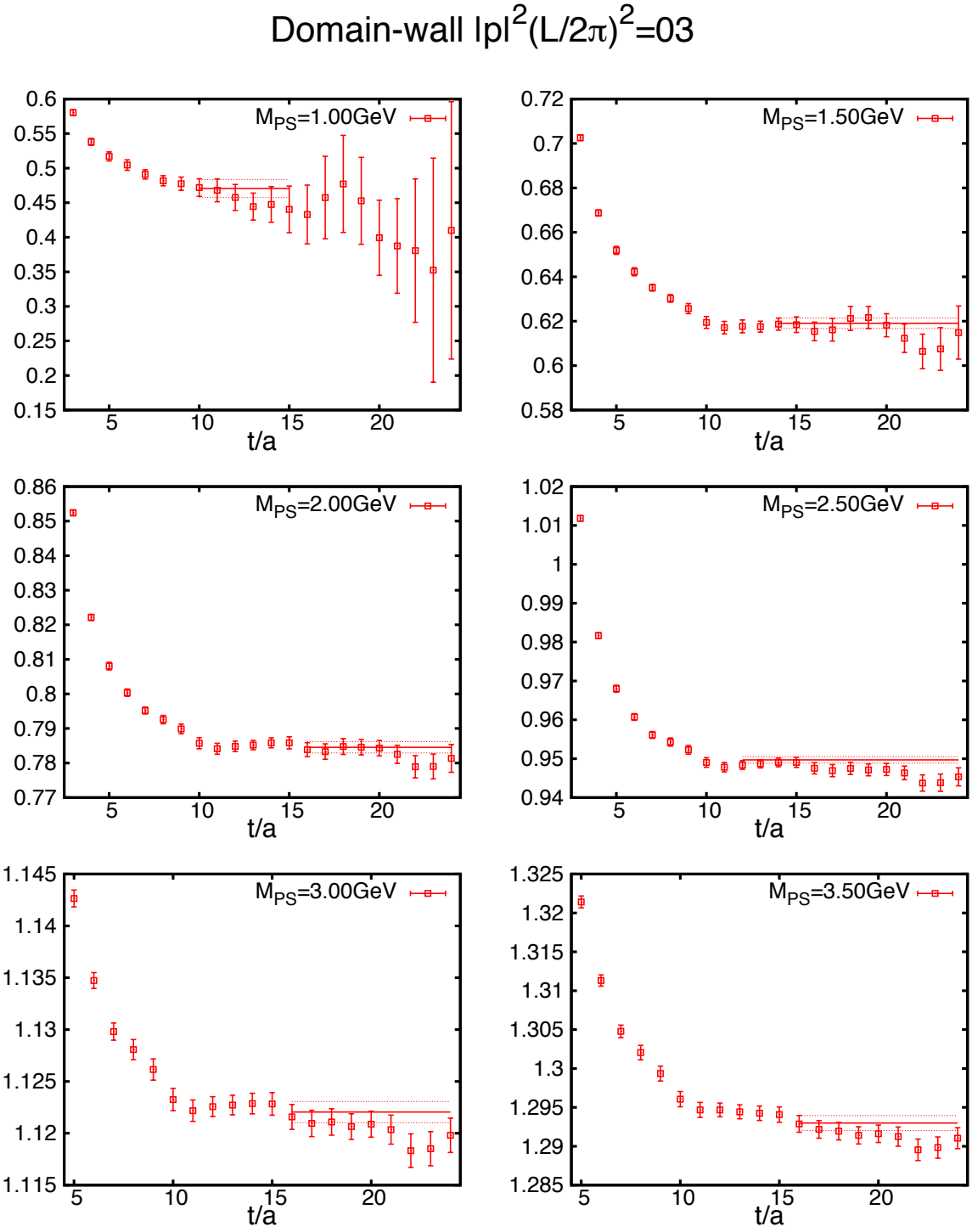

Figure 9.23: Effective masses for the domain-wall fermion on the $L/a = 24$ lattice.

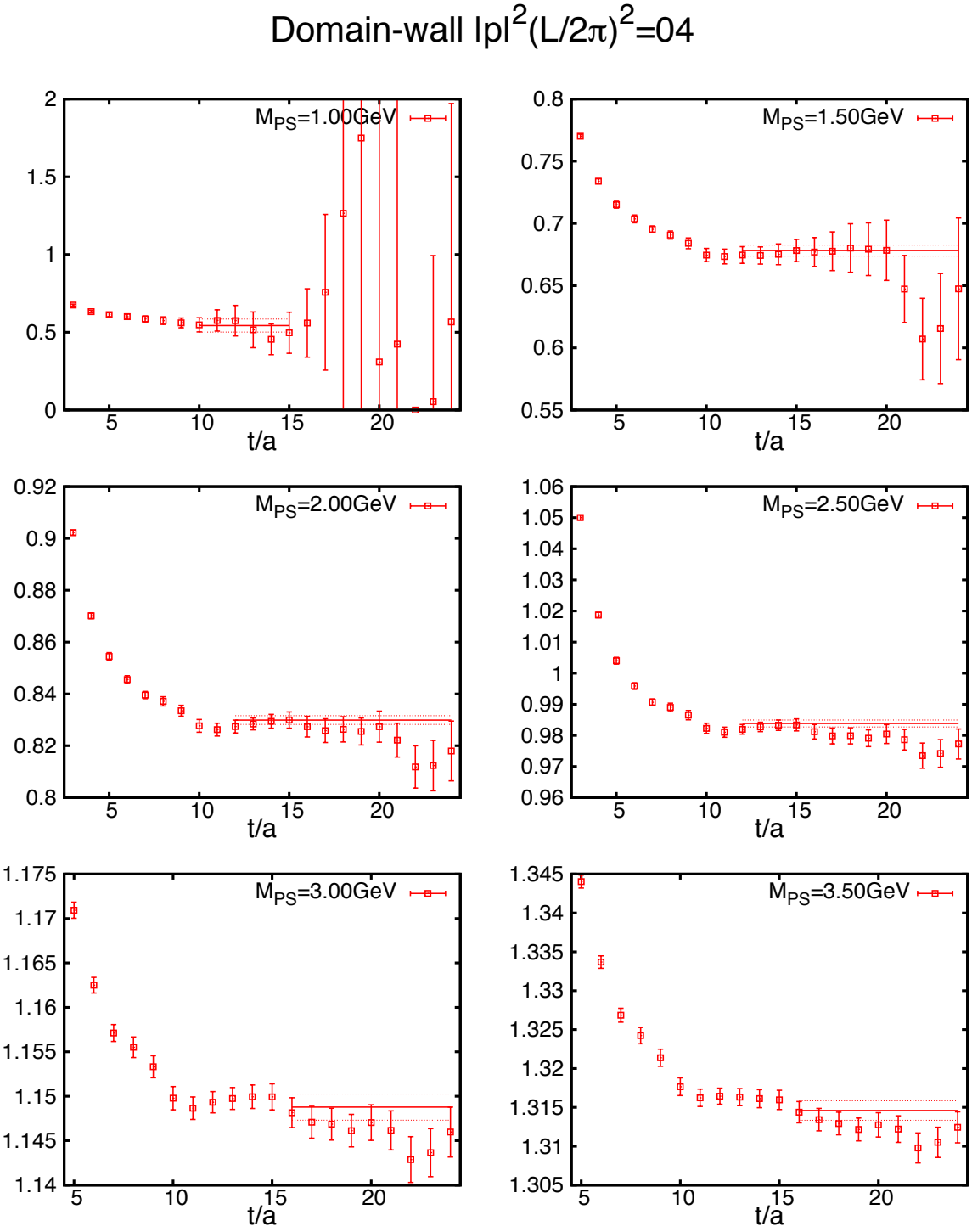

Figure 9.24: Effective masses for the domain-wall fermion on the $L/a = 24$ lattice.

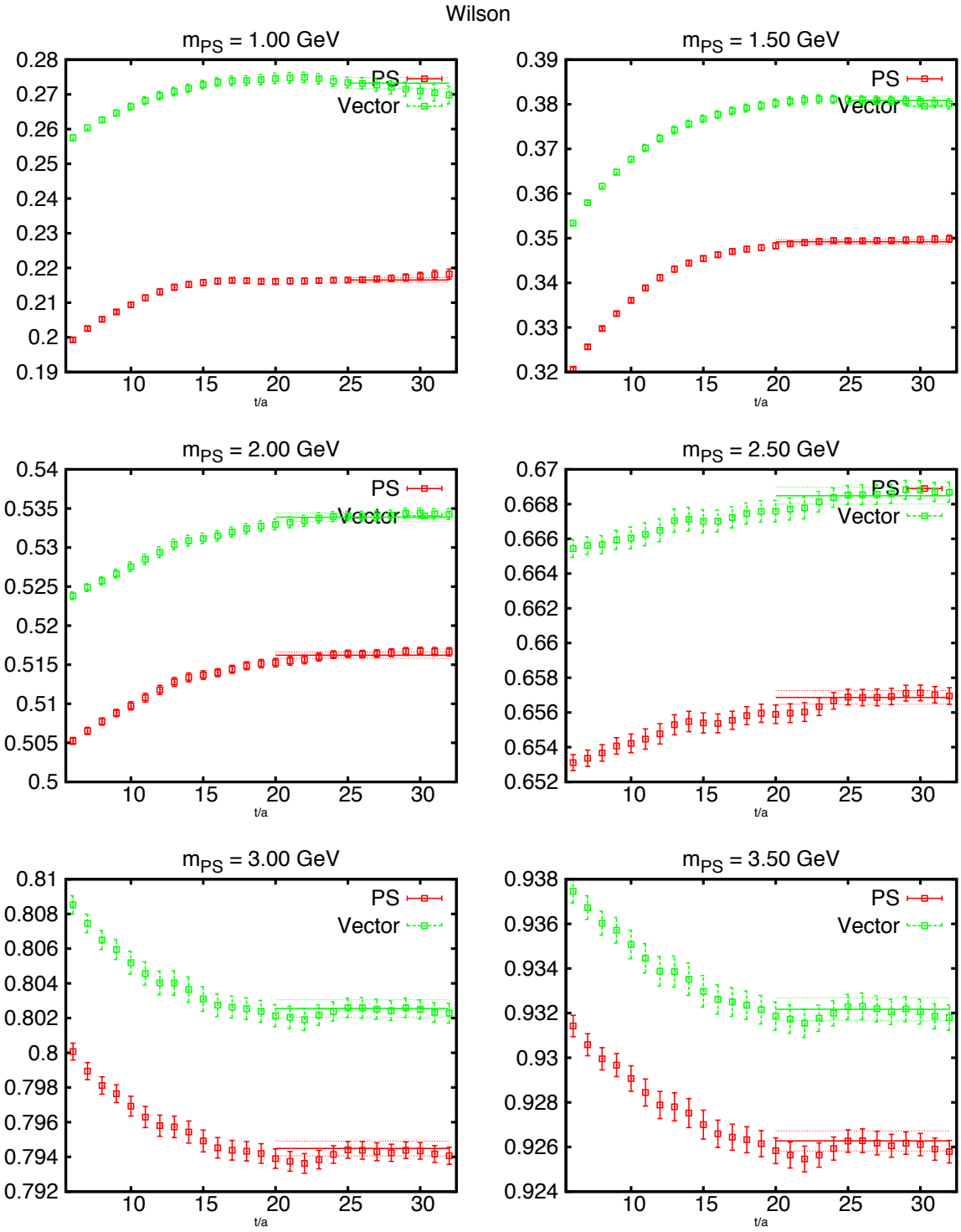

Figure 9.25: Effective masses for the Wilson fermion on the $L/a = 32$ lattice.

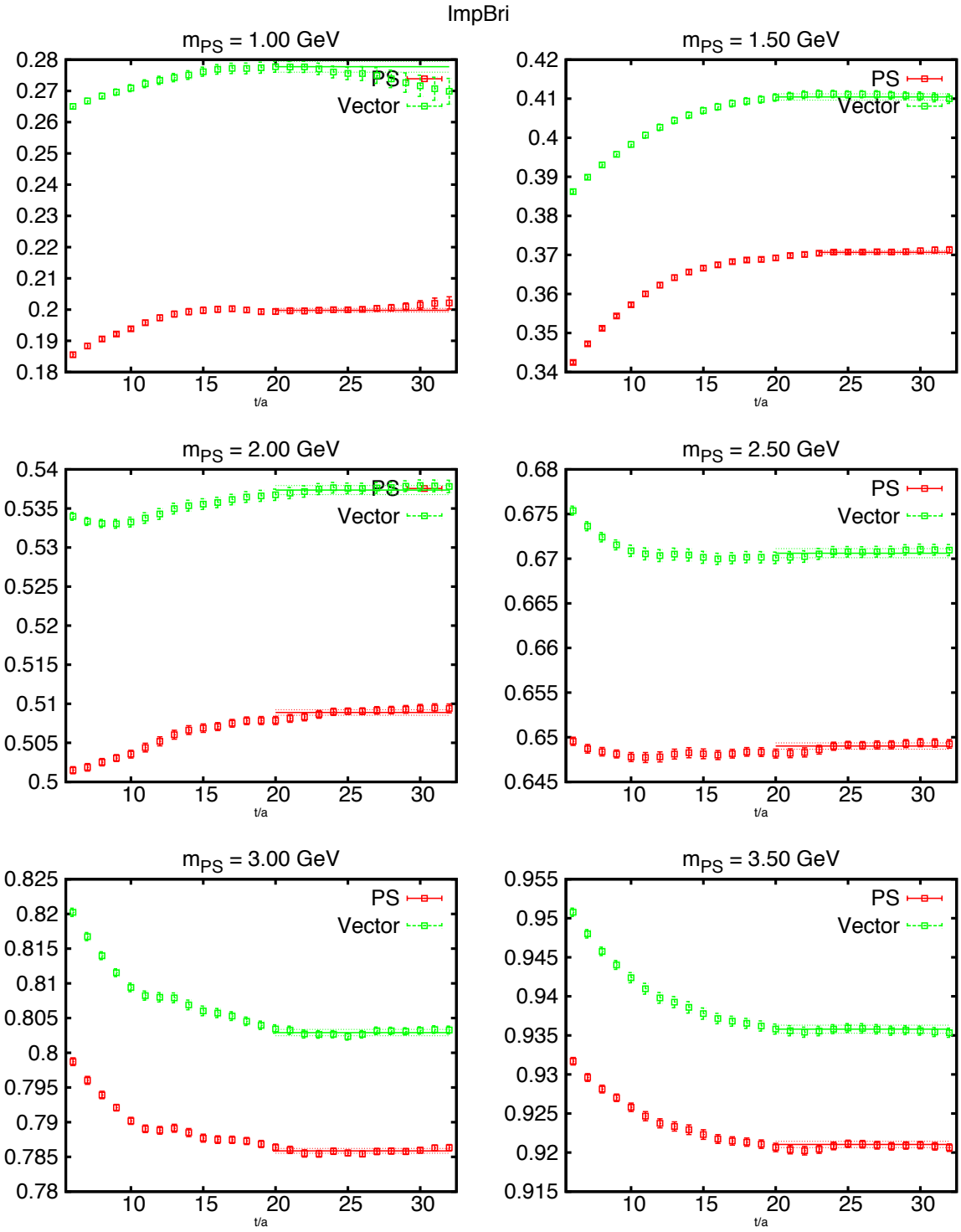

Figure 9.26: Effective masses for the improved Brillouin fermion on the $L/a = 32$ lattice.

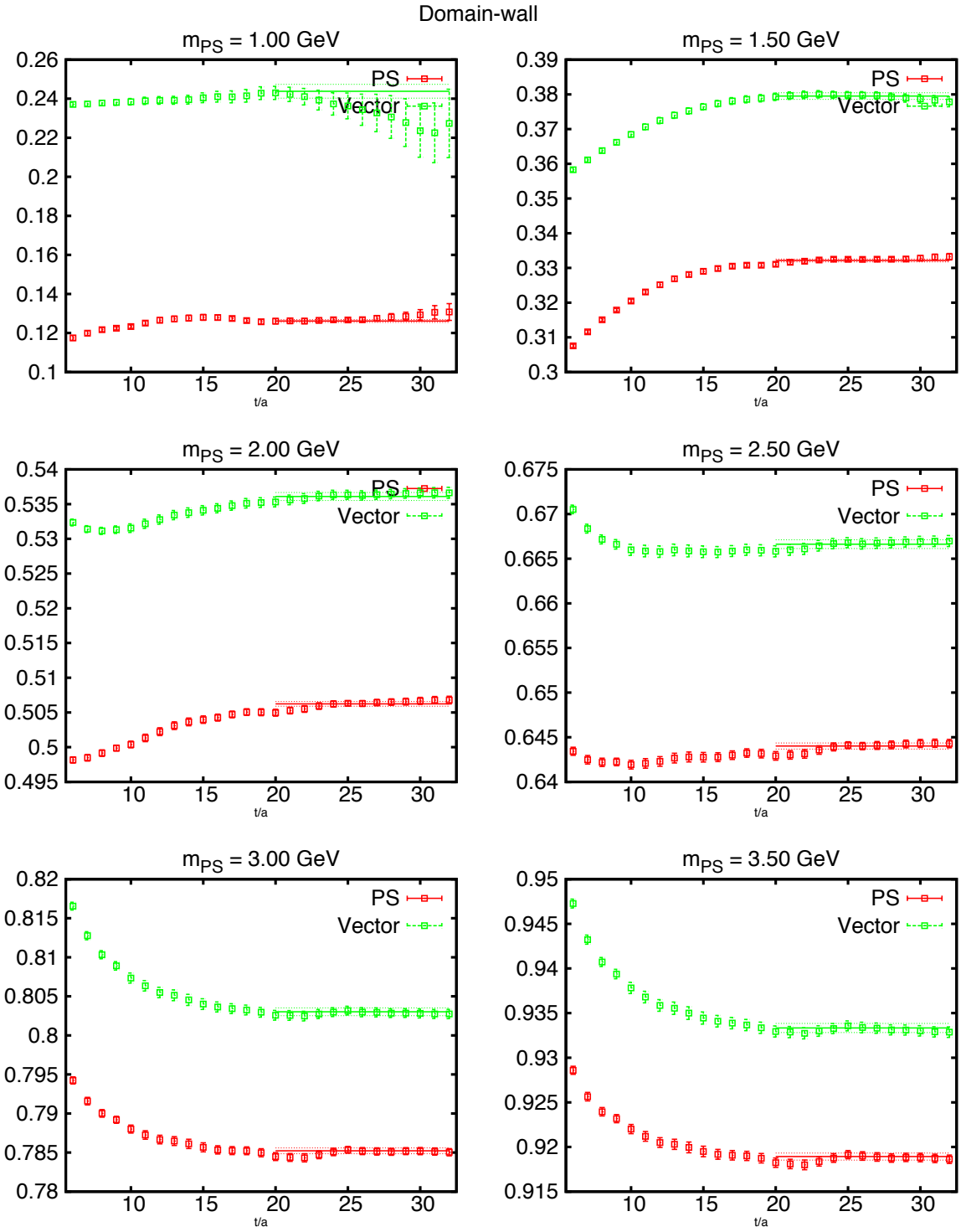

Figure 9.27: Effective masses for the domain-wall fermion on the $L/a = 32$ lattice.

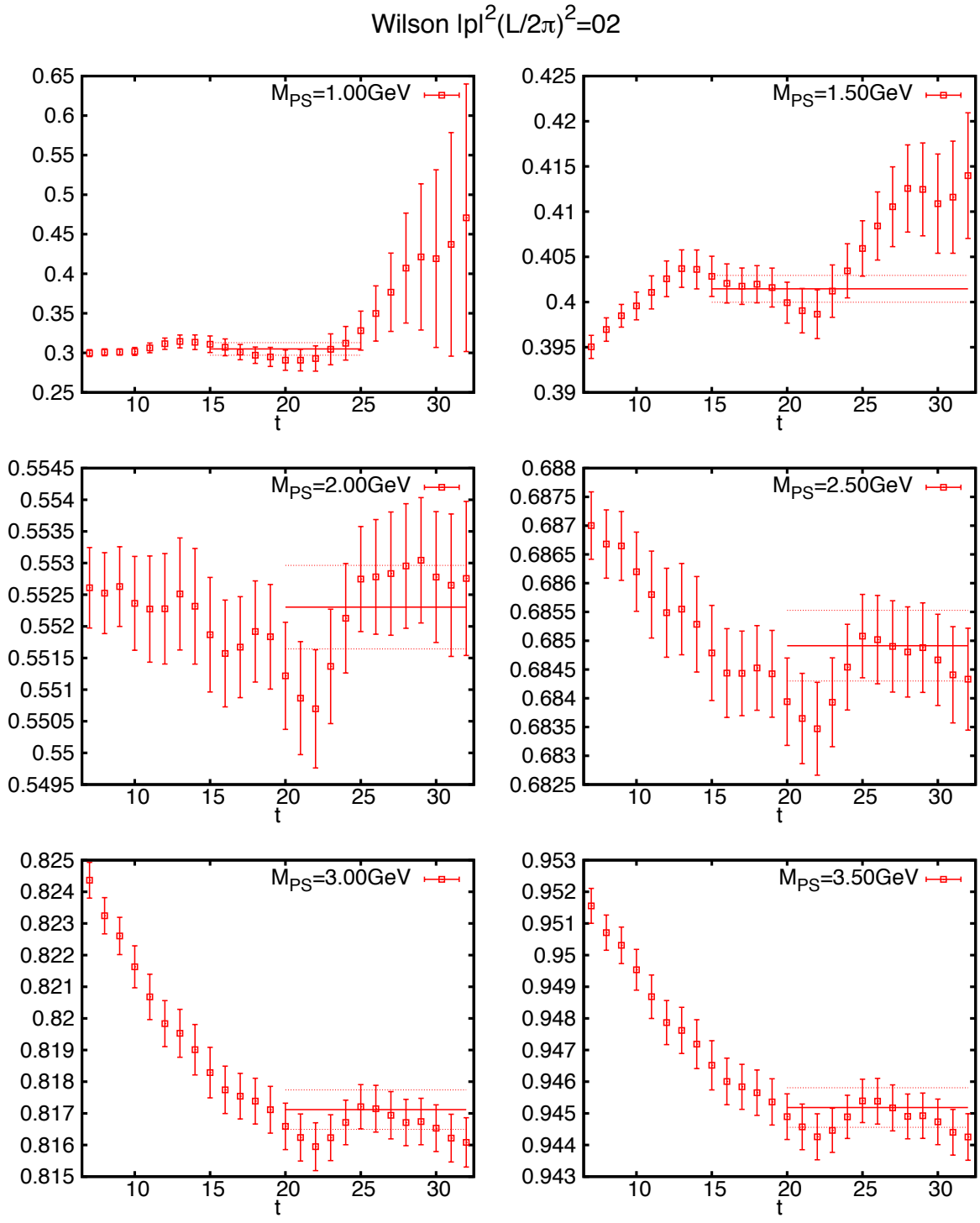

Figure 9.28: Effective masses for the Wilson fermion on the $L/a = 32$ lattice.

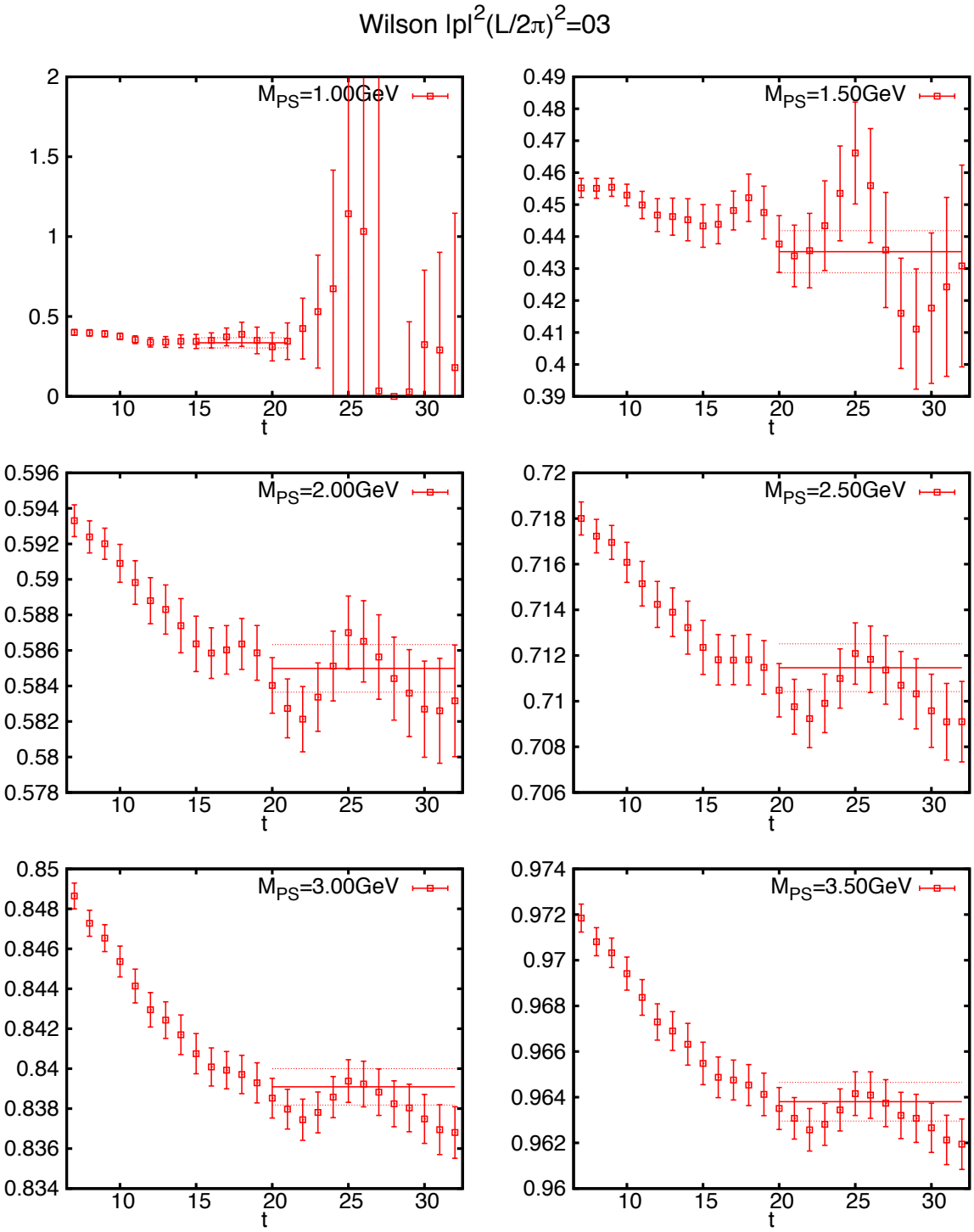

Figure 9.29: Effective masses for the Wilson fermion on the $L/a = 32$ lattice.

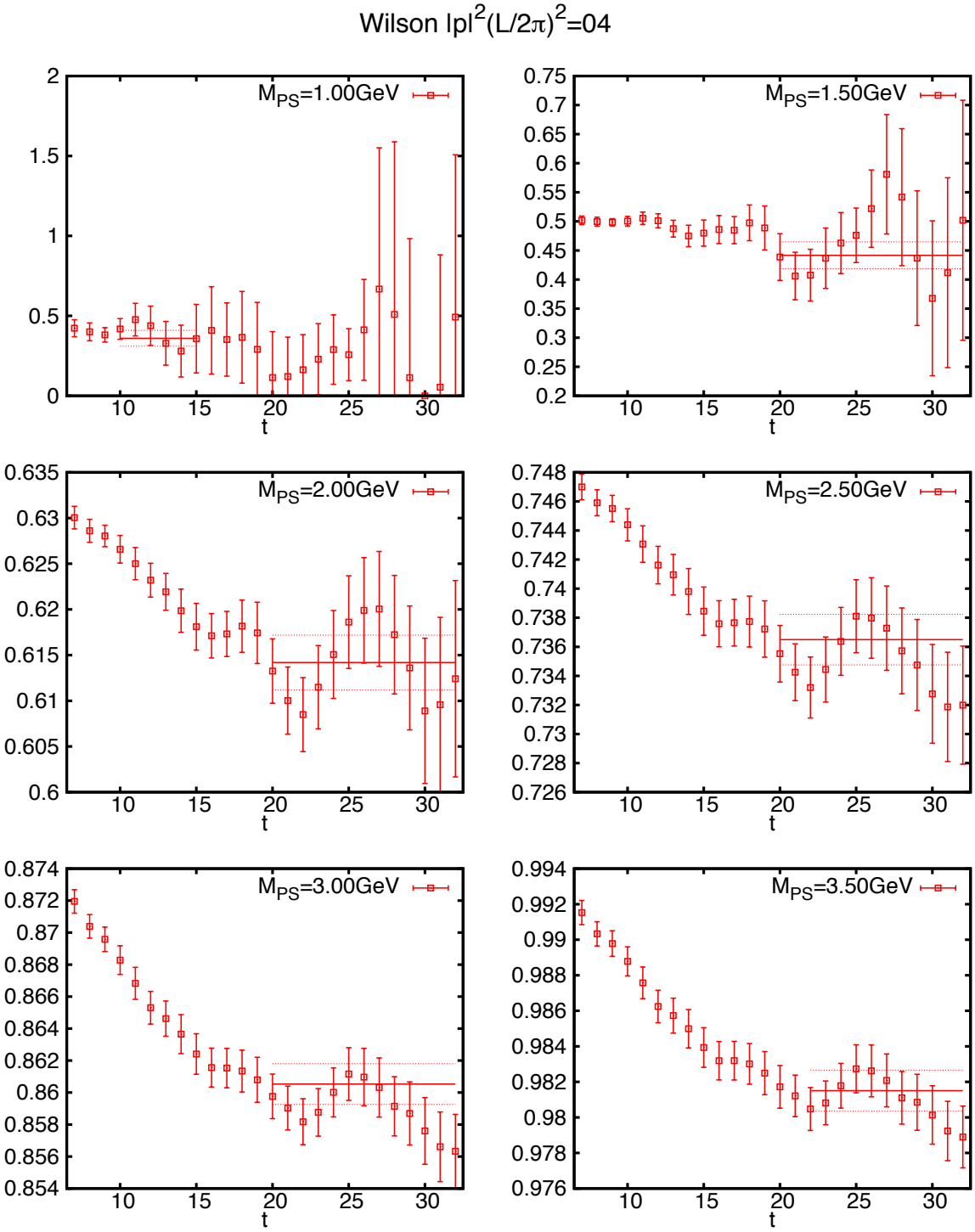

Figure 9.30: Effective masses for the Wilson fermion on the $L/a = 32$ lattice.

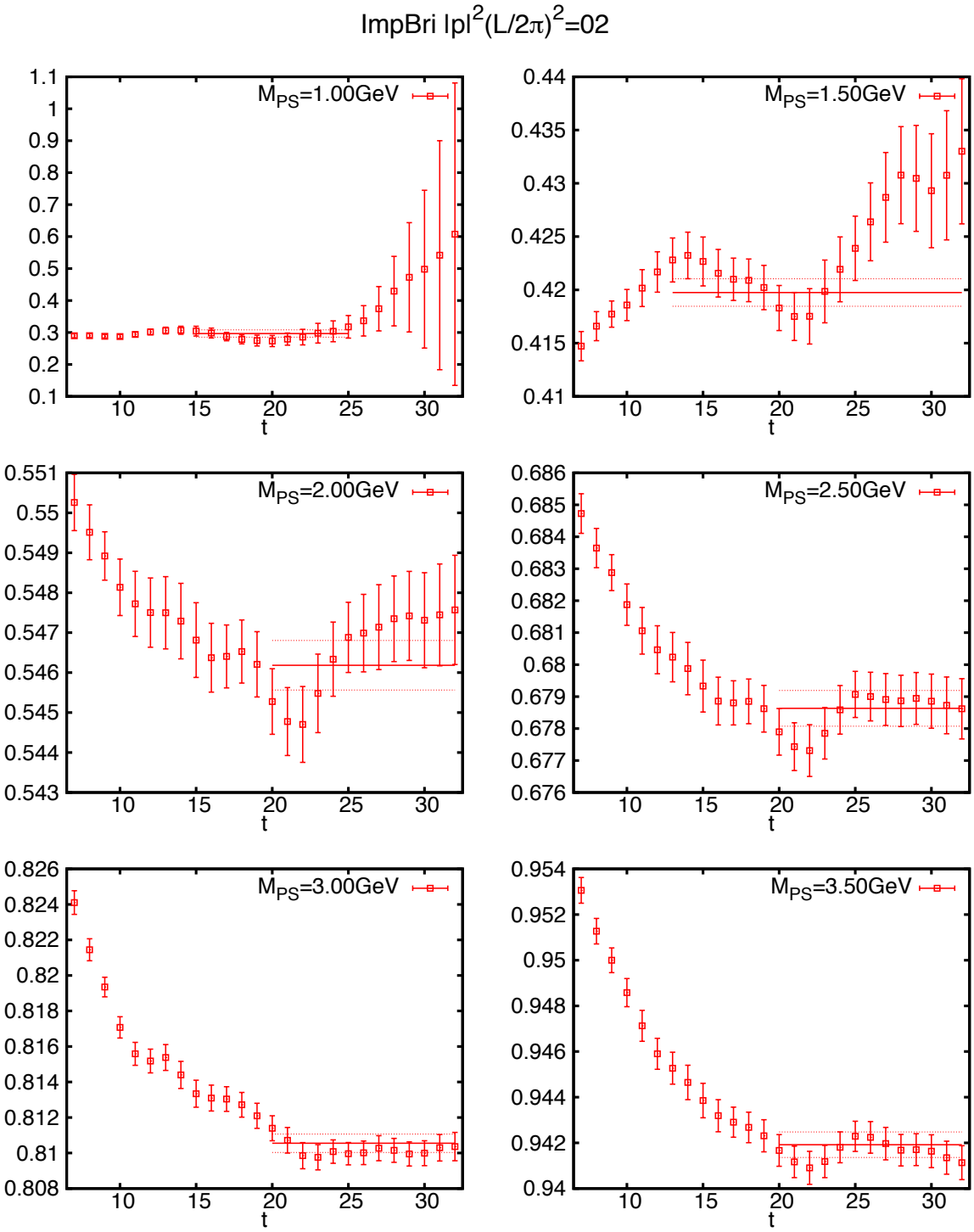

Figure 9.31: Effective masses for the improved Brillouin fermion on the $L/a = 32$ lattice.

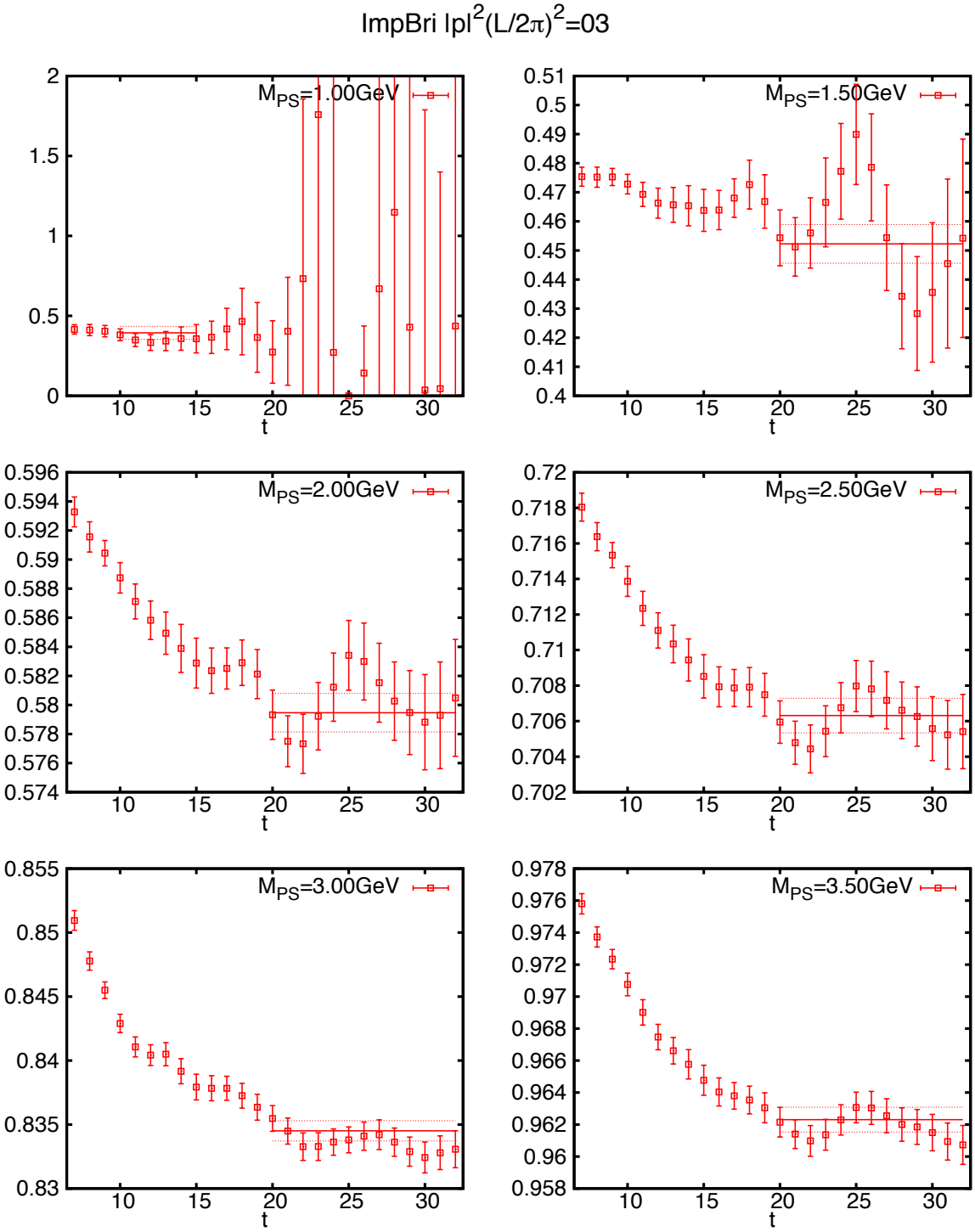

Figure 9.32: Effective masses for the improved Brillouin fermion on the $L/a = 32$ lattice.

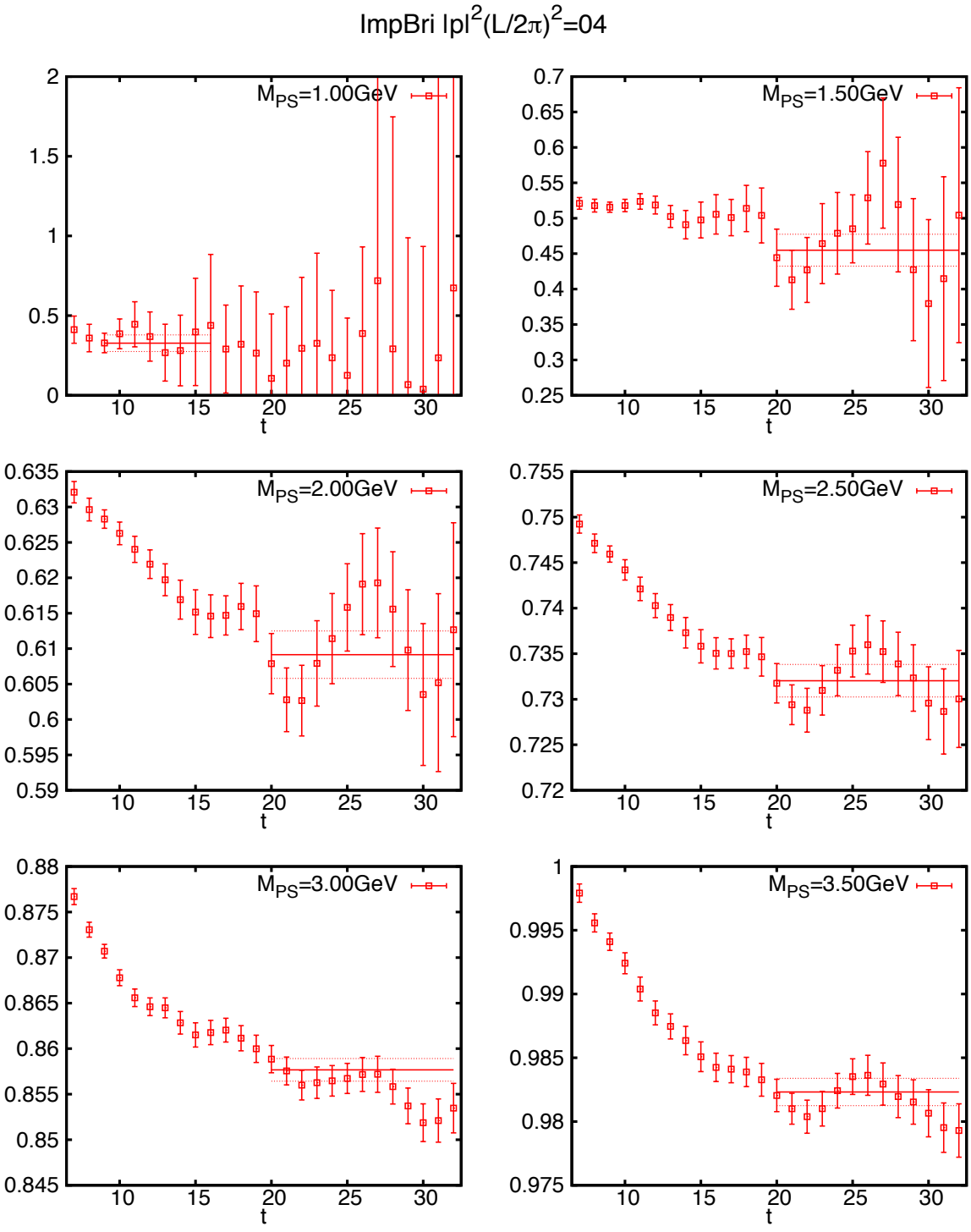

Figure 9.33: Effective masses for the improved Brillouin fermion on the $L/a = 32$ lattice.

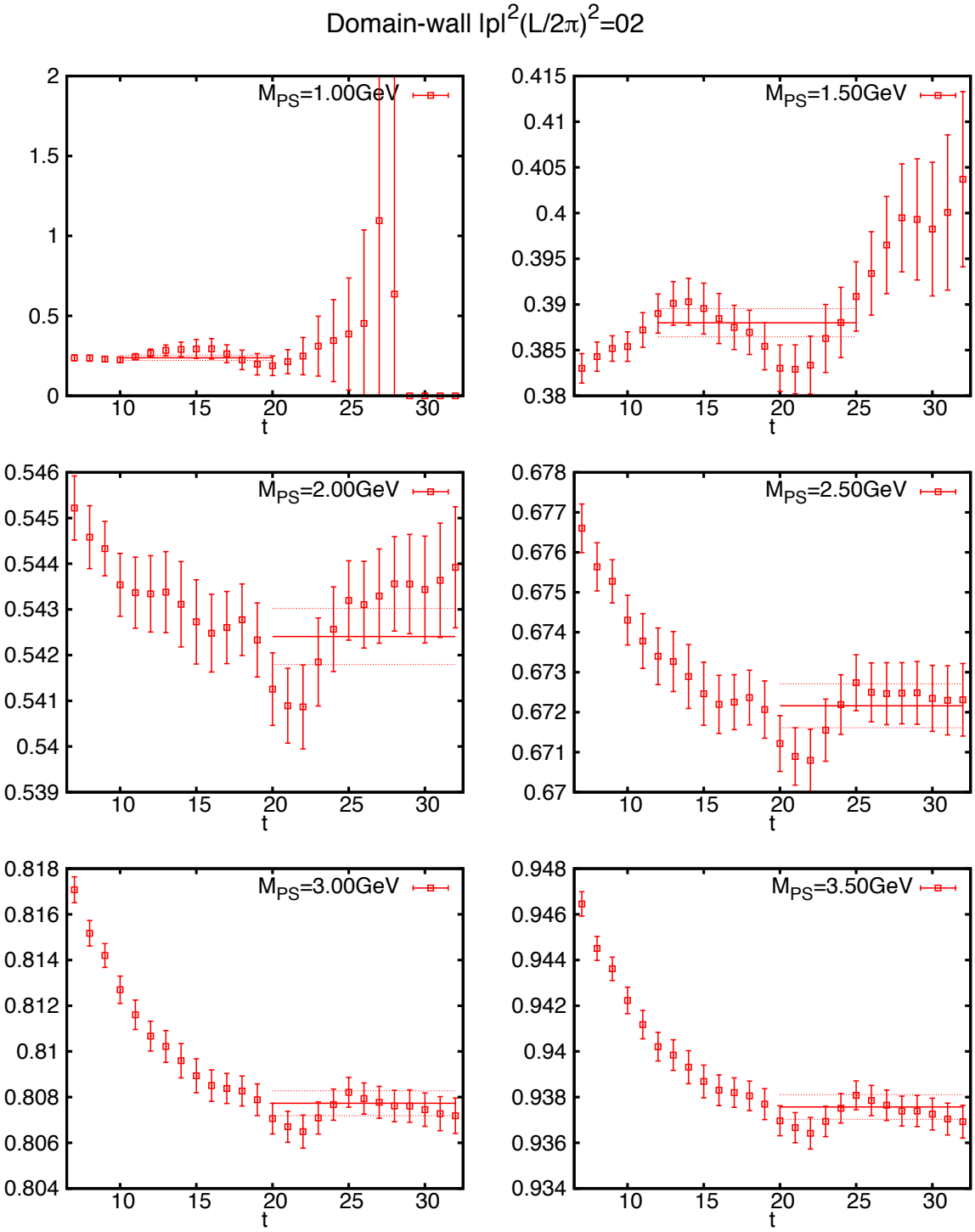

Figure 9.34: Effective masses for the domain-wall fermion on the $L/a = 32$ lattice.

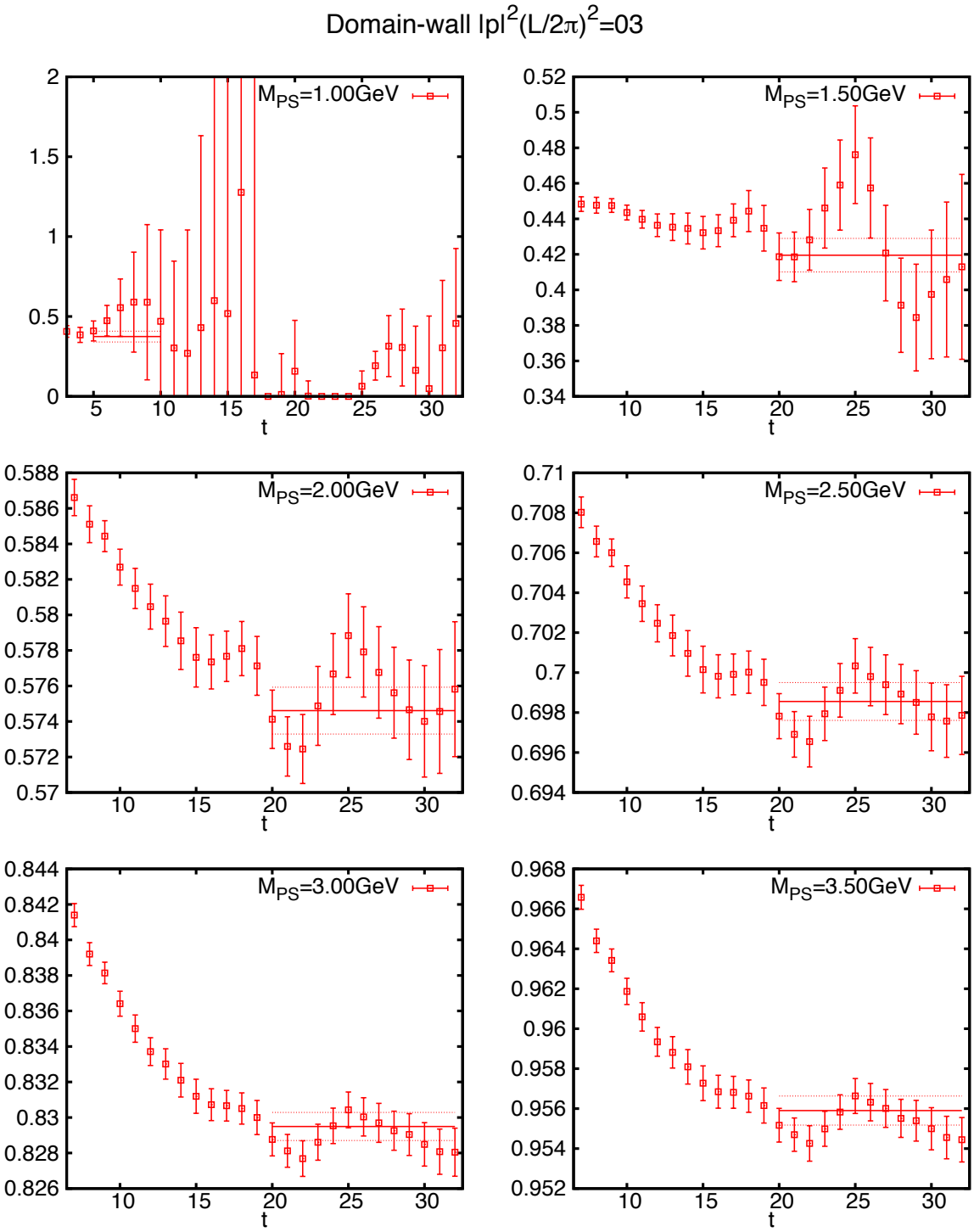

Figure 9.35: Effective masses for the domain-wall fermion on the $L/a = 32$ lattice.

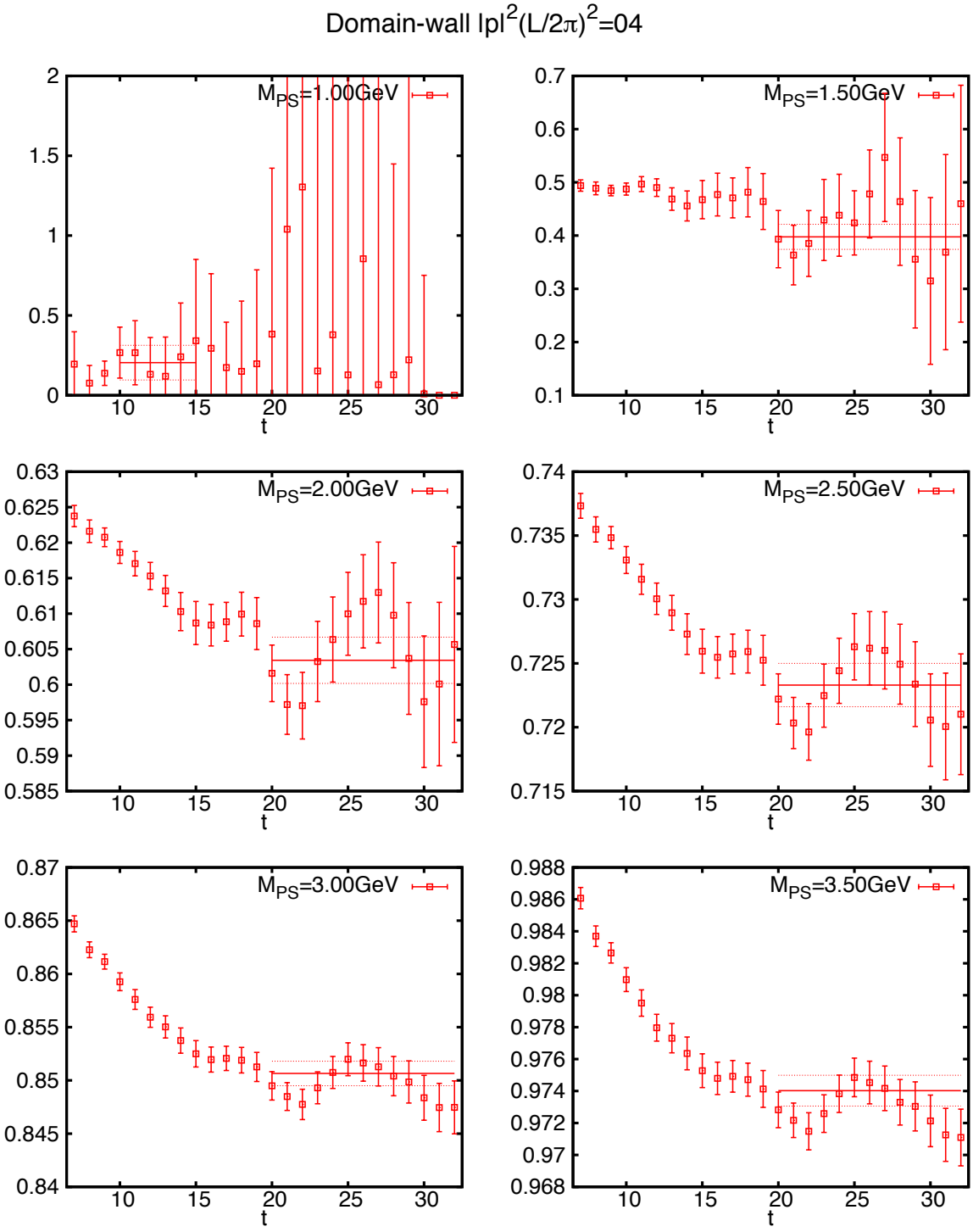

Figure 9.36: Effective masses for the domain-wall fermion on the $L/a = 32$ lattice.

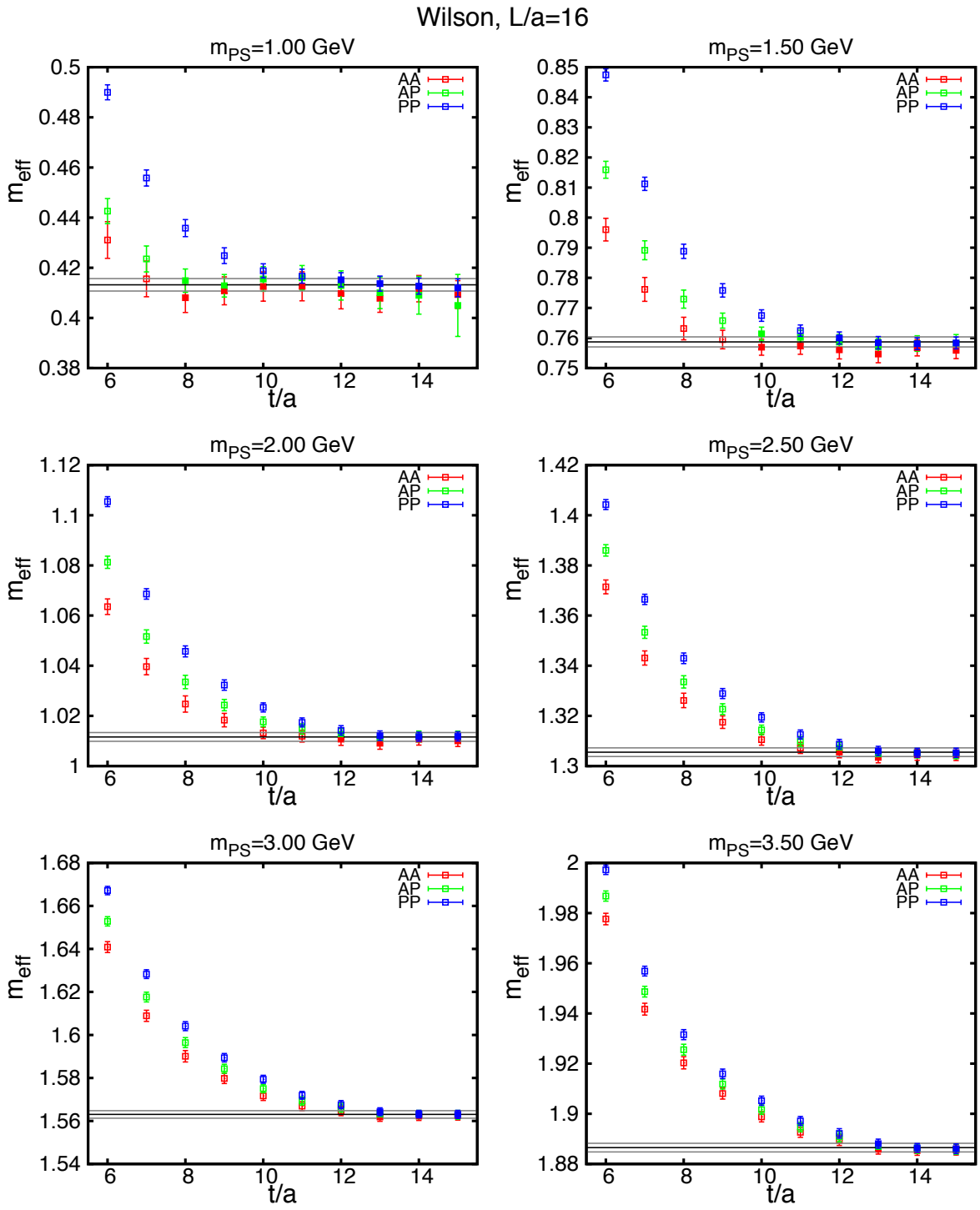

Figure 9.37: Effective masses for the Wilson fermion on the $L/a = 16$ lattice.

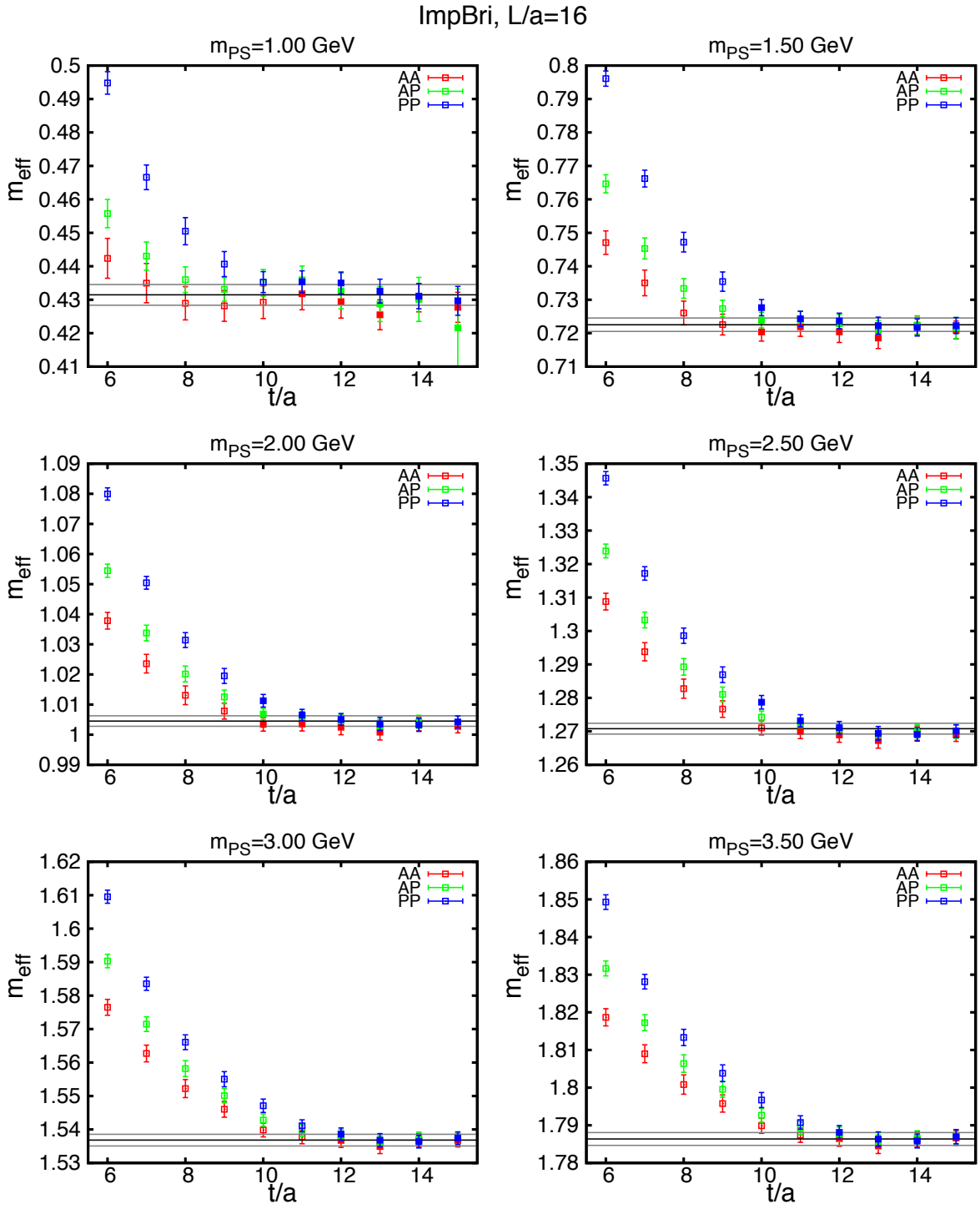

Figure 9.38: Effective masses for the improved Brillouin fermion on the $L/a = 16$ lattice.

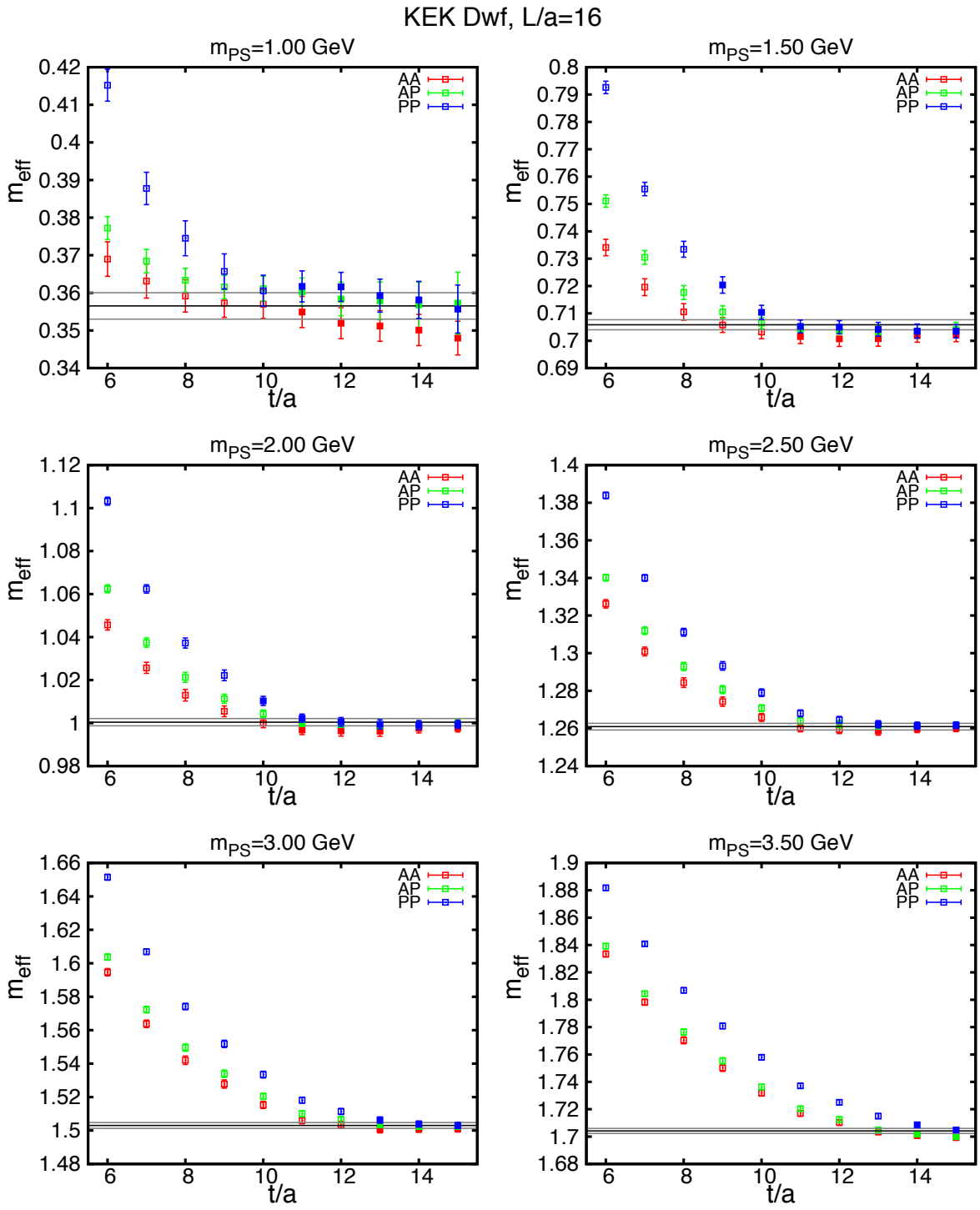

Figure 9.39: Effective masses for the domain-wall fermion on the $L/a = 16$ lattice.

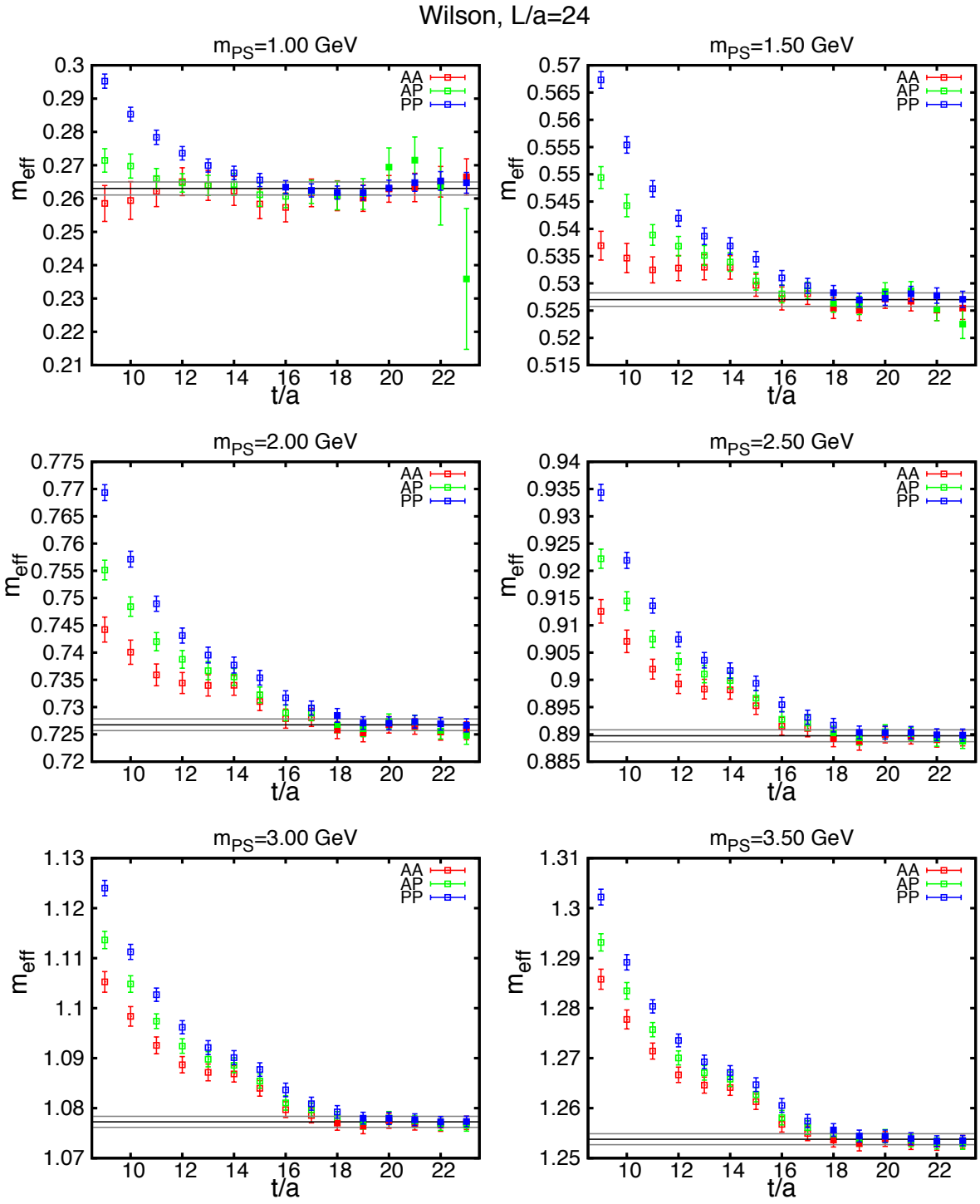

Figure 9.40: Effective masses for the Wilson fermion on the $L/a = 24$ lattice.

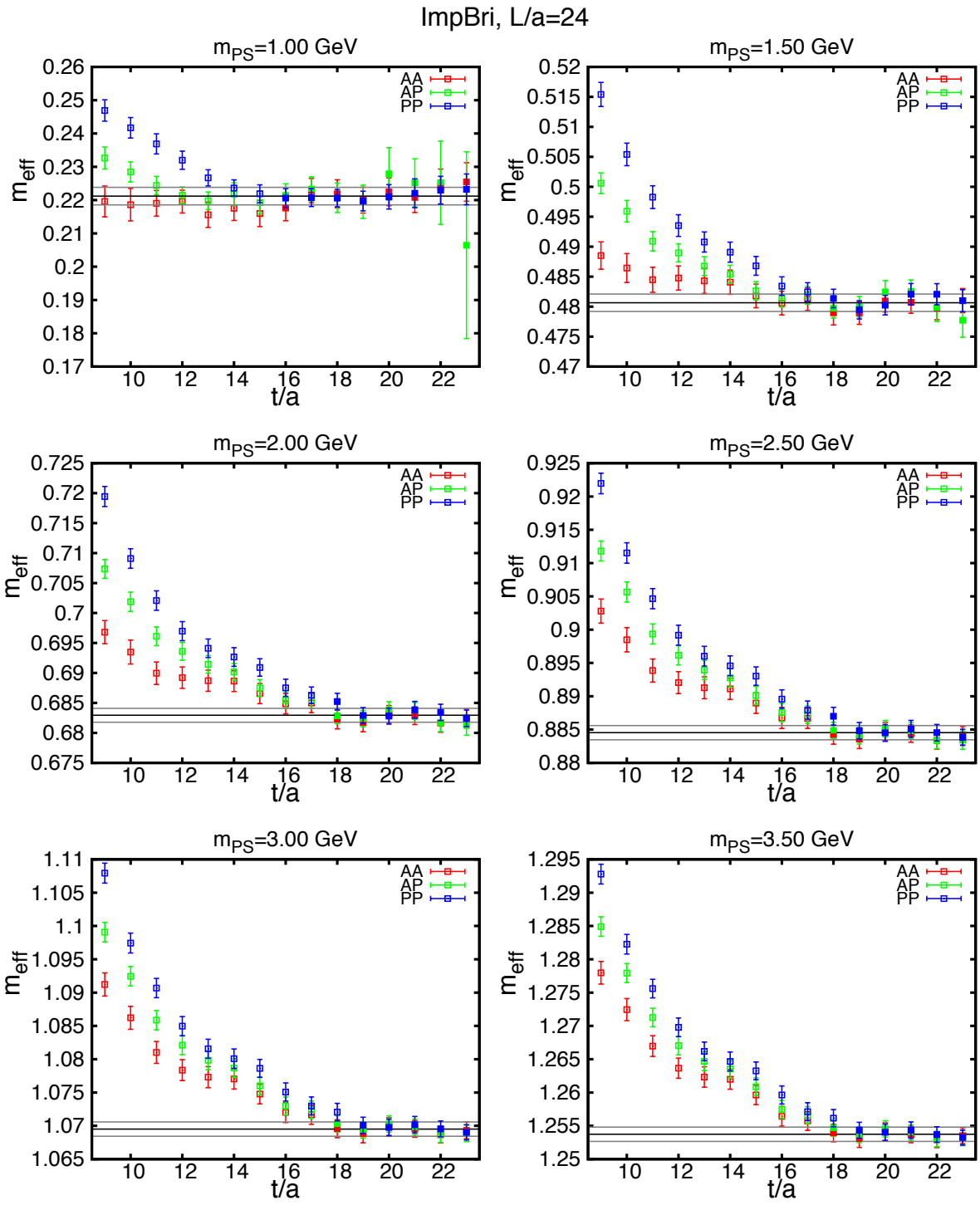

Figure 9.41: Effective masses for the improved Brillouin fermion on the $L/a = 24$ lattice.

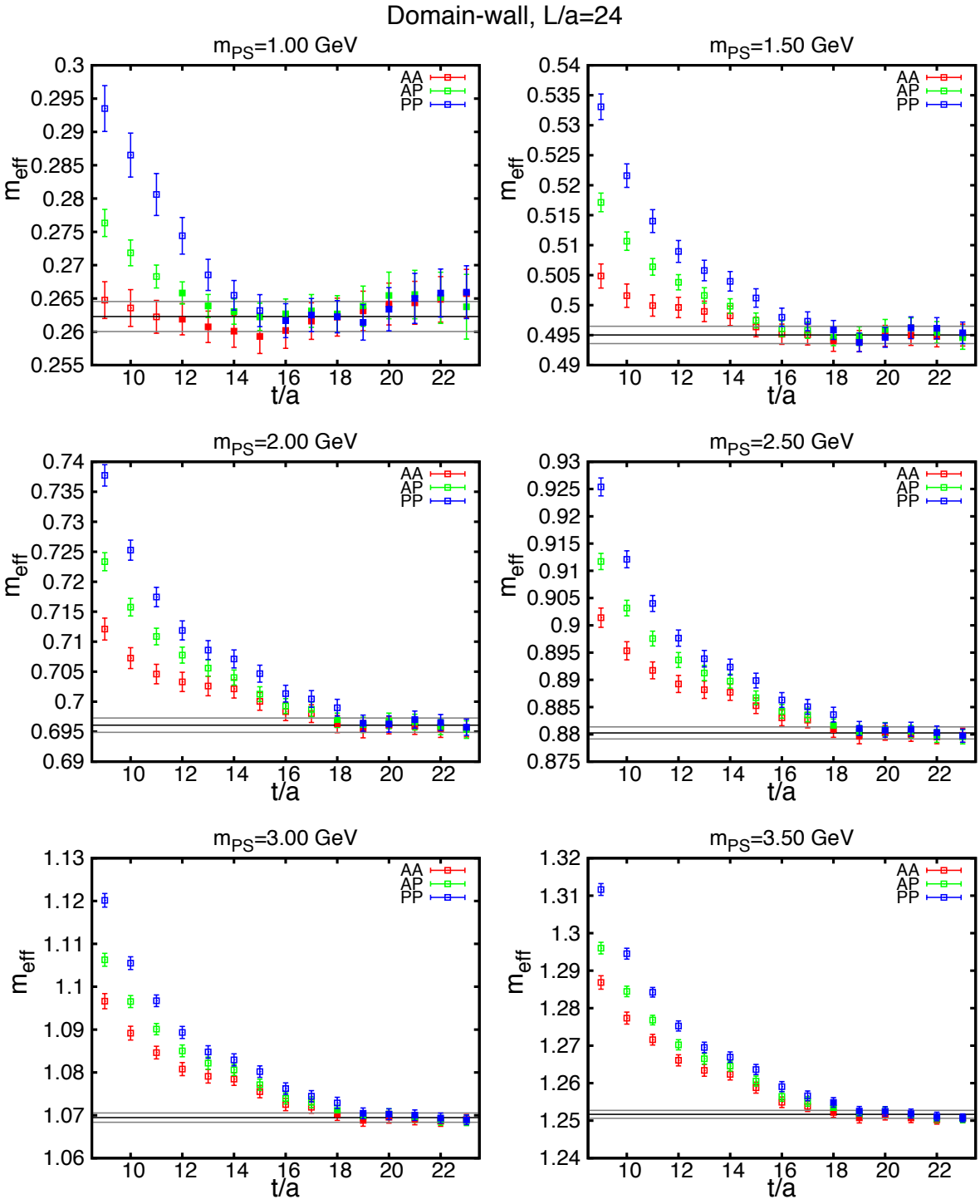

Figure 9.42: Effective masses for the domain-wall fermion on the $L/a = 24$ lattice.

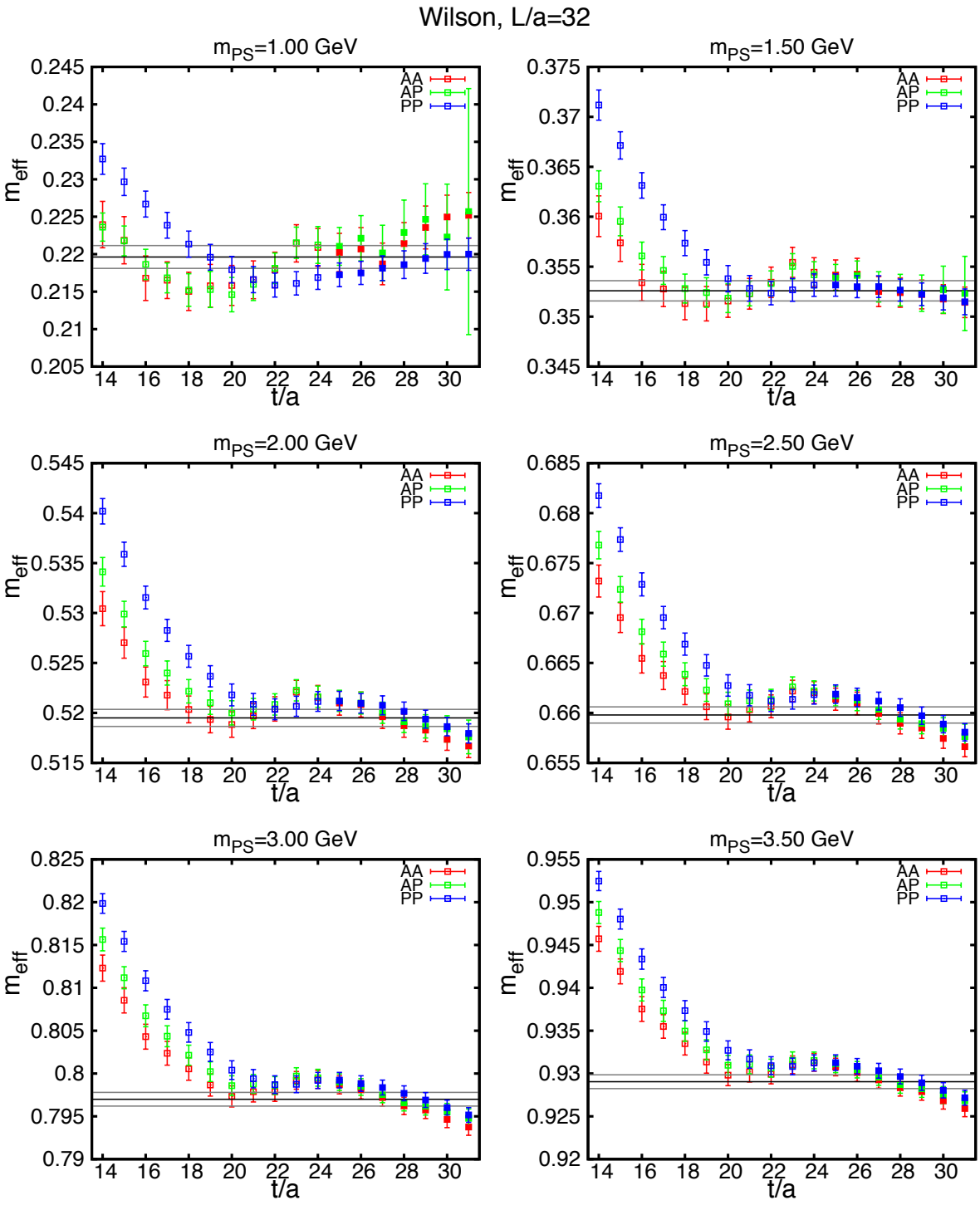

Figure 9.43: Effective masses for the Wilson fermion on the $L/a = 32$ lattice.

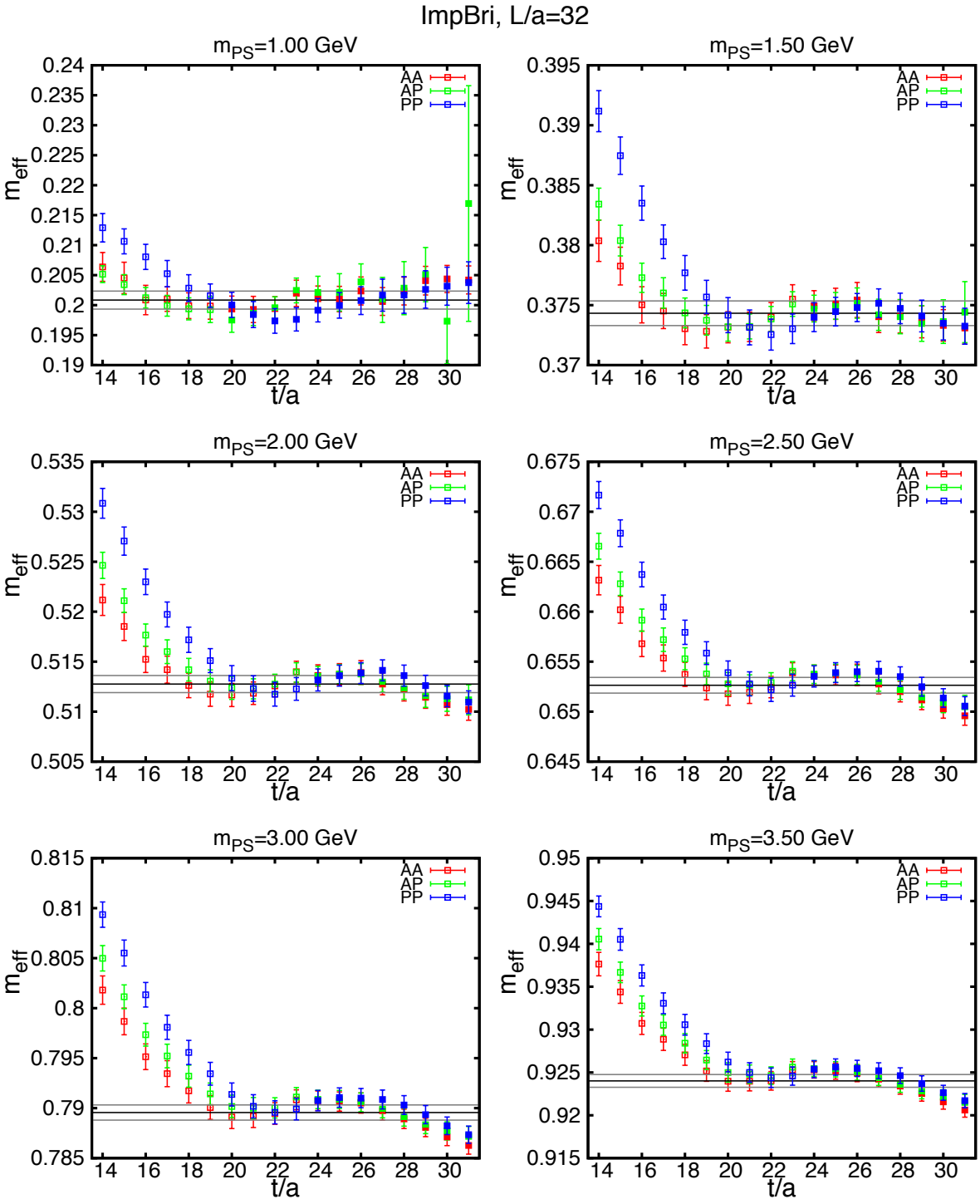

Figure 9.44: Effective masses for the improved Brillouin fermion on the $L/a = 32$ lattice.

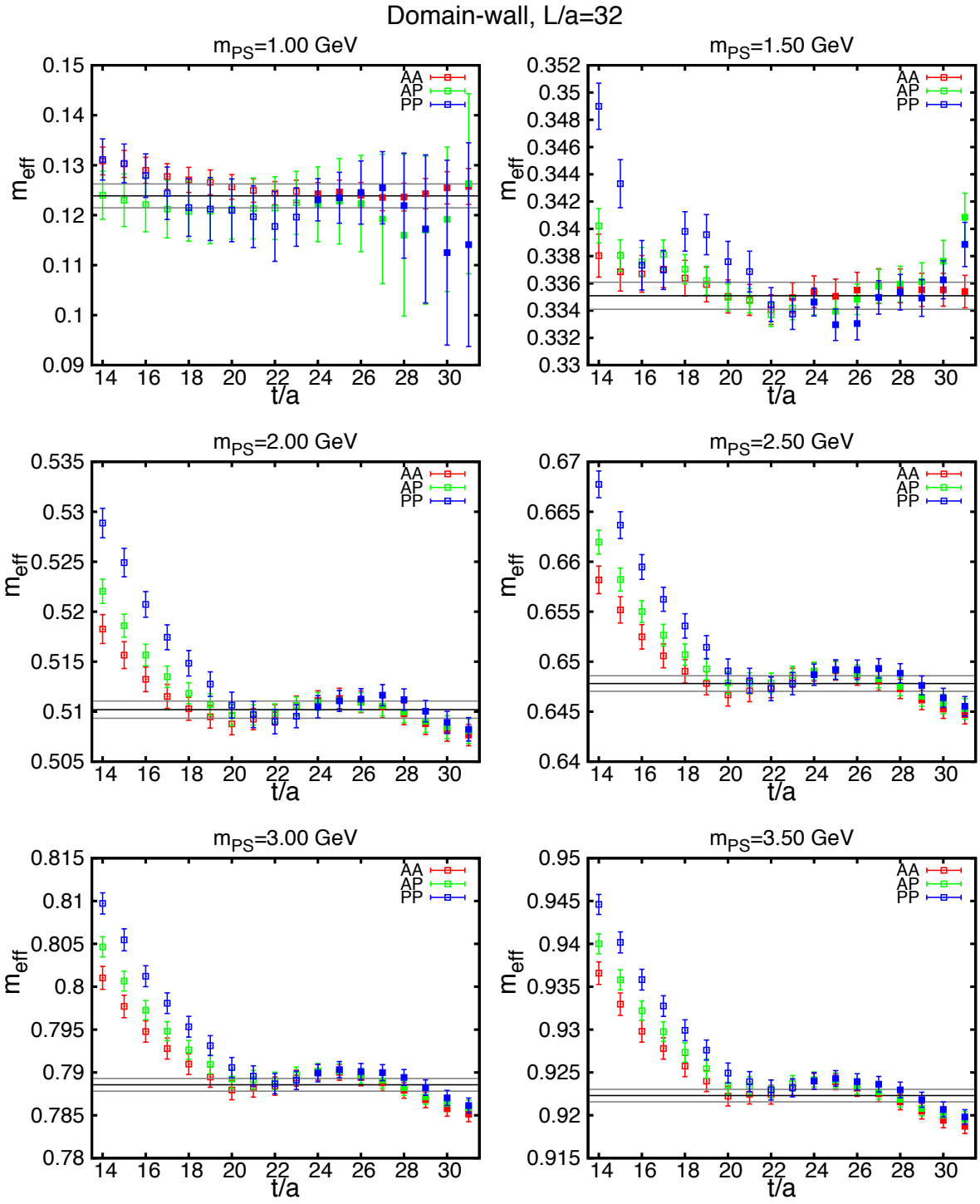

Figure 9.45: Effective masses for the domain-wall fermion on the $L/a = 32$ lattice.

Appendix A

κ of the Brillouin-type operator

The Brillouin operator is defined by

$$D = \sum_{\mu} \gamma_\mu \nabla_\mu^{iso} - \frac{r}{2}\Delta^{bri} + m. \tag{A.1}$$

Then we divide $\triangle^{bri}$ to a non-hopping term and any other hopping terms.

$$\triangle^{bri} = \triangle_{0-hop} + \triangle_{hop}, \tag{A.2}$$

where $\triangle_{hop}$ denotes hopping terms and

$$\triangle_{0hop} = -15/4. \tag{A.3}$$

we do not refer the detailed expression of the $\triangle_{hop}$, because now we are not interested in the specific form of hopping terms. Then the fermion action is

$$\begin{aligned} S_F &= \sum_{n,m} \bar{\psi}_n \left(\sum_{\mu} \gamma_\mu \nabla_\mu^{iso} - \frac{r}{2}\left(\triangle_{hop} - \frac{15}{4} \right) \right) \psi_m + \sum_n m \bar{\psi}_n \psi_n \\ &= \sum_{n,m} \bar{\psi}_n \left(\sum_{\mu} \gamma_\mu \nabla_\mu^{iso} - \frac{r}{2}\triangle_{hop} \right) \psi_m + \sum_n \left(m + \frac{15}{8} r \right) \bar{\psi}_n \psi_n. \end{aligned} \tag{A.4}$$

Thus we define the kappa in the case of the Brillouin operator as follows

$$\kappa^{bri} = \frac{1}{m + \frac{15}{8} r} \tag{A.5}$$

Then Eq.(A.4) becomes as follows

$$S_F = \kappa^{bri} \sum_{n,m} \bar{\psi}_n \left(\sum_{\mu} \gamma_\mu \nabla_\mu^{iso} - \frac{r}{2}\triangle_{hop} \right) \psi'_m + \sum_n \bar{\psi}_n \psi'_n \tag{A.6}$$

$$\psi'_n = \frac{1}{\kappa^{bri}} \psi_n \tag{A.7}$$

Next we will consider a 0-hop term of improved Brillouin operator. The improved Brillouin operator is defined as follows

$$D^{imp} = \sum_{\mu} \gamma_\mu (1 - \frac{1}{12} \triangle^{bri}) \nabla_\mu^{iso} (1 - \frac{1}{12} \triangle^{bri}) + c_{imp} \left(\triangle^{bri} \right)^2 + m. \tag{A.8}$$

If one needs 0-hopping contribution of the improved Brillouin operator, we have to perform some calculations.

$$\begin{aligned} \triangle^{imp} &= -\frac{1}{4} \left(\triangle^{bri} \right)^2 \\ &= -\frac{1}{4} \left(\triangle_{0-hop} + \triangle_{hop} \right)^2 \\ &= -\frac{1}{4} \left(\triangle_{0-hop}^2 + \triangle_{hop}^2 + 2 \triangle_{hop} \triangle_{0-hop} \right) \\ &= -\frac{1}{4} \left(\triangle'_{hop} + \triangle'_{0-hop} \right) \\ \triangle'_{0hop} &= \triangle_{0hop}^2 = \frac{225}{16} \end{aligned}$$

Thus the fermion action is given by

$$S_F = \sum_{n,m} \sum_{\mu} \bar{\psi}_n \left[\gamma_\mu \nabla_\mu^{imp} - \frac{r}{2} \left\{ -\frac{1}{4} \left(\triangle'_{hop} \right) \right\} \right] \psi_m + \left(m + \frac{225}{128} r \right) \sum_n \bar{\psi}_n \psi_n, \tag{A.9}$$

and the kappa of the improved Brillouin operator is defined by

$$\kappa^{imp} = \frac{1}{m + \frac{225}{128} r}. \tag{A.10}$$

Then Eq. (A.9) becomes as follows

$$S_F = \kappa^{imp} \sum_{n,m} \sum_{\mu} \bar{\psi}_n \left[\gamma_\mu \nabla_\mu^{imp} + \frac{r}{8} \triangle'_{hop} \right] \psi'_m + \sum_n \bar{\psi}_n \psi'_n \tag{A.11}$$

Bibliography

[1] Serguei Chatrchyan et al. Observation of a new boson at a mass of 125 GeV with the CMS experiment at the LHC. *Phys.Lett.*, B716:30–61, 2012.

[2] Georges Aad et al. Observation of a new particle in the search for the Standard Model Higgs boson with the ATLAS detector at the LHC. *Phys.Lett.*, B716:1–29, 2012.

[3] Sinya Aoki, Yasumichi Aoki, Claude Bernard, Tom Blum, Gilberto Colangelo, et al. Review of lattice results concerning low-energy particle physics. *Eur.Phys.J.*, C74(9):2890, 2014.

[4] R.J. Dowdall, C.T.H. Davies, R.R. Horgan, C.J. Monahan, and J. Shigemitsu. B-Meson Decay Constants from Improved Lattice Nonrelativistic QCD with Physical u, d, s, and c Quarks. *Phys.Rev.Lett.*, 110(22):222003, 2013.

[5] A. Bazavov et al. B- and D-meson decay constants from three-flavor lattice QCD. *Phys.Rev.*, D85:114506, 2012.

[6] Jochen Heitger and Rainer Sommer. Nonperturbative heavy quark effective theory. *JHEP*, 0402:022, 2004.

[7] G. Peter Lepage, Lorenzo Magnea, Charles Nakhleh, Ulrika Magnea, and Kent Hornbostel. Improved nonrelativistic QCD for heavy quark physics. *Phys.Rev.*, D46:4052–4067, 1992.

[8] Aida X. El-Khadra, Andreas S. Kronfeld, and Paul B. Mackenzie. Massive fermions in lattice gauge theory. *Phys.Rev.*, D55:3933–3957, 1997.

[9] Sinya Aoki, Yoshinobu Kuramashi, and Shin-ichi Tominaga. Relativistic heavy quarks on the lattice. *Prog.Theor.Phys.*, 109:383–413, 2003.

[10] Norman H. Christ, Min Li, and Huey-Wen Lin. Relativistic Heavy Quark Effective Action. *Phys.Rev.*, D76:074505, 2007.

[11] Mehmet B. Oktay and Andreas S. Kronfeld. New lattice action for heavy quarks. *Phys.Rev.*, D78:014504, 2008.

[12] K. Symanzik. Continuum Limit and Improved Action in Lattice Theories. 1. Principles and phi**4 Theory. *Nucl.Phys.*, B226:187, 1983.

[13] K. Symanzik. Continuum Limit and Improved Action in Lattice Theories. 2. O(N) Nonlinear Sigma Model in Perturbation Theory. *Nucl.Phys.*, B226:205, 1983.

[14] E. Follana et al. Highly improved staggered quarks on the lattice, with applications to charm physics. *Phys.Rev.*, D75:054502, 2007.

[15] B. Sheikholeslami and R. Wohlert. Improved Continuum Limit Lattice Action for QCD with Wilson Fermions. *Nucl.Phys.*, B259:572, 1985.

[16] B. Blossier et al. Light quark masses and pseudoscalar decay constants from N(f)=2 Lattice QCD with twisted mass fermions. *JHEP*, 0804:020, 2008.

[17] B. Blossier et al. f(B) and f(B)(s) with maximally twisted Wilson fermions. *PoS*, LAT2009:151, 2009.

[18] B. Blossier et al. A Proposal for B-physics on current lattices. *JHEP*, 1004:049, 2010.

[19] Stephan Durr and Giannis Koutsou. Brillouin improvement for Wilson fermions. *Phys.Rev.*, D83:114512, 2011.

[20] Wolfgang Bietenholz and I. Hip. The Scaling of exact and approximate Ginsparg-Wilson fermions. *Nucl.Phys.*, B570:423–451, 2000.

[21] Wolfgang Bietenholz. Approximate Ginsparg-Wilson fermions for QCD. pages 3–18, 2000.

[22] Christof Gattringer. A New approach to Ginsparg-Wilson fermions. *Phys.Rev.*, D63:114501, 2001.

[23] Christof Gattringer et al. Quenched spectroscopy with fixed point and chirally improved fermions. *Nucl.Phys.*, B677:3–51, 2004.

[24] Herbert W. Hamber and Chi Min Wu. Some Predictions for an Improved Fermion Action on the Lattice. *Phys.Lett.*, B133:351, 1983.

[25] Tohru Eguchi and Noboru Kawamoto. Improved Lattice Action for Wilson Fermion. *Nucl.Phys.*, B237:609, 1984.

[26] H. Ikeda and S. Hashimoto. O(a**2) improvement of the overlap-Dirac operator. *PoS*, LAT2009:082, 2009.

[27] Luuk H. Karsten. Lattice Fermions in Euclidean Space-time. *Phys.Lett.*, B104:315, 1981.

[28] J.W. Milnor. *Topology from the Differentiable Viewpoint*. Princeton Landmarks in Mathematics. Princeton University Press, 1997.

[29] Michael Creutz. Confinement, chiral symmetry, and the lattice. 03 2011.

[30] Martin Luscher, Stefan Sint, Rainer Sommer, and Peter Weisz. Chiral symmetry and O(a) improvement in lattice QCD. *Nucl.Phys.*, B478:365–400, 1996.

[31] Mark G. Alford, T.R. Klassen, and G.P. Lepage. Improving lattice quark actions. *Nucl.Phys.*, B496:377–407, 1997.

[32] M. Luscher and P. Weisz. On-Shell Improved Lattice Gauge Theories. *Commun.Math.Phys.*, 97:59, 1985.

[33] G. Curci, P. Menotti, and G. Paffuti. Symanzik's Improved Lagrangian for Lattice Gauge Theory. *Phys.Lett.*, B130:205, 1983.

[34] Paul H. Ginsparg and Kenneth G. Wilson. A Remnant of Chiral Symmetry on the Lattice. *Phys.Rev.*, D25:2649, 1982.

[35] Herbert Neuberger. More about exactly massless quarks on the lattice. *Phys.Lett.*, B427:353–355, 1998.

[36] M.F. Atiyah and I.M. Singer. Dirac Operators Coupled to Vector Potentials. *Proc.Nat.Acad.Sci.*, 81:2597–2600, 1984.

[37] Pilar Hernandez, Karl Jansen, and Martin Luscher. Locality properties of Neuberger's lattice Dirac operator. *Nucl.Phys.*, B552:363–378, 1999.

[38] Maarten Golterman and Yigal Shamir. Localization in lattice QCD. *Phys.Rev.*, D68:074501, 2003.

[39] Maarten Golterman, Yigal Shamir, and Benjamin Svetitsky. Mobility edge in lattice QCD. *Phys.Rev.*, D71:071502, 2005.

[40] Maarten Golterman, Yigal Shamir, and Benjamin Svetitsky. Localization properties of lattice fermions with plaquette and improved gauge actions. *Phys.Rev.*, D72:034501, 2005.

[41] Yong-Gwi Cho and Shoji Hashimoto. Locality of the overlap-Dirac operator on topology-fixed gauge configurations. *PoS*, LATTICE2012:255, 2012.

[42] Shoji Hashimoto. personal note. 2012.

[43] Y. Kikukawa and T. Noguchi. Low energy effective action of domain-wall fermion and the ginsparg-wilson relation.

[44] T. Blum, P. Chen, Norman H. Christ, C. Cristian, C. Dawson, et al. Quenched lattice QCD with domain wall fermions and the chiral limit. *Phys.Rev.*, D69:074502, 2004.

[45] Y. Aoki, T. Blum, N. Christ, C. Cristian, C. Dawson, et al. Domain wall fermions with improved gauge actions. *Phys.Rev.*, D69:074504, 2004.

[46] S. Hashimoto, S. Aoki, G. Cossu, H. Fukaya, T. Kaneko, et al. Residual mass in five-dimensional fermion formulations. *PoS*, LATTICE2013:431, 2014.

[47] Gunnar S. Bali, Sara Collins, and Andreas Schafer. Effective noise reduction techniques for disconnected loops in Lattice QCD. *Comput.Phys.Commun.*, 181:1570–1583, 2010.

[48] M. Albanese et al. Glueball Masses and String Tension in Lattice QCD. *Phys.Lett.*, B192:163–169, 1987.

[49] Colin Morningstar and Mike J. Peardon. Analytic smearing of SU(3) link variables in lattice QCD. *Phys.Rev.*, D69:054501, 2004.

[50] Thomas A. DeGrand. One loop matching coefficients for a variant overlap action: And some of its simpler relatives. *Phys.Rev.*, D67:014507, 2003.

[51] Anna Hasenfratz and Francesco Knechtli. Flavor symmetry and the static potential with hypercubic blocking. *Phys.Rev.*, D64:034504, 2001.

[52] R. Sommer. A New way to set the energy scale in lattice gauge theories and its applications to the static force and alpha-s in SU(2) Yang-Mills theory. *Nucl.Phys.*, B411:839–854, 1994.

[53] Martin Luscher. Properties and uses of the Wilson flow in lattice QCD. *JHEP*, 1008:071, 2010.

[54] Szabolcs Borsanyi, Stephan Durr, Zoltan Fodor, Christian Hoelbling, Sandor D. Katz, et al. High-precision scale setting in lattice QCD. *JHEP*, 1209:010, 2012.

[55] Stefano Capitani, Stephan Durr, and Christian Hoelbling. Rationale for UV-filtered clover fermions. *JHEP*, 0611:028, 2006.

[56] Christof Gattringer, Ivan Hip, and C.B. Lang. Approximate Ginsparg-Wilson fermions: A First test. *Nucl.Phys.*, B597:451–474, 2001.

[57] T. Misumi. . *in seminar at University of Tsukuba*, 2014.

[58] Yong-Gwi Cho, Shoji Hashimoto, Jun-Ichi Noaki, Andreas Jüttner, and Marina Marinkovic. $O(a^2)$-improved actions for heavy quarks and scaling studies on quenched lattices. *PoS*, LATTICE2013:255, 2014.

[59] T. Kaneko et al. Large-scale simulations with chiral symmetry. *PoS*, LATTICE2013:125, 2013.

[60] J. Noaki, S. Aoki, G. Cossu, H. Fukaya, S. Hashimoto, et al. Fine lattice simulations with chirally symmetric fermions. *PoS*, LATTICE2013:263, 2013.

[61] Guido Cossu, Jun Noaki, Shoji Hashimoto, Takashi Kaneko, Hidenori Fukaya, et al. JLQCD IroIro++ lattice code on BG/Q. 2013.

[62] G.S. Bali and K. Schilling. Static quark - anti-quark potential: Scaling behavior and finite size effects in SU(3) lattice gauge theory. *Phys.Rev.*, D46:2636–2646, 1992.

[63] M. Okamoto et al. Charmonium spectrum from quenched anisotropic lattice QCD. *Phys.Rev.*, D65:094508, 2002.

[64] Chris Stewart and Roman Koniuk. Unquenched charmonium with NRQCD. *Phys.Rev.*, D63:054503, 2001.

[65] Christoph Lehner. Automated lattice perturbation theory and relativistic heavy quarks in the Columbia formulation. *PoS*, LATTICE2012:126, 2012.